PANGEO

II PAN-AMERICAN WORKSHOP ON GEOMAGNETISM – II PANGEO
November (19- 24), 2017 – Vassouras - Brazil

Proceedings of the II Pan-American Workshop on Geomagnetism - II PANGEO

on Geomagnetic Observatories, Geomagnetic Instruments, Geomagnetism and Space Weather

Chairman: Luiz Benyosef

Observatório Nacional
Rio de Janeiro - Brazil
2018

ISBN: 978-85-99926-09-3

Observatório Nacional

FAPERJ
Fundação Carlos Chagas Filho de Amparo à Pesquisa do Estado do Rio de Janeiro

II PAN AMERICAN WORKSHOP ON GEOMAGNETISM – II PANGEO
November (19- 24), 2017 – Vassouras - Brazil

Proceedings of the II Pan-American Workshop on Geomagnetism - II PANGEO

on Geomagnetic Observatories, Geomagnetic Instruments, Geomagnetism and Space Weather

Chairman: Luiz Benyosef

Observatório Nacional
Coordenação de Geofisica
Rua General José Cristino, 77
São Cristovão
20921-400 Rio de Janeiro, RJ
BRAZIL

Preface

Between November (19 to 24), 2017, sixty three geomagneticists and students from all three Americas, Europe and Africa attended the II Pan American Workshop on Geomagnetism (II PANGEO) in Vassouras, Rio de Janeiro State, Brazil.

II PANGEO consisted of two parts: 1) The scientific session's helded at Mara Palace Hotel and 2) Magnetic comparative measurements and instrumental demonstration helded at Vassouras Magnetic Observatory (VSS).

So, magnetic observatory practices, magnetic instruments use for different purposes scientific, commercial and space wheater were carrefully discussed.

This workshop was too an excellent opportunity to know and discuss the situation of the geomagnetic observatories and magnetic measurement techniques in Latin America concerning the definitive data production.

Also, we discussed the need to continue with this workshop every two years and suggested the next one to be in Argentine.

I'm thankful to the FAPERJ (Rio de Janeiro's Research Support Foundation) for this publication.

Finally, I want to thank to the II PANGEO's Organizing Committee and all participants that sent scientific and technical contribution and done their presentations and geomagnetic measurements.

Luiz Benyosef
Chairman

II PANGEO's Organizing Committee:

André Wiermann: ON - Observatório Nacional - Brazil

Andrés Papa: ON - Observatório Nacional - Brazil

Angelo De Santis: INGV - Istituto Nazionale di Geofisica e Vulcanologia - Italy

Carol Finn: USGS - United States Geological Survey - USA

Clézio De Nardin: INPE - Instituto Nacional de Pesquisas Espaciais - Brazil

Gerardo Cifuentes-Nava: UNAM - Universidad Nacional Autónoma de Mexico - Mexico

Jean Rasson: IRM - Institut Royal Meteorologique de Belgique - Belgium

Jürgen Matzka: GFZ - German Research Centre Geosciences - Germany

Lívia Ribeiro Alves: INPE - Instituto Nacional de Pesquisas Espaciais - Brazil

Esteban Hernandez: UNAM - Universidad Nacional Autónoma de Mexico – Mexico: Co-Chairman

Luiz Benyosef: ON - Observatório Nacional - Brazil: Chairman

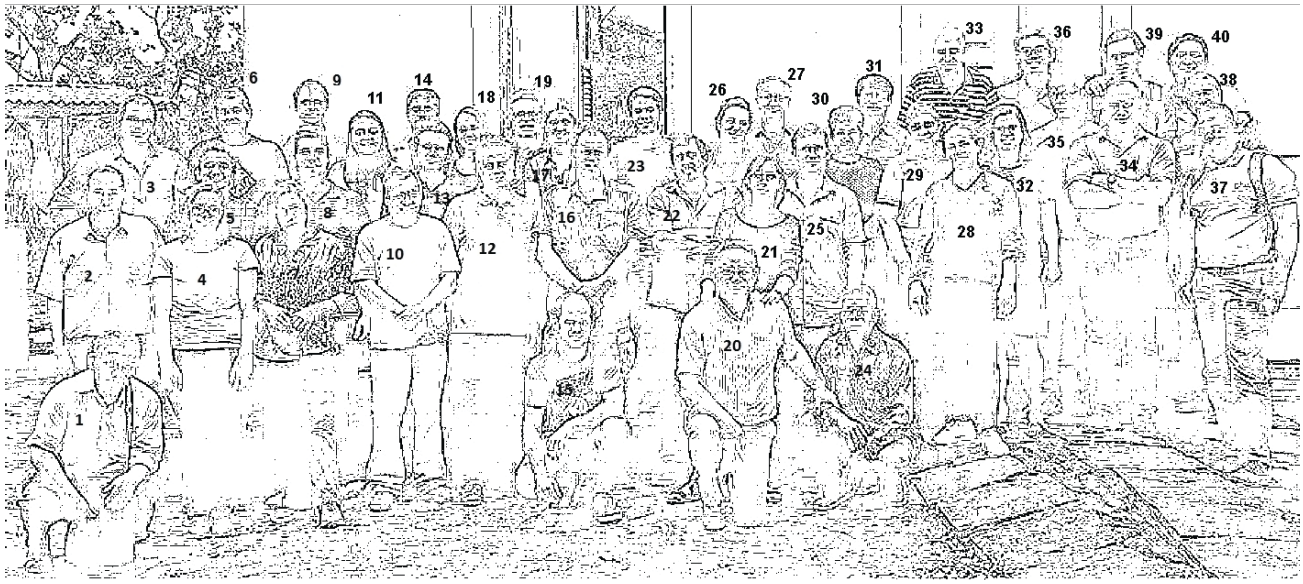

1: Edgard Rlcaldi Yarvi, 2: Domingos Rosales, 3: Bruno Canosa, 4: Yvelice Castillo, 5: Leandro Baptista 6: Jorge Brenes, 7: Marcela Nunes Almonaci, 8: Caio Gonçalves, 9: Paulo Ribeiro, 10: Luiz Benyosef, 11: Sophia Laranja, 12: Angelo De Santis, 13: Cezar F. Bellinghini, 14: Pedro Romero Corona 15: Alex Gonsette, 16: Jean Rasson, 17: Soledad Heredia, 18: Alex B. Nunes, 19: Thais Candido Silva, 20: Esteban Hernandez, 21: Leda S. Bettucci, 22: André Wiermann, 23: Facundo Poblet, 24: Armindo Nhatsave, 25: Gustavo Cabral, 26: Camila Farias, 27: Jürgen Matzka, 28: Keren Espinosa, 29: Carol Finn, 30: Maria Elena Muniz, 31: Wilson Quintero, 32: Denise Silva de Moura, 33: Ramon Caraballo, 34: Armando Ayala Fernandez, 35: Javier Quispe Mamani, 36: Sony S. Chen, 37: Antonio Mucussete, 38: Gerardo Cifuentes Nava, 39: Edwin Camacho, 40: Alejandro G. Serrano

Conclusions, Suggestions And General Comments:

Conclusions:

- The venue was a very good one. Its location was well-suited for easy walks to nearby restaurants; the meeting room was well-equipped and a good size for hosting the attendees; and having everyone stay at the same hotel made it conducive to fostering conversations with others outside of the main presentations, which is often where some of the most useful discussions take place.

- II PANGEO was successful because of the number of participants from different countries, and because of the large number of students in attendance. I believe that the students found it very valuable to learn from more senior scientists and to exchange ideas with them.

- The range of topics presented at the workshop was very good, covering a variety of areas of expertise.

Suggestions (for III PANGEO):

- I would recommend trying to schedule more time for hands-on measurement sessions at the observatory. If people are encouraged to bring their own theodolites to the workshop, they should have more opportunity to work with experienced observers who can advise them on their techniques and methods of recording their absolute measurements.
- I would encourage more time for hands-on equipment sessions, or demonstrations of software that can be used to view, analyze, or process data. I think this is one of the most important ways we can build capacity in other countries who may not have the means to develop such tools themselves.
- All of the attendees would benefit from having the full workshop schedule available to them before traveling to the workshop, so that they can plan their travel and presentations accordingly.

Carol A. Finn – USGS
Geomagnetism Group Leader
USGS/Geologic Hazards Science Center
PO Box 25046, MS 966
Denver, CO 80225

Comments:

- There is a significant amount of interested students, and scholars from the regions should do everything to make participation in interesting scientific projects possible for them.

- At the same time, geomagnetic data from the region is of global importance. The South Atlantic Magnetic Anomaly makes this a very interesting region and the American continent gives the possibility to deploy instruments on a broad range of latitudes, from the magnetic equator to the polar latitudes. The global importance of this data opens up for cooperation with institutes worldwide. This in turn gives the institutes in the region the chance for capacity building, both in observations, science and education.

Recommendation:

- The PANGEO is a great opportunity to meat. Please allow more time for training in the absolute house and give training time to interested parties.

Jürgen Matzka
GFZ German Research Centre for Geosciences
Section 2.3, Geomagnetism
Tel.: +49 (0)33843/624-18
Fax: +49 (0)33843/624-23
E-Mail: jmat@gfz-potsdam.de

Organization:

- Very good location;

- Convenient proximity of talks - rooms - meals, provides opportunity for contacts and discussions beyond session times.

- Interesting tours to the observatory

- Nice flexibility in resolving logistical challenges

- Would be good to have the schedule of talks / presentations distributed to participants in print or by e-mail. Preferably, in the evening, for next day sessions.

Important topics for further development and research:

- More stations in coastal regions, to support marine geophysical surveys

- Development and improvement of models and interpolation methods, to provide total field variation models for marine surveys

- Use of wavelet transformation methods for correction of magnetic variations in marine surveys

Dmitry Koryakin
Senior Geophysicist,
Marine Gravity & Magnetic Surveys
CGG Multi-Physics BL
Houston, Texas 77072 USA

Comments:

1. Meeting many scientists from all over the world with similar interest and passion for geomagnetism. I am sure the same passion will be a wonderful heritage to young researchers who attended with great attention and participation the conference.

2. Many interesting talks with particular focus on the state and the future development of geomagnetic networks in America and in the rest of the world. I hope many collaborations will consolidate or start from this unique event.

3. Sharing the space for most of the meeting, even after the conference itself, enjoying speaking on science as well as eating, drinking and singing together.

Angelo De Santis desantis@ingv.it
Senior Principal Research Fellow
Geomagnetic Observartories and National Magnetic Network
Via di Vigna Murata, 605 – 00143 Rome – Italy

General considerations

1. With a wide participation of researchers, technicians, observers and students from various continents, the meeting happened in an atmosphere of lively interest and discussion. An important set of works and studies were presented that gave a broad view of the various technical and theoretical questions of Geomagnetism and Space Weather. From the presentations on the simplest but fundamental technical issues related with the installation and good functioning of geomagnetic observatories, passing through the presentations of a new generation of magnetometers and the Brazilian space climate monitoring and forecasting program (EMBRACE), or even on the use of Swarm's magnetic data to study the large earthquake's precursory signals, were many the presentations of great interest and topicality.

2. The meeting took place in a beautiful space, where a warm atmosphere and great openness and informality promoted among all a wide sharing of experiences and knowledge that certainly contributed to the personal and scientific enrichment of all.

Suggestions

1. The inclusion of thematic short courses in a workshop is truly important not only for young technicians and researchers, but equally for all. However, for these short courses to be more productive, they should be scheduled for longer periods (e.g. 2-4 hours minimum!), and, if possible, should integrate a practical component (hands-on sessions: e.g. instrument training and or data processing) and a period of discussion & reflection.

Paulo Ribeiro
Magnetic Observatory of Coimbra
Coimbra University - Portugal

Final Considerations and Recomendations

By unamity all participants recommended to realize the Pan American Workshops on Geomagnetism (PANGEO) each two years in countries from the three Americas Continent.

The III PANGEO will be held in Argentine at November, 2019.

If the Argentine Local Committe decides that its realization will be not possible the Local Committees will choose among other candidates

We received from three Local Communitties some candidates countries to hold it, they are:

1 – Uruguay

2 – Honduras

3 – Costa Rica

Presentations, Titles and Authors:

01 - One century of data from Vassouras Magnetic Observatory (1915-2015):
Artur Benevides, Edwin Camacho, Vitor Silveira, Rodrigo Melhorato, Israelli Rodrigo e Katia Pinheiro - ON – Brazil

02 – Instruments Demo:
Jean Rasson and Alex Gonsette – Royal Meteorological Institute – Belgium

03 – Status of USGS Geomagnetism Program and Highlights from the 2017 Intermagnet Meeting:
Carol Finn – United States Geological Survey – United States of America

04 - Magnetic Anomalies at the Brazilian Equatorial Margin: from Ceará Plateau to Saint Peter and Saint Paul Archipelago:
Denise Silva de Moura, Eder Cassola Molina, Luigi Jovane, Yára Regina Marangoni, Márcia Maia. USP – UBO. Brazil and France

05 - Correction of Geomagnetic Field Variations in Marine Magnetic Surveys Using Observatory and Model Geomagnetic Data:
Dmitry Koryakin CGG - United States of America

06 - Nuevo Software Azmsole-2018 Para Determinacion De Azimuth:
Domingo Rosales and Erick Vidal - Observatorio Geomagnético de Huancayo – Instituto Geofísico del Perú – Perú

07 – **27 Day Variation in Solar-Terrestrial Parameters: Global Characteristics and an Origin Based Approach of the Signals:**
F. L. Poblet and F. Azpilicueta. Universidad de La Plata - CONICET – Argentina

08 - **The Tsallis Statistical Distribution Applied to Geomagnetically Induced Currents:**
C. S. Barbosa, R. Caraballo, L. R. Alves, G. A. Hartmann, C. D. Beggan, A. Viljanen, C. M. Ngwira, A. R. R. Papa, and R. J. Pirjola - INPE- ON-BGS. Brazil, Uruguay and UK

09 - Determinación del Lugar Para la Reubicación del Observatorio Geomagnético de la República de Cuba:
María Elena Muñiz; Ismael González; Antonio Alonso and Ramsés Zaldívar. Instituto de Geofísica y Astronomía – Cuba

10 - Cartas Magnéticas y Estructura del Bloque Andino a Partir de Observaciones Geomagnéticas en las Estaciones de Repetición de la Red Geomagnética de Colombia:
Wilson Quintero – Servicio Geologico Colombiano - Universidad Nacional – Colombia

11 - Estado Actual de los Observatorios Magnéticos Permanentes del Servicio Meteorológico Nacional de Argentina:
Soledad Heredia and Camila Farias; Servicio Meteorológico Nacional – Argentina

12 - Using Magnetograms to Understand and Probe the Magnetosphere:
Yvelice Castillo et al - National Autonomous University of Honduras and University of Coimbra. Honduras and Portugal

13 - Precursors of Disturbed Geomagnetic Conditions:
D.V. Blagoveshchensky, M.A. Sergeeva, A. Kozlovsky, P. Corona-Romero. SPSUAI - UNAM. Russia and Mexico

14 - Transient Phenomena into the SAMA During Geomagnetically Active Times: Solar Cycles 23 and 24 Case:
Ramon Caraballo y Leda Sánchez Bettucci. Universidad de la Republica y Observatorio Geofisico del Uruguay – Uruguay

15 - A Proposal for a Geomagnetic Observatory in Honduras:
Yvelice Castillo - National Autonomous University of Honduras – Honduras

16 – Analysis of Solar, Interplanetary and Geomagnetic Parameters in the Solar Cycle 24:
Yvelice Castillo et al - National Autonomous University of Honduras and University of Coimbra. Honduras and Portugal

17 - Reliability of the Geomagnetic Observation Data in The Villa Remedios And Patacamaya Observatories:
J. Quispe, M.; E. Ricaldi Y. and P. Miranda - Universidad Mayor de San Andres – Bolívia

18 - Estimativa Da Amplitude de Correntes Geomagneticamente Induzidas em Diferentes Locais no Brasil Durante a Tempestade Mais Intensa do Ciclo 24:
Espinosa, K.; Alves, L.; Padilha, A. - INPE – Brazil

19 - Comparison Between the Secular Variation at Tatuoca Magnetic Observatory Data (Brazil) and the Global Field Models IGRF12 and CHAOS6:
Baldez, Raissa Moraes; C. M. Martins; K.J. R. Pinheiro and C. E. P. Martins - UFPA and ON – Brazil

20 – Diurnal variations of the H Component in the South Atlantic Islands at Low magnetic Latitudes:
Freire, L.; Laranja, S. R.; Bellinghini, C. F. and Benyosef, L. - ON – Brazil

21 – Modelling Geomagnetically Induced Currents Using Data from a Remote Geomagnetic Observatory:
Ciaran Beggan and Gemma Richardson - BGS - United Kingdom

22 - Comparação do Comportamento de Pulsações Pc3 em Diferentes Latitudes da Anomalia Magnética do Atlantico Sul:
Piassi, A.; Alves, L. and Padilha, A. - INPE – Brazil

23 – Fulguraciones Solaes de los Primeros Dias de Septiembre 2017 Registrados Por el Observatorio Geomagnético de Villa Remedios y El Monitor de Neutrones Nm-64 de Chacaltaya Cortejados con Registros de Flujo de Rayos X Solares del Satelite:
Ricaldi Y.E.L., Ticona P.R., Miranda L.P., Quispe M.J. - Universidad. San Andreas – Bolívia

24 – Study for the Qualification of Magnetic Index Ksa:
Bilibio, A.V. et al - INPE – Brazil

25 - Response of the Δ*h* Made by the Embrace Magnetometer Network: A Case Study:
Chen, S.S. et al. - INPE – Brazil

26 - Geomagnetic Survey at Guárico, Bolívar and Carabobo in Venezuela for Repeat Stations and a New Magnetic Observatory:
Camacho, E, Gutierrez, E and Benyosef L. - C.I.D.A. and ON - Venezuela and Brazil

27 – **The Geomagnetic Observatory Niemegk Recent Activities and Global Geomagnetic Network:**
Jürgen Matzka – German Research Centre for Geosciences – Germany

28 - Magnetic Observatory of Nampula:
Antonio Mucussete – Magnetic Observatory of Nampula – Mozambique

29 - Kmex: the Mexican Geomagnetic K Index:
P. Corona-Romero et al - UNAM – Mexico

30 - The Magnetic Service and its relationship with Weather Space Services, experiences in Mexico University (UNAM):
Hernández-Quintero E., Cifuentes-Nava G. - UNAM – Mexico

31 – D-Z Geomagnetic Field Variations and Geological Features Observed at Low Magnetic Latitudes:
Laranja, S. R.; Cunha, C. Cândido, Thaís and Benyosef, L. - ON – Brazil

32 - Observatório Geofisico del Uruguay (Monitoreo Geomagnético y Sismológico):
Leda Sánchez-Bettucci and Ramón Caraballo. Universidad de la República and Observatorio Geofísico del Uruguay – Uruguay

33 – The Magnetic Observatory of Coimbra (COI): Past, Present Operating Status and Future Developments:
Paulo Ribeiro; M. Alexandra Pais and Anna L. Morozova - University of Coimbra – Portugal

34 - A Comparative Study of Pc 5-6 Geomagnetic Pulsations at Low and Middle Latitudes:
Werneck de Carvalho, Vinicius J.O.; Benyosef, Luiz and De Santis, Angelo - ON and INGV - Brazil and Italy

35 - Development of an Active Calibration System for Fluxgate Magnetometers:
Gustavo G. Cabral, André Wiermann and Luiz Benyosef - ON – Brazil

36 Development of an Automatic Device for the Determination of the Geographical North from the Measurement of the Solar Ecliptic and Georeferencing:
Natacha Oliveira, André Wiermann, Cosme F. Ponte-Neto - ON – Brazil

***37*- Análise Comparativa e Interpretação de Dados de Calibração de um Magnetômetro Fluxgate de Alta Resolução para Observatórios Geomagnéticos:**
Thaísa C.N. Melo e André Wiermann - ON – Brazil

38 – Research to Operation (and Operation to Research in Space Weather):
Clézio Marcos De Nardin - INPE – Brazil

39 - Evidence of an Abrupt Secular Variation Change during 2015 in Southern Africa and the Adjacent Atlantic Ocean Region:
Pieter Kotzé and Jürgen Matzka – SANSA and GFZ - South Africa and Germany

40 - A Study for Overhauser Magnetometer Development:
André Wiermann and Luiz Benyosef - ON – Brazil

41 – The Fluxgate Magnetometer Past, Present and Future:
Luiz Benyosef - ON – Brazil

42 – Magnetic Indices and Their Application to Space Weather
Clezio Marcos De Nardin – INPE - Brazil

43 - Production of a New Calibrated Dataset from the Tatuoca Geomagnetic Observatory in the Brazilian Equatorial Region:
Gabriel Soares, Jürgen Matzka and Katia Pinheiro - ON and GFZ - Brazil and Germany

44 – Conservation, Scanning and Digitalization of Historical Geomagnetic Data Archives from Brazil:
Daniel R. Franco et al – Brazil

45 – Space and Earth Weather – A Cloudy Relationship
Edson Alonso Falla Luza[1,2] *Daniel Ribeiro Franco*[2] *Alexandre Humberto Andrei*[2] *- UFF and ON – Brazil*

46 – Absolut Observations in the Vassouras Magnetic Observatory during II PANGEO:
Antonio Mucussette and Armindo Nhatsave – Nampula and Maputo Magnetic Observatories – Mozambique

Abstracts And Extended Abstracts

One Century of Data from Vassouras Magnetic Observatory (1915-2015).

Artur Benevides[1], Edwin Camacho[1], Vitor Silveira[1], Rodrigo Melhorato[1], Israelli Rodrigo[1] e Katia Pinheiro[1]*
1 ON Geophysics Department, Observatório Nacional, Rio de Janeiro, CEP: 20921-400, Brazil.

Vassouras Magnetic Observatory (VSS) was the first observatory in Brazil, starting its measurements in 1915. VSS is part of the INTERMAGNET (International Real-time Magnetic Observatory Network) since 1999 because of its high data quality and transmission in real time. The centennial observations of magnetic field components in VSS are fundamental to global models, especially because of lack of data in the Southern Hemisphere. Global models contribute significantly on the understanding of the Earth's magnetic field, both internal field caused by core dynamics, and external field, produced in the ionosphere and magnetosphere. Data from VSS is also applied to studies on geophysical prospection of metals and hydrocarbons. This work presents the history of VSS as well as its centennial dataset (1915-2015). We explore the main characteristics of the secular variation and external field temporal variations in VSS; comparison of VSS data with of IGRF (International Geomagnetic Reference Field) model and detection of possible geomagnetic jerks occurring in this period.

Keywords: Vassouras Magnetic Observatory, Earth's magnetic field, global model, geomagnetic jerks.

Instrument Demo

A.Gonsette, Royal Meteorological Institute of Belgium

J. Rasson , Royal Meteorological Institute of Belgium

We report here on the automatic magnetic observatories research. The Earth's magnetic field is in perpetual evolution, varying in time but also in space. The South-Atlantic anomaly is one of the several examples. The role of the magnetic observatories is to observe and record the vector field at fixed points for long term. The time series hence generated are at the early stage of any geomagnetic study; serving to build models; contributing to understand the Solid-Earth; being also important for space weather. The more we deploy observatories, the more we understand our planet.

The magnetic field is usually recorded from a set of at least three instruments. One of them, the variometer, continuously records the variations of the magnetic field. Those variations are relative and should therefore be calibrated by means of absolute observations. For that purpose, a scalar magnetometer gives the intensity of the field while an operator/observer measures its direction during the so-called absolute measurements. The need of an observer limits the deployment of magnetic observatories to the inhabited areas. Sometimes, it becomes difficult to find and train people. The instruments themselves are often old, second-hand and more and more difficult to find.

These critical points have led rmi Dourbes to work on both man-operated and automatic instrumentation. A new DIFlux based on a factory non-magnetic theodolite TD6JE has been developed in a wireless version particularly useful in the field. Moreover, the automation of the absolute measurement is a keystone in the development of automatic magnetic observatories. The AutoDIF is the result of several years of research at Dourbes. The instrument is a robotized version of a conventional DIFlux able to perform a completer D&I sequence in about 5 min. The possible high rate of measurements (more than 200/day) allows to get a very high definition of the variometer baselines and, from that, highlight and correct some calibration errors such as variometer scale factor and orientation errors. The automatic absolute measurement also allow to build the magnetic vector in near real-time.

AutoDIF needs a target for determining the True-North direction. This still limits its use to some "comfortable" locations. Indeed, fog, snow-storm, vegetation, water and so on… prevent the device from pointing the target. GyroDIF overcomes this problem by directly detecting the Earth rotation vector by means of an embedded fiber optical gyroscope (FOG) used as North-seeker. This evolution raises new possibilities of deployments in remote and areas such as Antartica and Seafloors.

Status of USGS Geomagnetism Program and Highlights from the 2017 INTERMAGNET Meeting

Authors: Carol A. Finn [1]

[1] U.S. Geological Survey (USGS)

Keywords: Geomagnetism, Intermagnet

Abstract

The U.S. Geological Survey (USGS) Geomagnetism Program has faced some challenges during the past year, especially with the proposed elimination of the Program in the President's fiscal year 2018 budget. The short- and long-term outlook for the Program remains unclear. Despite this, Geomagnetism Program employees continue to operate 14 magnetic observatories across the U.S. and its territories, and the Program continues to produce high-quality, high-resolution, continuous, real-time data for its national and international customers to the best of its ability. The Program also continues to perform important research on geomagnetic and geoelectric hazards of concern to the electric-power grid industry. Program staff also play important roles in a U.S. national program for Space Weather Operations Response and Mitigation (SWORM).

The 2017 INTERMAGNET (IM) Annual meeting was held at the offices of the South African National Space Agency (SANSA) in Hermanus, South Africa in Sep 2017, shortly after the IAGA Scientific Assembly in Cape Town, SA. Fifteen IM member-delegates attended either in person or online, and eleven guests participated. Simon Flower (United Kingdom) conducted his first meeting as Chair of the Operations Committee (OPSCOM) following the resignation of Jean Rasson (Belgium). Simon's goal is to make the work of IM more open and accessible, and will announce future meetings to the observatory community via the "worldobs" mailing list (worldobs@gfz-potsdam.de). The IM group hopes to improve how we communicate with the numerous INTERMAGNET Observatory (IMO) institutes. Progress is being made on one-second definitive data, with 38 IMOs contributing 2014 data in IAGA2002 format. Future data is requested to be provided in ImagCDF format. Discussions were held on licensing of IM data and digital object identifiers (DOIs), continuation of the annual DVDs, the IM web service, and a variety of other topics. The next meeting will be held 2-4 Jul 2018 in Vienna, Austria, after the IAGA Observatory Workshop in Conrad, Austria.

Magnetic Anomalies at the Brazilian Equatorial Margin: from Ceará Plateau to Saint Peter and Saint Paul Archipelago

Denise Silva de Moura[*1], Eder Cassola Molina[2], Luigi Jovane[1], Yára Regina Marangoni[2], Márcia Maia[3]*

1- University of São Paulo – Oceanographic Institute (IO-USP)

2- University of São Paulo – Institute of Astronomy, Geophysics and Atmospheric Sciences (IAG-USP)

3- Université de Bretage Occidentale – Institut Universitaire Européen de la Mer (IUEM-UBO)

Abstract:

Magnetic surveys along the Equator used to be difficult to interpret, due to the low magnetic field intensity near to the Magnetic Equator. This study, carried along the Brazilian Equatorial Transform Margin, presents the magnetic anomalies and models from two completely different seamounts, which differences may help the analysis. The Ceará Plateau is a 2 km high seamount, near to the continent, with very high magnetic anomalies. We propose that its basement is formed by volcanic edifices, below the flat sedimentary layer, based on magnetic and gravimetric anomalies. Its formation is unknown, so we correlated the ocean crust anomalies with the plateau ones. Around the Plateau, the crust was formed on the Cretaceous Normal Superchron (124-84 Ma), then the remanent magnetization has the same polarity as the induced one, since the two magnetic anomaly lows on the plateau seem to have a normal polarity as well, it can be an evidence of an old formation, related to the Brazilian Equatorial Ocean opening. Located on the Mid-Atlantic ridge, the St Peter and St Paul Archipelago is a mantle elevation, with more than 4 km and an active uplift. It is highlighted by a negative magnetic anomaly along the St Paul fracture zone. Its formation is dated to the last 10 Ma, and the induced magnetization seems to be predominant. Due to analyze the anomalies, from both sources, it was calculated a simple theoretical model able to simulate a homogeneous crust with constant spreading, magnetization and thickness. Both residuals, i.e., the differences between the observed and theoretical signal, helped to enhance the seamount anomalies. A defined magnetized layer is not a common approach, but may help the interpreter, mainly in complicated regions, as the Equator.

Correction of Geomagnetic Field Variations in Marine Magnetic Surveys Using Observatory and Model Geomagnetic Data

Dmitry KORYAKIN
CGG MultiPhysics, Houston, USA, dmitry.koryakin@cgg.com

CGG MultiPhysics performs marine gravity and magnetic surveys worldwide, mostly for geological prospecting purposes.

Marine magnetic measurements are greatly affected by geomagnetic field variations that produce erroneous anomalies often indistinguishable from anomalies of geological nature.

CGG MultiPhysics employs special decorrelation algorithm to produce effective correction of magnetic variations. The presentation shows examples of marine data correction using variations recorded at close and distant observatories, as well as estimated at survey location by interpolation between observatories and by HDGM-RT model algorithm. Combination of observed geomagnetic observatory data with modern high definition models leads to significant improvement in correction of magnetic variations.

1. D. Koryakin, dmitry.koryakin@cgg.com tel: +1-832-351-4838, fax: +1-832-351-4841. Address: 10300 Town Park Drive, Houston, TX 77072 USA.
1. OP

Nuevo Software Azmsole 2018 Para Determinacion de Azimuth

Domingo Rosales[1], Erick Vidal[1]*
[1] Observatorio Geomagnético de Huancayo – Instituto Geofísico del Perú, Huancayo, Perú.
[*]e-mail: drosales@igp.gob.pe.

Resumen

La determinación del “azimuth de marca” mediante observaciones de astros es una labor fundamental en trabajos de mediciones absolutas en un observatorio geomagnético, por lo que periódicamente es necesario verificar el valor de dicho azimuth. Así mismo en trabajos de levantamientos geomagnéticos se hace indispensable determinar con mucha precisión el norte verdadero, para poder medir la declinación magnética.

Para determinar el meridiano geográfico mediante observaciones astronómicas, recurrimos al azimut que tiene un astro en un momento dado, así como del ángulo horizontal que dicho astro hace con respecto a una línea de referencia, es decir se determina el azimut del astro y a partir de ella se obtiene la dirección del meridiano que pasa por el lugar del punto de observación. El proceso de reducción para la determinación del azimuth de marca, es realizado manualmente mediante la utilización de almanaques astronómicos o también mediante software que utilizan almanaques interactivos como por ejemplo el “Multiyear Interactive Computer Almanac” (MICA).

En el año 2007 se desarrollo el AZMSOLE y actualmente es utilizado en diversos trabajos de reducción de mediciones geomagnéticas para la de determinación del azimuth de marca.

Debido a que con forme va pasando el tiempo, las correcciones de tiempo y las proyecciones de las efemérides determinadas en el año 2007 al 2017 se hacen menos precisas. Se hace necesaria la actualización de dicho software, por lo que se ha desarrollado el nuevo “AZMSOLE_2018”.

El AZMSOLE_2018 toma como astros de medición además del Sol, a la Luna, Marte, Mercurio y las estrellas que conforman la Cruz del Sur, para lo cual se ha utilizado las más recientes correcciones de tiempo y las efemérides proporcionadas por la “Jet Propulsion Laboratory Horizons” (JPLH) con un rango valido desde el 1 de enero del 2010 al 31 diciembre del 2018.

Además con la finalidad de mantener actualizado este software y buscando que sea lo mas preciso posible, se ha determinado que en noviembre de cada año será actualizado el AZMSOLE con las más recientes efemérides y correcciones del tiempo, para que pueda ser utilizado durante el año siguiente.

27-Day Variation in Solar-Terrestrial Parameters: Global Characteristics and an Origin Based Approach of the Signals

Authors: F. L. Poblet [1], [2] and F. Azpilicueta [1], [2].

[1] Facultad de Ciencias Astronómicas y Geofísicas. Email: fpoblet@fcaglp.unlp.edu.ar
[2] Consejo Nacional de Investigaciones Científicas y Técnicas (CONICET).

Keywords: 27-day variation, solar wind, solar radiation, cross-correlation.

Abstract

The Earth and the near interplanetary medium is affected by the Sun in different ways. Those events generated in the Sun that induce large perturbations into the Magnetosphere-Ionosphere system are called geoeffective events and show a wide range of temporal variations, like the 11-year solar cycle (long term variations), the variation of ~27 days (recurrent variations), solar storms lasting for some days and particle acceleration events lasting for some hours, etc.

The periodicity of ~27 days associated with the solar synodic rotation period was investigated. The work was mainly focused on studying the resulting ~27 day periodic signal in the terrestrial magnetic activity, by the analysis of the H component of the magnetic field registered on a set of 103 magnetic observatories distributed around the world. The most important characteristics observed in the signal are two main amplitude modulations: the first and most prominent related to the solar cycle recurrence and the second one with a semiannual pattern. The amplitude of the resulting signal depends on the geomagnetic latitude of the observatory showing a significant discontinuity at approx. ±60º.

The 27-day signal in the magnetic activity was compared with similar signals found in other important parameters that are widely used to characterize the energy transfer from the Sun to the Earth. The radiative transfer was considered by studying the F10.7 and Mg II indices, and the vertical total electron content (vTEC). The non-radiative transfer, related to the interaction between the solar wind and the magnetosphere, was taken into account by analyzing the solar wind velocity. A series of cross-correlations between the previously mentioned parameters were performed. The most important conclusion reached is that the physical process that originates the 27-day signal in the magnetic activity is associated to a process in the solar wind (the non-radiative source) and not to the solar electromagnetic radiation.

The Tsallis Statistical Distribution Applied To Geomagnetically Induced Currents

C. S. Barbosa[1], *R. Caraballo*[2] , *L. R. Alves*[3], *G. A. Hartmann*[4], *C. D. Beggan*[5], *A. Viljanen*[6], *C. M. Ngwira*[7],[8], *A.R. R. Papa* [1],[9] *and R. J. Pirjola*[6],[10]

[1]*ON, Brazil,* [2]*UDELAR, Uruguay,* [3]*INPE, Brazil* [4]*UNICAMP, Brazil,* [5]*BGS, United Kingdom,* [6]*FMI, Finland,* [7]*CUA, United States,* [8]*NASA/GSFC, United States,* [9]*UERJ, Brazil,* [10]*NRC, Canada*

Geomagnetically induced currents (GICs) were first described by W. H. Barlow in 1849 as anomalous currents in telegraphic wires and they are currently understood as a ground effect arising from a chain of events in the Sun-Earth system. GIG are mainly observed at power networks and their amplitudes are controlled by a combination of geophysical conditions and network parameters. The magnetic disturbances detected on the ground came from the coupling of highly disturbed solar wind (SW) plasma propagating through the interplanetary medium which eventually impinges on the Earth's magnetosphere. The perturbed magnetospheric-ionospheric coupling can produce intense currents systems that can induce strong geoelectric fields at the Earth's surface, which in turn generate currents that can flow through grounded technological infrastructure. GICs have been measured and modeled in many countries, resulting in a considerable amount of data. The statistical analyses of such datasets have proposed various types of distribution functions, mainly based on extensive Boltzmann-Gibbs statistical to fit long-term GICs datasets. However, these extensive statistical approaches have been only partially successful in fitting the data sets. Here we use modeled GICs datasets calculated in four countries (Brazil, South Africa, United Kingdom, and Finland) using data from solar cycle 23 to show a plausible function based on a nonextensive statistical model of the *q*-exponential Tsallis function. The generalized Tsallis statistical mechanics function has been proposed as a more convenient way to describe those systems trapped into nonequilibrium conditions which eventually reach quasi-stationary states. The fitted entropic index, i.e. *q*-exponential, parameter was found as approximately the same for all locations, and the Lilliefors test shows good agreement with the *q*-exponential fits. From this fit, we compute that the likely numbers of extreme GICs events over the next ten solar cycles are 1–2 for both Finland and United Kingdom, at least one for Brazil and less than one event for South Africa. Our results indicate that the nonextensive statistics are a general characteristic of GICs, suggesting that the ground current intensity has a strong temporal correlation and long-range interaction.

Determinación del Lugar Para la Reubicación del Observatorio Geomagnético de La República de Cuba

María Elena Muñiz[1]; Ismael González [1]; Antonio Alonso [1]; Ramsés Zaldívar[1];

[1] Instituto de Geofísica y Astronomía. La Habana. Cuba

Keywords: geomagnetismo, levantamientos geomagnéticos

Abstract

En estos momentos debido al desarrollo urbano resulta imposible continuar con el emplazamiento que ocupa el Observatorio Geomagnético “HABANA”, por lo que se hace necesario buscar con la mayor brevedad un lugar para la reubicación del mismo. Para esto nos dimos a la tarea de buscar sitios que cumplieran con las características geológicas y geofísicas del CMT, además de cercanía y seguridad para la atención y cuidado del equipamiento.

Los trabajos previos incluyeron la búsqueda de información geológica de los sitios a investigar, consultas a especialistas (geólogos y geofísicos) y revisión de imágenes aéreas y satelitales.

En el trabajo se muestran los resultados de los levantamientos geomagnéticos realizados en las inmediaciones del área ecológica Sierra del Rosario, comunidad Las Terrazas; Provincia Artemisa.

Se trazó una cuadrícula de 20 x 20 m, en la que se procedió a realizar mediciones de la componente total del campo geomagnético “T” cada 1 m, a 2 alturas para medir tanto el gradiente horizontal como vertical. Las mediciones se ejecutaron con un magnetómetro protónico “Gem 19 T”.

Se utilizó la metodología aprobada por la International Association of Geomagnetism and Aeronomy (IAGA), para este tipo de investigación, confeccionándose los mapas de gradiente magnético horizontal y vertical.

Se concluye que el área estudiada cumple los requisitos de bajo gradiente, menos de 2 nT/m, recomendándose la misma para el traslado del observatório geomagnético cubano

Cartas Magnéticas Y Estructura del Bloque Andino a Partir de Observaciones Geomagnéticas en Las Estaciones de Repetición de La Red Geomagnética de Colombia.

Quintero, Wilson.[1,2]

[1] Servicio Geológico Colombiano; [2] Universidad Nacional de Colombia.

Palabras Clave: cartas magnéticas, estaciones de repetición, red Geomagnética.

Resumen

La república de Colombia cuenta con un observatorio geomagnético permanente instalado en la isla El Santuario de Fúquene en el año 1953. Paralelamente, en el año 1954 se inicia el diseño y ocupación de una red de estaciones geomagnéticas de repetición en todo el territorio colombiano que alcanza un total de aproximadamente 500 estaciones de repetición para el año 1993, año en el cual se cancela el proyecto de las reocupaciones por parte del Instituto Geográfico Agustín Codazzi (IGAC). Las componentes del campo geomagnético observadas en las estaciones de repetición dependieron de los instrumentos utilizados, en general se observada: declinación (D) y componente horizontal (H); declinación e inclinación (I); declinación, componente horizontal e intensidad total (F); y declinación, inclinación e intensidad total. La base de datos de estaciones de repetición geomagnética fue corregida por variación diurna, con los registros del Observatorio Magnético de Fúquene. De las 500 estaciones de repetición 100 tenían más de dos reocupaciones, sobre éstas se realizaron ajustes polinómicos y se rechazan 20 por no reflejar el comportamiento adecuado de la variación secular. Con las 80 estaciones magnéticas restantes que aún conservaban un buen cubrimiento del territorio colombiano se elaboraron las cartas magnéticas para las componentes declinación, componente horizontal e intensidad total. Se compararon las cartas magnéticas producto de las estaciones de repetición con las cartas sintéticas producto del modelo IGRF-1995, y se obtuvieron las siguientes diferencias promedio: declinación 4.5% que corresponde a 10.8' para una D media de 4° al W; componente horizontal 0.3% que corresponde a 84 nT para una H media de 28000 nT; e intensidad total 0.2% equivalente a 66 nT para una F media de 33000 nT. También se realizó un regrillado de las estaciones de repetición que cubrían el bloque andino, a éste se le restó el campo geomagnético principal (IGRF-1995). Al mapa de anomalías magnéticas resultantes se le realizó una reducción al polo, al cual se le realizó un análisis espectral, cuya separación regional-residual permitió delinear el bloque andino colombiano y diferenciar el carácter basáltico de las cordilleras Occidental y Central de la cordillera oriental de carácter granítico.

Estado Actual de los Observatorios Magnéticos Permanentes del Servicio Meteorológico Nacional, Argentina

Heredia Soledad [1], Farias Camila[1],

[1] Servicio Meteorológico Nacional, Argentina.

Palabras claves*: Observatorios magnéticos, SMN, Intermagnet, AMAS.*

RESUMEN

Una de las funciones del Servicio Meteorológico Nacional (SMN) es el estudio y medición del campo magnético terrestre además de monitorear el comportamiento de la Anomalía Magnética del Atlántico Sur (AMAS). Para ello, el SMN cuenta con Observatorios magnéticos permanentes (OMP) que registran continuamente las variaciones del campo magnético (Fig 1.). Con los datos obtenidos, se elaboran Boletines Mensuales, y se ejecutan trabajos de investigación y colaboraciones con organismos internacionales.

Sus OMP se fundaron a partir de 1904, el Observatorio magnético de Orcadas, Antártida (ORC) y el Observatorio de Pilar, Córdoba (PIL), y por último en 1917 el de la Quiaca (LQA). Este último se encuentra en reparación actualmente. Se cuenta con más de 100 años de registro, que en un principio, eran analógicos hasta el 2010 y 2012 donde, primero PIL y luego ORC, fueron actualizados a sistemas digitales.

Los Observatorios del SMN cuentan hoy con instrumental para medir la intensidad total (F) del Campo Magnético Terrestre (CMT), y las variaciones de las componentes; horizontal (H), vertical (Z) y declinación (D) del CMT. También poseen un Teodolito Magnético con el cual un observador determina en forma absoluta la Declinación e Inclinación, que junto con F permite calcular las líneas de base de los valores medidos por los variómetros.

A fines del 2015 el SMN sumo una nueva Estación Magnética Permanente, Estación Cipolletti (CPL), logrando así medir en otro punto de nuestro vasto territorio la Intensidad F.

Tanto PIL como ORC desde el año 2012 y 2013 respectivamente, integran la Red Mundial de Observatorios magnéticos (INTERMAGNET) gracias al Proyecto INDIGO, British Geological Survey, que permitió la implementación de un sistema digital de medición.

Además, la Universidad Nacional de La Plata cuenta con dos observatorios, el de Trelew (TRW), miembro de INTERMAGNET, y Las Acacias (LAS) de registro de F. Ellos intercambian información con el SMN y trabajan conjuntamente.

En este trabajo se presentan los datos históricos de las componentes del CMT, que muestran el comportamiento de la AMAS, y cómo los registros diarios de los Observatorios permiten analizar la actividad geomagnética y reconocer los eventos solares que la causan.

INTRODUCCIÓN

Fig 1. Localizacion de Observatorios

El Observatorio Magnético Pilar se localiza en la ciudad de Pilar, en la Provincia de Córdoba, zona centro de la Argentina. Sus coordenadas Geográficas y Magnéticas son 31°40´00´´ S 63°53´00´´ W y 20°02´00´´S 04°00´00´´W respectivamente y su altura sobre el nivel del mar es de 338 msnm.

En el Observatorio Geofísico y Meteorológico de Pilar confluyen diferentes disciplinas, Meteorología, Radiación, Ozono, Sismología y Geomagnetismo. Esta última dentro del Observatorio Magnético.

El Observatorio Magnético Pilar comenzó a operar en 1904 y sus registros datan desde entonces. Cuenta con instrumental el cual posee una configuración clásica acorde a la mayoría de los observatorios magnéticos.

En noviembre de 2010, el Observatorio se actualizó con la instalación del Sistema INDIGO (Digital Geomagnetic Observatory) para dar inicio a registros digitales. Luego de pruebas y de ajustes del sistema, en septiembre de 2012, el Observatorio fue aceptado como miembro de INTERMAGNET (Red Magnética Internacional en Tiempo Real).

El observatorio de la Base Orcadas es el más antiguo que ha estado operando en la Antártida desde su creación en 1903. El mismo, se localiza en la Isla Laurie, de las Islas Orcadas de Sur en la Antártida Argentina. Sus coordenadas Geográficas son 60° 44´16´´ S 44° 44´24´´ W y su altura es de 3 msnm.

En este Observatorio se miden ininterrumpidamente parámetros geomagnéticos que muestran la evolución y el comportamiento de una región situada cerca del polo magnético y lejos de las perturbaciones antropogénicas.

Al principio, la instrumentación utilizada en el Observatorio Orcadas era analógica. Desde 2012, se ha instalado el sistema INDIGO (Observatorio Geomagnético Digital de Intermagnet) para actualizar y digitalizar las mediciones. En el 2013, el Observatorio fue aceptado como miembro de INTERMAGNET (Red Magnética Internacional en Tiempo Real).

La estación Magnética Cipolletti se ubica en la ciudad de Cipoletti provincia de Río Negro, comenzó a operar en el año 2015. Dicha ciudad se localiza en un sitio de interés geomagnético y geológico, en una zona precordillerana donde la explotación de recursos naturales (gas, petróleo y minerales), es la actividad económica principal de la región. Por lo tanto, el registro obtenido es de fundamental importancia en los estudios de prospección de las industrias de petroleras y/o mineras.

El instrumental se localizó en un lugar en donde se encuentra protegido del viento y del sol, cuyas coordenadas son 38º56,45'S, 67º58,7'W. Desde el momento en que se instaló, se comenzaron a registrar valores de referencia del Campo Magnético Terrestre. Por el transcurso de casi un año, en conjunto con el área de Geomagnetismo de la UNLP, los datos obtenidos fueron validados con registros del Observatorio Geomagnético de Trelew, por ser el más cercano a la estación.

Los resultados arrojaron que el lugar era el adecuado para el registro de Intensidad del CMT (F).

INSTRUMENTAL

Los distintos observatorios cuentan con instrumental apropiado para el funcionamiento operativo de los mismos.

Magnetómetro Protónico

El magnetómetro de precesión protónica (ppm) (Fig.2) es así llamado porque utiliza la precesión de los spines protónicos, o núcleo del átomo de hidrógeno en el caso de un hidrocarburo o agua, para medir la intensidad total del campo magnético terrestre. Los spines protónicos del agua, alcohol, etc. se comportan como pequeños dipolos magnéticos. Estos dipolos son temporalmente alineados y polarizados mediante la aplicación de un campo magnético uniforme generado por una corriente en una bobina. Cuando se corta la corriente, el spin de los protones hace que estos precesen alrededor de la dirección del campo magnético de la Tierra.

Fig. 2 Magnetómetro de precesión protónico

Magnetómetro triaxial fluxgate

Este magnetómetro permite el registro simultáneo de las tres componentes, declinación (D) y las componentes, horizontal (H) y vertical (Z) del campo magnético de la Tierra. Las mismas, se registran cada 5 segundos y un minuto con una resolución de 0,1 nT. (Fig. 3) Mide la magnitud y la dirección del campo magnético de la Tierra. El dispositivo consta de dos núcleos ferromagnéticos rodeados por dos bobinas de alambre. Cuando el magnetómetro está activo, la corriente alterna pasa a través de una de las bobinas (la bobina), creando campos magnéticos inducidos de diferentes intensidades. Estos, generan una corriente eléctrica en la segunda bobina (bobina de detección), que luego se puede medir. La exposición a variaciones en el campo magnético de la Tierra provoca variaciones en los campos magnéticos de los núcleos ferromagnéticos y de alta permeabilidad magnética. Produciendo en estos, un flujo magnético. Si se hace variar la permeabilidad del núcleo, variará su flujo, como consecuencia se inducirá un voltaje en el arrollamiento receptor que proporciona unas medidas del campo externo. El funcionamiento del magnetómetro está, por tanto, basado en la variación con el tiempo de la permeabilidad del núcleo.

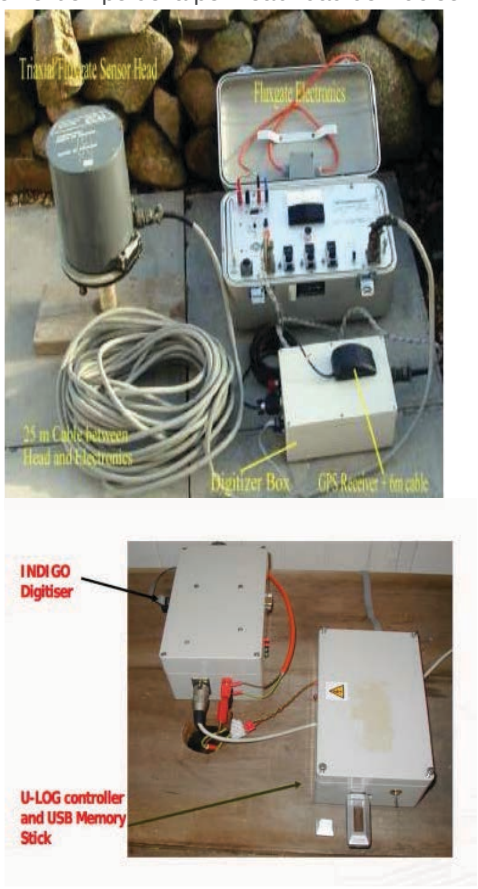

Fig. 3 Variometro y sus componentes

Teodolito

El teodolito convencional es el instrumento utilizado para determinar posiciones midiendo dos ángulos, uno horizontal (azimut) y otro vertical (altura).Éste está construido en material antimagnético y por tanto se podría utilizar para medir la declinación, acoplándole una aguja magnética (Fig. 4.

De esta manera se obtendría valores absolutos de la Declinación e Inclinación magnética en un determinado espacio y tiempo.

Fig 4. Teodolito

SISTEMA INDIGO Y OBSERVATORIOS MAGNÉTICO OPERATIVOS

Este sistema proporciona el hardware y el software para operar un Observatorio Magnético Digital básico. El hardware consiste en un magnetómetro triaxial fluxgate, un magnetómetro protónico, un Digitizador, un receptor GPS para proporcionar el tiempo exacto, un registrador de memoria USB y una fuente de alimentación DC alimentada por batería.

El software INDIGO WATCH captura los datos del magnetómetro digitalizado, registra en el disco y realiza el análisis de datos básicos. Los datos se registran cada 5 segundos del fluxgate y ppm, los mismos se almacenan en archivos diarios individuales usando el software INDIGO WATCH montado una PC (Fig 5.). Se generan valores medios de las componentes medidas cada 1 minuto los cuales se registran en el USB Logger.

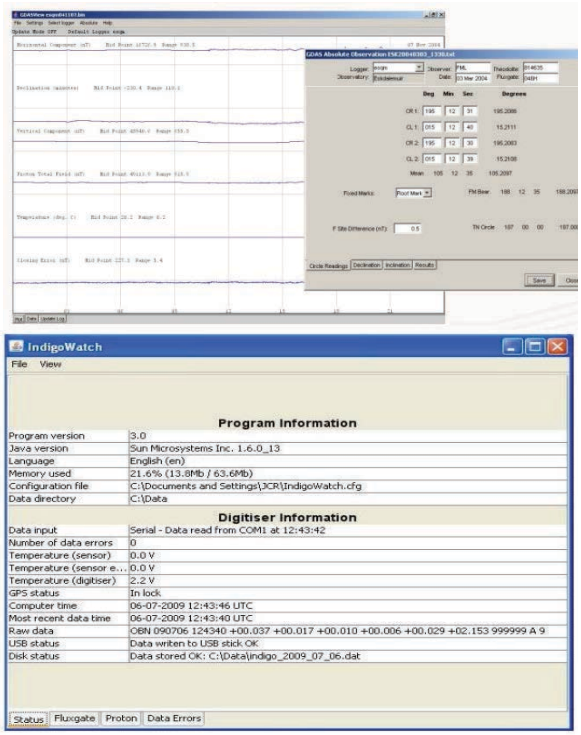

Fig. 5 Software utilizado

Los Observatorios de Pilar y Base Orcadas operan con Geomagnetic Data Acquisition System (GDAS) (Fig 5), el mismo fue desarrollado por la British Geological Survey (BGS). El INDIGO Watch registra las variaciones de las componentes del campo magnético, pero no los valores absolutos. Diariamente un Operador realiza más de una observación absoluta. Éstas son mediciones con el Teodolito Magnético que porta un sensor Fluxgate en la parte superior del mismo. Con él se obtienen datos de Declinación e Inclinación. Las observaciones absolutas conjuntamente con los datos obtenidos por el Sistema Indigo, se procesan en el software (GDAS), y producen un registro continuo de los **valores absolutos del campo magnético.**

Por su parte, la Estación Magnética Cipolletti (Fig.6), cuenta solo con un Magnetómetro Geometrics G856, con administración de energía externa. Las baterías utilizadas no afectan el registro magnético, las mismas son de gel, de 12v/7A o 12v/12A, y poseen una autonomía de 2 a 3 semanas aproximadamente.

El registro óptimo del sistema es cada 5 minutos a diferencia del sistema INDIGO de los Observatorios de Pilar y Orcadas que manejan intervalos de medición de 1 minuto. Los datos son almacenados en la memoria del equipo. Por lo que, cada 10-14 días aproximadamente, la serie de datos es descargada a una computadora y la batería intercambiada.
En gabinete los datos son procesados en una planilla Excel y validados constantemente con los registros de F de la red de Observatorios del país. Se obtienen promedios horarios, mensuales, y anuales. Luego se calculan, utilizando los días calmos establecidos por la IAGA, las curvas de variación diurna para cada mes de registro, y se comparan estos resultados con un índice de actividad geomagnética local, en formatos horarios,

trihorarios o diarios.

Fig. 6. Estación Cipolletti

INTERMAGNET

INTERMAGNET es una red mundial de Observatorios Magnéticos que operan casi en tiempo real. Existen varios nodos de información geomagnética (GINs) que son utilizados por todos los observatorios del mundo de la red INTERMAGNET para compartir los datos generados por cada uno de ellos. Cada observatorio, como los del SMN, adopta ciertos estándares para las mediciones geomagnéticas y para el monitoreo del equipamiento y transfiere información rápidamente al GINs (Geomagnetic Information Nodes). Esto es posible gracias a los satélites y a las comunicaciones en red. Estos nodos de información geomagnética recogen datos desde su posición en el globo para su difusión a la comunidad en forma oportuna. GINs puede, cuando sea necesario, intercambiar información y también puede difundir productos tal como índices geomagnéticos y modelos de actividad. En septiembre de 2012, el Observatorio Magnético Pilar fue aceptado como miembro de INTERMAGNET y las mediciones magnéticas generadas con el Sistema INDIGO en el Observatorio de Pilar, son reportadas diariamente a Edinburgo GIN.

http://www.intermagnet.org/

MAS DE 100 AÑOS DE REGISTRO

Los registros diarios de más de 100 años de los Observatorios argentinos han permitido visualizar el descenso en la Intensidad del CMT lo cual se correlaciona con la intensificación de la Anomalía del Atlántico Sur, como puede observarse en los mapas del modelo IGRF.

En todas las componentes, el CMT se comporta de manera similar para los observatorios de Pilar y La Quiaca, presentando variaciones anuales semejantes pero con diferencia en su escala de valores. En cambio, los registros en Orcadas del Sur a través de los años, muestran diferencias con respecto a los otros Observatorios.

En Orcadas la Intensidad F disminuye linealmente con una pendiente mayor que en los demás puntos de medición, lo que se puede vincular al correspondiente avance de la AMAS en esa región (Fig. 7).

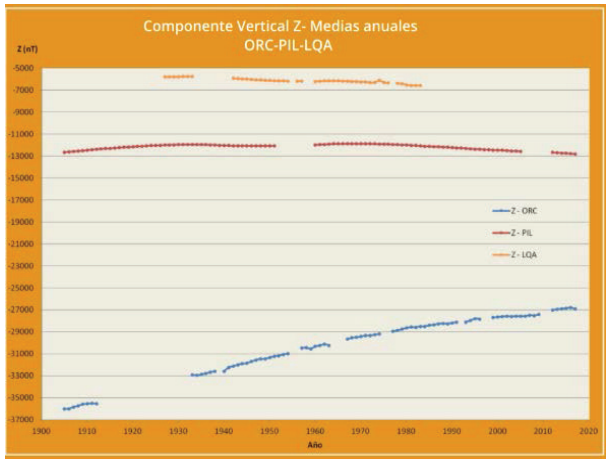

Fig. 7. Intensidad Total F

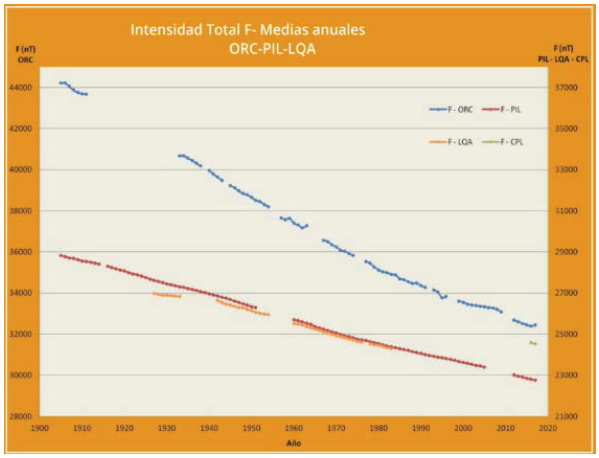

Fig 8. Componente vertical Z

Se destaca también el pronunciado aumento de su componente Z con respecto a Pilar y La Quiaca.(Fig.8)

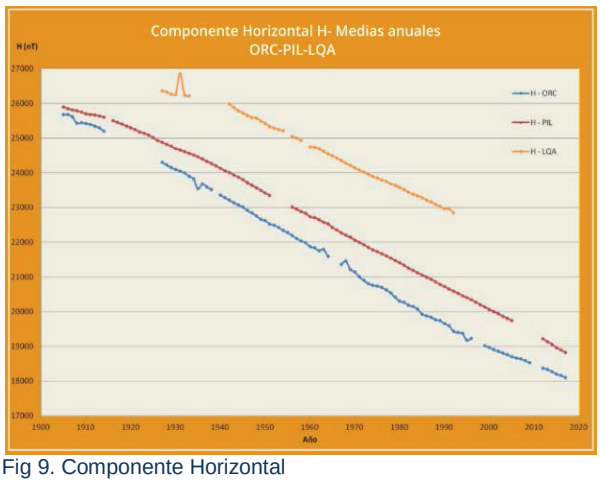

Fig 9. Componente Horizontal

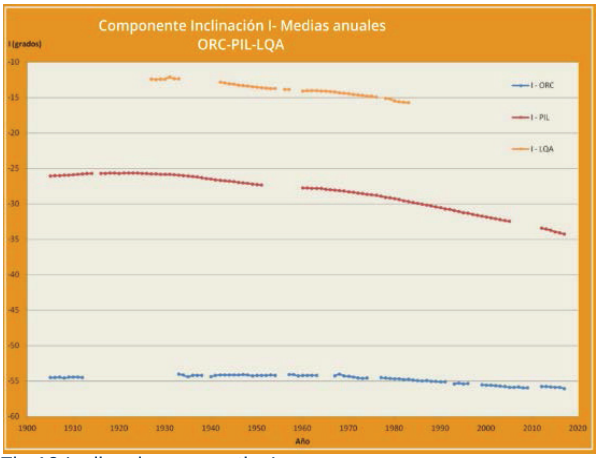

Fig 10.Inclinacion magnetical

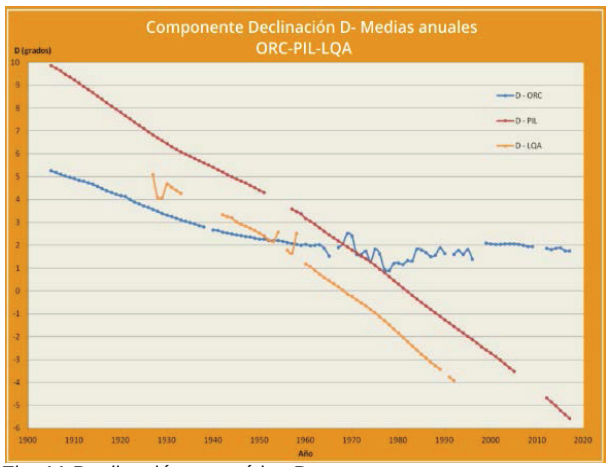

Fig. 11 Declinación magnética D

Pero lo más notable es cómo allí la Declinación se mantiene positiva cuasi constante durante aproximadamente los últimos 50 años, (Fig. 11) a diferencia de los Observatorios que se encuentran en el centro y norte del país, que con los años toman valores negativos (en 1968 La Quiaca y 1982 Pilar).

La diferencia en los sentidos de la componente D se evidencian en el modelo IGRF 2015 donde se ve que la curva isógona 0 pasa por encima de la ubicación del Observatorio Orcadas, manteniendo las mediciones de D positivas, a diferencia de Pilar y La Quiaca que se encuentran entre isógonas de valores negativos

TORMENTA MAGNÉTICA SEPTIEMBRE 2017

Durante el mes de Septiembre el Sol tuvo una actividad significativa sobre el CMT, emitiendo Fulguraciones Solares (flares) y Eyecciones de Masa Coronal (CME) clasificadas como las más grandes de este ciclo solar 24 que comenzó en enero de 2008. Estos eventos pueden relacionarse con las formas de la curva presentes en los magnetogramas de los distintos observatorios geomagnéticos instalados en todo el planeta. Nosotros haremos hincapié en los Observatorios del Servicio Meteorológico Nacional. El día 4 de Septiembre a las 20:33 UTC se produjo una fulguración de categoría M5.5
23:09 UTC. La componente Bz se mantuvo mayormente al norte para este evento con menores fluctuaciones de hasta -10 nT.El día 6 la misma región efectiva, continúa

(R2- Moderado) en la región activa 2673. Dicha fulguración finalmente formó una eyección de masa coronal completamente geoefectiva, observada por primera vez en imágenes SOHO / LASCO C2 a las 20:48 UTC. El 6 de septiembre se observó la primera de dos CME que se presentan en estos días. La primera CME, asociada con la llamarada M5 del 04 de septiembre, se observó por primera vez al atravesar el satélite DSCOVR a las 06/2308 UTC. El campo total aumentó a 16 nT a las 23:24 UTC y el viento solar aumentó a un máximo de 610 km /s a las

su alta actividad, generando una nueva fulguración severa X 2.2 y otra más tarde de X9.3 (R3-Extrema) que ocurrió a las 12:02 UTC. Esta también, trajo asociada

una CME, observada por primera vez en las imágenes SOHO / LASCO C2 a las 12:24 UTC.

Luego, el 07 de septiembre, la segunda CME llegó al satélite DSCOVR aumentando aún más el campo total, hasta un máximo de 34 nT a las 22:54 UTC, mientras que durante casi 5 horas la componente Bz apuntaba hacia el sur, alcanzando un máximo de -32 nT. El viento solar aumentó hasta un máximo de 842 km/s el día 08 de septiembre a las 08:48 UTC, antes de disminuir lentamente a cerca de 530 km/s hacia el 10 de septiembre.

Durante los últimos minutos del 7 de Setiembre, llegaba el roce directo de la eyección de masa coronal producida por la fulguración de categoría X9.3 producida el día 06 y en pocos minutos el campo magnético terrestre se alteró de tal manera que generó una tormenta geomagnética de nivel KP8 (G4) cual se mantuvo durante todo ese día.

NUESTROS REGISTROS

En los distintos observatorios se pudieron registrar estos importantes eventos (Fig. 12). La llegada de la fulguración el día 6, fue registrada casi instantáneamente (12:00 UTC). Por otro lado, el día 7 se constató la llegada de la CME perturbando las diferentes componentes fluctuando sus valores entre máximos y mínimos que difieren en 100nT aproximadamente. Dicha perturbación se extendió hasta el día 8 (Fig. 13).

Todos estos registros a su vez, fueron correlacionados con gráficos de Índices Kp, flares y viento solar obtenidas de la NOAA www.swpc.noaa.gov y de https://www.spaceweatherlive.com

Agradecimientos: La autoras expresan sus agradecimientos a Gil Ma. Inés y Ricci Silvana, del Área Geofísica del Servicio Meteorológico Nacional, por las contribuciones aportadas en la realización de éste reporte final.

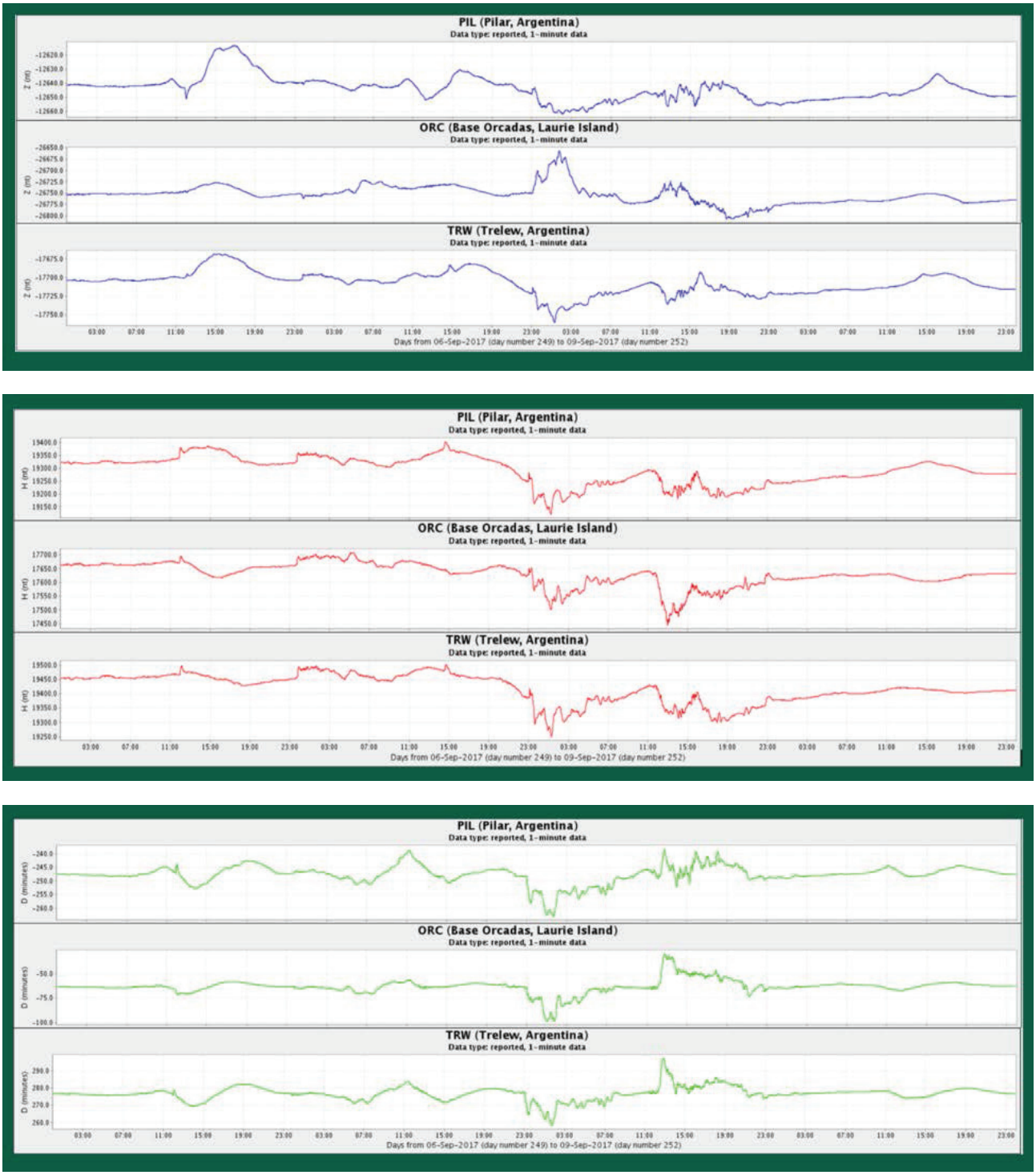

Fig. 12 Componente horizontal H, Componente vertical Z y la Declinación que muestran la perturbación debido a la Tormenta Magnética en Septiembre 2017.

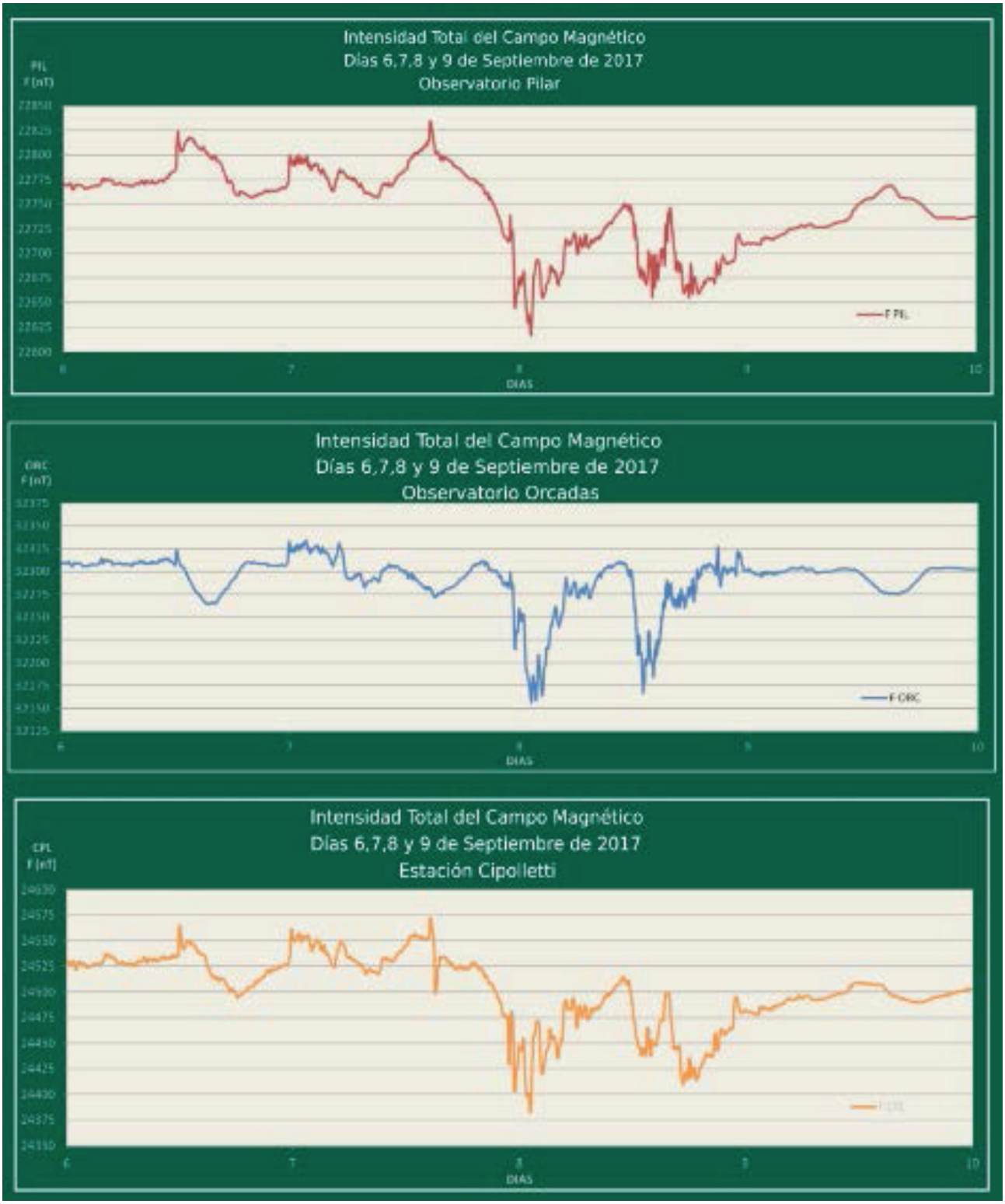

Fig 13. Registros de la Intensidad Total de Campo Magnético de los Observatorios de Pilar, Orcadas y Estación Cipolletti.

Using Magnetograms to Understand and Probe the Magnetosphere

Yvelice Castillo [1,2,3], M. Alexandra Pais [1,3], P. Ribeiro [1], João Fernandes [1,4], Anna L. Morozova [1], Fernando J. G. Pinheiro [1]

[1] CITEUC, Geophysical and Astronomical Observatory, University of Coimbra, 3040-004 Coimbra, Portugal; [2] Department of Astronomy and Astrophysics, National Autonomous University of Honduras; [3] Department of Physics, University of Coimbra; [4] Department of Mathematics, University of Coimbra. yvelicesoraya@gmail.com

Abstract

Recently, we tested Tsyganenko and Sitnov (2005) semi-empirical magnetospheric model (TS05) to evaluate how well its predictions could reproduce ground geomagnetic observations. The comparison was made at four Northern Hemisphere mid-latitude stations, including Coimbra (COI), Portugal, Panagyurishte (PAG), Bulgary, Novosibirsk (NVS), Russia, and Boulder (BOU), USA. We applied a statistical analysis on observatory and simulated hourly mean values of horizontal components (X, Y) for the 2007–2014 period (covering the long minimum of solar activity around 2008 and the rising phase of solar cycle 24).

Discussion:

In our study we observed that the TS05 model produces good estimates of the X geomagnetic activity at the four tested stations during more active days, with a percentage of ~50% showing correlation coefficient r > 0.7 between the observatory values and TS05 estimations. This percentage decreases to ~30% for the Y component. In these conditions, and although the TS05 model was aimed to predict the magnetospheric field at geosynchronous and high orbit satellites, our results strengthen the idea that the TS05 model can be used to successfully predict ground measured X component during geomagnetically active days, and, with some improvement, to also predict Y component.

A major advantage of the TS05 model is its modular structure, which allows to derive the possible configurations of magnetospheric sources contributing to the time variability of the geomagnetic field during periods of high activity and storms. Our analysis showed that the observed time variations of horizontal X component can be mostly explained by the tail, symmetric and partial ring currents, while the partial ring and field aligned currents contribute most to the time variability of Y.

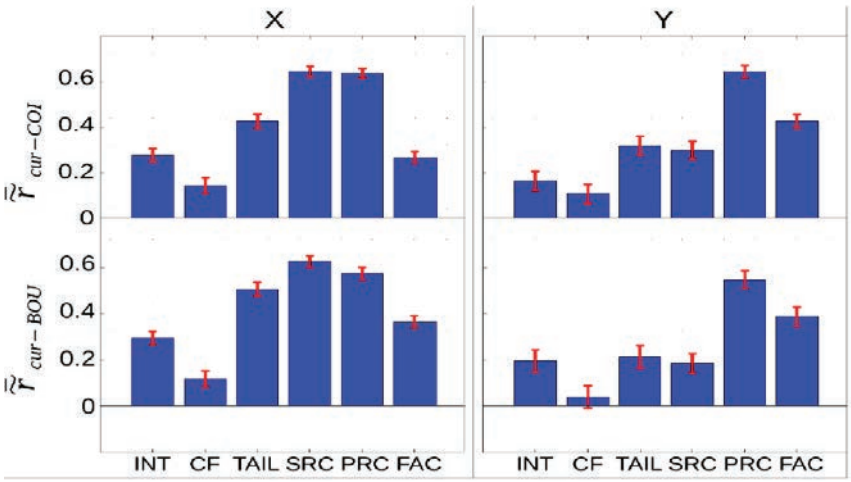

Figure 1. Mean values of correlations coefficients between data and each individual current (), in active days with r ≥ 0.7. X component at the left and Y at the right. COI station at the top and BOU station at the bottom. INT: penetration of the interplanetary magnetic field into the magnetosphere; CF: chapman-ferraro current: TAIL: cross-tail current; SRC: symmetric ring current; PRC: partial ring current; FAC: field-aligned currents.

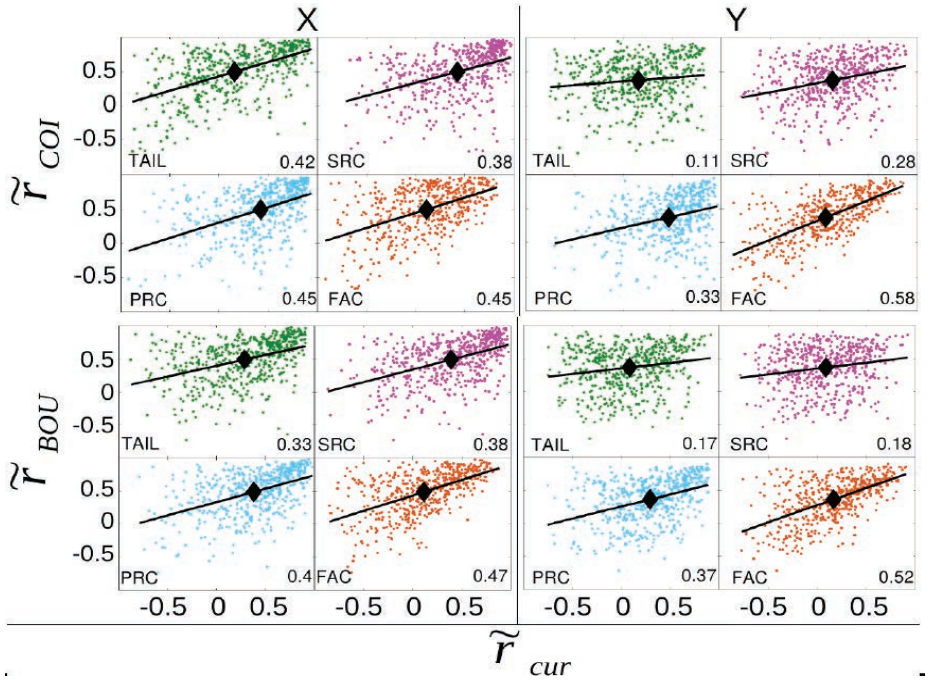

Figure 2. Scatter plots of r against the correlation coefficients between data and each current (). X at the left and Y at the right. COI at the top and BOU at the bottom. These plots represent the sensitivity of r to each current. Values of the slope, as inset. Black diamonds mark the location of the cloud center-of-distribution.

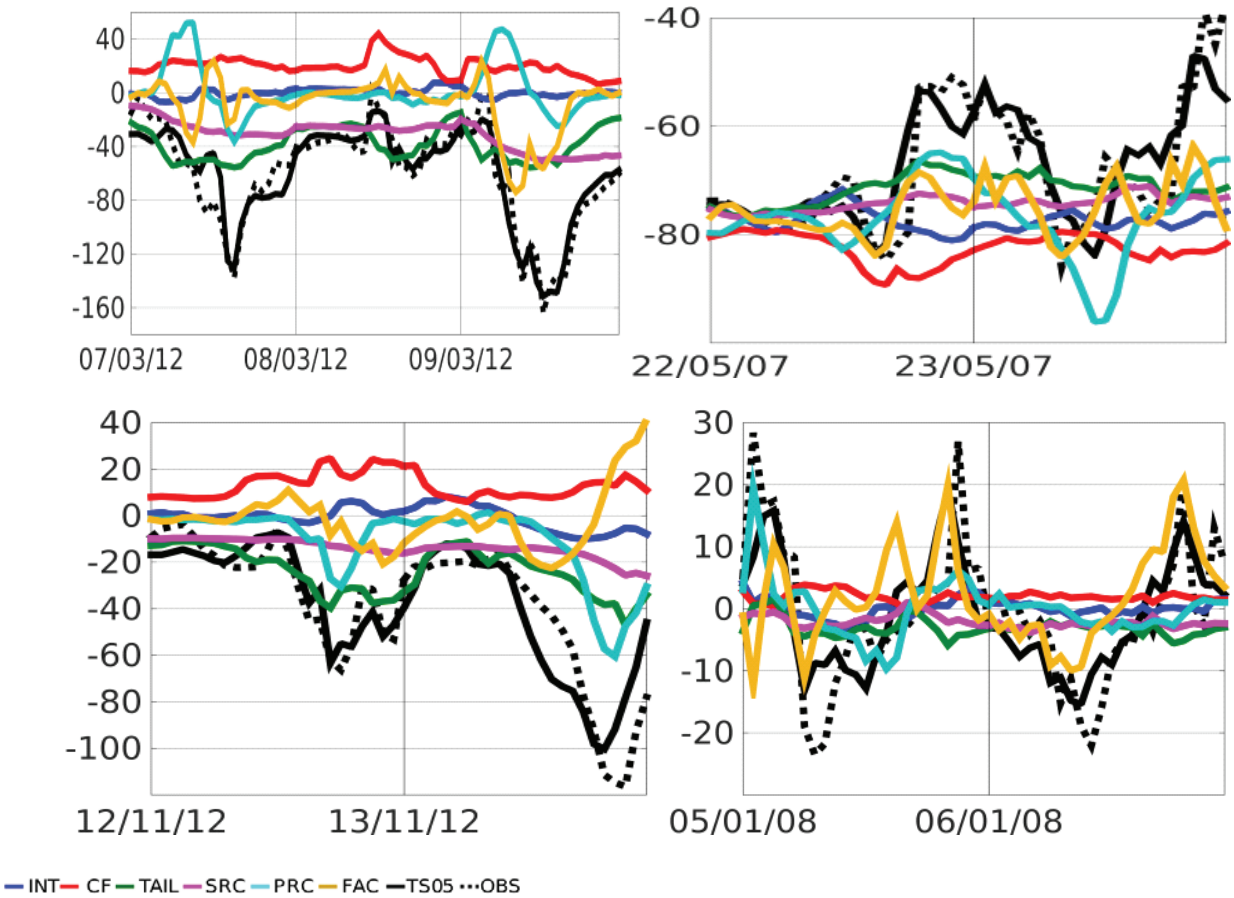

Figure 3. Case examples of daily series in more active days (K ≥ 4) when TS05 simulations perform the best (r ≥ 0.7). COI at the top and BOU at the bottom. X at the left and Y at the right. Data (black dotted lines) is shifted and scaled in order to compare with estimations from TS05 (black solid line). Separate results for X (left) and Y (right) series. Colored lines represent individual contributions from different current sources (see legend).

Conclusions

1. TS05 model produces good estimates of the X geomagnetic activity at the four tested stations during more active days, with a percentage of ~50% showing correlations r ≥ 0.7. Results are clearly worse for the Y component, with a percentage of ~ 30% of the total number of geomagnetically active days with correlation values of r ≥ 0.7. The closing of field aligned (FAC) currents through the Earth's center in the TS05 model can be the reason for the lower performance in Y predictions.

2. During more active days, all tail, symmetric ring and partial ring currents contribute to the time variability of X while the partial ring and field aligned currents contribute most to the time variability of Y (as seen on Fig. 3).

3. The tail and symmetric ring currents are main contributors to the magnitude of X, both during quiet and disturbed days. The field aligned and partial ring currents have a higher relative contribution for the Y than for the X component magnitudes.

Acknowledgements

CITEUC is funded by National Funds through FCT - Foundation for Science and Technology (project: UID/Multi/00611/2013) and FEDER - European Regional Development Fund through COMPETE 2020 Operational Programme Competitiveness and Internationalization (project: POCI-01-0145-FEDER-006922).

Yvelice Castillo's Ph. D. thesis related to this poster was funded by a grant in the Erasmus Mundus Action 2 Consortium AMIDILA, Lot 15 – strand 1, 2013-2588/001-001-EM Action 2 Partnerships.

References

Castillo, Y., Pais, M.A., Fernandes, J., Ribeiro, P., Morozova, A.L., Pinheiro, F.J.G. 2017. Geomagnetic activity at Northern Hemisphere's mid-latitude ground stations: How much can be explained using TS05 model. Journal of Atmospheric and Solar-Terrestrial Physics. Vol 165-166. Pag. 38-53. DOI: 10.1016/j.jastp.2017.11.002. ISSN: 1364-6826. http://www.sciencedirect.com/science/article/pii/S1364682617303668

Precursors of Disturbed Geomagnetic Conditions.

D.V. Blagoveshchensky[a], M.A. Sergeeva [b,c], A. Kozlovsky[d], P. Corona-Romero [b,c,]*

[a]Saint-Petersburg State University of Aerospace Instrumentation, 67, Bolshaya Morskaya, Saint- Petersburg, 190000, Russia
[b]LANCE, SCiESMEX, Instituto de Geofisica, Unidad Michoacan, Universidad Nacional Autonoma de Mexico, Antigua carretera a Patzcuaro 8701, Morelia, Michoacan, C.P.58089, Mexico.
[c]CONACYT, Instituto de Geofisica, Unidad Michoacan, Universidad Nacional Autonoma de Mexico, Antigua carretera a Patzcuaro 8701, Morelia, Michoacan, C.P.58089, Mexico. [d]Sodankylä Geophysical Observatory of the University of Oulu, Tähteläntie 62, FIN-99600 Sodankylä, Finland

We studied the ionospheric processes before, during and after magnetic storms and substorms to reveal ionospheric precursors that can be used to forecast geomagnetic disturbances beginning at high latitudes. Data from Sodankylä Geophysical Observatory was used (geomagnetic coordinates: 64.1oN, 119.2oE). In earlier works the Main Effect (ME) was revealed for substorms. It consists of the following steps: (a) the increase of critical frequency foF2 from its quiet median before and during the substorm growth phase, four-five hours before To moment that is the moment of the expansion phase onset, (b) the foF2 decrease to the level lower than its median just after To and until Te that is the moment of the end of the expansion phase, (c) the issue “a” repeated during the recovery phase (d) two bell-shape spikes in the cutoff frequency values foEs: first spike occurs three hours before To, second spike – during the expansion phase within the interval between To and Te. In the present study we revealed that the similar ME takes place in the case of magnetic storms but within the different time scale. We show how ME manifestations can be used as precursors of magnetic substorms and storms at high-latitudes (geomagnetic latitudes 50oN – 65oN).

Transient Phenomena into the SAMA during Geomagnetically Active Times: Solar Cycles 23 and 24 Case

Ramón Caraballo MSc.[1,3] , Dra. Leda Sánchez Bettucci[2,3]

[1] *Facultad de Ingeniería - Universidad de la República.*

[2] *Facultad de Ciencias - Universidad de la República.*

[3] *Observatorio Geofísico del Uruguay.*

Abstract

The south Atlantic Magnetic Anomaly (SAMA) constitutes an unique feature of the main field due to its eccentricity with respect of the Earth's center. As the main field magnetic moment decreases the SAMA continues drifting westward and increasing its area. The weakened magnetic field, (c. 23000 nT) acts like a sink for particles trapped into the inner radiation belt. Of those particles, the electrons by its small size penetrate deeply into the atmosphere where they suffer pitch angle scattering due to collision with neutrals. Since the proton precipitation variability has been studied, electron precipitation impact on the high atmosphere is not well understood yet. The present study intends to provide an outlook intending to assess the actual impact of electron precipitation on the geomagnetic variability in the SAMA area. Wavelet transform and Wavelet coherence analysis were performed to compare electron fluxes and geomagnetic H component records during two of the major magnetic storms of the solar cycle 23 and 24.

Additionally geomagnetic records of Vassouras and Trelew magnetic observatories were compared with registers of two observatories outside the SAMA to compare the degree of coherence between the H-component and precipitation flux signals.

The results suggest a certain degree of correlation between low frequency transients into the H component and electron precipitation flux detected by the MEPED instruments onboard the NOAA/POES satellites. An unexpected high coherence between both signals was obtained during the wavelet coherence analysis (WCO). On the other hand, some constant phase islands in the WCO spectra suggest a large scale correlation.

Keywords: Geomagnetic Activity, Rapid Time Variations, Particle Precipitation, South Atlantic Anomaly.

Introduction

As the South Atlantic Magnetic Anomaly (SAMA) continues drifting and passing over South America it leads to a unique opportunity to study some phenomena which can contribute to increase the geomagnetic variability at short time scales during geomagnetic active times. The SAMA constitutes a particular feature of the main field due to its weak intensity. The weak field acts as a sink for trapped particles from the inner radiation belts. Particle precipitation, mainly protons, electrons and cosmic rays in the range of few keV up to several MeV, has been observed as a relevant phenomenon inside the SAMA area [Asikainen & Mursula 2005, 2008]. The enhanced particle fluxes at the SAMA result harmful for electronic devices on board satellites at low orbits and constitutes a direct biological threat for human space activities close to Earth.

The SAMA can be ascribed to the eccentricity of the Earth's magnetic dipole by ca. 550 km off Earth's center. The anomaly has been drifting c.a 0.3º/yr [Badhwar 1997], and expanding its area which currently cover the main part of South America. In this way, the SAMA temporal evolution is close related with the temporal evolution of the higher order multi polar components of the main field [Hartmann & Pacca 2009]. If this trend continues, it is expected to have a very low field intensity zone covering the South Atlantic Ocean and South America at the beginnings of the XXII century [Heirtzler 2002] .

Solar protons and cosmic rays can penetrate deeply into the atmosphere in this area (at heights as low as 60 km), increasing the risk of radiation exposition on flight crews Fig. 1. But all these particles impinging into the high atmosphere can produce distortions into the physics and chemistry of ionosphere and mesosphere.

The electron precipitation contributes to the formation of OH^- and NO_x radicals which contribute to ozone destruction at mesospheric heights [Callis et al. 1991]. Such phenomena result more significant during the geomagnetic storms.

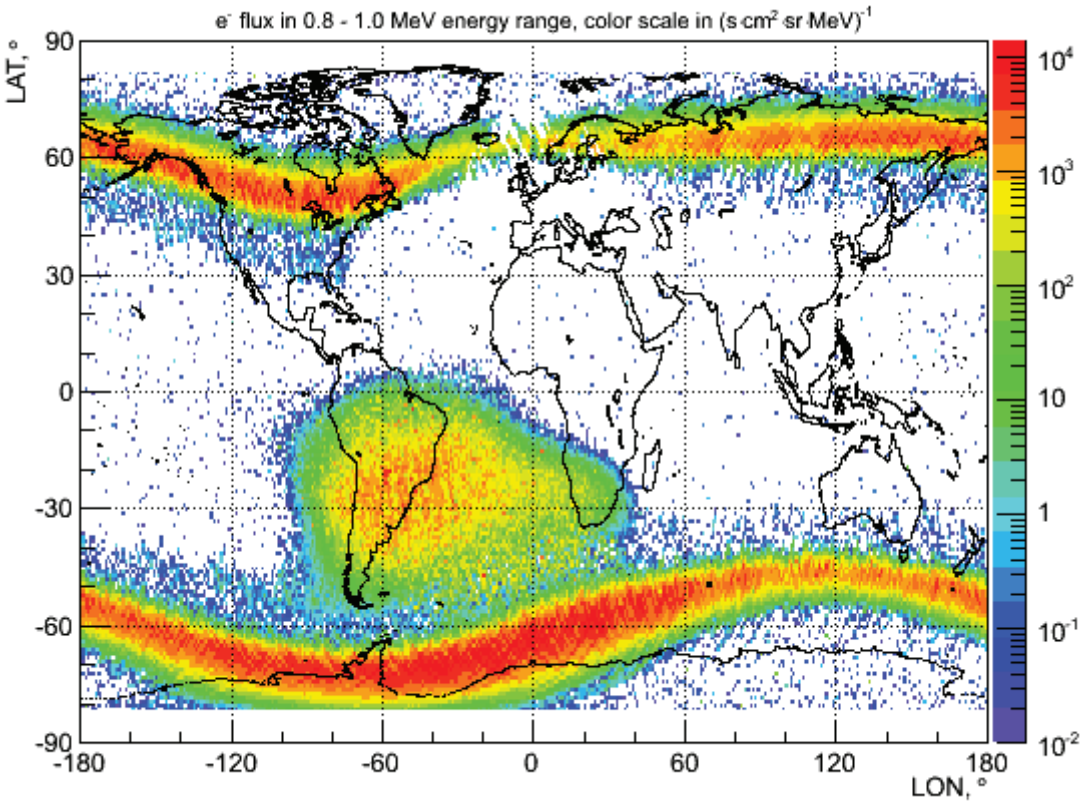

Figure 1: Electron precipitation in the range of 0.8 – 1.0 MeV. The central feature corresponds to precipitation into the SAMA. Particle precipitation at the SAMA is the most relevant phenomenon between +30 and -30 geomagnetic latitudes. Courtesy: **:** SPENVIS, NASA.

As the main field continues decreasing inside the SAMA, more particles from the inner radiation belt will precipitate as a result of the broadening of the trapped particles loss cone. This will enhance the risk of radiation exposure on crews and equipments in flight through this area.

In this way, the SAMA shares some unique features with the auroral zones where the particle precipitation plays an important role regarding the energy influx into the ionosphere.

Despite the anomaly's continuous increase in its geographical extent, little insight have been provided in such processes and its possible impact into the local ionosphere. The conditions in the ionosphere can determine the local geomagnetic variability, particularly during periods of strong geomagnetic activity. The former constitutes the main reason to study short time transients that could increase the geomagnetic activity into the area and enhance the space weather effects on the human activities.

The transient temporal scale ranges from seconds to several minutes. Phenomena related to rapid time variations: Sudden impulses, pulsations, geomagnetically induced currents (GIC), etc. Ionospheric ionization enhancements have been ascribed to particle precipitation events into the SAMA at disturbed times [Pinto et al. 1990a,b]. Several studies since the 60's, focused mainly on particle precipitation. But the main question is: what is the particle precipitation leverage on the local geomagnetic variability?.. If there is one.

This study constitutes an initial approach to answer this question and lot of work has to be done to provide a definitive explanation.

Methodology

We started to analyze the geomagnetic data available for the observatories located into the SAMA area during two of the major storms occurred during the solar cycle 23 and 24. Specifically looking for transitory phenomena which could contribute to enhance the geomagnetic disturbances in the area that can lead to the generation of the strong geoelectric fields on the Earth`s surface. As the magnetosphere-ionosphere system behaves in a very complex way, wavelet spectral analysis (WT) was used to study the geomagnetic time series during the major events during solar cycles 23 and 24 respectively. Additionally a detailed analysis of particle precipitation data from the POES observational satellites as it passes over the SAMA was performed in order to estimate the impact of the precipitation influx into the ionosphere and in the consequent local magnetic activity. The NOAA/POES program is a long term projects which dates back to 70`s and maintains a large collection of data related to the near Earth environment. POES satellites are located in sun-synchronous orbits with an inclination ca. 90º at 840 km above the Earth`s surface and an orbital period of 101 min. Each POES satellite passes at the same local time by each longitude sector.

All these satellites are equipped with the MEPED SEM-1/2 instrument to measure electron and proton fluxes in two perpendicular directions. MEPED can detect protons in six energy channels from 30 keV up to E > 6900 keV and electrons in three energy channels covering an energy range from 30 keV to > 2500 keV. Almost all electron telescopes are sensible to cross contamination by protons in the range of 210 – 2700 keV.

Despite that proton flux variability has been studied in the past [Zou et al. 2015], electron precipitation effects into the SAMA are not well understood yet. Moreover, there is some evidence of their influence into the geomagnetic variability [Jayanthi et al. 1997a] .

Horizontal component H from Vassouras and Trelew magnetic observatories and integral electron precipitation data were analyzed.

In this way, wavelet power spectrum of the H component measured at the Vassouras and Trelew magnetic observatories during two of the most intense events for the solar cycle 23 and 24 namely, the Halloween Storm on 29-31 October 2003 and the 8-10 March 2012 storm.

An additional wavelet coherence analysis (WCO) was performed for magnetic data from each observatory and other two located in Australia approx. 180º off the SAMA longitude sector in order to compare the similarities and possible teleconnections between electron flux and H variations at all sites. The coherence is a measure of the similitude of two signals and it is bounded to the interval $0 < wco <\leqslant 1$, where $wco = 0$ implies no similitude and $wco = 1$ identity between both signals. In all cases 95% confidence significance test was used to ensure the reliability of each point of the spectrum.

The main challenge when working with satellite and geomagnetic datasets is to manage and convert data from several different formats to a common one more suitable to analyze it. In this case, 16s-means integral electron flux data from the MEPED instruments was converted to minute means centered on the minute using a gaussian filter. The output was electron integral flux data with the same sampling frequency as the magnetic datasets. Another difficult arose in the irregular and partial coverage for the satellites across the years. Moreover, each satellite performs 14 orbits by each solar day, leading to a poor global coverage.

To overcome this difficulty, we know that the SAMA covers a narrow latitudinal sector close to the magnetic equator. Hence, satellite data was considered only in a ± 30º latitudinal strip centered on the magnetic equator. Almost all particle precipitating at such geomagnetic latitudes comes from the inner radiation belt defined at $1.01 <\leqslant L <\leqslant 2.0$, being *L* the McIlwain's *L*-Shell parameter [McIlwain 1961]. Particles outside this strip are confined into higher *L*-Shells and precipitate mainly into the auroral zone. Another fact is that at low geomagnetic latitudes, particle precipitation into the SAMA longitudinal sector is several orders of magnitude higher than other locations (see Fig. 1). In this way, to workaround the problem of the lack of full coverage, all electron flux data was binned by *L*-shell and time in the interval defined by $(1.01 \leqslant< L \leqslant< 2.0) \times (1 <\leqslant t <\leqslant 4320)$ where the temporal window was centered on the magnetic storm commencement covering a total width of 4320 min (3 days)

Inside these data interval, particle precipitation into the SAMA is the most relevant phenomenon. Then, each three-day interval includes data from several passes through the anomaly. Data inside each bin was averaged and a posterior interpolation filled the gaps and provided a smooth dataset. This method avoids the use of running averages which is a common practice, but acts like a selective filter in frequency which is not desirable in transient analysis. Due to the intensity of the electron precipitation inside the SAMA precipitation contributions from outside the longitude sector of the anomaly does not contribute significantly to the averaging process inside the latitudinal strip.

Observations and Conclusions

Wavelet analysis of the H component variations measured at Vassouras and Trelew magnetic observatories for the events considered are shown on Fig.2. At first look, flux periodicities in the range of 10-64 min seem to correspond to a faint signal in the H spectrum close to the end of the storm commencement day. This could be a signature of low frequency Pc5 pulsations or ULF waves as reported in the past [Jayanthi et al. 1997a,b] . This feature is more visible in the case of the Trelew spectra for the March 2012 storm. Despite the high coherence, we can only suggest some association between the mean electron flux at $L \leq 2$ and H-component observed at the surface, but not more than that. During several instances the cross correlation analysis have shown significant results regarding large deviations in geomagnetic parameters which are in good agreement with particle precipitation episodes registered at L values such $1.01 << L << 2.0$. This suggests an interesting perspective to characterize several physical processes occurring in the anomaly region.

Wavelet coherence analysis (WCO) shown in Fig. 3 revealed some areas at lower frequencies where particle precipitation variations maintains a quasi-constant phase shift respect analogous variations in H component (black arrows).

The overall spectrum gives a high coherence in the background; a possible explanation of this feature is that we are observing ring current particles which at last, contribute to the modulation of the H-component. Regarding the phase difference between H-component and precipitation signals, the spectra at low frequencies looks more structured than at higher ones. In the plot, horizontal black arrows towards the right indicate in phase evolution, whilst pointing leftward, upward and downward indicates 180º, 90º and -90º out of phase respectively.

This is a very promising and unexpected result, considering the great complexity related with the two phenomena. Such features are robust to a change in the wavelet basis which ensures that is not an artifact of the WCO calculation process.

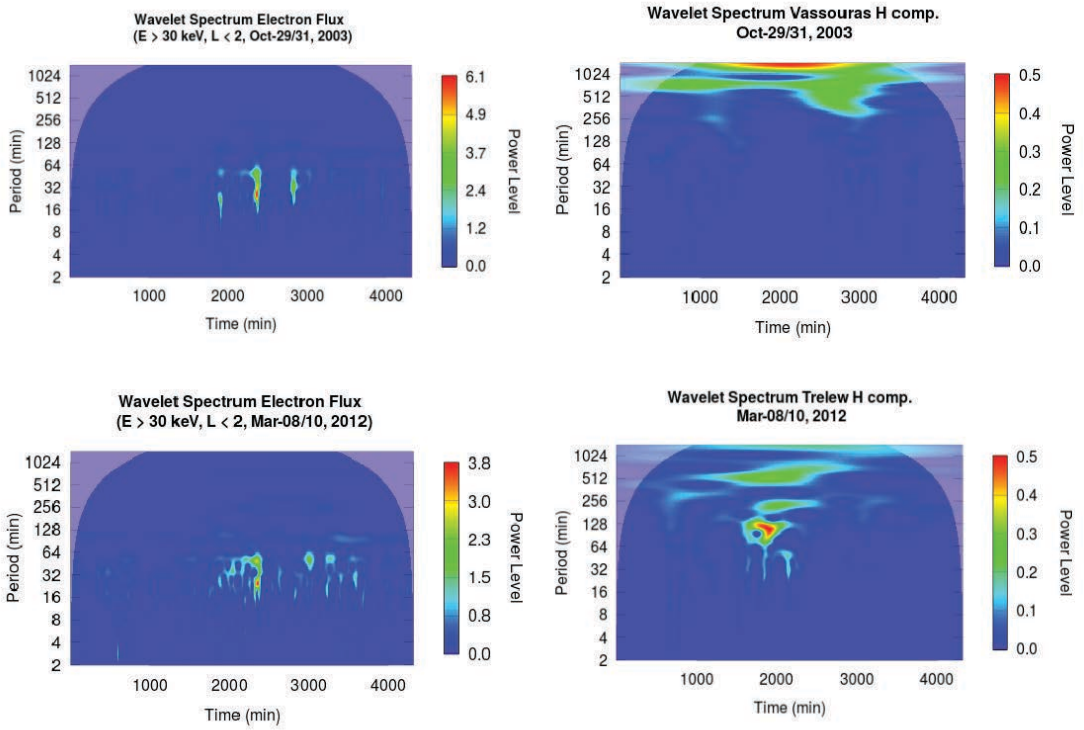

Figure 2: Wavelet Spectrum of electron precipitation flux and magnetic H-component during two great magnetic storms for Vassouras and Trelew magnetic observatories respectively. The central features suggest some correlation between long periodicity transients in H and electron fluxes during the day of the storm commencement (between 1440 and 2880 min.). This characteristic is more visible in the case of the Trelew record.

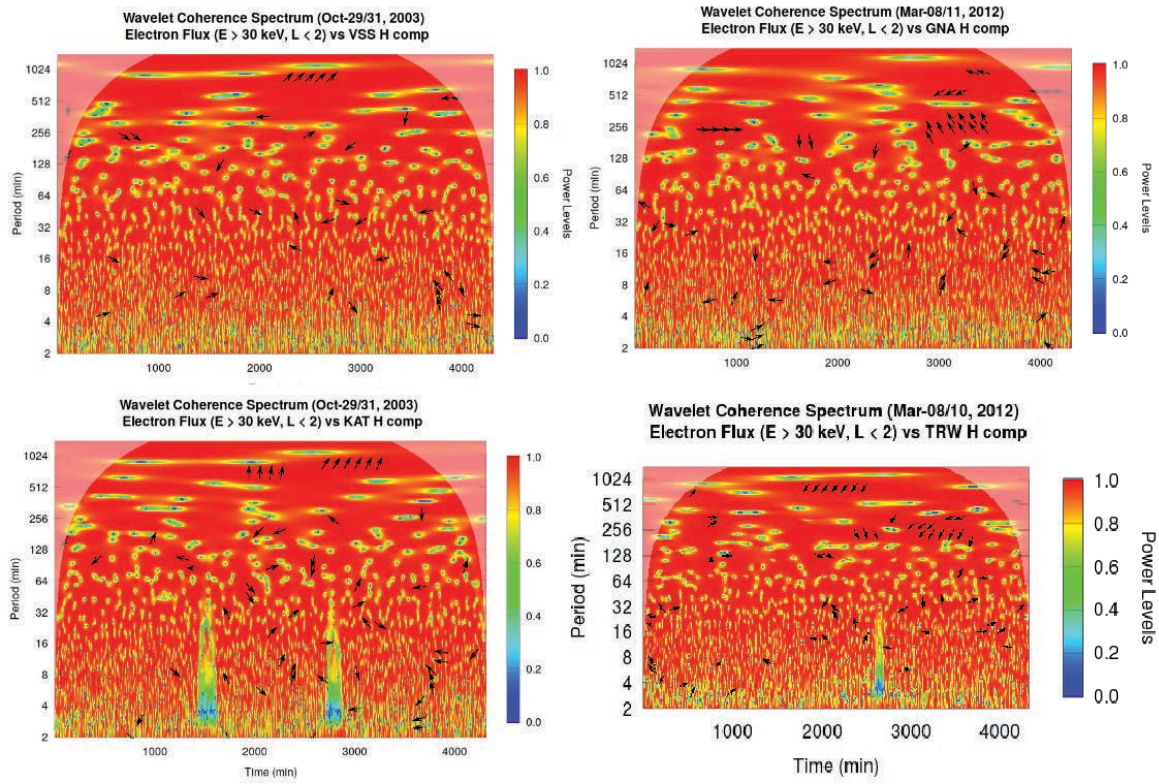

Figure *3*: Wavelet coherence spectrum from Vassouras and Trelew during the same magnetic storms and the comparison with the observatories magnetic records of Gnangara (GNA) and Katanning(KAT) 180 deg. Off the SAMA. The coherence is tested with the precipitation flux on each event. The central features on the low panel correspond to gaps in the time series. The black arrows point the phase shift differences between both signals. It is possible to appreciate some "islands" at low frequencies where the phase difference between both signals seems to be constant for some time. At higher frequencies the coherence is poor and phase difference tends to be chaotic.

Coherence spectra for data from observatories outside the SAMA appear quite "unstructured", when comparing with similar data from inside the SAMA. The strong phase variability at short periods suggests a association between both phenomena at short frequencies.

Lot of work is necessary to provide a good assessment of the transients inside the SAMA. We need to improve time resolution and increase the definition to resolve the fine grained structures hidden into the signal. Finally we need to extend the study to address all the storms of 23-24 cycles.

Acknowledgements

The authors wish to thank the invitation of the members of the organizing committee of the II Pan American Workshop on Geomagnetism as well as the opportunity to share experiences with colleagues more than a dozen of countries around the world during our stay in Vassouras. Also we gratefully acknowledge to SuperMag network and its partner institutions and to the NASA Space Physics Data Facility for offer freely all the magnetometer and satellite data.

References

Asikainen, T. and Mursula, K. (**2005**). *Filling the South Atlantic anomaly by energetic electrons during a great magnetic storm*, Geophysical Research Letters 32.

Asikainen, T. and Mursula, K. (**2008**). *Energetic electron flux behavior at low L-shells and its relation to the South Atlantic Anomaly*, J. Atmos. Solar-Terrestrial Phys. 70 : 532-538.

Badhwar, G. D. (**1997**). *Drift rate of the South Atlantic Anomaly*, Journal of Geophysical Research: Space Physics 102 : 2343-2349.

Callis, L. B.; Baker, D. N.; Blake, J. B.; Lambeth, J. D.; Boughner, R. E.; Natarajan, M.; Klebesadel, R. W. and Gorney, D. J. (**1991**). *Precipitating relativistic electrons: Their long-term effect on stratospheric odd nitrogen levels*, Journal of Geophysical Research: Atmospheres 96 : 2939-2976.

Hartmann, G. A. and Pacca, I. G. (**2009**). *Time evolution of the South Atlantic Magnetic Anomaly*, Anais da Academia Brasileira de Ciencias 81 : 243 - 255.

Heirtzler, J. R. (**2002**). *The future of the South Atlantic anomaly and implications for radiation damage in space*, Journal of Atmospheric and Solar-terrestrial Physics 64 : 1701-1708.

Jayanthi, U.; Pereira, M.; Martin, I.; Trivedi, N. and Lazutin, L. (**1997b**). *X-ray observations in the SAA - pulsations in electron precipitation accompanied by Pc4 events*, Advances in Space Research 20 : 509-512.

Jayanthi, U. B.; Pereira, M. G.; Martin, I. M.; Stozkov, Y.; D'Amico, F. and Villela, T. (**1997a**). *Electron precipitation associated with geomagnetic activity: Balloon observation of X ray flux in South Atlantic anomaly*, Journal of Geophysical Research: Space Physics 102 : 24069-24073.

McIlwain, C. E. (**1961**). *Coordinates for mapping the distribution of magnetically trapped particles*, Journal of Geophysical Research 66 : 3681-3691.

Pinto, O.; Gonzalez, W. and Leme, N. (**1990a**). *VLF disturbances at the south atlantic magnetic anomaly following magnetic storms*, Planetary and Space Science 38,(5) : 633 - 636.

Pinto, O.; Pinto, I. and Gonzalez, W. (**1990b**). *On the effect of electron precipitation on the fair-weather electric field*, Journal of Atmospheric and Terrestrial Physics 52 : 21 - 22.

Zou, H.; Li, C.; Zong, Q.; Parks, G. K.; Pu, Z.; Chen, H.; Xie, L. and Zhang, X. (**2015**). *Short-term variations of the inner radiation belt in the South Atlantic anomaly*, Journal of Geophysical Research: Space Physics 120 : 4475-4486.

A proposal for a Magnetic Observatory in Honduras

Yvelice Castillo [1,2,3], M. Alexandra Pais [1,3], P. Ribeiro [1], João Fernandes [1,4], Anna L. Morozova [1], Fernando J. G. Pinheiro [1]

[1] CITEUC, Geophysical and Astronomical Observatory, University of Coimbra, 3040-004 Coimbra, Portugal; [2] Department of Astronomy and Astrophysics, National Autonomous University of Honduras; [3] Department of Physics, University of Coimbra; [4] Department of Mathematics, University of Coimbra. yvelicesoraya@gmail.com

Abstract

The Department of Astronomy and Astrophysics of the National Autonomous University of Honduras (UNAH) is interested in installing the first magnetic observatory of Honduras. The nearest magnetic observatories are located in Costa Rica, Cuba, México, Puerto Rico and Colombia. During the II PANGEO we made the first approaches to people of those observatories. We are also in touch with the Magnetic Observatory of the University of Coimbra (COI) in Portugal, where we will make a traineeship in magnetic measurements and data treatment. Later, with local colaborators we are planning to purchase the equipment to make local geomagnetic field measurements in different places of Honduras, in order to define the best location for our future magnetic observatory. We also want to establish alliances with the nearest observatories

Introduction

Space weather studies the interaction of large amounts of radiation and charged particles that come from the Sun (protons, electrons and ions) and the interestelar medium (i.e., cosmic rays), with the Earth and its environment, both in its magnetosphere, at some terrestrial radius distance, and in its atmosphere and surface. Specially hazardous are the induced currents in the Earth's mantle and crust, that can cause surges in the electrical systems, currents in the seabed, in pipelines, etc. At higher altitudes they can cause scintillation and damages in satellites, UHF, UHF, GPS and GNSS signals, large doses of radiation in polar flights and astronauts.

Magnetic observatories can monitor the geomagnetic activity and give information on the arrivalof energetic particles from the Sun. They can contribute to a deeper understanding and a better prediction of space weather events

Acknowledgements

CITEUC is funded by National Funds through FCT - Foundation for Science and Technology (project: UID/Multi/00611/2013) and FEDER - European Regional Development Fund through COMPETE 2020 Operational Programme Competitiveness and Internationalization (project: POCI-01-0145-FEDER-006922).
Yvelice Castillo is supported by the Department of Astronomy and Astrophysics of the UNAH.

References

Gose, W. A., Finch, R. C. (1992). “Stratigraphic implications of palaeomagnetic data from Honduras”. In: Geophysical Journal International, 108, pp. 855–864.

Schrijver, C. J. (2015). “Understanding space weather to shield society: A global road map for 2015-2025 commissioned by COSPAR and ILWS”. In: Adv. in Space Res. 55, pp. 2745–2807.

Ribeiro, P., Vaquero, J. M., Trigo, R. M. (2011). “Geomagnetic records of Carrington's storm from Guatemala”. In: Journalheric and Solar Terrestrial Physics, 73, pp. 308 – 315.

***Figure 1 - The nearest magnetic observatories are located in Costa Rica, Cuba, México, Puerto Rico and Colombia. Image adapted from Edinbugh Data Center*.**

Analysis of solar, interplanetary and geomagnetic parameters during solar cycle 24 A proposal for a Magnetic Observatory in Honduras

Yvelice Castillo [1,2,3], M. Alexandra Pais [1,3], P. Ribeiro [1], João Fernandes [1,4], Anna L. Morozova [1], Fernando J. G. Pinheiro [1]

[1] CITEUC, Geophysical and Astronomical Observatory, University of Coimbra, 3040-004 Coimbra, Portugal; [2] Department of Astronomy and Astrophysics, National Autonomous University of Honduras; [3] Department of Physics, University of Coimbra; [4] Department of Mathematics,

Summary:

A prospective study was made using different proxies that describe the Sun surface, the interplanetary medium and geomagnetic activity, to identify those parameters that should be more meaningfully used to relate the Sun to the geomagnetic activity observed on Earth. Correlations between 33 solar, interplanetary magnetic field (IMF) and geomagnetic activity proxies were analyzed for the 2009-2016 time interval. t was found that series of 27-day averages (Bartels' rotation) give higher correlations than daily or annual series.

Parameters that show higher cross-correlations among different groups are the Sun's northern and southern facular areas (FA-N and FA-S), two geomagnetic indices derived from the Tsyganenko and Sitnov 2005 (TS05) magnetosphere's model, the total IMF intensity (*B*), the percentage of IMF southward component (B_{ZS} GSM) and the interplanetary Newell's coupling function. We propose that these parameters are the best candidates to use if we want to relate meaningfully the solar surface events to geomagnetic activity felt on the Earth's surface.

Two new proxies were tested: 1) TI-indices, calculated from the North-South (*X)* TS05-derived series of cross-tail current (TAIL), symmetric ring current (SRC), partial ring current (PRC) and field-aligned currents (FAC) for the four observatories and 2) B_{ZS} GSM, calculated as the daily percentage of IMF southward component along the GSM Z-axis.

Helio-magnetic asymmetries were calculated for the 33 parameters, as the difference between their averaged values in the towards (interplanetary magnetic field – IMF – pointing inward the Sun) and away (IMF pointing outward the Sun) magnetic sectors. When these asymmetries are taken into account, the absolute values of some correlation coefficients increase. The most probable explanation for this is the Russell-McPherron effect: B_{ZS} GSM and B_Z GSM have a well-defined annual modulation, therefore, corresponding proxies for geomagnetic activity indices also have annual oscillation and high correlation coefficients with B_{ZS} GSM and B_Z GSM. TI-indices have annual oscillation at declining phase of the cycle, but insignificant oscillation near the minimum.

A major percentage of toward days in negative polarity epoch and of away days in positive polarity epoch means that the Earth has been mostly at the northern magnetic hemisphere during the solar cycle 24.

List of analyzed parameters

Solar Parameters

SN-N: the SILSO international northern solar hemisphere's sunspot number.

SN-S: the SILSO international southern solar hemisphere's sunspot number.

SN-T: the SILSO international total sunspot number.

SN-NS: difference between northern and southern sunspot number.

FA-N: northern hemisphere's facular area (calculated by CITEUC), in % of solar disk.

FA-S: southern hemisphere's facular area (calculated by CITEUC), in % of solar disk.

FA-T: total facular area (calculated by CITEUC), in % of solar disk.

FA-NS: difference between northern and southern facular areas (FA-N minus FA-S).

F10.7: the solar radio flux at 10.7 cm wavelength, originating in the chromosphere and corona of the Sun, in solar flux units (s.f.u.).

Solar Wind Parameters (SWP)

V: bulk flow speed, in km/s.

T: proton temperature, in 10^3 Kelvin degrees.
p: flow pressure, in nPa.
ρ: proton density, in number of protons per cubic centimeter.

Geomagnetic Activity Indices (GAI)
NLL: Newell's coupling function, that includes the rate of magnetic flux removed from the day side magnetopause, dΦMP/dt that is itself an electric field.
PCN: polar cap (north) index (mV/m).
Dst: storm-time disturbance index (nT).
Kp planetary index.
Ap planetary index (nT).
AE, AU, AL indices (nT). Auroral index horizontal component disturbances. The magnetograms of the horizontal components from the *AE* stations are superimposed: the upper envelope defines the *AU* index, and the lower envelope define the *AL* index; then *AE = (AU - AL)*.

TI Indices
TI indices were calculated from the X component of four TS05 currents: TAIL, SRC, PRC, FAC (nT).

IMF components
IMF components BX, BY, BZ (nT).
BZS (the percentage of southward BZ component) both in GSM and GSE systems.
B, the magnitude of the averaged total IMF field vector.

Conclusions

Facular areas as solar activity proxies. Facular areas computed independently for the northern and southern hemispheres of the Sun, as averages over 27-day periods, is a solar parameter that correlates better with the IMF field (B), but particularly with GAI and TI parameters than do the sunspot numbers (northern and southern solar hemispheres) or the F10.7 cm solar radio flux (see Table 1). The proposed here T-SRC and T-PRC indices, averaged over 27-day periods, are the geomagnetic activity parameters that best correlate with solar and IMF parameters (see Table 2).
Our results show that the proposed here B_{ZS} index shows higher than B_Z GSM correlations with all GAI parameters, and we consider it as a better parameter to characterize the geo-effectiveness of a solar event. The B values averaged over 27-days and the Newell ious cycles.

coupling function are parameters that correlate with all other groups of variables.

Par	FA-T	FA-N	FA-S	SN-T	SN-S	F10.7	B	B_Z GSM	B_{ZS} GSM
B	0.58	0.54	0.53		0.41	0.48			
T							0.58		
V							0.52		
p		0.53					0.74		
NLL	0.46	0.45	0.49		0.45	0.41	0.79	-0.48	0.57
Kp		0.41	0.41				0.77		0.43
Ap		0.41					0.76		0.41
AE			0.43				0.74		0.46
AU			0.42				0.66		0.42
AL			-0.41				-0.74	0.41	-0.46
PCN							0.62	-0.41	0.46
Dst							-0.5		
T-TAIL		0.46					0.65		0.45
T-SRC	0.53	0.48	0.53	0.46	0.52	0.51	0.66		0.41
T-PRC	0.52	0.51	0.5	0.4	0.44	0.47	0.76		0.45
T-FAC							0.57	-0.4	0.46

Table 1. s for 27-day averaged series of solar parameters, interplanetary magnetic field parameters and geomagnetic indices.

	V	p	NLL	Kp	Ap	AE	AU	AL	PC-N	Dst	T-TAIL	T-SRC	T-PRC	T-FAC
T	0.92	0.70	0.78	0.80	0.76	0.74	0.65	-0.77	0.65	-0.52	0.65	0.57	0.61	0.70
V		0.73	0.78	0.84	0.80	0.79	0.70	-0.81	0.71	-0.56	0.68	0.56	0.61	0.75
p			0.77	0.88	0.84	0.75	0.67	-0.78	0.68	-0.50	0.81	0.62	0.76	0.67
NLL				0.94	0.92	0.91	0.82	-0.93	0.82	-0.64	0.85	0.86	0.89	0.86
Kp					0.97	0.94	0.85	-0.96	0.83	-0.61	0.82	0.76	0.84	0.81
Ap						0.93	0.82	-0.96	0.86	-0.67	0.80	0.78	0.85	0.82
AE							0.95	-0.98	0.87	-0.55	0.73	0.76	0.80	0.81
AU								-0.88	0.79	-0.40	0.61	0.71	0.72	0.74
AL									-0.88	0.62	-0.77	-0.76	-0.81	-0.82
PC-N										-0.56	0.69	0.70	0.73	0.75
Dst											-0.59	-0.50	-0.56	-0.54
T-TAIL												0.78	0.88	0.83
T-SRC													0.92	0.84
T-PRC														0.85

Table 2. s for 27-day averaged series of interplanetary medium parameters and geomagnetic indices.

Distribution of toward and away polarity over solar cycle 24. Major percentage of the toward days in 2009-2012 (negative polarity) and of the away days in 2015-2016 (positive polarity),see Figure 1, means that Earth was at the north of the heliospheric current sheet (HCS) most of the time, as has been observed in previous cycles.

It means that the Earth is most constrained by the polarity of the Sun's North hemisphere during those time intervals. It also agrees with Ulysses mission discovery of an offset of the HCS toward south by about 10º.

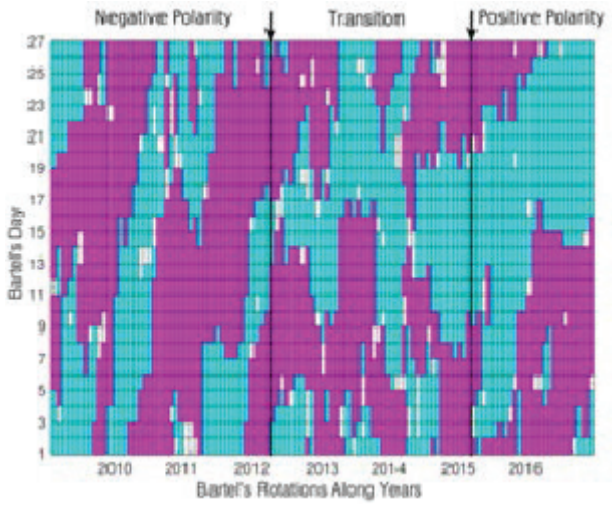

Figure 1. Days with toward (pink) or away (cyan) IMF direction. White days means missing data or polarity that could not be determined. Vertical axis shows days during each of Bartels' rotation (27 days). Horizontal axis represents consequent Bartels' rotations during 2009-2016.

Annual oscillation in toward-away asymmetries. Correlations among toward-away asymmetries of IMF, GAI and TI parameters increase when going from annual series to series of 27-day averages (compare Tables 1 and 3). GAI 27-day asymmetries have good correlations with BZS GSM and BZ GSM. These asymmetries show annual variations with smaller amplitudes in 2009 and larger amplitudes in 2015-2016 (declining phase of the 24th solar cycle with Sun's positive polarity). It is in agreement with Nair and Nayar (2009) conclusions, that geomagnetic activity is associated with coronal holes and enhances at declining phase of solar cycle. This conclusion also agrees with Zhao and Zong (2012), who show that geomagnetic activity is higher around equinoxes and maximal during positive polarity epochs. TI 27-day asymmetries also present an annual variation pattern and higher values at declining phase of the cycle, but no significant asymmetries at minimum.

Par	p	NLL	Kp	Ap	AE	AU	AL	PCN	Dst	T-TAIL	T-SRC	T-PRC	T-FAC
FA-S	-0.44												
BZ GSM		-0.87	-0.74	-0.72	-0.87	-0.86	0.85	-0.86	0.79	-0.50	-0.54	-0.54	-0.67
BZS GSM		0.88	0.74	0.70	0.85	0.85	-0.84	0.85	-0.76	0.53	0.53	0.53	0.68

Table 3. s for 27-day helio-magnetic asymmetries of solar parameters, interplanetary magnetic field parameters and geomagnetic indices. Only parameters showing increase of the absolute values of s are shown.

Acknowledgements

CITEUC is funded by National Funds through FCT - Foundation for Science and Technology (project: UID/Multi/00611/2013) and FEDER - European Regional Development Fund through COMPETE 2020 Operational Programme Competitiveness and Internationalization (project: POCI-01-0145-FEDER-006922). Yvelice Castillo's Ph. D. thesis related to this poster was funded by a grant in the Erasmus Mundus Action 2 Consortium AMIDILA, Lot 15 – strand 1, 2013-2588/001-001-EM Action 2 Partnerships. A.L.M. is supported by FCT -Foundation for Science and Technology, post-doc grant SFRH/BPD/74812/2010. The software for computation of facular aereas was developed by the CITEUC group Teresa Barata, Sara Carvalho, João Fernandes and Fernando Pinheiro.

References

Barata, T. et al. (2017). "Software tool for automatic detection of solar activity features in the Coimbra Observatory spectroheliograms". Submitted for publication.

Castillo, Y., Pais, M.A., Fernandes, J., Ribeiro, P., Morozova, A.L., Pinheiro, F.J.G. 2017. Geomagnetic activity at Northern Hemisphere's mid-latitude ground stations: How much can be explained using TS05 model. Journal of Atmospheric and Solar-Terrestrial Physics. Vol 165-166. Pag. 38-53. DOI: 10.1016/j.jastp.2017.11.002. ISSN: 1364-6826. http://www.sciencedirect.com/science/article/pii/S1364682617303668

Owens, Mathew J. and Robert J. Forsyth (2013). The Heliospheric Magnetic Field. Living Reviews in Solar Ph.

Nair, V. S. and S. R. Prabhakaran Nayar (2009). Features of long term evolution of solar wind and IMF and their signature on geomagnetic activity. Indian Journal of Radio & Space Physics 38.

Tsyganenko, N.A., Sitnov, M.I., 2005. Modeling the dynamics of the inner magnetosphere during strong geomagnetic storms. J. Geophys. Res. 110, A03208.

Zhao, H. and Q.G. Zong (2012). Seasonal and diurnal variation of geomagnetic activity: Russell-McPherron effect during different IMF polarity and/or extreme solar wind conditions. Journal of Geophy. Res. 117.

Reliability of the Geomagnetic Observation Data in the Villa Remedios and Patacamaya Observatories

J. Quispe M.1,2, E. Ricaldi Y.1,2, P. Miranda L.1,2
1Universidad Mayor de San Andrés U.M.S.A.
2 Instituto de Investigaciones Físicas I.I.F. − U.M.S.A.
J. Quispe M.: javierlinux21@gmail.com
E. Ricaldi Y.: ericaldi@gmail.com
P.Miranda: pmiranda@fiumsa.edu.bo

Abstract

In this work we describe the Geomagnetic observatories installed in Villa Remedios and Patacamaya(Andean Altiplano). The obtaining and treatment of geomagnetic data in its H, D and Z components is explained. In addition, for the case of the Patacamaya observatory, the form of magnetogram processing, digitization and data collection is shown. Both observatories have the capacity to process and publish the data set in a reliable way for the use of the scientific and technological community

I. Introduction

geomagnetism is an important branch of geophysics. Geomagnetic observatories
are the main sites for obtaining data for geomagnetic observation, which show the various physical processes related to solar energy or Earth activities. Geomagnetic observation data has been widely used in various fields, such as space, environmental prediction, oil well drilling, etc., and the reliability of the data is fundamental for scientific research and commercial applications. To have the proper reliability of the observation data, it is necessary to track and monitor the data over a long period of time Cite [1],[2] and [4]. The geomagnetic observatories of Villa Remedios and Patacamaya both located at a latitude of $-16^o46'0''$ N and longitude of $-68^o10'0''$ E with 3949 meters above sea level, and at a latitude of $-17^o14^0 27.30^{00}$ N and longitude of $-67^o54^0 38.27^{00}$ E at 3799 meters above sea level, respectively, both belonging to the Physical Research Institute of the University of San Andrés (U.M.S.A.) of the city of La Paz-Bolivia, is responsible for the processing, reliability and obtaining of geomagnetic data records, whether these are absolute measurements and/or relative measurements Cite [1],[4]. The data obtained from Villa Remedios geomagnetic observatory are in collaboration with the GeoForschungszentrum Potsdam Research Center, GFZ (Potsdam Geophysical Research Center). Each observatory is equipped with variographs to make recordings of daily geomagnetic variations, a fluxgate theodolite for each observatory, a proton precession magnetometer for absolute measurements. Then the observatories are equipped as detailed: a La Cour variograph, a Danish triaxial magnetometer, a Hungarian hybrid theodolite MG2KP, a Overhauser fluxgate MAG-01H theodolite and a proton precession magnetometer Cite [1,2,4] and [5]. Observation data of Villa Remedios are transmitted to the GeoForschungszentrum Potsdam, GFZ research center by email every month. This document focuses on the content and process of control, reliability and the obtaining of geomagnetic data. The publication of the data set is done through of GFZ Potsdam Research Center and the Physics Research Institute of the Physics career U.M.S.A.

II.The elements of the magnetic field of the Earth

The geomagnetic field has a direction and magnitude at each point in the space that define the magnetic field. This intensity of the geomagnetic field is usually represented Cite [5]:

− Components *X*, *Y* and *Z*: Three components orthogonal to each other, with *X* and *Y* being horizontal components pointing North and East respectively. *Z* is the component that points towards the center of the Earth.

− Components *H*, *D* and *I*: *H* is the magnitude of the horizontal component that is considered positive whatever its direction; *D* is the magnetic declination: angle that is measured from component *X* to *H*; and I is the angle formed between the total intensity and the horizontal component (Fig [1]).

− F is the magnitude of the total magnetic field (see Fig [1] center).

From Fig. [1(b)] by simple geometry we obtain the relationship between the variables that are:

$$F = \sqrt{X^2 + Y^2 + Z^2}, \qquad (1)$$

$$H = \sqrt{X^2 + Y^2}) \qquad (2)$$

$$I = arctan\left(\frac{Z}{H}\right), \qquad (3)$$

$$D = arctan\left(\frac{Y}{X}\right) \qquad (4)$$

The components in Cartesian coordinates are:

$$X = Hcos(D) \qquad (5)$$

$$Y = Hsin(D) \qquad (6)$$

$$Z = Fsin(I) \qquad (7)$$

The components of the geomagnetic field *X*, *Y*, *Z* and *H* are expressed in Nanoteslas [*nT*]. *I* and *D* angles measured in sexagesimal degrees

Geomagnetic observatories always perform measurements of the components of the magnetic field as shown in the equations [1,2,3,4 and 7]. These measurements, whether these can be absolute and / or relative are carried out continuously over several years, which allow to the magnetic field event of the Earth to be recorded, and where definitive data recorded are regularly published for the scientific community in general Cite[8].

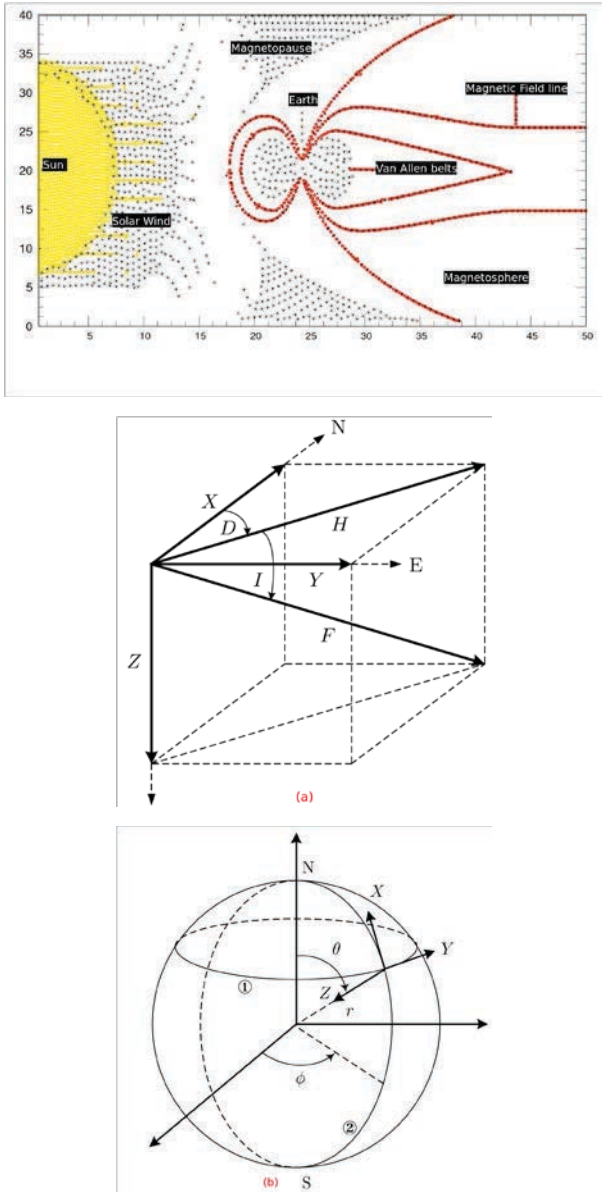

Figure 1: (upper part) Solar Wind, (a) Cartesian components of the geomagnetic field. (b) Polar components of the geomagnetic field (spherical coordinates).

III. RELATIVE GEOMAGNETIC MEASURING INSTRUMENTS

I. VILLA REMEDIOS OBSERVATORY

Variographs The triaxial fluxgate 3component Danish Variographs, installed in Villa-Remedios is new and modern. Record events of *x*, *y* and *z*, calculating the other components *D*, *I* (declination and inclination magnetic) Fig.[2].

Proton Magnetometers It is of Canadian manufacture, it registers values of the total magnetic field *F*, and attached we have *GPS* for the Time record *t* Fig.[2].

The behavior of the Earth's Magnetic Field is recorded, continuously, measured at a relative level with a resolution of the order of nanoteslas. In Villa Remedios the data acquisition is automatically (Data-logger) and the registration of events is digital Fig.[2, 4].

Figure 2: (Top) 3-component Fluxgate sensor head (modern variograph) installed in Villa Remedios, together with a (middle) proton precession magnetometer and (below) data-logger recorder

II. PATACAMAYA OBSERVATORY

Variographs The Patacamaya Variographs are constructed based on optical-mechanical principles, record events of the HDZ geomagnetic components by suspended needles and helzmoltz coils for the calibrations Fig.[3].

In Patacamaya the events are recorded in an optical way on photographic paper (Magnetograms), these magnetograms can be digitized as shown below (see Fig.[6]).

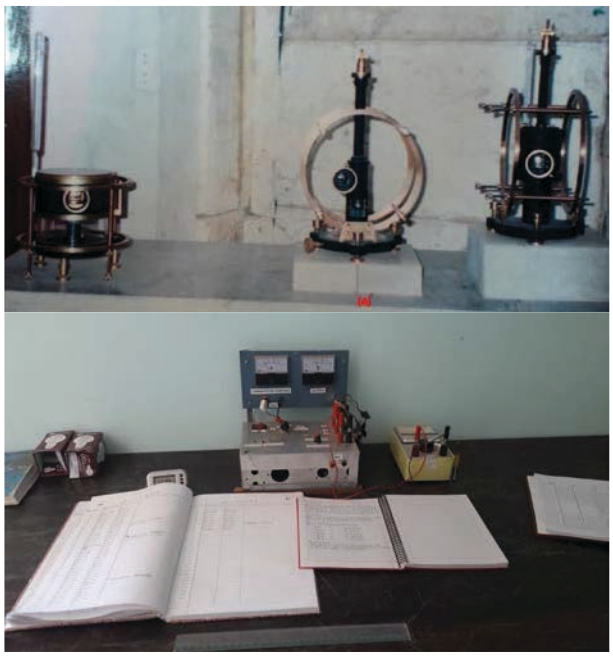

Figure 3: (upper part)*H*, *D* and *Z* magnetic components measured by suspended needles helmholtz coils. (lower part) Electronics for the calibrations of each component *H*, *D* and *Z*, together with the record bitacoras. Equipment belonging to the patacamaya observatory.

IV. ABSOLUTE GEOMAGNETIC MEASUREMENTS

The absolute measurements are made from time to time with the theodolites of declination and inclination with fluxgate sensor, with which the angles of inclination and declination of the vector F with respect to the horizontal plane and the geographic north are measured. For absolute geomagnetic measurements we have the following equipment:

- 1 Theodolite Fluxgate German Zeiss MAG01H (Villa Remedios)
- 1 Theodolite Fluxgate Hungarian MG2KP (Patacamaya)
- There is no proton magnetometer for *F*field measurements

V. Records and temporary

VARIATIONS

MEASUREMENTS OF THE GEOMAGNETIC FIELD AND OTHER GEOPHYSICAL STUDIES SHOW THAT THE EARTH'S MAGNETIC FIELD CHANGES SIGNIFICANTLY WITH TIME. TEMPORAL VARIATIONS EXTEND FROM THE TIME SCALE OF SECONDS TO MILLIONS OF YEARS, THEY CAN BE PERIODIC OR COMPLETELY RANDOM, THEY CAN ALSO INCLUDE CHANGES IN THE SLOPE AND DECLINATION ALONG WITH THE MAGNITUDE OF THE TOTAL FIELD *F* FROM A FEW NANOTESLAS TO HUNDREDS OF [*NT*] CITE [2, 5, 6] AND [7].

These temporary changes to know are:

− **Secular Variations:** variations that extend over several years. These originate from changes in the interior and the values of the secular variation of the components of the field go from 10 [*nT*] per year to 150 [*nT*]/year.

− **Periodic Variations:** They originate due to the influence of external fields and in general they are equivalent to less than 100 [*nT*]. Characteristic periods are 12 [h], 1 [day],

27 [days], 6 [months], 1 [year], 11 [years], 22 [years], etc. These are related to rotation of the Earth and the influence of the Sun and the Moon.

− **Magnetic storms:** They are sudden disturbances of the magnetic field, which can last from hours to several days and modify the field by more than 500 [*nT*].

VI. RESULTS I. RECORD OF EVENTS IN VILLA REMEDIOS

The geomagnetic observatory in the town of

Villa Remedios distant 40 [km] from the City

of La Paz Bolivia, due to the digital technology with which it operates, the data are taken daily for to study the variations of the Earth's magnetic field in these latitudes, being that the geomagnetic H component at these latitudes very close to the equator are more sensitive that the Z component, where this component is much less sensitive Cite [2]. Fig.[4] shows the geomagnetic components *H*, *D* and *Z* [1].

The Fig.[5] shows the register of each magnetic component separately.

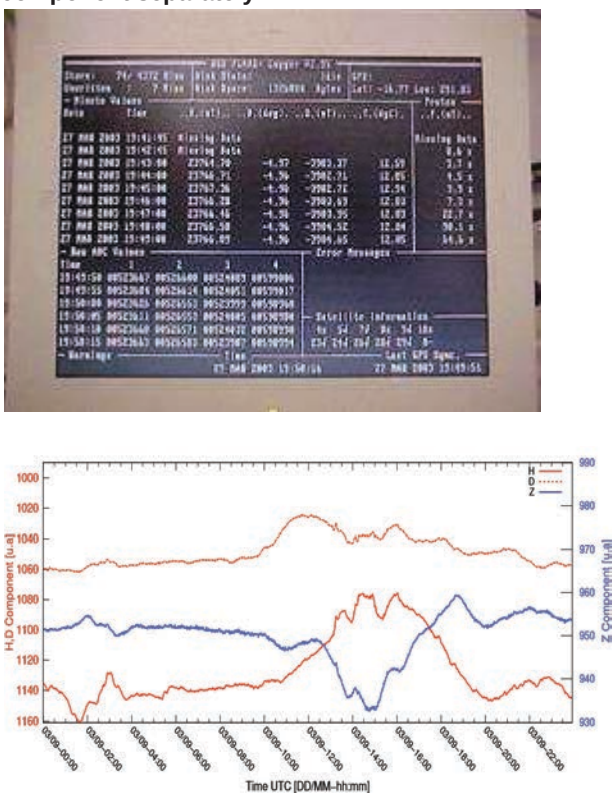

Figure 4: (upper part)Data-logger continuous data acquisition (lower part) Data processed for components *H*, *D* and *Z* in the observatory of Villa remedios.

II. RECORD OF EVENTS IN PATACAMAYA

The Geomagnetic Observatory of Patacamaya,

101 [km] away from the city of La Paz, operates with La Cour variographs of continuous optical-photographic record (see Fig.[6]). These varigraphs are installed in such a way that they are free of the influence of magnetic materials (see Fig.[3]). The current scale values are: for the magnetic declination (D) 0.91 [arc minutes] per [mm], the horizontal intensity (H) 3[nT] per [mm] and the vertical field intensity of 4.28

[1] **horizontal component of the magnetic field, magnetic declination and the vertical geomagnetic component**

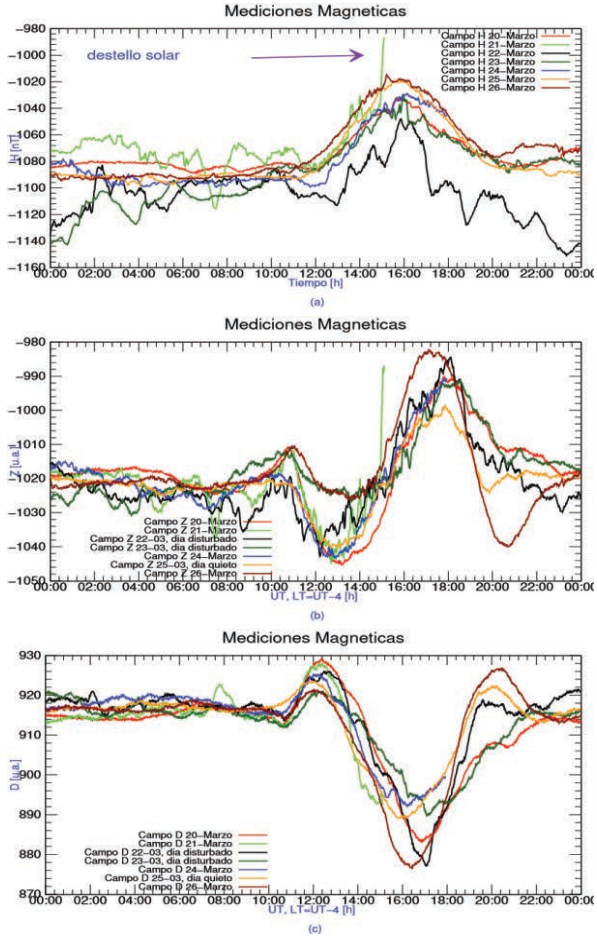

Figure 5: *H*, *D* and *Z* recorded by the variometers of Villa Remedios.

[nT] per [mm]. The instruments of this observatory are in good working condition where the recorded values are obtained using Heltmholz coils, these coils are located on each of the variographs since each one uses a different intensity of current.The magnetograms are digitized and controlled by means of free software modified and developed by the physical research institute (Cite [1, 2, 4]), which allows obtaining data from the magnetograms to a digital form for later analysis (see Fig.[6] and Fig.[7]).

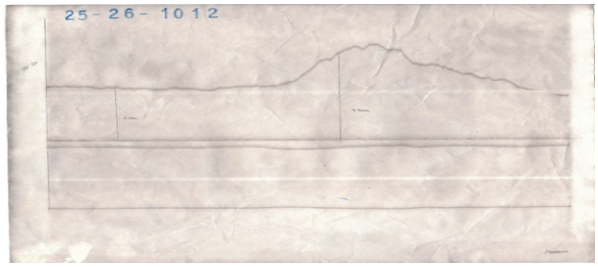

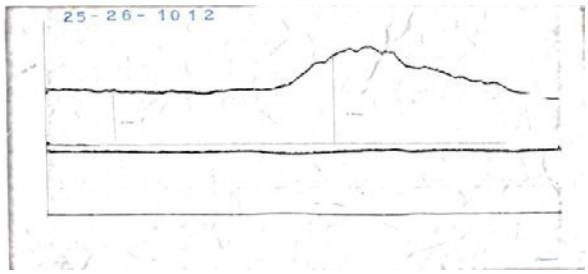

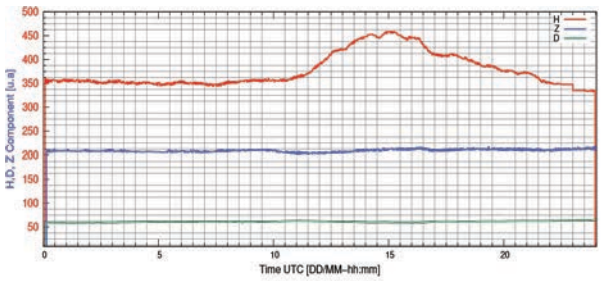

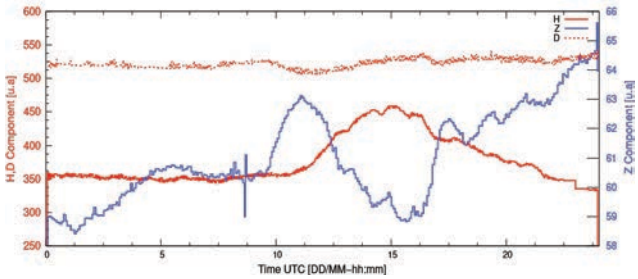

VII. CONCLUSIONS

The reliability of the data is directly related to the quality of the subsequent investigation. It is the responsibility of all the personnel involved

Figure 6: Magnetograms, one day records of the geomagnetic observatory of Patacamaya: the *H*, *D* and *Z* components can be observed.

Figure 7: Digitization of magnetograms (photographic paper) of the geomagnetic observatory of Patacamaya: the *H*, *D* and *Z* components can be observed in digital form. with the data output to guarantee and improve the reliability of the data. To date, the physical research institute is responsible for verifying the data quality operations, focused mainly on the control of reliability and quality (No background noise) of data per minutes. The precise quality control of the geomagnetic data is in the process of improvement; as yet, no efficient and feasible mechanisms have been identified, mainly for our Patacamaya observatory. Future efforts will be directed at solving these problems. The identification of incorrect records when pre-processing Patacamaya data can be observed with digitization methods. In the future, we hope to identify alternative methodologies to improve the automation of quality monitoring with data simulation (events). Finally, the data of our observatories are being used by our collaborators of the geomagnetic research center of GFZ, the research teachers and students of the Physics career of the U.M.S.A.

References

Ricaldi, E. Miranda P., Observaciones Geomagneticas en el observatorio de Patacamaya. Revista Boliviana de Fisica NUMERO 2 Julio 1996.

Vilca Salinas, R. 2001, Master's thesis, Carrera de Física, Universidad Mayor de San Andrés, La Paz, Bolivia

Mendoza, M. & Morales, J. 2004, Analysis of the Interaction of the Solar Wind with the Terrestrial Magnetosphere, Tech, rep., Departamento de Física, Universidad Nacional de Colombia, Ciudad Universitaria, Bogotá, D.C., Colombia

Ricaldi, E. 2007, Observación simultánea de neutrones solares en asociación con una fulguración solar del 7 de septiembre de 2005 (HF-UMSA).

Calcina, M.. Un modelo dinámico para el campo Geomagnético. Revista Boliviana de Física [online]. 2009, vol.15, n.15, pp. 44-62. ISSN 1562-3823.

World Data Center. 2008, http://spidr.ngdc.noaa.gov/spidr WEA:WEA2329,Thomson, Alan W. P., Geomagnetic observatories: monitoring the Earth's magnetic and space weather environment,Journal - Weather,69,9,John Wiley & Sons, Ltd, 1477-8696, http://dx.doi.org/10.1002/wea.2329, 10.1002/wea.2329, pp 234–237,2014.

http://www.fiumsa.edu.bo/

Estimativa da Amplitude de Correntes Geomagneticamente Induzidas Em Diferentes Locais no Brasil Durante a Tempestade Mais Intensa do Ciclo 24

Espinosa, K. ; Alves, L. ; Padilha, A.
INSTITUTO NACIONAL DE PESQUISAS ESPACIAIS, INPE
karen.sarmiento@inpe.br , antonio.padilha@inpe.br , livia.alves@inpe.br

Resumo

As variações temporais do campo geomagnético medido na superfície da Terra estão associadas às correntes geomagneticamente induzidas (GIC), que constituem um parâmetro determinante na análise de efeitos do clima espacial que podem ser observados na Terra. Partindo dos registros das variações do campo geomagnético, registradas em quatro estações da Rede do programa de Estudo e monitoramento de Clima Espacial (EMBRACE) do INPE, com magnetômetros do tipo "fluxgate", e com o conhecimento prévio do modelo de condutividade elétrica do subsolo nas regiões de localização das estações magnéticas, são estimadas as variações de campo geoelétrico induzido na superfície da Terra. Deslocando hipoteticamente a malha de transmissão de energia elétrica de $500\mathrm{kV}$ da qual se possui informação, localizada na região central do Brasil (mais especificamente, em torno do nodo da subestação de São Simão) e por último, usando o modelo de engenheira Lehtinen-Pirjola (LP), é estimada a amplitude das GIC durante a tempestade do dia 17 de março de 2015 ($\mathrm{Dst} = -222\ \mathrm{nT}$). A máxima amplitude da GIC calculada foi de ~$6\mathrm{A}$ para a estação de Alta Floresta (ALF), durante a fase principal da tempestade. Os valores das GIC foram comparados entre estações, para mostrar a influencia do eletrojato equatorial e a estrutura de condutividade do subsolo.

Introdução

As variações do campo geomagnético estão associadas às GIC, de maior amplitude em regiões de alta latitude devido às intensas correntes aurorais na cercania dos polos. Deve-se observar que, além da intensidade das variações do campo magnético em função da latitude geográfica, fatores como a estrutura geométrica, características de engenharia da rede elétrica e a composição geológica do subsolo contribuem significativamente para a amplitude das GIC durante uma tempestade magnética. Desse modo, têm sido observadas GIC com amplitudes significativas (dezenas de Ampères) em diferentes regiões de baixas latitudes. No Brasil, onde GIC com amplitudes de $15\ a\ 20A$ foram medidas durante uma tempestade de Novembro de 2004, com $Dst = -373nT$ (TRIVEDI et al., 2007). Embora esses valores da ordem de dezenas de Ampères não sejam suficientes para trazer efeitos imediatos nos transformadores ou mesmo levar ao colapso de uma rede nessas regiões de baixa latitude, eles ainda podem gerar efeitos indesejados por fazer os instrumentos operar por períodos prolongados fora de seu regime ideal, podendo causar saturação, geração de harmônicos e a consequente diminuição do seu tempo de vida útil. Por essas razões é importante continuar o monitoramento e a análise dos vários parâmetros envolvidos na ocorrência e amplitude das GIC em regiões de baixas latitudes, visando contribuir para explicar seus efeitos e assim desenvolver novos mecanismos que permitam minimizar seu possível impacto. Neste trabalho foram estimadas as GIC em torno do nodo da subestação de São Simão, durante a tempestade do dia 17 de março de 2015, a mais intensa ocorrida durante o ciclo 24 ***($Dst = -222nT$)***.

Metodologia

Neste trabalho, priorizou-se as estações do programa EMBRACE com dados disponíveis para a tempestade do dia 17 de março de 2015 e que dispunham do modelo de condutividade $1D$ para o cálculo do campo geoelétrico. As quatro estações usadas neste estudo, foram: Alta Floresta (MT), Jataí (GO), São José dos Campos (SP) eSão Martinho da Serra (RS) (Figura 1).

Partindo das séries temporais do campo geomagnético durante a tempestade escolhida, a mais intensa ocorrida durante o ciclo 24 ($Dst = -222nT$), e usando os dados do modelo de condutividade das quatro regiões de estudo (Tabela 1) (BOLOGNA et al., 2011, PADILHA et al., 1991), foram obtidas as **variações de campo geoelétrico $\boldsymbol{E(t)}$,** que constituem o componente geofísico.

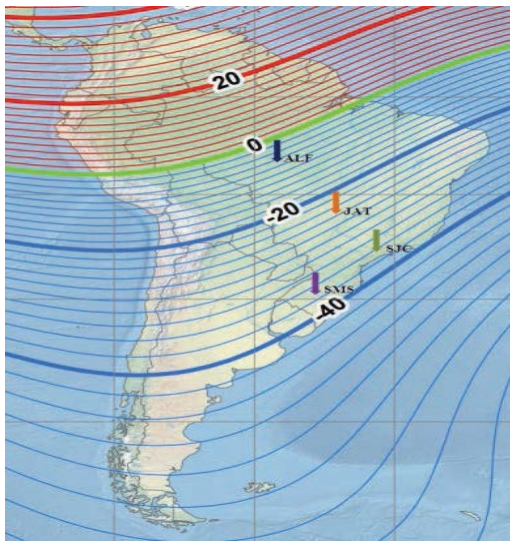

Figura 1 – Localização das quatro estações segundo a latitude DIP, para o ano 2015.

Estação	Propriedade	Número de Camadas						
		1	2	3	4	5	6	7
ALF	Resistividade (Ωm)	2000	10000	1100	7000	300		
	Espessura (Km)	1	10	20	230	-		
JAT	Resistividade (Ωm)	60	20	80	7000	50	5000	300
	Espessura (Km)	0.5	0.7	0.6	42	36	120	-
SJC	Resistividade (Ωm)	5	10000	100	10000	5000	300	
	Espessura (Km)	0.2	10	2	10	200	-	
SMS	Resistividade (Ωm)	160	12	5000	500	5000	300	
	Espessura (Km)	0.2	1	20	20	160	-	

Tabela 1 – Modelo de condutividade para as regiões das quatro estações de estudo.

Foram desenvolvidas rotinas na linguagem de programação MatLab que consideram as series temporais de **campo geomagnético** e o **modelo de condutividade** do subsolo, além da configuração da **rede elétrica**, a fim de obter uma **estimativa das GIC**. O processo esquematizado se apresenta na Figura 3.

Partindo dos resultados da **variação do campo geoelétrico** e da **configuração da rede elétrica**, foram calculadas as **amplitudes das GIC**. Estas amplitudes são calculadas baseadas no deslocamento hipotético da rede, composta por sete subestações (Figura 2) com voltagem entre as linhas de transmissão de $500kV$, e os dados de engenheira obtidos do trabalho de (BARBOSA et al., 2015).

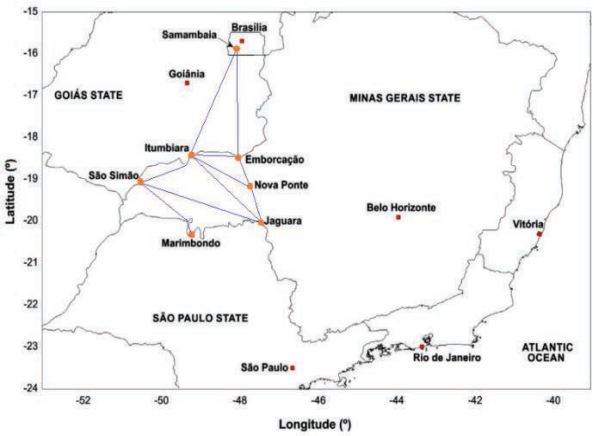

Figura 2 – Subestações elétricas da linha de altatensão localizada na parte central do Brasil.

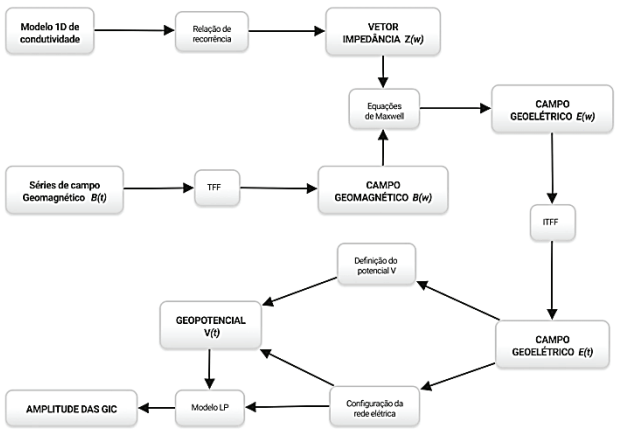

Figura 3 – Sequência de passos para o cálculo das GIC.

Resultados

Análise dos dados de campo geomagnético

Uma vez que os registros confirmam que a ocorrência das GIC está relacionada com a variação da componente $\boldsymbol{X}$ $(Norte - Sul)$ do campo geomagnético, e que a sua variação temporal tem o mesmo comportamento dos registros das GIC, na Figura 4 é representado o comportamento para cada estação.

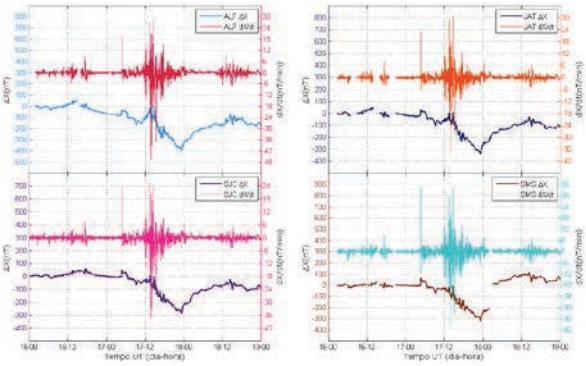

Figura 4 – Variação e derivada temporal da componente X.

Análise geofísica

A partir do modelo de condutividade elétrica e a série temporal de campo geomagnético, obtém-se os valores da série temporal do campo geoelétrico $\boldsymbol{E_y}(t)$.

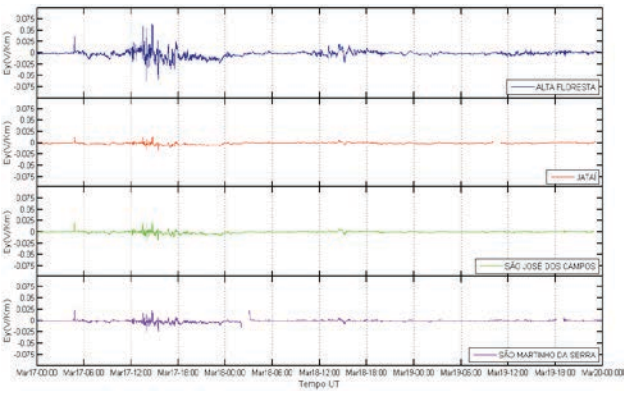

Figura 5 - Campo geoelétrico na direçãoY Modelo de engenheira

Séries temporais das GIC na subestação elétrica de São Simão, estimadas a partir do modelo LP.

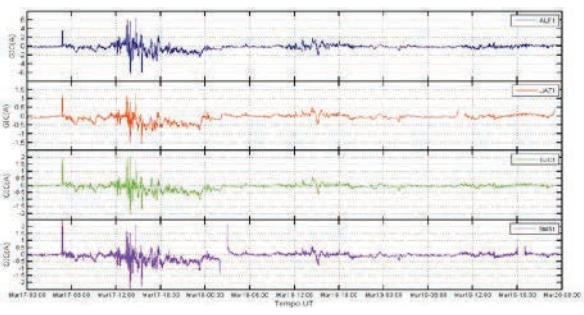

Figura 6 - GIC estimada em São Simão, para a tempestade de 17 de março de 2015.

Na figura 7, evidencia-se que a variação temporal da componente $\boldsymbol{X}$ $(Norte - Sul)$ do campo geomagnético, a componente $\boldsymbol{Y}$ $(Leste - Oeste)$ do campo geoelétrico e a série temporal das GIC apresentam o mesmo comportamento.

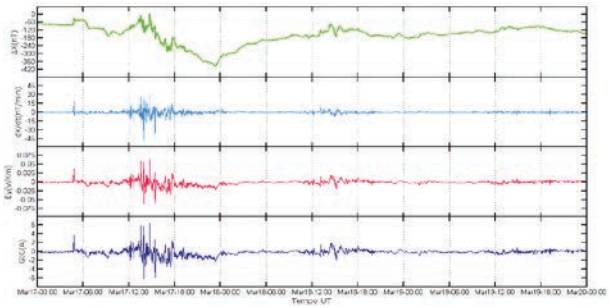

Figura 7 – Variáveis para ALF durante a tempestade de 17 de Março de 2015.

Conclusões

• Para o evento analisado, se registra maior magnitude da componente Norte-Sul do campo geomagnético, nas estações que ficam mais próximas do Equador magnético.
• Observa-se que a taxa de variação do campo é bem mais significativa nas componentes $\boldsymbol{H}$ e $\boldsymbol{X}$, um resultado típico para baixas latitudes magnéticas.
• Os maiores valores da derivada, que dão origem às GIC de maior intensidade, ocorrem durante o ssc $(04{:}44\ UT$ de 17 de março) e na fase principal (maiores amplitudes concentradas entre $13{:}30$ UT e $15{:}30$ UT desse mesmo dia). A máxima taxa de variação é de cerca de $38\ nT/min$ registrada às $13{:}47$ UT , durante a fase principal da tempestade.
• A estação Alta Floresta registrou a maior variação do campo geomagnético, possivelmente devido à influência do Eletrojato, assim, evidenciou-se também amplitudes do campo geoelétrico induzido na superfície mais intensas nesta região.
• A estação de Alta Floresta, localizada em uma região de alta resistividade, oferece menor atenuação ao sinal eletromagnético, em consequência o campo geoelétrico induzido na superfície registra maiores amplitudes, o que está em concordância com o modelo.
• O inicio da tempestade durante a noite hora local, mostra uma maior variação do campo geomagnético na estação São Martinho da Serra, como evidência da sua posição no centro da anomalia magnética do Atlântico Sul (AMAS). Porém, e de acordo com o modelo de condutividade, por ter estruturas pouco resistivas, não são registrados as maiores amplitudes das GIC no inicio da tempestade, nessa estação.
• Na procura de mitigar o impacto das GIC em estruturas tecnológicas aterradas, é necessário contar com dados experimentais que permitam a validação dos modelos.

Acknowledgements

Ao Conselho Nacional de Desenvolvimento Científico e Tecnológico (Cnpq) e à Coordenação de Aperfeiçoamento de Pessoal de Nível Superior (Capes), a bolsa de Mestrado e auxílios concedidos. Aos organizadores do II PANGEO pela receptividade e as entidades financiadoras pelo auxílio concedido.

Referências

TRIVEDI, N., VITORELLO, Í., KABATA, W., DUTRA, S., PADILHA, A., BOLOGNA, M., … VILJANEN, A. (2007). Geomagnetically induced currents in an electric power transmission system at low latitudes in Brazil: A case study. *Space Weather*, *5*(4), 1–10. https://doi.org/10.1029/2006SW000282

BOLOGNA, M., PADILHA, A., VITORELLO, I., & PÁDUA, M. (2011). Signatures of continental collisions and magmatic activity in central Brazil as indicated by a magnetotelluric profile across distinct tectonic provinces. *Precambrian Research*, *185*(1–2), 55–64. https://doi.org/10.1016/j.precamres.2010.12.003

PADILHA, A., TRIVEDI, N., VITORELLO, I., & DA COSTA, J. (1991). Geophysical constraints on tectonic models of the Taubaté Basin, southeastern Brazil. *Tectonophysics*, *196*(1–2), 157–172. https://doi.org/10.1016/0040-1951(91)90294-3

BARBOSA, C., ALVES, L., CARABALLO, R., HARTMANN, G. A., PAPA, A. R. R., & PIRJOLA, R. J. (2015). Analysis of geomagnetically induced currents at a low-latitude region over the solar cycles 23 and 24: Comparison between measurements and calculations. *Journal of Space Weather and Space Climate*, *5*. https://doi.org/10.1051/swsc/2015036

Comparison between the Secular Variation at Tatuoca Magnetic Observatory Data (Brazil) and the Global Field Models IGRF12 and CHAOS6

Baldez, Raissa Moraes[1], C. M. Martins[1], K. J. R. Pinheiro[2], C. E. P. Martins[1]
1 - Universidade Federal do Pará, 2- Observatório Nacional

Abstract

The secular variation (SV) represents the changes observed in Earth's magnetic field due to the dynamics of the core. The SV occurs in long timescales hence it is better observed by magnetic observatories. Tatuoca Magnetic Observatory (TTB) is located at an island 30km from Belém, Brazil and 132km south from the geographic equator. This location is important for three reasons: it lies at the magnetic equator; it is useful to study the Equatorial Electrojet (EEJ) and the Counter Electrojet (CEJ) behaviors; and to observe the South Atlantic Magnetic Anomaly (SAMA) growth and effect. TTB produces high quality data since 1957 but its data were not used in global field models because it is not an INTERMAGNET member yet. In this work, we compared the observed SV at TTB and the calculated SV by the IGRF12 and CHAOS6 models for two distinct periods. The first is from 1981 to 1999 for D, H and Z and the second is from 2009 to 2015 for X, Y and Z components. TTB data corresponds to hourly mean values for the chosen periods, while the IGRF12 and CHAOS6 models give the daily mean. Using the available data sets to calculate the SV and the application of the root mean square error (RMSE), we were able to determine which model better fits the SV observed at TTB. The comparison among SV from TTB and the global models showed that they agreed with TTB data.

.

Introduction

The geomagnetic field is the sum of the fields produced by internal and external sources. The major contribution for the internal source correspond to the field generated by the geodynamo, a process where convection in the liquid outer core generates electric currents and consequently a magnetic field. The magnetized crust is another source of the internal field, produced by the remnant and induced magnetization of rocks in the crust. The external field sources are the electrical currents in the ionosphere and the magnetosphere. Additionally, the variations of the internal and external fields induce electrical currents in the crust and mantle producing induced fields (HULOT et al, 2007). The sources of the Earth's magnetic field are dynamics and they cause changes in the magnetic field. The geomagnetic field changes on long and short timescales. The focus of this work is the study of the variations on timescales of years to tens of years known as Secular Variation (SV). It corresponds to changes in time directly associated to the core dynamics (STEVENSON, 2003). These changes occurs due to the process of convection in the outer core, driven by cooling of the planet and by chemical differentiation at the Inner Core Boundary (ICB) (Finlay et al, 2010). The IGRF (International Geomagnetic Reference Field) is a field model produced from satellite, observatory and survey data (THÉBAULT et al, 2015). It calculates the geomagnetic field and the SV at any point at the Earth's surface. It is important to know that the IGRF12 model gives values for the core field only. This model also gives a future estimation of the SV up to five years. Since the magnetic field changes with time, the IGRF model is revised each five years before its release to the public. The CHAOS6 model is the most recent model in the CHAOS series and spans from 1999 to 2016. It contains satellite, ground-based activity indices and observatory monthly means data (FINLAY et al, 2016). The primary objective of CHAOS6 is the study of SV and Secular Acceleration (SA) with high resolution in space and time. The recent addition of two years of Swarm data makes it an excellent model to analyze recent SV. As for the external field, CHAOS6 has a parametrization of the quiet-time, near-Earth magnetospheric field, with no representation of the fields produced by the magnetosphere-ionosphere coupled currents.

Method

From the hourly mean values at TTB we calculated the daily means, annual means and SV. Figure 1 and 2 show the available TTB data for each chosen period. It is important to clarify that for this work we made no separation between quiet, disturbed and normal days at TTB. In addition, without access to the TTB yearbooks we could not certificate that some too high or too low values from the digital data were indeed correct. Because of that we decided to exclude them from this analysis, hence our data coverage is low for some components. These issues will be addressed at future works. To calculate the predicted values for each model we used as input the days for which we had daily means at TTB. From the calculated daily means, we determined the annual means and SV for each model. Since the CHAOS6 model starts at 2000, it did not participate in the comparison with TTB from 1981 to 1999. Additionally, we used only the core field part of this model since the IGRF models only the core to field. After calculating the SV for each time period we applied the RMSE to quantify the difference between the observed data (TTB) and the predicted data (models).

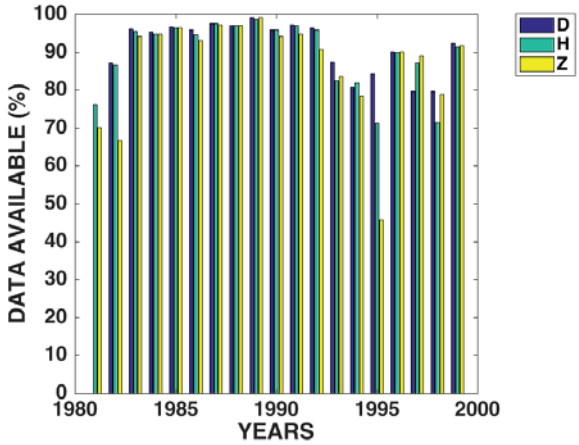

Figure 4 TTB data from 1981 to 1999 showing the available data used in this work in percentage for declination D (blue), horizontal field H (green) and vertical field Z (yellow).

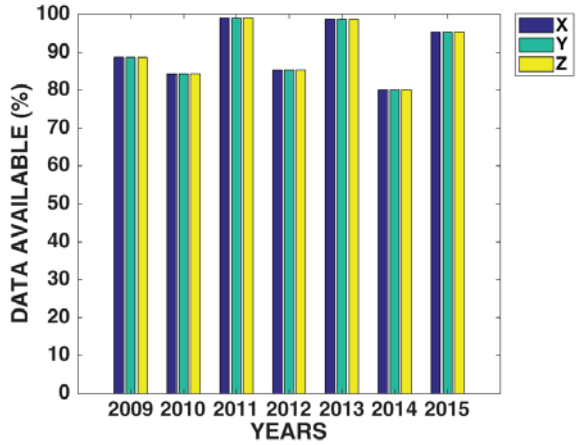

Figure 5 TTB data from 2009 to 2015 showing the available data used in this work in percentage for North Field X (blue), East field Y (green) and vertical field Z (yellow).

Results

Figures 3, 4 and 5 show the annual means for D, H and Z from 1981 to 1999. They show that the IGRF calculated annual means follow the trend line exhibited by TTB data. Their difference in amplitude is because IGRF gives values relative to the core field while TTB sums up all the field contributions in its record. This characteristic will show off more pronounced in the difference in amplitude for the SV.

Figures 6, 7 and 8 represents the SV for D, H and Z from 1981 to 1999. Here the most notable feature is the sharp contrast of amplitude from one year to the next in TTB data when compared to the well-behaved IGRF data. This is explained by three different factors. First, as explained

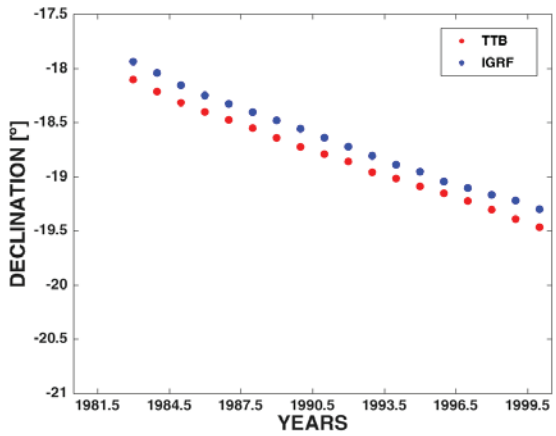

Figure 6 Annual means for declination (D) from 1981 to 1999. Red is TTB data and blue is IGRF data.

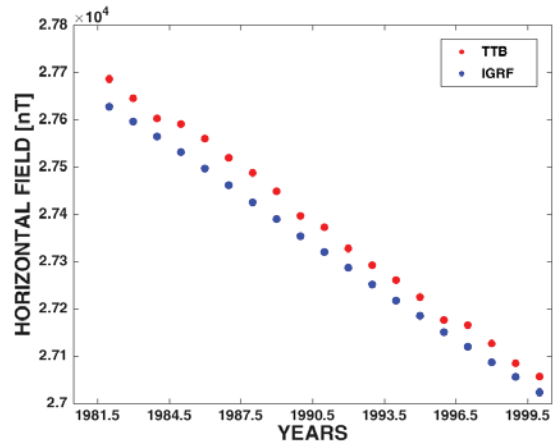

Figure 7 Annual means for horizontal field (H) from 1981 to 1999. Red is TTB data and blue is IGRF data.

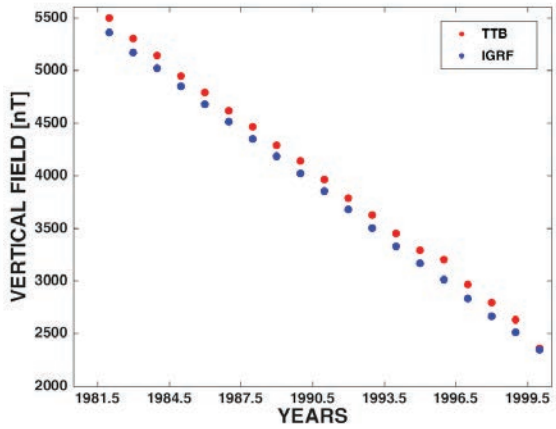

Figure 8 Annual means for vertical field (Z) from 1981 to 1999. Red is TTB data and blue is IGRF data.

before, the digital record of TTB data has some values that were too high or too low when compared to others for the same year. This affected the calculation of the daily and annual means and consequently the SV, since it is derived from the difference between an annual mean the one of the previously year. Furthermore, for some components, we had less than 50% of available data to use in the calculations and that put a strain in the representation of a field component value at TTB. Moreover, as mentioned before, the IGRF model used in this comparison only gives values for the core field and since TTB data represents the sum of all magnetic field sources it is expected to show difference in amplitude among them due to the influence of the external field and mostly notable the EEJ for the horizontal field in the region. In addition, the presence of disturbed days in the TTB data might have affected the calculated means. Table 1 shows the RMSE values for this comparison.

Table 1 RMSE values for the SV comparison between TTB SV data and IGRF SV data from 1982 to 1999.

TIME INTERVAL: 1982 to 1999		
COMPONENT	IGRF	UNITS
D	0.0153	degrees
H	10.5688	nT
Z	33.8164	nT

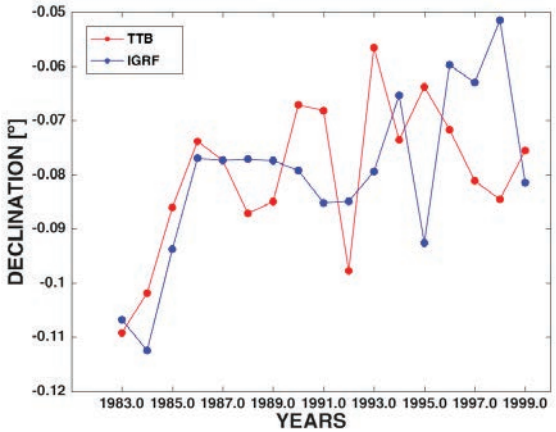

Figure 9 SV from 1981 to 1999 for declination. Red is TTB data and blue is IGRF data.

Figures 9, 10 and 11 show the annual means for X, Y and Z from 2009 to 2015. They show that the both models followed the same trend line as TTB data with lesser differences in amplitude when compared with the data set from 1981 to 1999. It happens due to the higher data coverage for this particular comparison (Figure 2). Once again, this difference in amplitude occurs due to the distinction in core field modeled values and total field observed at TTB.

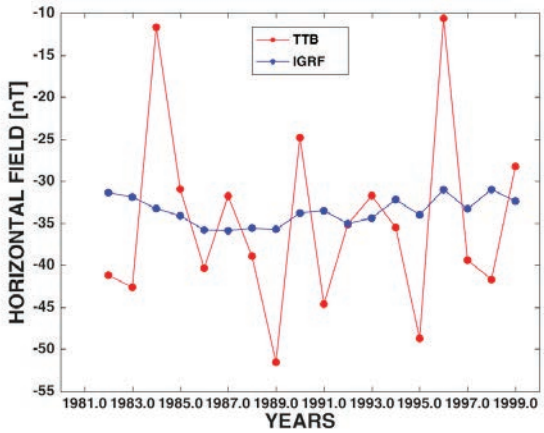

Figure 10 SV from 1981 to 1999 for horizontal field. Red is TTB data and blue is IGRF data.

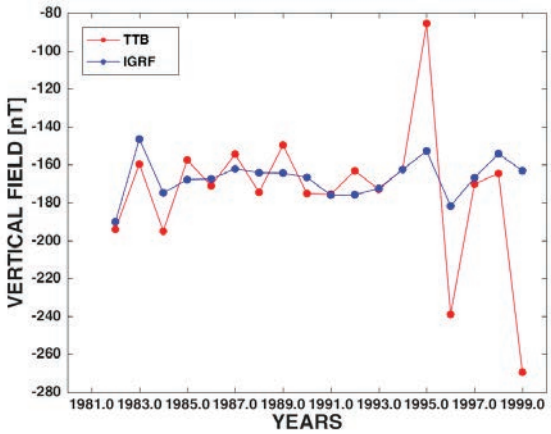

Figure 11 SV from 1981 to 1999 for declination. Red is TTB data and blue is IGRF data.

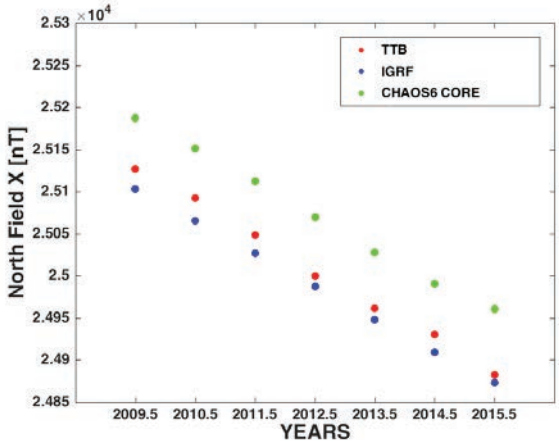

Figure 12 Annual means for north field (X) from 2009 to 2015. Red is TTB, blue is IGRF and green is CHAOS6 Core data.

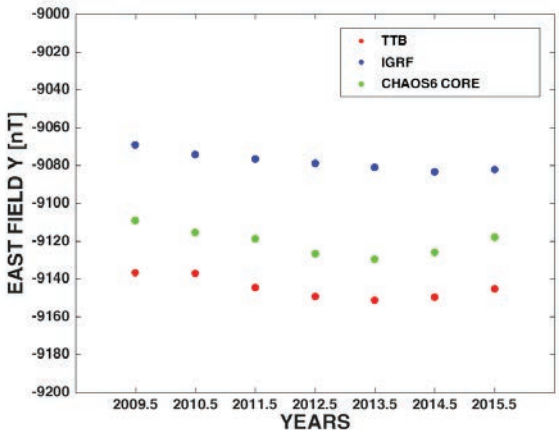

Figure 13 Annual means for east field (Y) from 2009 to 2015. Red is TTB, blue is IGRF and green is CHAOS6 Core data.

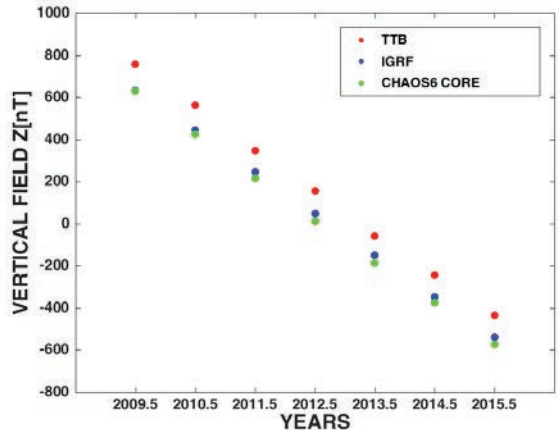

Figure 14 Annual means for vertical field (Z) from 2009 to 2015. Red is TTB, blue is IGRF and green is CHAOS6 Core data.

Figures 12, 13 and 14 represents the SV for X, Y and Z from 2010 to 2015. In this data set, TTB also presents the sharped contrast in values between some years, although it is less frequent than in 1981 to 1999 period. Observing these figures, we noticed that the IGRF model had low amplitude difference from 2011 to 2014 for all analyzed components, appearing as a straight line whereas the TTB data showed high and low amplitude values. The CHAOS6 Core SV data followed the same pattern as TTB but with less amplitude differences. Table 2 shows the RMSE values for this comparison.

Table 2 RMSE values for the SV comparison between TTB SV, IGRF SV and CHAOS6 Core SV data from 1982 to 1999.

TIME INTERVAL: 2009 to 2015			
COMPONENT	IGRF	CHAOS6 CORE	UNITS
X	7.3142	8.1172	nT
Y	3.6640	3.6369	nT
Z	11.9532	10.7306	nT

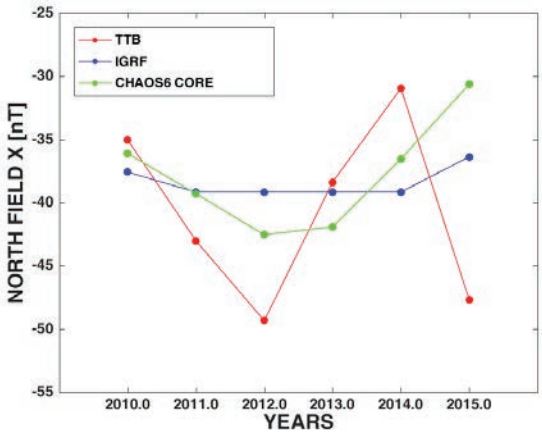

Figure 15 SV from 2010 to 2015 for north field. Red is TTB, blue is IGRF and green is CHAOS6 Core data.

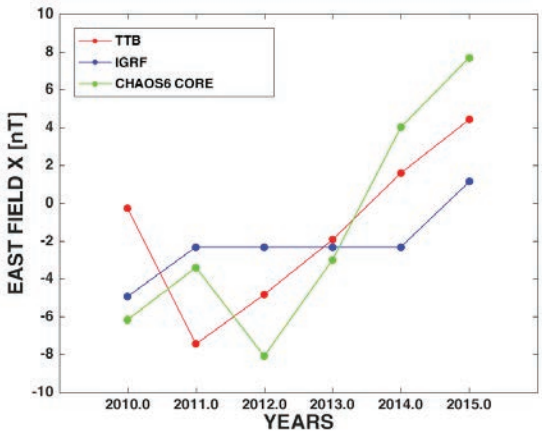

Figure 16 SV from 2010 to 2015 for east field. Red is TTB, blue is IGRF and green is CHAOS6 Core data.

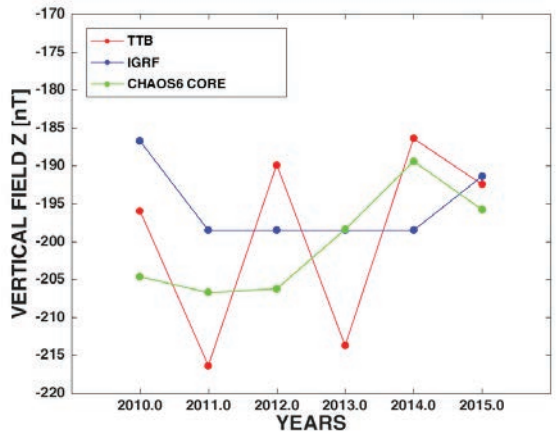

Figure 17 SV from 2010 to 2015 for vertical field. Red is TTB, blue is IGRF and green is CHAOS6 Core data.

Conclusions

Both models had appropriated responses to TTB data, mainly in relation to the trend of the data and the variation. However, specifically in relation to the SV, the discrepancy between the calculated from the TTB data and the predicted by the models is greater. For the 1981 to 1999 period, we faced difficulties in terms of available data and that reflected in the results for the calculated SV for TTB. With access to the yearbooks and a better data selection we aim to correct these issues in future works. For the 2009 to 2015 period, CHAOS6 model had a better fit to SV of Y and Z in in terms of RMSE, while the SV X had better approximation by IGRF. The SV of the Y component shows a behavior compatible with the Jerks for the years of 2011 verified in other publications. The search for other documented jerks will also feature in our future works. Maybe the difference between the predicted and observed data in TTB would be lower if there were more magnetic observatories near the equator and in the south hemisphere. It remains to extend this comparison to the entire period of TTB data, and include other models, such as CM4 for example.

Acknowledgements

Dr. João Batista Miranda, IG, UFPA; PROEX-UFPA; Jürgen Matzka, GFZ, Potsdam; and Tatuoca Staff.

References

FINLAY, C. et al. International Geomagnetic Reference Field: the eleventh generation. *Geophysical Journal International*, Oxford University Press, v. 183, n. 3, p. 1216–1230, 2010.

FINLAY, C. et al. Short timescale core dynamics: theory and observations. *Space Science reviews*, Springer, v. 155, n. 1-4, p. 177–218, 2010.

HULOT, G.; SABAKA, T.; OLSEN, N. The present field. *Treatise of Geophysics*, 2007.

STEVENSON, D. J. Planetary magnetic fields. *Earth and planetary science letters*, Elsevier, v. 208, n. 1, p. 1–11, 2003.

THÉBAULT, E. et al. International geomagnetic reference field: the 12th generation.

Earth, Planets and Space, Springer, v. 67, n. 1, p. 1–19, 2015.

Diurnal Variations of the H Component in the South Atlantic Islands at Low Magnetic Latitudes

Sophia Laranja, [1,2] *Caio Gonçalves* [1,2] *Thaís Cândido* [1,2] *and Luiz Benyosef* [2]

[1] *Universidade Federal Fluminense*

[2] *Observatório Nacional*

Abstract

The geomagnetic variations recorded in the equatorial region are known to present an enhanced behavior when compared to those at off-equatorial latitudes. This pattern can be attributed to the phenomenon of the Equatorial Electrojet (EEJ), which is a narrow belt of intense electric current in the ionosphere confined to about ±3º at the dip equator (Chapman, 1951a, and Adimula, et al, 2011). We intend to analyze the Sq variations of the geomagnetic components D, Z from two EEJ and one SAMA (ASC) observatories, being one of them a south atlantic island. Our purpose is to correlate these results with the geology of the regions studied, in both quiet and disturbed conditions.

.

INTRODUCTION

The geomagnetic variations on the ground in the equatorial ionosphere region are known to have an enhanced behavior when compared to those at non-equatorial latitudes. The phenomenon called "Equatorial Electrojet" (EEJ) is believed to be responsible for this distinct pattern. At the magnetic dip equator the global dynamo generates the midday eastward polarization field, which gives rise to a downward Hall current. A strong opposite vertical polarization field is set up due to the presence of non-conducting boundaries, making arise the intense Hall current named the Equatorial Electrojet (EEJ) (Chapman, 1951). The typical extent of the EEJ is within ±3° of the dip equator, confined at the E region in a height of about 95 - 115 km. The Equatorial stations respond primarily to the directly overhead EEJ, but also to the ring current and the global quiet time Sq current system, therefore two EEJ stations were chosen to analyze and compare their Sq variations in the geomagnetic components D and Z, in both quiet and disturbed conditions.

The South Atlantic Ocean is a region of large interest due to its anomalous geomagnetic field, caused by the South Atlantic Magnetic Anomaly (SAMA). In this region the strength of the internal magnetic field is significantly lower when compared to elsewhere in the world. The SAMA originates from an inverse magnetic flux at the core mantle boundary beneath South America and South Africa, which existence is noted over the last 200 years (Gubbins et al., 2006). The low geomagnetic field in this region causes a strong increase of radiation due to the distortion of the inner van Allen radiation belt, affecting satellites when passing through the SAMA (Heirtzler et al., 2002). The growth of this reversed flux region may be related to the Earth's magnetic field attempting to reverse (Gubbins, 2008).

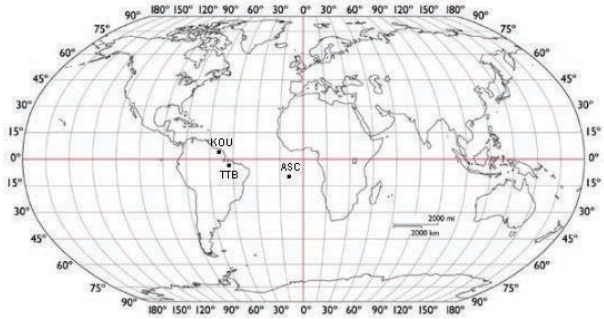

Figure 1. Geographic distribution of the observatories studied.

	Geographic		Geomagnetic	
Observatory	Latitude (º)	Longitude (º)	Latitude (º)	Longitude (º)
Tatuoca (TTB)				
Ascension Island (ASC)	7.949 South	345.624 East	2.809 South	057.530 East
Kourou (KOU)	5.209 North	307.267 East	14.55 North	20.11 East

Table 1. Geographic and Geomagnetic coordinates of the stations.

Method

First of all, the three quietest and disturbed days were chosen for the analysis, using the same method, according to planetary magnetic index, kp for the quietest one and the ap index for the disturbed days. The kp and ap indexes are provided by the international service of geomagnetic indices (isgi).

The data used has one-minute resolution and one-hour median values were derived. A quiet level baseline was defined for each day as the mean of six nighttime values. dH and dZ were computed by subtracting the baseline from D and Z geomagnetic components (Yamazaki, Y.,et al., 2011), according to the equation 1.

$$dD(UT) = D(UT) - \frac{D(0) + D(1) + D(2) + D(22) + D(23) + D(24)}{6} \quad (1)$$

After that we compared the behavior of the Z component with the geology of the regions studied. We made a correlation of the Z component morphology with how much we believe that the geology can affect the curves obtained.

Results

The quiet daily variations for both D and Z geomagnetic components are in figure 2, and the disturbed condition for the same component is in figure 3. The pattern obtained in figures 2 and 3 clearly revealed that D has deviated from the normal known variation of morning trough and afternoon crest. This could be attributed to change in electric field (Okeke et al., 1998). However, D seems to increase around noon for TTB and KOU, showing its minimum between 14 and 16 UT.

The diurnal variation curves in Z component for the three stations might be interpreted according to the Sq current system. ASC is a volcanic island, so the geology of this region might influence in a very small scale the curves in Z. Induction effects can influence stations off the continent, like ASC.

The morphology of the curves in TTB and KOU has a more pronounced diurnal variation when compared to ASC. This might be due to the stations location. TTB and KOU are located in the equatorial region and within the EEJ zone, thus this can influence the behavior of Z component.

The diurnal variations for both D and Z components at ASC exhibits an opposite sign from those at TTB and KOU. This might be due to the localization of the observatories. For the stations at the northern side of the dip equator the curves are negative in the afternoon and for the southern stations they are positive (Obiezekie, 2012).

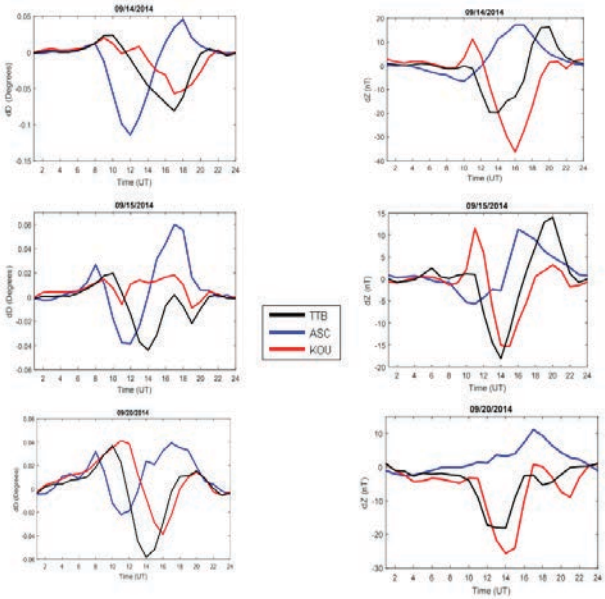

Figure 2. Diurnal variations for D and Z components on quiet condition.

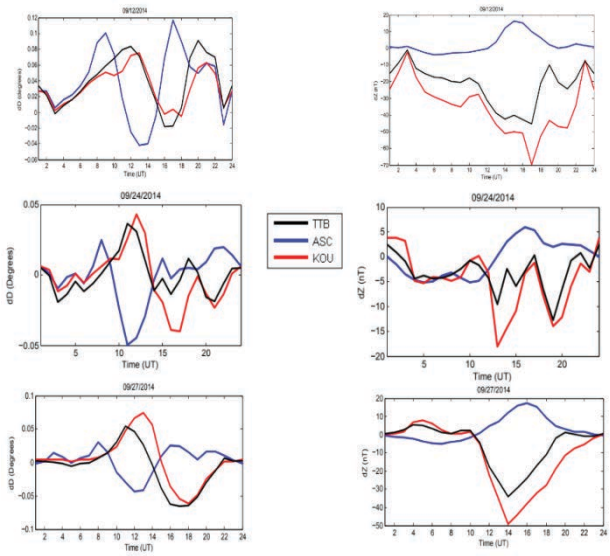

Figure 3. Diurnal variations for D and Z components for the disturbed condition.

Geological considerations

Ascension is a volcanic island, but although there are lots of vents on the island, it is only a single volcano. In fact, the area above the water level is only 1% of the volcanic landmass.

Ascension lies on the South America plate, while the hotspot is on the other side of the Mid Atlantic Ridge under the African plate, and the magma flows along the ridge to reach Ascension Island.

Larger explosive eruptions produce pumice and ash. The ash and pumice can be laid down in two main ways, as pyroclastic and pyroclastic flow, both of which are found on Ascension. Pumice is very light volcanic rock filled with holes, from the rapidly expanding gas that drove the eruption.

Most of the outcrops are scoria cones. These are built up during relatively small-scale explosive eruptions where red-hot rocks are thrown from the vent into the air, cool and then land. The magma on this island is usually basaltic.

Mafic and silicic pyroclastic deposits are distributed across Ascension Island, much of them are trachyte, rhyolite and obsidian, all igneous rocks. These types of rocks have a medium magnetic susceptibility, which is considerable for correlation to Z component. A geological map of Ascension is in figure 4.

The two South Atlantic islands of this paper are better represented by igneous rocks, and basalt is the most common one in both islands. The iron oxide content of basalt can vary from 3.8 to 8.1% and because of this high iron content magnetite is a common mineral in basalts. The magnetic susceptibility of basalt (as in all igneous rocks) is relevant as well, and this is an important feature that can affect the behavior of Z component in these two islands.

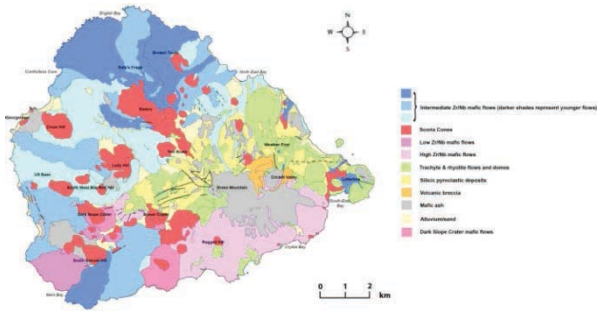

Figure 4. Geological map of Ascension Island

The Tatuoca region has predominantly estuarine sediments, the source of its sediments is both fluvial and marine. They are holocene post-barrier sediments, with variable thicknesses from 2 to 5 meters, compound by fine to very fine sands, well selected with dispersed charcoal fragments and, eventually, ceramic fragments. These sediments cover the older post-barrier lower sediments, which form a package with a thickness of up to 10 meters, consisting predominantly bioturbated sands, from moderate to good selection, fine to medium granulometry, and may be locally coarse to conglomerate.

Kourou has the geology very similar to Tatuoca, having in its majority sedimentary rocks.

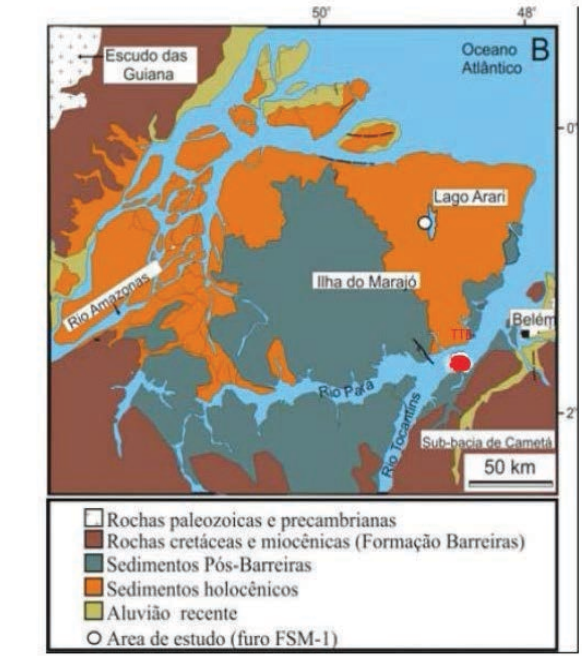

Figure 5. Geological map of the region of Tatuoca

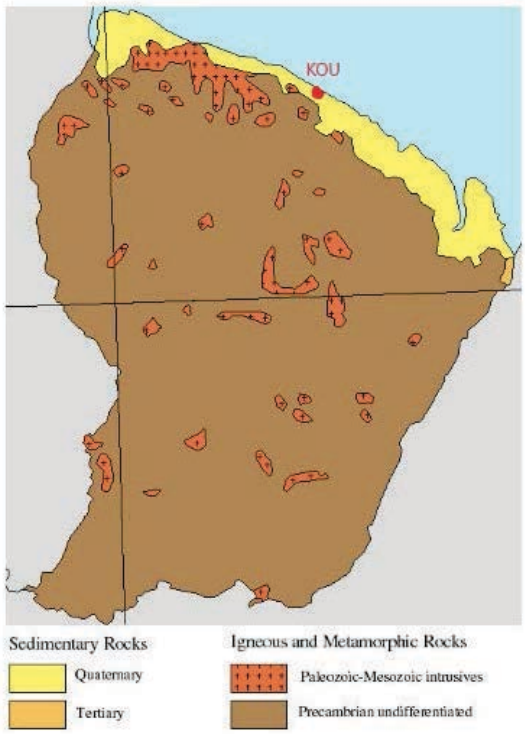

Figure 6. Geological map of the region of Kourou

Conclusions

The present work showed that the morphology of the curves obtained for Z might be interpreted to be due to the Equatorial Electrojet (EEJ) and the SAMA.

It can be seen that the variation in the Z component is a result of the great influence of the Sq current system and in a smaller scale it is due to induction effects in the ocean (Kuvshinov *et al.,* 2007).

The geological influence is imperceptible in the graphs seen, because it is very small when compared with the Sq system.

For a better understanding of the geological influence in the curves, it will be necessary to use a longer period of days, and a statistical analysis should be done using the frequency domain in the same diurnal variation for comparison with the depth of the crust. Finally, a model should be made aggregating all of these influences

The diurnal variation of the Z component displayed an opposite sign from the northern side of the dip equator to the southern side.

The EEJ can enhance the Sq current system in the equatorial region, however, a kind of phase difference was observed between the three stations studied. This phase shift may be attributed to the differences in their latitudinal locations.

The data of Z component from ASC can be a problem in some cases, because of all the variations in the magnetization that a volcanic island can have.

The pattern obtained in the curves revealed that D has deviated from the normal known variation of morning trough and afternoon crest. This could be attributed to change in electric field at the magnetosphere (Okeke et al., 1998).

Acknowledgements

The authors are thankful to the Observatório Nacional, CNPq and CIEE for the financial support. Also, we thank the INTERMAGNET for the KOU, TTB and ASC data. And to the 2 Pangeo's committee for the opportunity.

References

Baker, P. E., Gass, I. G., Harris, P. G., and Le Maitre, R. W., 1964, The volcanological report of the Royal Society expedition to Tristan da Cunha, 1962: Philosophical Philosophical Transactions of the Royal Society of London. Series A, Mathematical and Physical Sciences, v. 256.

Brandl, W., "Erdmagnetische Untersuchungen im Brockenmassif", Abh. der Preuss. Geol. Landes., N. F., 188 (1939) 82 pp.

Freire, L., Laranja, S. R. and Benyosef, L, 2016. Geomagnetic Field Variations in the Equatorial Electrojet Sector, VII Simpósio Brasileiro de Geofísica.

Gelvam A. Hartmann and Igor G. Pacca. Time evolution of the South Atlantic Magnetic Anomaly, Annals of the Brazilian Academy of Sciences (2009) 81(2): 243-255.

International Service of Geomagnetic Indices.

James Cresswell (UK), The geology of Saint Helena, Ascension Island and Tristan da Cunha, Deposits Magazine - Issue 45 (2016), pages 17-23.

Jürgen Matzka, et al.,2009. Geomagnetic observations on Tristan da Cunha, South Atlantic Ocean, ANNALS OF GEOPHYSICS, VOL. 52, N. 1, February 2009.

Kuvshinov, A., C. Manoj, N. Olsen, and T. Sabaka (2007), On induction effects of geomagnetic daily variations from equatorial electrojet and solar quiet sources at low and middle latitudes, J. Geophys. Res., 112, B10102, doi:10.1029/2007JB004955.

Le Sager, P., and T. S. Huang, Longitudinal dependence of the daily geomagnetic variation during quiet time, J. Geophys. Res., 107(A11), 1397, doi:10.1029/2002JA009287, 2002.
Richard A. Geyer, 1951: Geomagnetic Survey of a Portion of Southeastern New York State. Geophysics, vol. 16, issue 2, p. 228.

Susan Macmillan, Chris Turbitt and Alan Thomson, 2009. Ascension and Port Stanley geomagnetic observatories and monitoring the South Atlantic Anomaly, ANNALS OF GEOPHYSICS, VOL. 52, N. 1, February 2009.

Weaver, B. 2002: A Guide to the geology of Ascension Island and Saint Helena, ebook.

Weaver, B. Website:
http://mcee. ou.edu/bweaver/Ascension/sh.htm.

Yamazaki, Y., et al., 2011. An empirical model of the quiet daily geomagnetic field variation, Journal of Geophysical Research, 116, A103112.

Modelling Geomagnetically Induced Currents Using Data from a Remote

Ciaran Beggan[1] *Gemma Richardson*[1]
[1] *British Geological Survey, Edinburgh, UK*

Keywords: Geomagnetically Induced Currents, Space Weather, Rapid Time Variations

Space weather effects on grounded infrastructure such as high-voltage power networks have been well documented over the past three decades. Current research on Geomagnetically Induced Currents (GIC) seeks to understand both the detailed effects of extreme geomagnetic storms on transformers as well as methods for nowcasting or forecasting the magnitude of such events in real-time, particularly where only sparse measurements may be available.

We examine the use of remote observatories (up to 1000 km away) to model the GIC flowing in two hypothetical power grids. The first grid is the benchmark test grid of Horton et al (2012) with 15 'transformers' and the second is a simplified version of the UK power network with around 250 nodes.

We place the grids at high geomagnetic latitudes in the auroral to sub-auroral zone around Hudson Bay in Canada and use data from three local magnetic observatories (Baker Lake: BLC; Fort Churchill: FCC and Poste de-la-Baleine: PBQ). We use magnetic data from three large storms of March 1989, June 1991 and October 2003 and a simple land/sea conductance model to calculate the geo-electric field using the thin-sheet modelling method. The GIC flowing with each grid is computed, both separately and jointly, from the magnetic field recorded at the observatories. As a second experiment we site the same grids in the UK and use up to five observatories within and around the UK to compute GIC both jointly and separately.

Using Taylor plots to compare the resulting GIC models we find that, although the correlation between the GIC flows computed from the different observatories varies with distance to the instrument, the magnitude of the GIC are similar to within 20%, particularly if they are at a similar latitude. This suggests that remote observatories can provide useful information for nowcasting GIC flow at high latitudes if they are within 500 km and at a similar latitude to the power grid.

Comparação do Comportamento de Pulsações Pc3 em Diferentes Latitudes da Anomalia Magnética

Piassi, A. [1]; Alves, L. [1]; Padilha, A[1]

[1] Instituto Nacional de Pesquisas Espaciais,

Av. dos Astronautas, 1758, 12227-010 São José dos Campos (SP) - CEP: 12227-010;

RESUMO

No presente trabalho é realizado um estudo sobre a ocorrência, amplitude e densidade de potência de pulsações magnéticas do tipo Pc3 na região da Anomalia Magnética do Atlântico Sul (AMAS) durante o período de recuperação da tempestade de 17 de março de 2015, a maior tempestade geomagnética do ciclo solar atual. A AMAS é uma região caracterizada por um mínimo no campo geomagnético principal, ocorrendo assim um enfraquecimento das linhas de campo magnético nessa região. Este enfraquecimento do campo apresenta alterações ao longo do tempo em sua topologia, principalmente devido ao deslocamento dos polos magnéticos e à diminuição global do campo magnético, o qual já perdeu cerca de 10% de sua intensidade desde o século 19. Como consequência desse deslocamento do campo, a AMAS já esteve sobre a África e continua a deslocar-se no sentido oeste. Também, pelo fato de o campo magnético ter menor intensidade na região da anomalia, os cinturões internos de radiação de Van Allen situam-se mais próximos da Terra o que faz com que partículas carregadas provenientes desses cinturões aproximem-se mais da superfície da Terra e se precipitem na alta atmosfera da região. Esse incremento na precipitação de partículas implica que os níveis de radiação sejam mais altos nesta área o que prejudica os satélites em sua passagem pela região. Apesar de a anomalia ser conhecida há bastante tempo e prevista pelo modelo do IGRF, ainda há carência de estudos sobre que a sua dinâmica, os mecanismos associados à geração desse mínimo de intensidade e em como este enfraquecimento das linhas de campo pode influenciar em perturbações da condutividade da ionosfera. Com o objetivo de estudar esse último aspecto, o presente trabalho apresenta resultados preliminares da avaliação do comportamento de pulsações geomagnéticas, medido por magnetômetros fluxgate instalados em estações geomagnéticas operando em diferentes latitudes na região da anomalia. Os resultados obtidos mostram uma variação sistemática no comportamento das pulsações em função da distância do centro da anomalia, um resultado que pode ser utilizado para fornecer informações a respeito dos efeitos da diminuição do campo principal sobre a condutividade da ionosfera.

Autor para contato: Amanda Piassi(amanda.piassi@inpe.br)

Fulguraciones Solares de los Primeros Dias de Septiembre 2017 Registrados Por el Observatorio Geomagnetico de Villa Remedios Y El Monitor de Neutrones Nm-64 de Chacaltaya Cotejados con Registros de Flujo de Rayos X Solares del Satelite GOES

Ricaldi Y.E.L.1,2, Ticona P.R.1,2, Miranda L.P.1,2, Quispe M.J.1,2

1Universidad Mayor de San Andrés U.M.S.A.

2 Instituto de Investigaciones Físicas I.I.F. − U.M.S.A.

ericaldi@gmail.com, pmiranda@fiumsa.edu.bo, rticona@fiumsa.edu.bo & javierlinux21@gmail.com

Abstract

Because the conditions of the sun involve intense magnetic fields and in them live electrons moving at high energies, this is a natural source of X-ray emission by synchrotron effect. It is known that solar X-rays are produced in its Atmosphere, in its crown, characterized by containing very hot gases at millions of degrees of temperature.
The sun's magnetic field varies from complex structures in years of active sun to simpler configurations in years of quiet sun. Many of the observable magnetic variations on the surface of the Earth have their origin in the behavior of the Sun. Establishing relationships between the interior of the sun with the solar crown and consequently relations between the behavior of the sun and the Earth. Solar events, especially those that occur in the sun's activity zones, (sunspots) produce electromagnetic radiation that can be recorded by the corresponding sensors installed in research satellites, continuously, as the GOES satellite that measures the flow of X-rays from the sun (NOAA / SPWC), and geomagnetic observatories installed on the surface of the Earth. The geomagnetic observatory of Villa Remedios located at a latitude of −16o460 000 N and longitude of −68o100 000 W at 3949 meters above sea level, located 13 [km] south of the city and the Neutron Monitor (NM-64) of the Cosmic Physics Laboratory located at Mount Chacaltaya of latitude −16o250 6000 N and longitude −68o100 0.100 E at 5220 meters above sea level, both observatories located in La Paz − Bolivia, continuously record the geomagnetic behavior of the earth where sufficiently intense solar events can be observed in both observatories. We show and identify 5 signs of storms of notable disturbances that are in correspondence (correlation) with the records of solar X-ray flow of the GOES satellite that occurred on the days of September 3 to 12. These events are classified and analyzed statistically as Crochets and geomagnetics storms. The results of the main causes for the production of geomagnetic storms are discussed in this document.Keywords: X-ray; GOES satellite; Geomagnetic Observatories; Geomagnetic storm; Disturbance time

Introducción

Los primeros días del mes de septiembre 2017, la NOAA/SWPC anuncia la evolución de al- gunas regiones activas del sol a la producción de potentes fulguraciones. Debido a que las condiciones del sol implican: poderosos cam- pos magnéticos, una temperatura promedio de 60000 K en su superficie y que su atmosfera en la parte de su corona es muy caliente, al- canzando millones de grados kelvin, genera dos hipótesis que tratan de explicarla: Calen- tamiento de la corona solar a través de interac- ciones magnéticas, Los bucles magnéticos coro- nales realizarían re conexiones y chasquidos desprendiendo calor. Ondas magnéticas que se originarían al interior de la superficie de sol que por burbujeo liberarían energía mag- nética a la corona, la cual se tornaría en energía térmica. Estas estructuras convierten al sol en un acelerador formidable de partículas permi- tiendo el estudio detallado de la aceleración de los electrones pero aun inconclusa de los iones, que a veces alcanzan energías correspondientes a velocidades relativísticas. La superficie solar emite la mayor parte de la radiación electro- magnética como luz visible. Con la finalidad de evitar el efecto de los campos magnéticos se estudian (observan) las partículas secundarias neutras y las radiaciones solares, además que estas se registran con excelente resolución es- pacial y temporal. Los neutrones solares se producen por reacciones nucleares a través de la interacción entre los iones acelerados con energías alrededor de los 100 MeV y la atmos- fera solar librándose de la contaminación de radiación de electrones. Los electrones acelera- dos que habitan la atmosfera solar se mueven a energías extremadamente elevadas, convir- tiendo a esta, la atmosfera solar, en una fuente natural de rayos X por efecto sincrotrón, de- saceleración de electrones, reducción de su ve- locidad en trayectorias espirales alrededor de las líneas de campo magnético de las protuber- ancias solares, produciendo perdida de energía que genera rayos X. La energía de estos rayos X se reduce grandemente durante su viaje a la Tierra y pueden ser registrados de diversas for- mas, de manera directa o por sus efectos secundarios entre

estos por variaciones del campo magnético de la tierra en los observatorios geo- magnéticos.

II. Registros de Flujo de Rayos X y otros, por sensores instalado en el satélite GOES de la noaa/swpc.

Las figuras 1 y 2 ilustran por separado los reg- istros temporales de incremento significativo del flujo de rayos X, obtenidos por los sensores del satélite GOES de la noaa/swpc en las fechas 6 y 10 de septiembre 2017, respectivamente.

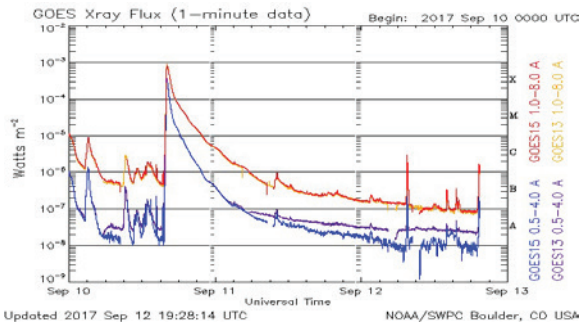

Figure 1: Registro Flujo de Rayos X el 20170906

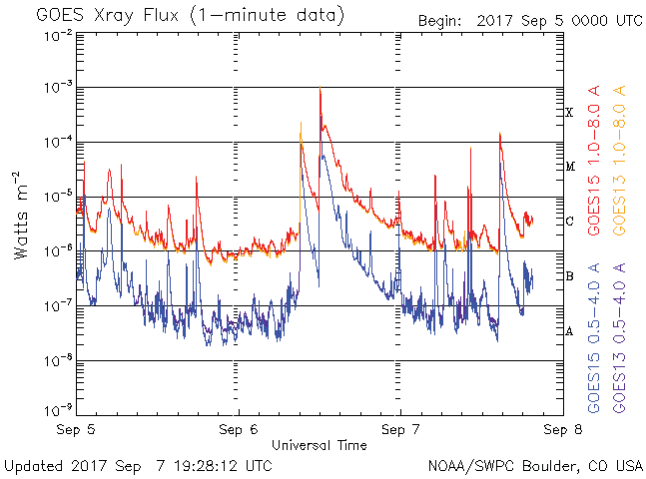

Figure 2: Registro Flujo de Rayos X del 20170910.

En la figuira 3 se procede a describir el com- portamiento de la actividad solar, momentos de tiempo de los eventos de Fulguraciones solares que se dieron en el transcurso del tiempo (3 al 13 de septiembre), el Flujo en Watts/m2, su clasificación correspondiente de acuerdo a escala en uso, la localización de la zona activa sobre el disco solar y se incluyen dos de sus efectos más notables sobre el campo magnético de la tierra, los Crochets y Tormentas magnéti- cas, con finalidades de correlación.

III. Registros del Monitor de Neutrones NM-64 de Chacaltaya

Las figuras 4 y 5 que se presentan a contin- uación ilustran el incremento temporal de las cuentas de neutrones solares para promedios de 5 y 10 minutos, respectivamente. La línea azul representa los eventos de neutrones y la línea roja la presión en el observatorio para fines de corrección

IV. Interacción Sol-Tierra

El campo magnético del sol varia de estruc- turas complejas en años de sol activo a configuraciones mas simples en años de sol quieto. Muchas de las variaciones magnéticas observables en la superficie de la tierra tienen su origen en el comportamiento del sol.

CORRELACION: DATOS FLUJO DE RAYOS X CON REGISTROS MAGNETICOS

Registros: GOES X - ray Flux (1-Minute data)

Registros: Componentes H,D y Z, Observatorio Villa Remedios - Bolivia (1-Minute data)

AÑO	MES	DIA	INICIO	MAXIMO	FINAL	Flujo, Watts/m2	Clase	Registro magnetico del Flare	Tiempo viaje radiacion	Posicion Area activa solar	Registro magnetico, componente H	Tiempo viaje Nube plasma
2017	9	3	4:58	4:41	4:54	10^-5	C1.0	Imperceptible			Quieto	
2017	9	4	8:08	8:14	8:24	10^-5	C2.9	Imperceptible			Quieto	
2017	9	4	12:12	12:25	12:33		C8.3	Imperceptible			Quieto	
2017	9	4	20:45	20:50	20:55	10^-5	C1.9	Imperceptible			Quieto	
2017	9	5	0:30	0:36	0:41	10^-5	C9.8	Imperceptible			Quieto	
2017	9	5	4:33	4:53	5:07		M3.2	Imperceptible			Quieto	
2017	9	5	16:14	16:19	16:22	10^-5	C3.7	Imperceptible			Quieto	
2017	9	5	17:20	17:39	17:48	10^-5	C6.0	Crochet, 17:47:00, aperus reconocible	0:08	Casi frontal, 12674-E	Quieto	
2017	9	6	7:29	7:34	7:48		C2.7	Imperceptible			Quieto	
2017	9	6	8:57	9:10	9:17	10^-6	X2.2	Crochet, 09:18:00, reconocible	0:08	Casi frontal, 12674-E-N	Quieto	
2017	9	6	11:53	12:02	12:10	10^-3	X9.3	Crochet, 12:10:00, bien definida	0:08	Frontal, 12673-E-S	Quieto	
2017	9	6	21:06	21:12	21:20		C1.5	Imperceptible			Quieto	
	9	6	23:50								Variable, 23:50 SSC, Tormenta, Kp=5, G1	1 dia 6 h 3 min
2017	9	7	4:59	5:02	5:08	10^-4	M2.4	05:12:00 , aperus reconocible.	0:08		Disturbado	
2017	9	7	6:19	6:28	6:42		C8.2	Imperceptible			Disturbado	
2017	9	7	10:11	10:15	10:18		M7.3	10:23:00, apenas reconocible.	0:08		Disturbado	
2017	9	7	14:20	14:36	14:55		X1.3	Crochet, 14:44:00, reconocible.	0:08	Casi frontal, 12673-E-S	Disturbado	
	9	7	20:50								Variable, 20:50, sin SSC, Tormenta, Kp=6, G2	1 dia 11h 42min
	9	7	23:05								Variable, 23:05 SSC, Tormenta, Kp=6, G2	1 dia 10h 50min
2017	9	7	23:33	23:39	23:44		M1.2	Imperceptible				
2017	9	8	5:31	5:48	5:53	10^-4	C8.2	05:56:00 , aperus reconocible	0:08		Disturbado	
2017	9	8	7:40	7:49	7:58		M8.1	07:57:00, aperus reconocible	0:08		Disturbado	
2017	9	8	15:09	15:47	16:04		M2.9	Crochet, 15:55:00, reconocible	0:08	12673, Lejano E	Disturbado	
	9	8	22:50								Variable, 22:50 SSC, sin Tormenta	1dia 8h 4min
	9	8									Disturbado, alta frecuencia entre 12:00-18:00	
2017	9	9	0:36	0:39	0:46	10^-4	C1.0	Imperceptible			Quieto	
2017	9	9	3:57	4:01	4:07		C4.2	Imperceptible			Quieto	
2017	9	9	10:57	11:04	11:42		M3.7	Crochet, 11:12:00, aperus reconocible	0:08	12673 en el limbo E	Quieto	
2017	9	9	23:33	23:45	23:56		M2.1	Imperceptible			Quieto	
2017	9	10	2:40	3:09	3:25	10^-5	C9.0	Imperceptible			Quieto	
2017	9	10	9:02	9:20	9:37		C2.9	09:28:00, aperus reconocible	0:08		Quieto	
2017	9	10	12:38	12:54	13:24	10^-5	C1.9	13:02:00, aperus reconocible	0:08		Quieto	
2017	9	10	15:35	16:02	16:31	10^-3	X8.2	Crochet, 16:10:00, bien definida	0:08	Frontal, 12678	Quieto	
	9	10	22:45								Variable, 22:45 SSC, Tormenta, Kp=5, G1	1dia 11h 33min
2017	9	11	10:00	10:12	10xx	10^-6		10:19			Quieto	
2017	9	12	7:22	7:27	7:34	10^-6	C3.0	07:35:00, aperus reconocible	0:08		Disturbado	
											Variable, 00:40 SSC, sin Tormenta	1dia 9h 26min
2017	9	12	20:01								Variable, 20:01 SSC, Tormenta, Kp=6, G2	1dia 9h 32min

Figure 3: El comportamiento de la actividad solar

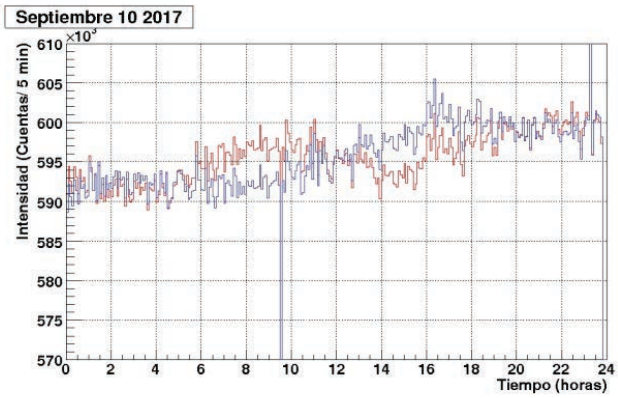

Figure 4: Registro de la fulguración solar Del 20170910 por el Monitor de Neutrones (MN) del Observatorio de Rayos Cósmicos de Chacaltaya (OR- CCh) con una resolución promedio de cuentas cada 5 minutos. Línea azul eventos de neutrones, línea roja registro de la presión en el observatorio para corregir datos.

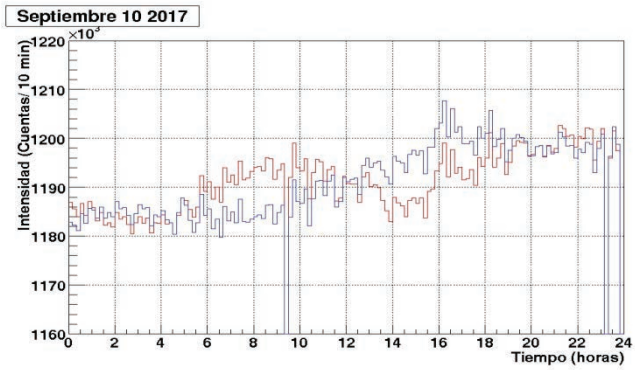

Figure 5: Registro de la fulguración solar Del 20170910 por el Monitor de Neutrones (MN) del Observatorio de Rayos Cósmicos de Chacaltaya (OR- CCh) con una resolución promedio de cuentas cada 10 minutos. Línea azul eventos de neutrones, línea roja registro de la presión en el observatorio para corregir datos.

Estableciéndose relaciones entre el interior del sol con la corona solar y en consecuencia relaciones entre el comportamiento del sol y la Tierra. Eventos solares, especialmente aquellos que ocurren en las zonas de actividad del sol, las manchas solares, que producen radiación electromagnética pueden ser registrados por los correspondientes sensores instalados en satélites de investigación, de manera continua, como el satélite GOES de la NOAA/SPWC, que pueden medir el flujo de rayos X que provienen del sol. Los observatorios geomagnéticos instalados sobre determinados puntos de la superficie de la tierra, pueden también registrar estos eventos solares si son suficientemente intensos y únicamente en horas en que estos puntos están de frente al disco solar, es decir durante las horas en que se tiene al sol de frente y en consecuencia no registraran eventos que se produzcan en horas de la noche terrestre, puesto que estos eventos, los electromagnéticos se producen a tremendas velocidades por cortos intervalos de tiempo. Entonces muchas de las fulguraciones del sol no dejaran huellas en los registros magnéticos de otros puntos de la superficie de la tierra. Las masas coronales eyectadas (MCE, CME, Coronal Mass Ejection en ingles) consecuencia de las Fulguraciones Solares también son registrados por los Observatorios Magnéticos de Superficie (OMS) con determinadas características. Con por ejemplo, CRT (Comienzo Repentino de Tormenta, SSC, Sudden storm commencement por sus siglas en ingles) nítidas o difusas, a cualquier hora del día, incluidas horas de la noche, continuadas de las Tormentas Magnéticas (TM, MS, Magnetic Storm por sus siglas en ingles), intensas o débiles, como resultado de la interacción de la Nube de Plasma Eyectada (CME-Coronal Mass Ejection) por el sol con el Campo Magnético (propio) de la Tierra. El nexo entre los fenómenos solares y los de la tierra se realiza a través del Viento Solar (VS, SW, Solar Wind) radiación solar constante y el Campo Magnético Interplanetario (CMI, IMF, Interplanetary Magnetc Field), espacio entre el Sol y la Tierra, ocupado por el Campo Magnético del Sol que se extiende más allende la posición de la tierra, a través de los cuales viaja la MCE (CME, Coronal Mass Ejection) del Sol.

V. Registros del Observatorio Geomagnético de Villa Remedios

El Observatorio Geomagnético de Villa Remedios (VRE) localizado en las coordenadas geográficas, 19K588448.58 m E – 8145634 m S y 3949 m de elevación sobre el nivel del mar, ubicada a 13 Km al sur de la ciudad de La Paz, en sus registros correspondientes a los primeros días de Septiembre, 3 al 12, del 2017, en sus tres componentes: H, D y Z, muestra señales muy claras de origen solar. Las figuras 6 y 7 por separado ilustran los Crochets magnéticos, señales magnéticas impresas por los rayos X y por los Neutrones emitidos por las fulguraciones solares del 6 y el 10 de Septiembre 2017,respectivamente.

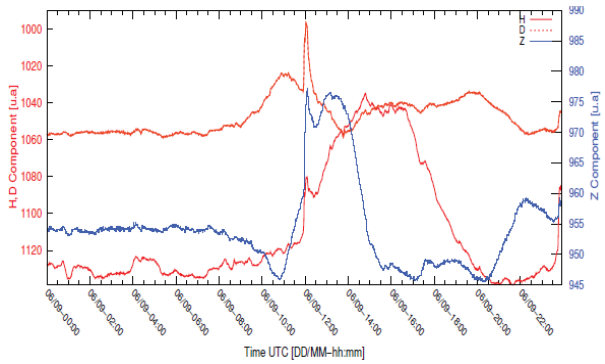

Figure 6: Registro de un Crochet, en las tres componentesdel campo magnético, mejor definido en sus componentes Z y H, correspondiente al 20170906, obtenido por el Observatorio Geomagnético de Villa Remedios (VRE) - Bolivia.

De todos los registros disponibles y la información contenida en la Figura 3, a continuación se esumen los eventos más notables :

- 20170905 17:47 crochet magnético claramente perceptible.
- 20170906 09:16 Crochet magnético apenas perceptible, Fulguración clase X8.3

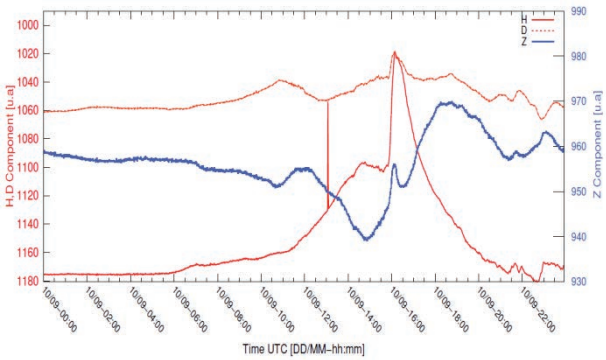

Figure 7: Registro de un Crochet, en las tres componentes del campo magnético, notable en su componente H, correspondiente al 20170910, obtenido por el Observatorio Geomagnético de Villa Remedios (VRE) □ Bolivia.

- 20170906 12:10 crochet magnético bien definido, 30 nT/10 min en la componente H, Recuperando altura apuntando hacia el W., Fulguración X9.3, muy intensa.
- 20170907 14:44 crochet magnético perceptible, circuito horizontal hacia el E, cambio al W.
- 20170908 15:55 Crochet magnético perceptible, compresión de H y Z, cambio hacia el W.

_ 20170909 11:12 crochet magnético apenas perceptible con cambio hacia el W.

_ 20170910 16:10 crochet magnético bien definido, 120 nT/80 min en H, cambio de dirección al W., Fulguración X8.2

_ 20170911 10:19 crochet magnético apenas perceptible, cambios muy pequeños.

Sea enlistado algunas de las señales magnéticas perceptibles que están en correspondencia (correlación con desfases constantes) con los registros de Flujo de rayos X solares del satélite GOES de las mismas fechas. Ver Tabla 1 y Graficas correspondientes para mayor detalle. Las figuras 7, 8 y 9 ilustran los registros magnéticos de días continuados en sus: Componente H superpuesto con el modelo (primera aproximación) de su Variación Diaria Solar (VDS), aclarando los excesos de campo magnético, correspondientes a circuitos eléctricos ionosfericos, Crochets y otros, y déficits de campo magnético producidos por interacción entre la Masa Coronal Eyectada solar, (MCE) con la Magnetosfera terrestre, Tormenta Magnética (MT). Componente D superpuesto con su modelo VDS correspondiente y la Componente Z, también superpuesta con su VDS, respectivamente.

VI. Crochets magnéticos

Dos de los Crochet magnéticos enlistados están muy bien definidos y claros, están en correspondencia con la emisión de Rayos X, emitidos desde una posición frontal de la Región Activa (Mancha Solar) Nro. 12673 en Septiembre 6 y de la Región Activa Nro. 12678 no frontal en Septiembre 10, respectivamente, observados con relación a la posición terrestre de Villa Remedios donde fueron registrados a las 12:10 y 16:14 UT, horas de la mañana, 8:10 y 12:14 Hora local (LT), en el lugar de registro, respectivamente. En los registros de Flujo de Rayos X del GOES, lo momentos de máxima intensidad de las Fulguraciones son indicadas con las horas 12:02 y 16:06 UT, respectivamente. De los datos indicados se
infiere una diferencia de tiempo igual a 8 minutos que correspondería al tiempo de viaje entre el Sol y la Tierra de esta radiación de alta energía. La intensidad de la Variación del Campo Magnético Terrestre producidas por ambas Fulguraciones solares son relativamente pequeñas, de 30 nT con 20 min de duración y 120 nT con 80 min de duración en la componente H, respectivamente. Son campos magnéticos adicionales que se enganchan al Campo Magnético Propio de la Tierra y son denominados Crochets magnéticos (CM).

El primer crochet magnético sería el resultado de un chorro de corriente eléctrica que se mueve hacia el Este hacia alturas mayores con un gran cambio de dirección hacia el Oeste en horas de la mañana (8:10 LT). El segundo provendría de un chorro de corriente eléctrica
que se mueve horizontalmente hacia el Este sin un cambio de dirección significativo hacia el Oeste, comenzando justo al medio día con un tiempo de duración de 80 minutos, que como se dijo anteriormente están en correspondencia con las Fulguraciones solares que emitieron rayos X de gran intensidad de clase X.

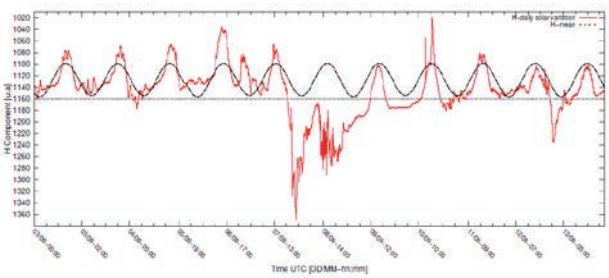

Figure 8: Record continuous days component H, superposition model VDS, highlighting of magnetic fieldsurpluses (electrical circuits), Crochets and others and field deficits product of the interaction of the CME with terrestrial Magnetosphere. (Magnetic storms). Registros de días continuados de la componente H incluyendo la superposición del modelo de la Variación Diaria solar (VDS), el remarcado con amarillo de los excesos de campo magnético correspondientes a Crochets y otros eventos magnéticos producto de corrientes eléctricas ionosféricas incrementadas y con azul los déficits de campo magnético producto de la interacción de la Masa Coronal Eyectada (MCE) con la Magnetosfera terrestre, Tormentas Magnéticas (TM).

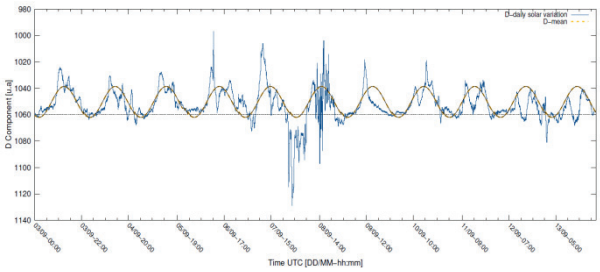

Figure 9: Continuous days record component D, superposition VDS model. Registro de días continuados de la componente D con superposición del modelo de la VDS correspondiente.

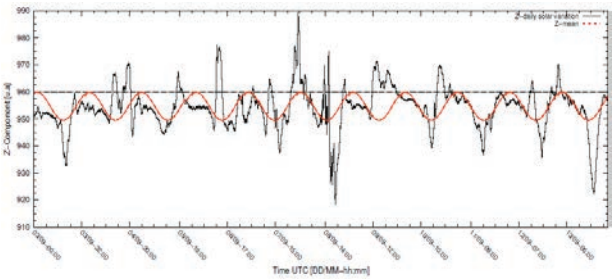

Figure 10: *Continuous days record Z component, superposition model VDS. Registro de días continuados de la componente Z con superposición del modelo de la VDS correspondiente*

VII. Tormentas magnéticas

Ambas Fulguraciones solares han logrado la Eyección de Masa Coronal (CME), Nube de Plasma Solar (NPS), que producen Tormentas Magnéticas (TM) en el Campo Magnético Propio de la Tierra (CMTP). La primera de aproximadamente 800 nT, y la segunda de muy escasa magnitud, al haberse producido el contacto de la MCE con el Campo Magnético de la Tierra (CMT, Magnetósfera) a:

_ Las 23:05 UT del 7 de Septiembre, significando un tiempo de viaje de 34h 45min, es decir 1día 10 horas y 45 min, generando un Comienzo Repentino de Tormenta (CRT=SSC, Sudden Storm Commencement) pequeño de 30 nT y 15 minutos de duración, correspondiente a la etapa de compresión del CMT para continuar con una abrupta caída de su Fase Principal (FPT), descompresión o expansión de la magnetosfera terrestre o del CMT, a niveles muy bajos respecto del Nivel de Referencia Normal (NRN), 250 nT aproximadamente.

Continuada por una fase de recuperación (FR) suave de más de 1 día de duración. El nivel de la componente H

retorna a valores bajos durante todo el día, 8 de Septiembre. Debido a la ocurrencia de una nueva perturbación se presentan altas frecuencias a partir de las 12:00 UT hasta las 16:00 UT para luego alcanzar una fase recuperativa nueva suave hasta el medio día del siguiente día, 9. Tormenta Magnética (TM) que puede ser calificada de nivel: Índice Kp =7 a 8, G3 a G4.

_ Las 00:40 UT del 12 de septiembre que no genera un CRT (Storm Sudden Commencement) claro, 8 nT/20 min., tampoco genera una Tormenta (Magnetic Storm) de características intensa, pero si logra generar una fase principal de 100 nT y una fase recuperativa suave característica de 1 día de duración. Los demás registros de las Fulguraciones Solares (Flares) muestran características similares pero son difíciles de reconocerlas magnéticamente.

En fecha 20170910 el Monitor de Neutrones NM64 localizado en el monte Chacaltaya, también en sus registros muestra una señal notable en sus graficas construidas en base a promedios de 5 y 10 minutos, que coinciden con los tiempos de arribo del flujo de rayos X

del sensor del satélite GOES. Los rayos X junto con otros penetrantes no cuentan con masa ni carga viajan a velocidades iguales a la de la velocidad de la Luz y no son interferidos por los campos magnéticos interplanetarios y tiene capacidad de ionización. Los neutrones que si tienen masa se mueven a velocidades por debajo de la velocidad de la luz, es decir tardan un poco más que las radiaciones y tienen capacidad de ionización por interacción nuclear. Estos eventos solares, como ya dijimos, impactan de acuerdo a su comportamiento sobre los átomos de la ionosfera que principalmente son de oxigeno, generando circuitos eléctricos intensos de corta duración que modifican de acuerdo a dirección de arribo los circuitos eléctricos a nivel ionosfera circunscriptos al lado iluminado de la tierra que son los responsables para la generación de los campos magnéticos secundarios denominados Crochets magnéticos. En 20050907 los Observatorios Geomagnéticos de Villa Remedios y Patacamaya registraron un crochet magnético a las 17:40 UT (13:40 LT, medio día local) correspondiente a una Fulguración

Solar frontal, corroborado por los registros de: un Detector de Neutrones Solares TNS y un Monitor de Neutrones 12-NM64 del Laboratorio de Rayos Cósmicos de Chacaltaya y el Detector de Flujo de Rayos X del satélite GOES, caracterizado por una intensidad de campo magnético cercano a los 400 nT. Este evento se produjo durante el periodo de Máxima Actividad Solar, Sol Activo, del Ciclo Nro. 23.

VIII. Conclusiones

La observación cuidadosa de los registros y la tabla de resumen de características del comportamiento del campo magnético terrestre relacionado al comportamiento del Sol, motivo de estudio, nos conducen a las siguientes conclusiones:

_ Las imágenes del Sol en diferentes frecuencias y para diferentes radiaciones y los registros del flujo de rayos X logrados por el satélite GOES proporcionan abundante información de lo que sucede en la superficie y la atmosfera solar: Velocidad de movimiento rotacional del sol alrededor de su propio eje de rotación, numero y posición de las regiones activas (manchas) del Sol y proporciona la posibilidad de estudiar los mecanismos de generación de las diferentes radiaciones como: los rayos gamma, rayos X, protones e iones en general, las estructuras que las disparan al especio exterior, las direcciones preferenciales de emisión de las radiaciones electromagnéticas y la eyección de masa coronal (partículas), además de otros.

_ Que es muy importante considerar la posición relativa de los observatorios geomagnéticos de superficie a la hora de observar lo que sucede en la atmosfera solar por medio de sus registros. Como son la posición de frente del observatorio geomagnético respecto del disco solar, la posición de las regiones activas del sol respecto de su meridiano central, si están adelantadas retrasada o de frente al mismo.

_ No todas las señales de flujo de radiación X registradas por los detectores y las cámaras fotográficas de los satélites están registradas como señales magnéticas en los registros de los observatorios de superficie. Porque, sin importar la posición de la región activar solar que la genera, La dirección de emisión de los rayos X emitidos por el sol parece ser radial (hay
que estudiar con mas detenimiento para determinar si tiene alguna dirección preferencia, que parece que la tiene!), producen señales de diferente intensidad. Y/o las
fulguraciones se produjeron en horas de la noche correspondiente al observatorio en consideración. Los efectos magnéticos de la radiación X y del proceso de fulguración en sí, son tan rápidos que no pueden dejar huellas en otros instantes.

_ Fulguraciones poderosas de regiones activas del sol que no estuviera en posición frontal no están en posibilidad de generar señales geomagnéticas observables en horas del día del observatorio.

_ No todas las Eyecciones de masa coronal (CME) que pudieran generar las fulguraciones solares están en posibilidades de generar Tormentas magnéticas, ni siquiera SSC claras debido a que;

_ Las CME son direccionales, con dirección preferencial radial. Para lograr generar tormentas magnéticas deben tener una posición muy cercana a la frontal, adelante o atrás, observada desde el observatorio geomagnético. De lo contrario, por más que en la superficie del sol se produzcan poderosas fulguraciones con gran emisión de CME estas no impactaran sobre la magnetosfera terrestre.

References

[1] Ricaldi, E. Miranda P., Observaciones Geomagneticas en el observatorio de Patacamaya. Revista Boliviana de Fisica NUMERO 2 Julio 1996.

[2] Vilca Salinas, R. 2001, Master's thesis, Carrera de Física, Universidad Mayor de San Andrés, La Paz, Bolivia

[3] Mendoza, M. & Morales, J. 2004, Analysis of the Interaction of the Solar Wind with the Terrestrial Magnetosphere, Tech, rep., Departamento de Física, Universidad Nacional de Colombia, Ciudad Universitaria,

Bogotá, D.C., Colombia

[4] Ricaldi, E. 2007, Observación simultánea de neutrones solares en asociación con una fulguración solar del 7 de septiembre de 2005 (HF-UMSA).

[5] Calcina, M.. Un modelo dinámico para el campo Geomagnético. Revista Boliviana de Física [online]. 2009, vol.15, n.15, pp. 44-62. ISSN 1562-3823.

[6] E. Ricaldi et al.; OBSERVACION SIMULTANEA DE NEUTRONES SOLARES EN ASOCIACION CON UNA FULGURACION SOLAR DEL 7 DE SEPTIEMBRE DE 2005; Revista Boliviana de Física, No.13. 200710.

[7] Saco et al. ; EMISION NEUTRONICA SOLAR DE LARGA DURACION COMPARADA CON LA RADIACION PRODUCIDA POR ELECTRONES EN LA FULGURACION SOLAR DEL 7 DE SEPTIEMBRE DE 2005; Revista Boliviana de Física, No. 13; 200710.

[8] Murphy R.; EXPLORANDO LAS FULGURACIONES SOLARES CON RAYOS GAMMA Y NEUTRONES; NRL Review 2008.

[9] NOAA/AWPC Boulder, CD USA; GOES Xray Flux data; 2017.

[10] Observatorio de Rayos Cósmicos de Chacaltaya, IIF-UMSA, Monitor de Neutrones NM64, 2017. [11] Observatorio Geomagnético de Villa Remedios, IIF-UMSA, 2017.

[12] Echer E. et al.; A STUDY OF SOLAR GEOMAGNETIC INDICES CORRELATION;

INPE, 12201-970, Sao Jose dos Campos, SP, Brazil.

[13] TI2AMX – Indices Solares..

[14] http://www.fiumsa.edu.bo/

Study for the Qualification of Magnetic Index Ksa

Bilibio, A. V. [1]; Chen, S. S. [1]; Denardini, C. M. [1];
Resende, L. C. A. [1]; Moro, J. [2,3]; Bertollotto, T. O [1];
Barbosa Neto, P. F [1]; Picanço, G. A. S; [1] Schuch, N. J. [2].
[1] National Institute for Space Research (INPE),
Av. dos Astronautas, 1758, S. J. Campos, SP, Brasil - CEP: 12.227-010;
[2] Southern Regional Space Research Center (CRS/INPE),
Mailbox 5021, Av. Roraima, 1000, Campus Universitário, Santa Maria, RS - CEP: 97105-970;
[3] National Space Science Center, Chinese Academy of Science (NSSC/CAS), Beijing, China.

Abstract

The Brazilian Studies and Monitoring of Space Weather (Embrace) Program of the National Institute for Space Research (INPE) developed the new South American K (Ksa) index. In order to qualify this index, we use magnetometer data collected by the Embrace Magnetometer Network (Embrace MagNet) and the same data collected by a magnetometer of the International Real-time Magnetic Observatory Network (Intermagnet) chain at the same Vassouras Magnetic Observatory, Brazil (VSS, 22.4° S, 43.6° W). These magnetometers provide measurements of the temporal variation of the Earth's magnetic field and, thus, allow us to constructs magnetic activity indexes such as Ksa. In turn, it provides an estimate of the energy deposition in the terrestrial magnetospheric system due to magnetic storms. In this study, we present the methodology used for the validation study of the Ksa index, which consists of mathematical techniques. The results are presented and discussed in terms of an analysis of the quality and precision of the magnetic data of the Embrace MagNet.

Response of the ΔH Made by the Embrace Magnetometer Network: A Case Study

Chen, S. S. [1]; Denardini, C. M. [1]; Resende, L. C. A. [1]; Moro, J. [2,3]; Bilibio, A. V. [1]; Paulo, C. M. [4]; Barbosa Neto, P. F. 1]; Nogueira, P. A. B. [5]; Picanço, G. A. S. [1]; Bertollotto, T. O [1].

[1] National Institute for Space Research (INPE),
Av. dos Astronautas, 1758, S. J. Campos, SP, Brasil - CEP: 12227-010;
[2] Southern Regional Space Research Center (CRS/INPE),
Mailbox 5021, Av. Roraima, 1000, Campus Universitário, Santa Maria, RS - CEP: 97105-970;
[3] National Space Science Center, Chinese Academy of Science (NSSC/CAS), Beijing, China;
[4] Center of Radio Astronomy and Astrophysics Mackenzie (CRAAM), Engineering School, Mackenzie Presbyterian University, Rua da Consolação, 930, Bairro Consolação, São Paulo, SP, Brazil - CEP: 01302-907;
[5] Federal Institute of Education, Science and Technology of São Paulo (IFSP),
Rua Antônio Fogaça de Almeida, 200, Jacareí, SP, Brasil - CEP: 12322-030.

Abstract

In the present work, the magnetometer data of the Embrace Magnetometer Network (Embrace MagNet) are evaluated for uses in space weather studies. The analysis was carried out to investigate the response of the evolution of ΔH derived from the Embrace MagNet throughout the Saint Patrick's Day geomagnetic storm as compared to the evolution of the Dst index during the same period. This comparison consisted of three steps: (a) deriving the ΔH for the Embrace MagNet network and compare it straight to the evolution of the Dst index; (b) deriving the ΔH considering a different number of Embrace MagNet station comprised in its derivation and then compare it to the evolution of the Dst index; and (c) deriving the ΔH for some selected Intermagnet observatories (split into two groups) and compare it to the evolution of the Dst index. The last step was included to verify the application of our methodology for deriving the ΔH. Among the results, we were able to show that ΔH derived from the Embrace MagNet data closely follows the Dst variation with pretty good accuracy in the time of occurrence of the peaks, valleys, and phases of the magnetic storm afterwards. We attributed the discrepancies in the amplitude between the Embrace MagNet ΔH and the Dst to regional characteristic of the magnetic field over the South American sector, e.g. the presence of the South American Magnetic Anomaly (SAMA) and the large declination angle (~ 20° westward) that may act on the Sq current system and, in turn, in the equatorial electrojet (EEJ). Other few longitudinal time-lag dependencies between the Intermagnet ΔH and the Dst observed during the main phase of the magnetic storm were attributed to the time elapsed for the solar particles to distribute themselves into the Van Allen belts leading to different particles densities over the different longitudinal sector of the Earth.

Geomagnetic Survey for Repeat Stations and/or a New Magnetic Observatory at Guárico, Bolívar and Carabobo States in Venezuela

Camacho E.[1,2], Gutierrez E. [1], Benyosef L.[2]

[1] Astronomy Research Center C.I.D.A. – Venezuela
[2] Nacional Observatory (ON) - Brazil

Abstract

The Bolivarian Agency for Space Activities (ABAE) and the Astronomy Research Center (CIDA) are two specialized institutes which interested in magnetic measurements obtained in observatories or repeat stations in Venezuela. In this work are presented the results of four geomagnetic surveys carried out in different locations in Venezuela, with the aim of choose the best location to install a new magnetic observatory and/or repetition stations. Absolute intensity measurements were done nearby the ABAE's premises using two proton precession magnetometers.

Introduction:

A geomagnetic observatory is a place where continuous measurements of the geomagnetic field components are made for long periods of time with the best possible accuracy, preferably the INTERMANET's accuracy. Venezuela has one geomagnetic observatory, located in Mérida state, Venezuela (8°33'N, 71°19'O, 1755 m), installed in 2012 (Camacho et al., 2014), which belongs to the Astronomy Research Center (CIDA). Its construction was carried out following the recommendations of IAGA (*International Association of Geomagnetism and Aeronomy*). Despite the effort to build this observatory, we consider that only one observatory is not enough for the entire territory of Venezuela, so we recommend additional stations to be build. Magnetic repeat stations are a fixed and well iditified point on the Earth's surface, where the three components of the geomagnetic field are regularly measured to the highest possible accuracy. Repeat stations provide an important and cost-effective means of supplementing observatory data. Unfortunately, Venezuela does not have actuality a magnetic repeat stations network. For the CIDA is a priority to start the surveys with the aim
to create a magnetic repeat station network in Venezuela. For this, CIDA is asking the collaboration of other institutions of the country.
The Bolivarian Agency for Space Activities (*ABAE*), was created in 2007, at the present time ABAE has three satellites: VENESAT-1 (launched in 2008), VRSS-1 (launched in 2012), VRSS-1 (launched in 2017), (Jose P. and Tan Y., 2017). Considering the relevance of space weather information for its operations ABAE and CIDA established a cooperation agreement since 2012, with the aim to install a new magnetic observatory and repeat stations to provide magnetic data for its satellite network.
ABAE has infrastructure consisting on two operative ground stations and its equipment, including TT&C antennas, monitoring and telecom services administration, the main ground control station is located in the Aerospace Base Capitan Manuel Rios (BAEMARI), in the central state of Guarico whereas the backup earth station is located in Luepa, Bolivar state. ABAE also has a headquarters building of the Space Research and Development Center (CIDE), located in Borburata, Carabobo state. The objective of these surveys is to select areas near the ABAE's buildings to find the more adequate locations for installation of a new magnetic observatory and/or repeat stations.

Method:

In order to develop the study four areas near of the ABAE's buildings were selected to carry out the magnetic exploration studies. The locations were:

1.- Borburata, Carabobo state.
2.- El Sombrero, Guárico state.
3.- Calabozo, Guárico state.
4.- Luepa, Bolívar state.

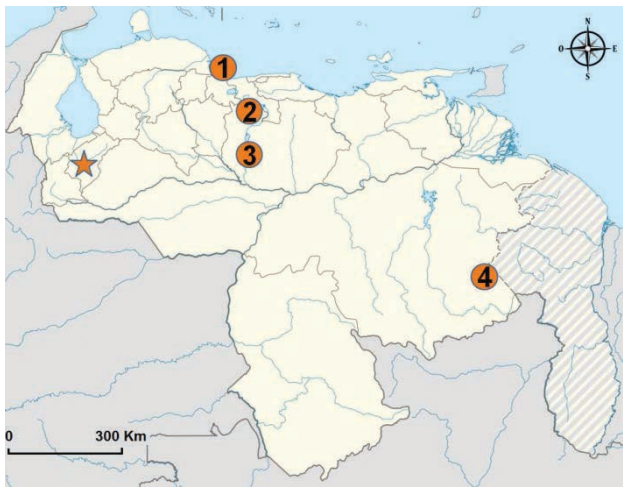

Figure 1: Venezuela's map, circles: survey areas, star: geomagnetic observatory of the Mérida.

First work was the collection of preliminary information of the survey areas. In this process, the team obtained geological information and possible sources of magnetic noise, to identify a good place that meets the requirements for the observatory site (Jankowski & Sucksdorff, 1996), to carry out the geomagnetic field explorations.
After find candidate locations the more likely to be appropriated were selected for the survey. The measurements were done at morning (before 10 am) with two proton precession magnetometers (0.01 nT of resolution), one as a reference for temporal variations of the field and another one at survey. The temporal measurements were done at sampling rate of 3 seconds.

The surveys areas were defined as a square grid with a total size of 50x50 meters and 5 meters spacing. This measurements were done twice over the same area at different heights (0.9 m and 1.9 m), to obtain the vertical gradient between the two surveys. All measurements were georeferenced using a GPS (1m of resolution).

Geomagnetic Surveys

1.- Borburata, Carabobo state. Here is a headquarters building of the Center of Research and Development Space (CIDE). CIDE is a nanosatellites factory focused on building small satellites of up to 1 ton, is an institution that belongs to ABAE. CIDE is located in a small coastal town in Carabobo state, in the north of the country. Its local geology of the study area is sedimentary rock (alluvium).
Some artificial magnetic sources disturbances founded in the study area: roadway, buildings, building site, naval artillery emplacement and an electrical power substation 36 MVA.

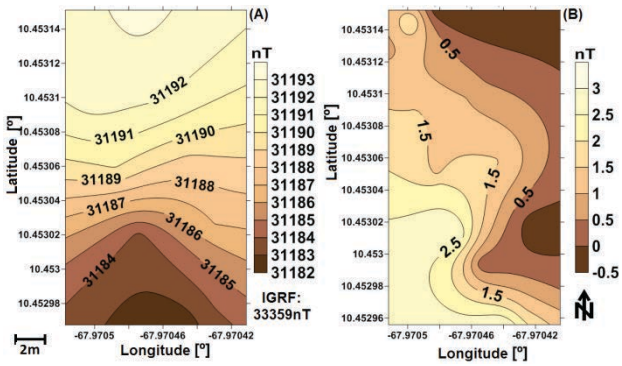

Figure 2: Borburata's contour maps: (A) magnetic survey and (B) vertical gradient values

2.- El Sombrero, Guárico state. The ABAE's main ground control station is located within the Captain Manuel Ríos Aerospace Base (BAEMARI) grounds, this is located in the heart of Venezuela and It has an area of 3400 Hectares approximately. From the geological formation point of view, BAEMARI is located on the boundary or geological contact between the formations Quebradón to the East and Roblecito to the West, both are sedimentary rocks.

Artificial magnetic sources disturbances founded in BAEMARI were: roadway, runway, military buildings, satellite dish antenna and an electrical power substation 1250 kVA.

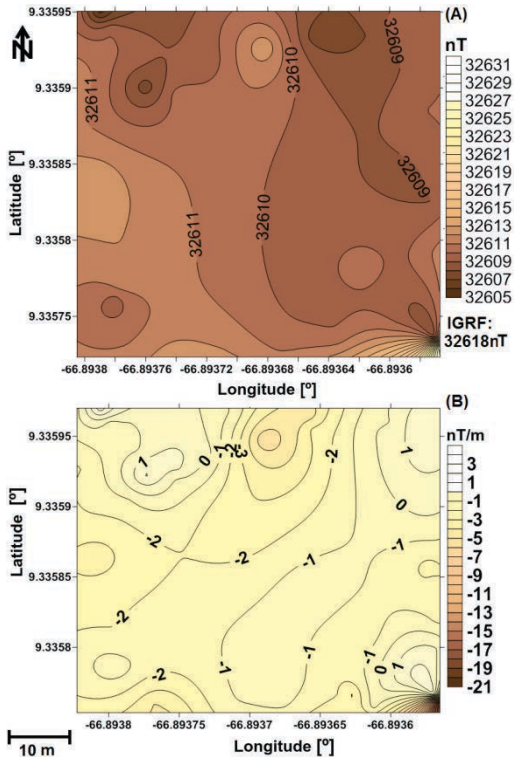

Figure 3: El Sombrero's contour maps: (A) magnetic survey and (B) vertical gradient values.

Considering the favorable geology of Guárico state for a geomagnetic observatory and its location in the center of the country, we decided to look for other areas to carry out the magnetic survey away from the El sombrero´s electrical power substation.

3.- Calabozo, Guarico state. The area of study is located about 50 km south of the city of Calabozo, on the ALBA's rice farm grounds, this farm belongs to the Ministry of Agriculture and Lands, and it is constituted by two conjuncts parcels, one of them with 176 hectares and the other with 213 hectares. In terms of geology, the study area is located on sedimentary rocks, alluvial sediments

The study area presents few sources of artificial magnetic disturbances, because it is a rural area far away from urban developments, the main sources finded were a few diesel engines to extract groundwater.

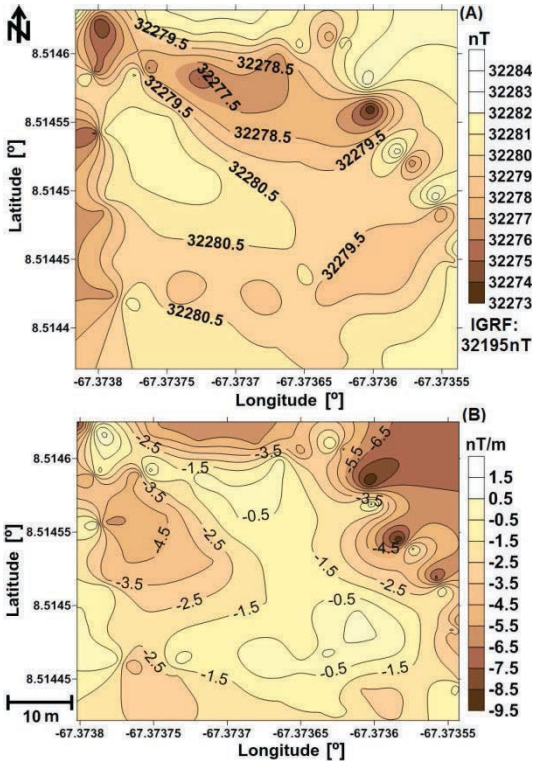

Figure 4: *Calabozo's contour maps: (A) magnetic survey and (B) vertical gradient values.*

4.- Luepa, Bolívar state. The magnetic survey were carried out in the area near the Manikuyá military fort (5° 50'11" N and 61°26'40" W), located in the southeastern of Venezuela. In this military fort is located ABAE's backup satellite ground control station. Luepa's geology consist of sedimentary rocks, belongs to Roraima group.

The main sources of magnetic disturbances in the surroundings of the fort are: roadway, runway, military buildings, satellite dish antenna and an electrical power substation 13.8 kVA. Electric power substation is a backup system, that operates only in case of an electrical outage in area.

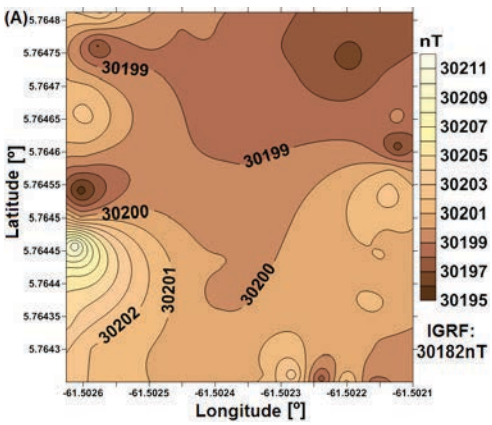

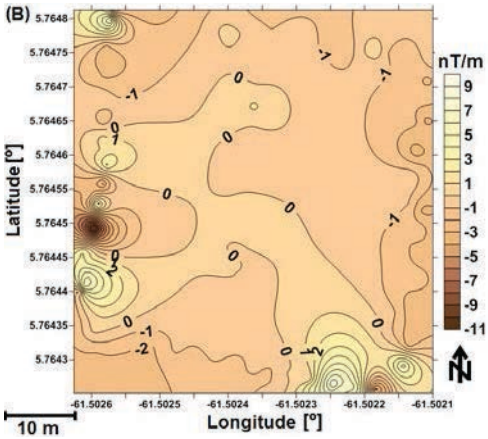

Figure 5: *Luepa's contour maps: (A) magnetic survey and (B) vertical gradient values.*

Discussion

1.- Borburata, Carabobo state. The isolines maps of total intensity (F), figure 2 shows gradients about 2 nT/m or less. Despite this low spatial gradient of the surveyed data, there is big offset of about 2000nT against the IGRF (*International Geomagnetic Reference Field*) values. The source of this magnetic anomaly is likely to be an elétrica power station (36MVA) nearby the ABAE headquarters

2.- El Sombrero, Guárico state. The areas near the ABAE headquarters in El Sombrero have a high level of magnetic disturbance, mainly due the presence of an electrical substation. However, the survey area presents vertical gradients around 2 and horizontal gradients less than one (figure 3).

3.- Calabozo, Guarico state. Figure 4 shows horizontal and vertical gradients in ALBA's rice farm are less than 2 nT/m and sources of magnetic disturbances are very low.

4.- Luepa, Bolívar state. The horizontal and vertical gradients maps, figure 5 shows that survey area has less than 1 nT/m. Luepa's electric power substation of 13.8 KVA is very small, this would imply that the "safe" distance required to move away from source of magnetic disturbance would be significantly lower. Furthermore, Luepa has a low population density, which is ideal to instal an observatory or repeat station..

Conclusions

- Borburata (CIDE) and El Sombrero (BAEMARI), these areas are not adequate for installing a new magnetic observatory and/or repeat stations, considering the artificial magnetic disturbances sources found as electrical power substations.

- Luepa, Manikuyá military fort does not have enough space to install an observatory, but the exploration carried out 10 km from the electric substation and the military fort, shows evidence of the existence of places with adequate conditions for an observatory or a repeat station with low magnetic gradients and minimal magnetic disturbances.

- Calabozo, ALBA's rice farm, has adequate places for installing a new magnetic observatory and/or a repeat station.

Acknowledgements

We would like to thank the staff of the ABAE for the collaboration and help during the magnetic surveys.

Referencies

Camacho E. at al., 2014 Construcción del Observatorio Geomagnético de Mérida, Venezuela. Revista Geofisica - Instituto Panamericano De Geografía E Historia (IPGH), No 64, 143-153.

Camacho E., at al., 2014. Estudio de factibilidad para la instalación de estaciones de observación geomagnéticas, en zonas cercanas a las sedes de la ABAE en Guárico, Bolívar y Carabobo. Informe técnico ABAE-CIDA.

Jose P. and Tan Y., 2017. The role of Venezuelan space technology in promoting development in Latin America. International Journal of Social Science and Humanity, Vol. 7, No. 7.

Gubbins D.and Herrero E., 2007. Encyclopedia of Geomagnetic and Paleomagnetism. Springer, 61-66. Dordrecht, Netherlands.

Jankowski J. and Sucksdorff C., 1996. Guide for magnetic measurements and observatory practice. Published by Association International of Geomagnetism and Aeronomy, 36-50. Warsaw, Poland.

Newitt L., Barton E., Bitterly J., 1996. Guide for magnetic repeat station surveys. Published by Association International of Geomagnetism and Aeronomy. Warsaw. Poland.

St-Louis B. and Sauter E. 2004. INTERMAGNET Technical Reference Manual. Version 4.2. download: www.intermagnet.org.

Wienert K., 1970. Notes on geomagnetic observatory and survey practice. Unesco,15-23. Belgium.

The Geomagnetic Observatory Niemegk: Recent Activities and Global Geomagnetic Network

Authors: Jürgen Matzka

[1] GFZ German Research Centre for Geosciences, Telegrafenberg, 14473 Potsdam, Germany

Keywords: Geomagnetic Observatory Network, Niemegk, Neumayer Station, Antarctica, Huancayo

ABSTRACT

In this talk we will report recent activities at the geomagnetic observatory Niemegk with special focus on the global geomagnetic observatory network, we will show new geomagnetic observations from Antarctica, and present a scientific study with data from the geomagnetic observatory Huancayo in Peru

Magnetic Observatory Of Nampula

Antonio Mucussete
Magnetic Observatory of Nampula - Mozambique

Abstract

Eleven years after the reopening of Nampula Magnetic Observatory (NMP), Nampula continuously is conducting monitoring activities of the Earth's magnetic field. And so we think that is open a path to a common future in the field of geomagnetic studies.
The main purpose of this presentation is to show the participants here and the tasks carried out in the magnetic observatory Nampula, as opportunities like these are rare.
This work is the result of the commitment that Mozambique in general has in the field of physical studies of the planet we live in, giving their contribution from absolute observations and recording data on components X, Y, Z and F.
We have challenges yes, related to improving the quality of our data, as they are sometimes recorded with interruptions caused by power supply.
The present work shows the magnetic declination of Nampula and Maputo as well as the wide differences between them, opening way from the real cause of this phenomenon.
We would like to take this opportunity to thank everyone who direct or indirectly have contributed to the renewal of our observatory

Introduction

In Nampula was built a Magnetic Observatory, during colonial period, after 1975 Nampula Magnetic observatory stopped. According to some reports, Magnetic Observatory of Nampula (NMP) was installed in the late of seventies and was operative only a few years, below I will give the some historical.

1982 Start of observations in the Magnetic Observatory of Nampula.

1987 Magnetic Observatory of Nampula is closed.

2006. Magnetic Observatory of Nampula was upgraded.

I cannot finish this introductory note without acknowledging the very large contribution of British Geological Survey (BGS), United Geological Survey (USGS) and other countries members of intermagnet. I also appreciate the prudence work of many individuals (let me mention Mr Jean Rasson, Allan Berrarducci, Chris Turbbit, John Riddick, Peter Kontze and others of BGS, USGS and Hermanus Magnetic Observatory).

MAGNETIC OBSERVATORY OF NAMPULA IN 2001

TASKS IN MAGNETIC OBSERVATORY OF NAMPULA

TASKS IN MAGNETIC OBSERVATORY OF NAMPULA

The main tasks made from Magnetic observatory of Nampula are:

- Absolutes measurements;
- Recording raw data of X, Y, Z and F component;
- Convert into IAGA 2002 one minute format using GdasView software;
- Send to Geomagnetic Information Note (GIN);
- Calculate Declination and Inclination monthly mean;
- Measurement of Declination and Inclination from repeat station.

To Record raw data of X, Y, Z and F component, we use a magnetometer connected with a digitizer, as can be seen from the picture:

MAGNETIC OBSERVATORY PLAN

ABSOLUTES INSTRUMENTS

LMM MANGETIC DECLINATION (NOV 2015)

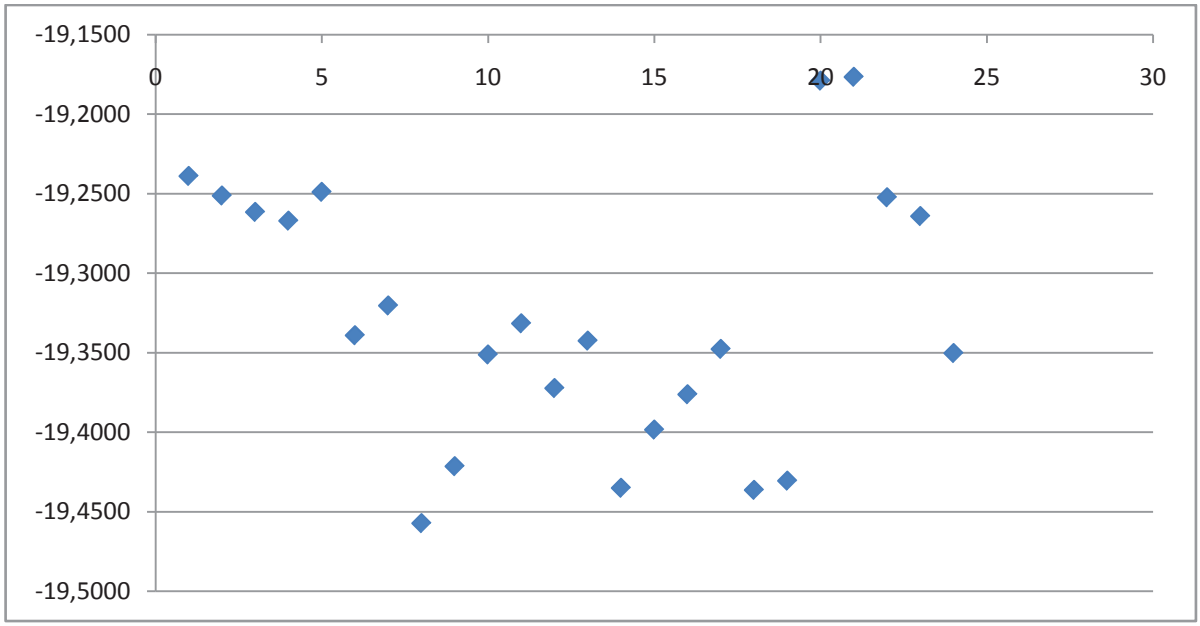

NMP MANGETIC DECLINATION (NOV 2015)

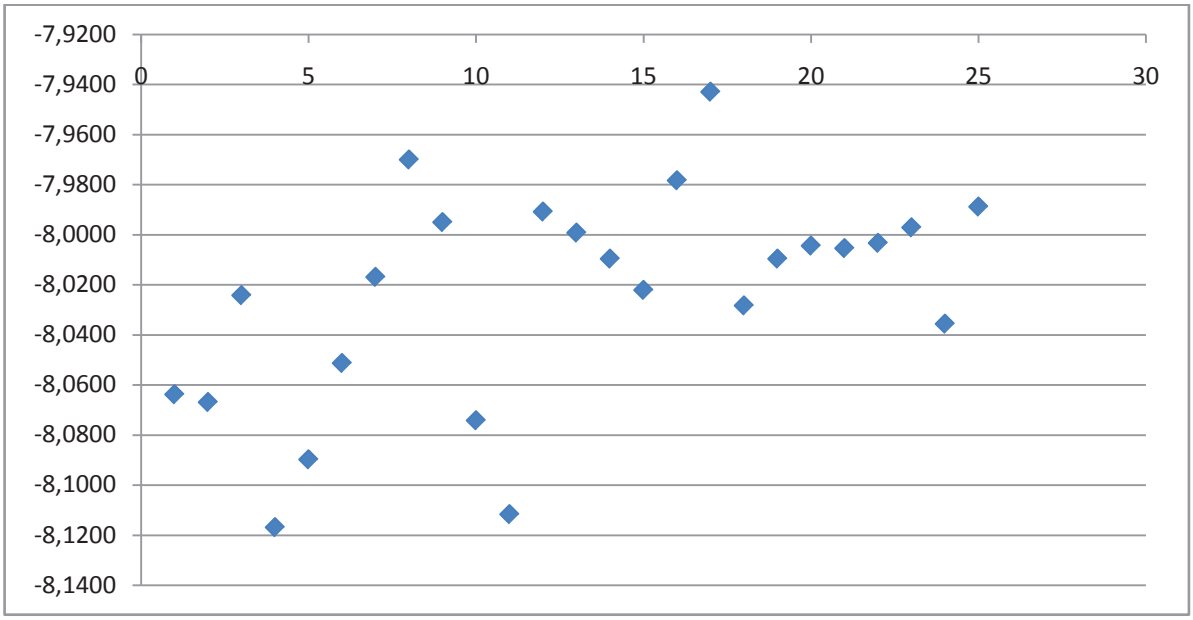

MAP OF MOZAMBIQUE

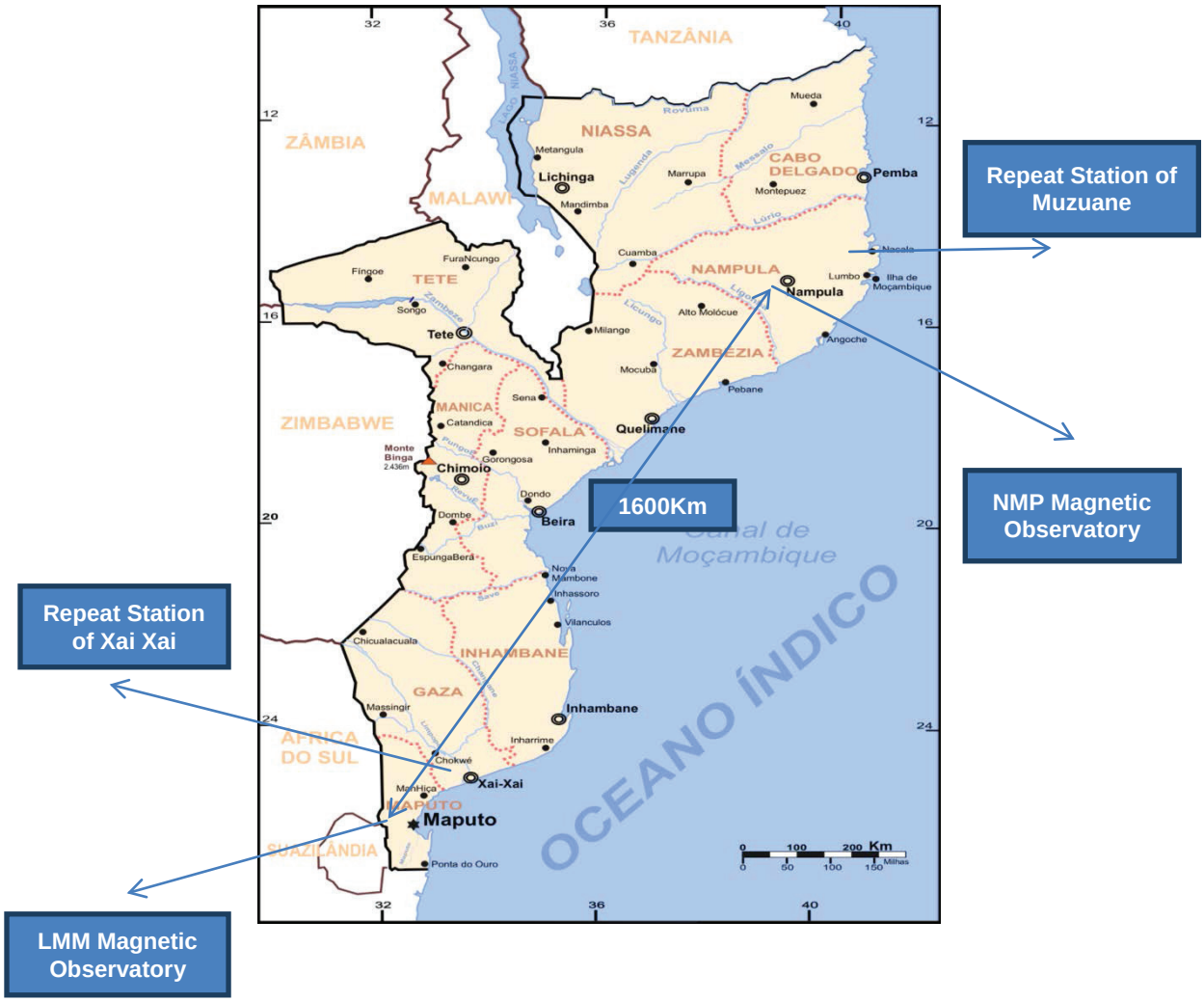

DIFERENCE OF DECLINATION BETWEEN NMP AND LMM

November 2015

LMM = -19,3251º

NMP = -8,0235º

Difference = LMM – NMP = -19,325º - (-8,0235º)

= -11,3011º

REPEAT STATION MEASUREMENTS IN MUZUANE

GDASVIEW COMPUTING DEFINITIVE DATA

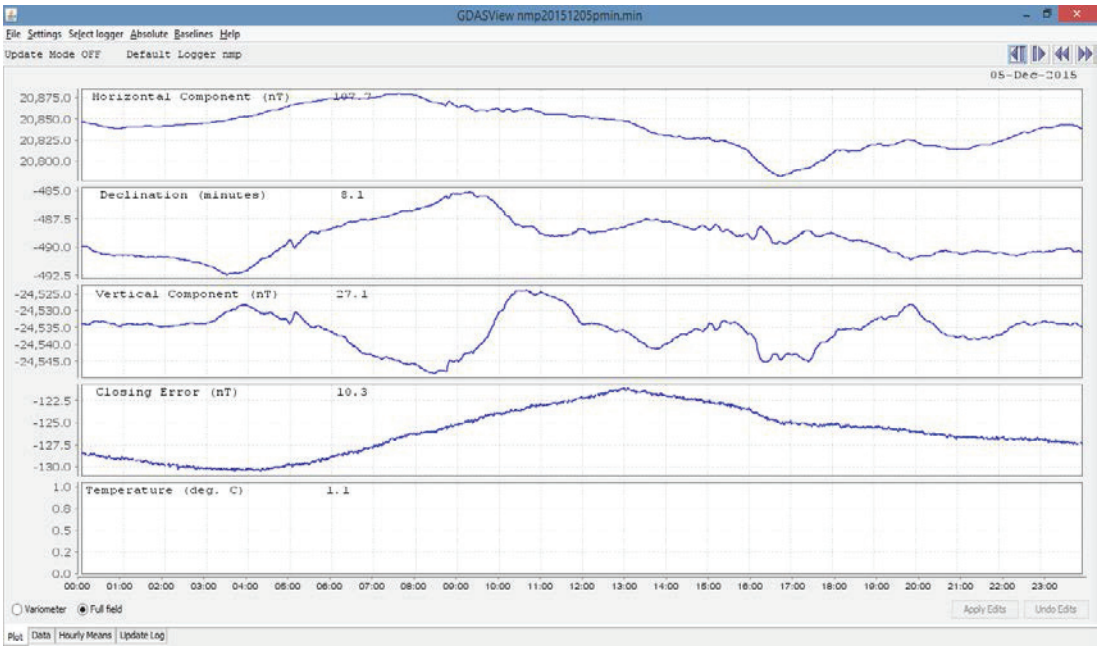

DELIVERY DATA TO CGG

We have received requests of our data from Dr Dmitry Koryakin, he has used data for Marine Gravity and magnetic Survey. This kind of request has results in saving some payments. Thanks of this payment, we saved some money to buy a GSM 19 over house magnetometer, as may be seen from the picture below.

OUTLOOKS

1. Acquisition of new geomagnetic instruments and improve the quality of the works;

2. Expand our know how for the region and many countries of the world;

3. The main perspective of this work, is become Magnetic Observatory of Nampula in high level like those Observatories that are members of INTERMAGNET.

CONCLUSION

1.To conclude this presentation, we would like to understand more about the magnetic phenomenal from the earth;

2. We are very interested to ex-change our knowledge and give our contribution with other scientists around the world.

Kmex: the Mexican Geomagnetic K index

P. Corona-Romero[1,2], E. Sanchez-Garcia[3], M. Sergeeva[1,2], J.A. Gonzalez-Esparza[1], G. Cifuentes-Nava[4], E. Hernandez-Quintero[4], A. Caccavari[4], E. Aguilar-Rodriguez[1],J.C. Mejía-Ambriz[1,2], V. de-la-Luz[1,2], L.X. Gonzalez[1,2]*

[1]*Space Weather National Laboratory (LANCE), Instituto de Geofisica, UNAM, Morelia, Mexico.*

[2]*CONACYT Reaserch Fellow, National Council of Science and Technology (CONACYT), Mexico, Mexico.*

[3]*Earth-Sciences Postgraduate Program, Instituto de Geofisica, UNAM, Morelia, Mexico.*

[4]*Magnetic Service, Instituto de Geofisica, UNAM, Ciudad de México, Mexico.*

[*]*Contact: p.coronaromero@igeofisica.unam.mx*

Abstract

Space weather affects the Earth's magnetic field in multiple ways. A geomagnetic storm is probably the most intense effect of space weather over Earth's magnetosphere. Geomagnetic storm effects threaten the distribution of energy (electricity, oil and gas) as well as systems of geopositioning and telecommunication, and compromise technology and facilities related with security of nations. For this reason, the magnetosphere of Earth is continuously monitored in order to detect the occurrence of geomagnetic storms. One of the main tools to detect a geomagnetic perturbations is the geomagnetic K index. The K index is a scale for assessing the effects associated with the (3-hourly) variations of the geomagnetic field. In this work we present the procedures to calibrate, calculate, and validate the geomagnetic K index for the central region of Mexico (Kmex). Additionally, we present a geomagnetic storm recorded by the Kmex index. Kmex index is a collaboration between the National Space Weather Laboratory (LANCE) and the Magnetic Service of the Geophysics Institute (UNAM).

Introduction

Possibly the most extreme space weather-effects on the terrestrial magnetosphere are geomagnetic storms. Geomagnetic storms occur when interplanetary magnetic field reconnects with the geomagnetic field. The phenomenon allows charged particles, from interplanetary medium, to get into the environment of the Earth's magnetosphere. This perturbs the currents of Earth's ionosphere, specifically the ring current, that induce perturbations on the whole geomagnetic field known as geomagnetic storms. [1]

The Space Weather studies the effects of solar activity on the terrestrial environment, and its effects on our technology. Geomagnetic storms are of great interest for Space Weather purposes, since they may derive into harmful effects in: telecommunications, global positioning systems and production and distribution of energy, and others. Because of this, there are tools to assess the effects of geomagnetic storms like the disturbance storm time (Dst) index or the geomagnetic index K. [1]

A regional geomagnetic K index is an attempt to estimate the effects of both, interplanetary medium as well as the local ionospheric currents on the geomagnetic field at a given region. Besides to regional K indexes, there is a planetary K index (Kp), which averages a number of K indexes from different Earth's locations. In order to calculate the K index it is necessary to remove the cyclic variations from H geomagnetic-component (<H>). Subsequently, in intervals of three hours, one must calculate the maximum and minimum values of H - <H>. Subsequently the minimum value is subtracted to the maximum one in order to calculate the largest 3-hourly difference. Finally, the K index grows almost linearly with the logarithm of such maximum variations. [2]

Recently, the National Space Weather Laboratory (LANCE) and the Magnetic Service (MS), both of the Geophysics Institute at the National and Autonomous University of Mexico (UNAM), have been given the task of calculating the K index for the central region of Mexico (Kmex). Whereas the MS provides the data of the terrestrial magnetic field; the LANCE provides the computational infrastructure for the calculation of the Kmex. It is important to emphasize that the Kmex is an experimental product in validation process

2 MEXICAN GEOMAGNETIC K INDEX

2.1Geomagnetic data from central Mexico

As previously mentioned, we use data delivered by the Magnetic Service (MS). The magnetic data is measured at the Teoloyucan Geomagnetic Observatory (TGO) located in central Mexico (LAT 19.746 °, LON -99.190 °). The TGO is the main magnetic observatory of the MS housted in the Institute of Geophysics of the National Autonomous University of Mexico (UNAM). The TGO operates with a 3 components variograph fluxgate DFI, a magnetometer Overhauser POS N 129 and a DI-flux ZEISS THEO20B, with a backup variograph FGE HDZ. The MS reports the data recorded by the TGO in near real time with a cadence of one minute and a resolution of 1 nT. The MS release one file per day in Extended IAGA2002 format. These are the files we use in the calculation of the Kmex index.

2.2Kmex calculation

We follow the method expose by Corona-Romero et.al. [3]. In order to remove the cyclic variations from H, we calculate the median value of H (<H0>) along the previous 27 days, for a given time t = t0. We select a period of 27 since it is the duration of a solar rotation and thus, this period is long enough to take into account many of the solar and terrestrial cyclic effects of H. This allows us to define the variations of H (dH) for a given time t0 as:

$$dH(t0)=H(t0)-<H0> \quad (1)$$

Once known the value of dH(t), our next step is to calculate its maximum (MH) and minimum (mH) values in lapses of 3 hours. With MH and mH known, we proceed to calculate the maximum tri-hourly variation of dH (DH):

$$DH=|MH-mH|. \quad (2)$$

We calculate eight different values of DH per day through equation (2). Next we use DH to calculate the Kmex.

Next we compared the values of the natural logarithm of DH (*Ln*(DH)) with values of the planetary K index (Kp). The purpose of this is to find out a relation between thevalues of Kp and the corresponding values pf DH. In other words, we aim to calibrate the TGO measurements

.

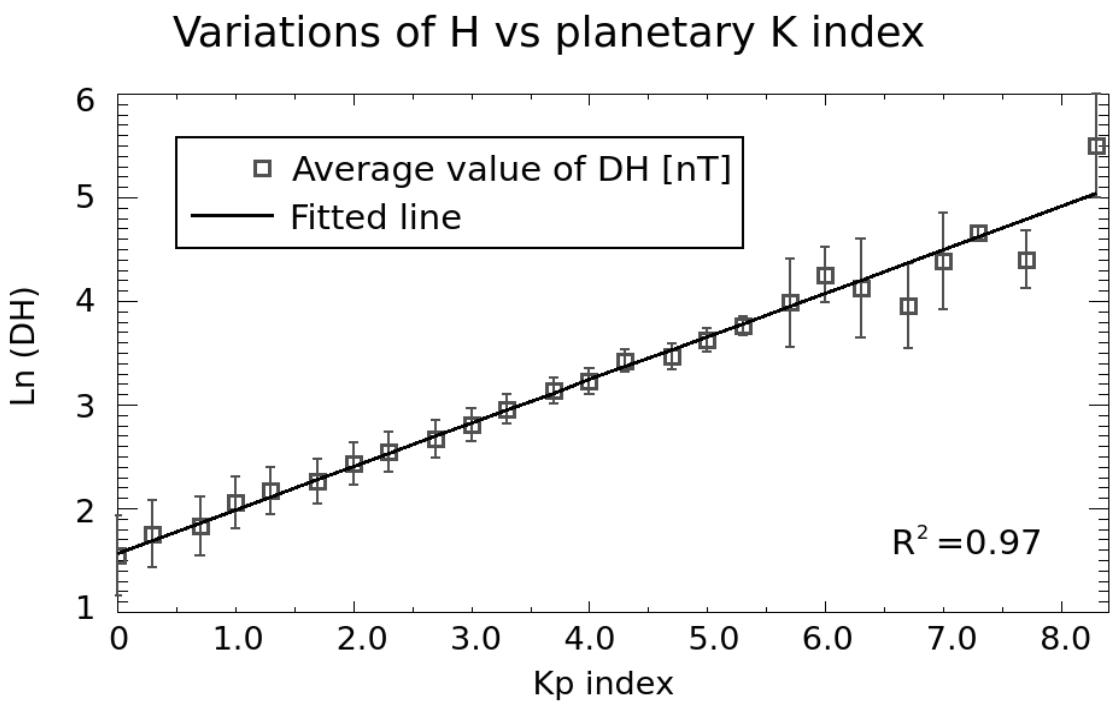

Figure 1. Average values of DH as function of Kp during 01-Jan-2014 to 01-Jan-2017. Solid black line is the fit to the data.

Figure 1 shows a comparison between DH and Kp values, for the period 01-Jan-2014 to 01-Jan-2017. In the figure we appreciate an almost linear tendency (solid black line) between *Ln*(DH) and Kp. Tendency that

allows us to define the scale between the calculated values of DH and a regional value of K index, *i.e.* Kmex. Table 1 shows the resulting scale to calculate the Kmex from the TGO measurements.

It is important to note that the values presented in Table 1 are not definitive. This is relevant for Kmex values above 6. Because in the period used for calibration, there were very few events with Kp larger than 6. We can appreciate this in Figure 1, where data relative to Kp>6 detach away from the linear tendency commented on before.

Table 1: Values of Kp according the calculated value of DH.

Kmex	DH [nT]	Kmex	DH [nT]
00	[0, 5.5)	47	[34.4, 39.0)
03	[5.5, 6.4)	50	[39.0, 44.2)
07	[6.4, 7.3)	53	[44.2, 52.3)
10	[7.3, 8.3)	57	[52.3, 59.2)
13	[8.3, 9.8)	60	[59.2, 67.2)
17	[9.8, 11.1)	63	[67.2, 79.4)
20	[11.1, 12.6)	67	[79.4, 90.0)
23	[12.6, 14.9)	70	[90.0, 102.1)
27	[14.9, 16.9)	73	[102.1, 120.7)
30	[16.9, 19.1)	77	[120.7, 136.9)
33	[19.1, 22.6)	80	[136.9, 155.2)
37	[22.6, 25.6)	83	[155.2, 183.5)
40	[25.6, 29.1)	87	[183.5 208.0)
43	[29.1,34.4)	90	[208, ...)

3 KMEX AND SPACE WEATHER ON MEXICO

Kmex preliminary results already registered recent space weather events. The reader can find such registers in the special and quarterly reports that the LANCE generates and distributes through its space weather service (SCiESMEX). The most recent geomagnetic storm occurred during May 27 and 28, 2017. The LANCE and its collaborators registered this phenomenon and SCiESMEX made two different special reports of the event (both in Spanish, www.sciesmex.unam.mx/productos-y-servicios/).

3.1 May 27thand 28thevent

Figure 2 shows data from the geomagnetic field between May 27 and 29. The upper panel shows the Dst index (solid black line) and the hourly averaged dH (solid blue line). It is important to note that both profiles are significantly similar. In both of them it is observed a sudden commencement (spontaneous increment) at the end of May 27. Such a signature was due to the arrival of an interplanetary shock wave that compressed the geomagnetic field.

A few hours later, in the early hours of May 28, a coronal mass ejection (CME) impacted the Earth's space environment. The magnetic configuration of the CME allowed it to interact with the geomagnetic field, resulting in a "Strong" geomagnetic storm, according to NOAA scales. In the upper panel of Figure 2 we can appreciate the main phase of the geomagnetic storm as an abrupt descent that decreases the Dst and dH values to -122 nT and -150 nT, respectively.
The middle and bottom panels of Figure 2 show the Kmex and Kp index values during the event. Notice that Kmex index is qualitatively similar to its planetary

counterpart. The sudden increase in the values of the K indexes observed at the end of May 27 is due to the arrival of the shock wave. The high values of the K indexes are maintained due to the geomagnetic storm, and they reached a maximum value of 7 and 8 for Kp and Kmex, respectively.
From midday on May 28, the magnetic configuration of the CME no longer favored the reconnection with the Earth's magnetosphere. This triggering the beginning of

the recovery phase. We appreciate this in the panels of Figure 2 as a tendency to return to the pre-storm conditions for mid May 29.

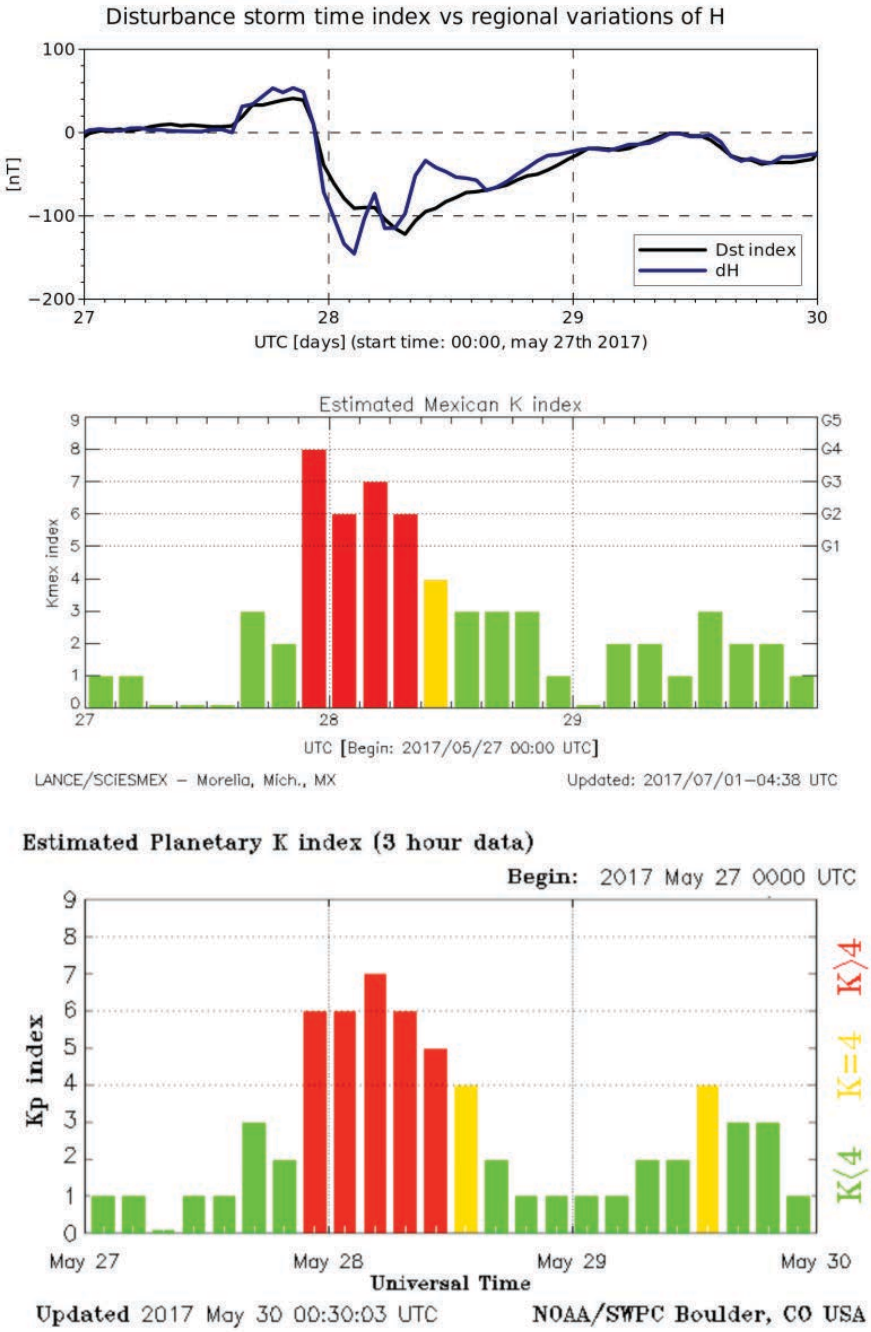

Figure 2. Upper: Dst (black) index and hourly averaged dH (blue). Middle: Estimated Kmex index. Bottom: Estimated Kp by SWPC/NOAA.

4 DISCUSIÓN Y CONCLUSIONES

We presented the calibration and preliminary calculations of Kmex. Which is calculated from OGT data, whose calibration (see Table 1) is based on Kp index. It is important to mention that Kmex calibration is not finished, for we require geomagnetic data related with large values of Kp.

Additionally, we described the geomagnetic storm of May 27-28, 2017 with the mexican geomagnetic data.

We notice consistencies between the Kmex index and the Kp. Which suggests that our methodology for calculating Kmex might be adequate. Additionally, we found significant agreements between dH values and the Dst index. However, it is important to notice (in the upper panel of Figure 2) the presence of differences between the Dst and dH at the last(first) hours of May 27(28). The upper panel of Figure 3 shows such differences between these profiles. A detailed inspection allows us to conclude that such differences are possibly local ionospheric effects.

Although the Kmex index is in validation stage, the results showed in this work suggest that it is possible to use the Kmex index for the analysis of space weather events. In addition, an additional result derived from the Kmex calculation is the value of dH, which is consistent with the Dst index. Finally, our results highlight the local effects of space weather on the regional geomagnetic field.

REFERENCES:

[1] Mark Moldwin. An Introduction to Space Weather, Cambridge University Press, New York, 2008.

[2] Mayaud, Pierre Noel. Derivation, Meaning, and Use of Geomagnetic Indices. American Geophysical Union, Washington, D. C., USA, 1980

[3] Yasyukevich et al., Influence of GPS/GLONASS Differential Code Biases on the Determination Accuracy of the Absolute Total Electron Content in the Ionosphere, Geomagnetism and Aeronomy, 55(6), 2015

[4] P. Corona-Romero, et.al. Mexican Geomagnetic K index. Latinmag Letters, Vol. 7, 2017.

The Magnetic Service and its relationship with Weather Space Services, experiences in Mexico University (UNAM)

E. Hernández-Quintero and Cifuentes-Nava G.
Magnetic Service. Instituto de Geofísica. Universidad nacional Autónoma de México

Abstract

According to the increasing interest in the study and measure the external magnetic field and its relation to the effects on strategic technologies in Mexico (power grids or satellite for example), it was just created the Space Weather Service (February 2016). This service has great potential to study and solve problems related to solar activity and its influence on technology (communications, gps-networks, satellites, human health, for example).
Nevertheless we assume that Mexico is outside the area of influence of this kind of effects, there is some ambiguity between the scope that this new service would be, and the magnetic service with a long tradition, in subjects such as the infrastructure of Earth surface; geomagnetic observatories, repeat stations, or temporary diurnal variation monitoring.
Geomagnetic data used for modeling the earth's magnetic field of internal origin, and secular variation have been studied based mainly in data obtained from geomagnetic observatories, and repeat stations distributed throughout the earth's surface. Nowadays new applications for this information had become more important, considering several hazards and its significance from the magnetic point of view, such as volcano or earthquake activity. Surface surveys, airborne and satellite contributes to characterize the crustal, and main geomagnetic field and they are part of the Magnetic Service in Mexico.
The influence of external electric currents whose origin are in the magnetosphere and ionosphere, are features with relevance in data acquisition in satellites and spacecraft, ground stations are less important.
The Space Weather Service and the Magnetic Service apparently have a common field of study in this work we remark several aspects in order to discuss a frontier between such views of the whole geomagnetic field: internal and external sources. The goal of this work is to separate clearly the differences between these two lines of researching, and enhance that lines that fit well with both of them.
Conclusions are not easy to reach when there are some very close lines of study. These experiences will help to understand such qualitative differences
This service must absorb the other? There should be both to complement the activities? Here are some examples where they were to find answers to such lines of work are presented.

Introduction

Several of the Geomagnetic Observatories in Latin America have been operating since more than 100 years, such as Vassouras (Brazil) or Teoloyucan (Mexico). These observatories have used its data to model the terrestrial magnetic field of internal origin and the secular variation based mainly on their information and magnetic repeat stations distributed over the earth's surface. Nowadays the new applications of this information have become more important, taking into account the risks of solar phenomena and their importance from the geomagnetic point of view, also associated with volcanic or seismic activity. The magnetic surveys on the surface of the Earth, the aerial or satellite surveys to characterize the earth's crust have been part of the Magnetic Service objectives in Mexico (UNAM) since its conception and in most of the countries are integrated as programs of research in geomagnetism, such as government agencies or universities.
Historically, the influence of electric currents witch origin is in the magnetosphere and the ionosphere have been studied with less interest in the acquisition of data on satellites and stations on the surface of the earth at low geomagnetic latitudes (50 degrees of north or south latitude). In contrast, today is a very important issue to compare and know the influence of this phenomenon in mid latitude geographical positions.
Magnetic Service inside the national university in Mexico is in charge of teach, diffusion, and researching the knowledge on geomagnetism; guard historical data bases of geomagnetic data (1879-2018 historical observatories, data charts 1906).
The interest of government agencies in Mexico, encouraged the creation of a new Space Weather Service in order to pay attention to those planetary risks associated with the solar activity and its real influence over countries such as Mexico.

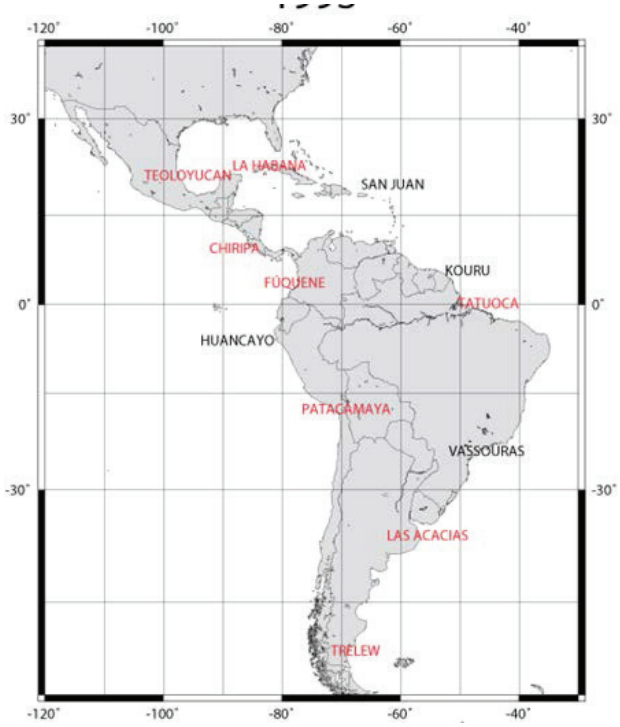

Figure 1.Geomagnetic observatories in Latin America in the year 2000.

Practice of Geomagnetic Service independent of Space Weather

During the existence of the geomagnetic practice in Mexico, it is well known several applications concerned specially with observatory geomagnetic data.

Secular variation of the magnetic field

Teoloyucan magnetic Observatory (IAGA code:TEO) is located near Mexico City. Its location is of great interest in Mexico because is the unique and singular magnetic observatory during the last 103 years and offers a high scientific value of the observatory's data. The history of this observatory is close to its data; several published papers make a description and evaluation of its time series data; some recent improvements, and plans for the near future will give some results on the behavior of the geomagnetic field in this geographical position (Hernández et al., 1997; Campos-Enriquez et Al.; 1994).

Geomagnetic Signals as precursor of volcano activity

In the developing of new lines of research, such as Martin del Pozzo and others (2003); demonstrates how the local magnetic field variations near an active volcano, present a clear correlation with the activity increase of magnetic field; including various features such as diurnal magnetic variation, occurrence of geomagnetic storms, for example. Even though this is not a determinative tool to evaluate directly an eruption process, the twenty years of experiences had been very helpful to conclude that magnetic monitoring is very helpful to support the volcano activity.

Workshops and Schools of Geomagnetism an Latin America

The recent history of meetings in Latin American countries, had demonstrate the increase of collaboration projects among different countries in this area. The Pan American Institute of Geography and History play a significant role as supporter and organizer. In 1993 an effort to know this discipline and how it its develop in such countries (Table 1).

year	Magnetic Service (Mexico),
1993	I School on Geomagnetism, Fuquene Magnetic observatory, Colombia (FUQ)
1995	II School on Geomagnetism, Taxco, México (TEO)
1996	First Workshop on Geomagnetic Instruments in Latin America(TEO)
1997	III School on Geomagnetism (HUA)
2000	IV School on Geomagnetism (CHI)
2004	V School on Geomagnetism (JUR)
2005	Annual Intermagnet Meeting in Latin America (México)
2007	VI school on Geomagnetism (VSS)
2012	First Latin American Workshop on Geomagnetism (Mexico). IAGA (SF-Spain).
2013	First IAGA Meeting in México (Mérida)
2014	First Legal step (National Civil Protection) for SPACE WEATHER hazards (Mexico)
2016	XVII IAGA Workshop on Geomagnetic Observatory Instruments (DOU)
2017	Second PANGEO- VASSOURAS

was

Table1. Twenty four years of geomagnetic work in Latin America

The organization of such kind of events, have positive agreements in developing scientific relationships between institutions such as National University of Mexico; the Observatorio Nacional de Rios de Janeiro; the Agustin Codazzi Geographical Institute in Colombia, for example.

Conclusions

During the last decades geomagnetism in Latin America have clear lines of study, such as maintenance and instrumental updating in the existing Geomagnetic Observatories in the next years; Deploy new observatories into national interest geographical areas; spread the national observatory repeat stations grids in order to study and analyze anomalies in Secular Variations terms; Volcano Activity and its relationship with magnetic expression; and to solve problems such as .- Reach a Proper operation observatory: lack of institutions interest; urban effects; social and security risks; overload of personnel activities.

Along with Space Weather global groups in the Americas, Europe and Asia this area of the world should increase the knowledge about the effects in low latitudes of phenomena related with Space Weather; Designing of a proper grid of variographs over the countries; Increasing knowledge of conductivity in strategic geographic areas in the countries; funding and refreshing staff.

Acknowledgements

Authors want to thanks the PAIG (Panamerican Institute of Geography and History) in funding and Observatorio Nacional de Rio de Janeiro and Universidad Nacional Autónoma de México (UNAM) for the organizing og this succesful Second PANGEO.

References

Hernández, E. ,A. Orozco.1997. "Magnetic Field work and IGRF models for México, three examples for the 20th Century" J. Geomag. Geoelectr., vol 49, pp 387-392.

Campos-Enríquez, J.O., E. Hernández-Quintero, H. Nolasco-Chávez, A. Orozco-Torres, C. Cañón-Amaro, G. Alvarez-García, J. Urrutia-Fucugauchi. 1994. A Preliminary Assesement of IGRF-1990 for Mexico. Physics of the Earth and Planetary Interiors. 82 p 105-111.

Cifuentes G.; 2009. Monitoreo Geomagnético del Volcán Popocatépetl. Thesis for MsC degree. Universidad Nacional Autónoma de México. DOI: 10.13140/RG.2.2.29315.91682.

D-Z Geomagnetic Field Variations and Geological Features Measured in low Magnetic Latitudes

Sophia R. Laranja [1,2] *Caio C. Gonçalves* [1,2] *Thais Cândido* [1,2] *and Luiz Benyosef* [2]

[1] *Universidade Federal Fluminense(UFF)*

[2] *Observatório Nacional (ON)*

Abstract

The geomagnetic variations recorded in the equatorial region are known to present an enhanced behavior when compared to those at off-equatorial latitudes. This pattern can be attributed to the phenomenon of the Equatorial Electrojet (EEJ), which is a narrow belt of intense electric current in the ionosphere confined to about ±3º at the dip equator (Chapman, 1951a, and Adimula, et al, 2011). We intend to analyze the Sq variations of the geomagnetic components D, Z from two EEJ and one SAMA (ASC) observatories, being one of them a south atlantic island. Our purpose is to correlate these results with the geology of the regions studied, in both quiet and disturbed conditions.

.

Introduction

The geomagnetic variations on the ground in the equatorial ionosphere region are known to have an enhanced behavior when compared to those at non-equatorial latitudes. The phenomenon called “Equatorial Electrojet” (EEJ) is believed to be responsible for this distinct pattern. At the magnetic dip equator the global dynamo generates the midday eastward polarization field, which gives rise to a downward Hall current. A strong opposite vertical polarization field is set up due to the presence of non-conducting boundaries, making arise the intense Hall current named the Equatorial Electrojet (EEJ) (Chapman, 1951). The typical extent of the EEJ is within ±3° of the dip equator, confined at the E region in a height of about 95 - 115 km. The Equatorial stations respond primarily to the directly overhead EEJ, but also to the ring current and the global quiet time Sq current system, therefore two EEJ stations were chosen to analyze and compare their Sq variations in the geomagnetic components D and Z, in both quiet and disturbed conditions.

The South Atlantic Ocean is a region of large interest due to its anomalous geomagnetic field, caused by the South Atlantic Magnetic Anomaly (SAMA). In this region the strength of the internal magnetic field is significantly lower when compared to elsewhere in the world. The SAMA originates from an inverse magnetic flux at the core mantle boundary beneath South America and South Africa, which existence is noted over the last 200 years (Gubbins et al., 2006). The low geomagnetic field in this region causes a strong increase of radiation due to the distortion of the inner van Allen radiation belt, affecting satellites when passing through the SAMA (Heirtzler et al., 2002). The growth of this reversed flux region may be related to the Earth’s magnetic field attempting to reverse (Gubbins, 2008).

Ascension is a volcanic island, therefore the nature of this island can influence the magnetic records of the Z component, even if it is a very small influence, because of the magnetic susceptibility of the rocks on the island.

We intend to correlate these results with the geology of the three observatories selected, which was succinctly described.

The results of this preliminary study confirm that the morphology of the curves obtained for D and Z on ASC can be related to the SAMA, as well as the curves of KOU and TTB can be attributed to the EEJ.

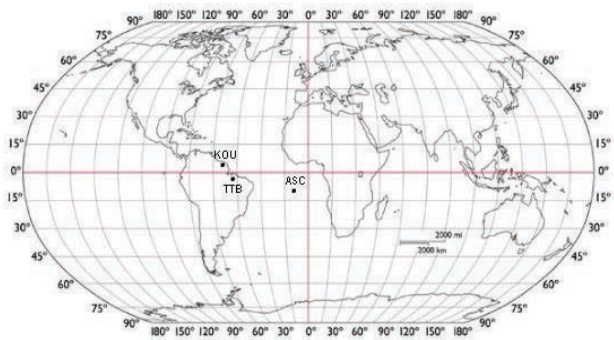

Figure 1. Geographic distribution of the observatories studied.

	Geographic		Geomagnetic	
Observatory	Latitude (º)	Longitude (º)	Latitude (º)	Longitude (º)
Tatuoca (TTB)				
Ascension Island (ASC)	7.949 South	345.624 East	2.809 South	057.530 East
Kourou (KOU)	5.209 North	307.267 East	14.55 North	20.11 East

Table 1. Geographic and Geomagnetic coordinates of the stations.

METHOD

First of all, the three quietest and disturbed days were chosen for the analysis, using the same method, according to planetary magnetic index, kp for the quietest one and the ap index for the disturbed days. The kp and ap indexes are provided by the International Service of Geomagnetic Indices (isgi).

The data used has one-minute resolution and one-hour median values were derived. A quiet level baseline was defined for each day as the mean of six nighttime values. dH and dZ were computed by subtracting the baseline from D and Z geomagnetic components (Yamazaki, Y.,et al., 2011), according to the equation 1.

$$dD(UT) = D(UT) - \frac{D(0) + D(1) + D(2) + D(22) + D(23) + D(24)}{6} \quad (1)$$

After that we compared the behavior of the Z component with the geology of the regions studied. We made a correlation of the Z component morphology with how much we believe that the geology can affect the curves obtained.

Results

The quiet daily variations for both D and Z geomagnetic components are in figure 2, and the disturbed condition for the same component is in figure 3. The pattern obtained in figures 2 and 3 clearly revealed that D has deviated from the normal known variation of morning trough and afternoon crest. This could be attributed to change in electric field (Okeke et al., 1998). However, D seems to increase around noon for TTB and KOU, showing its minimum between 14 and 16 UT.

The diurnal variation curves in Z component for the three stations might be interpreted according to the Sq current system. ASC is a volcanic island, so the geology of this region might influence in a very small scale the curves in Z. Induction effects can influence stations off the continent, like ASC.

The morphology of the curves in TTB and KOU has a more pronounced diurnal variation when compared to ASC. This might be due to the stations location. TTB and KOU are located in the equatorial region and within the EEJ zone, thus this can influence the behavior of Z component.

The diurnal variations for both D and Z components at ASC exhibits an opposite sign from those at TTB and KOU. This might be due to the localization of the observatories. For the stations at the northern side of the dip equator the curves are negative in the afternoon and for the southern stations they are positive (Obiezekie, 2012).

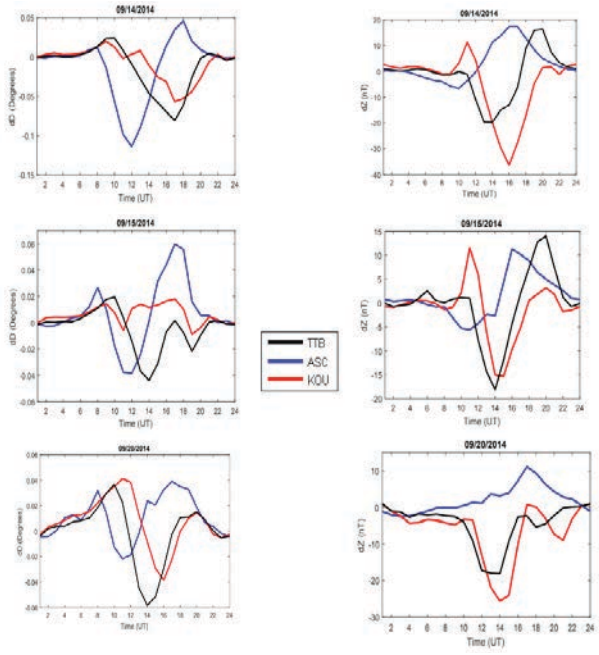

Figure 2. Diurnal variations for D and Z components on quiet condition.

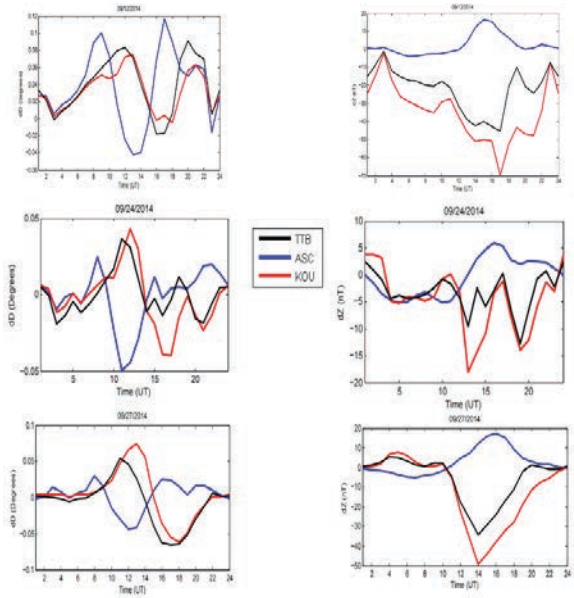

Figure 3. Diurnal variations for D and Z components for the disturbed condition.

Geological considerations

Ascension is a volcanic island, but although there are lots of vents on the island, it is only a single volcano. In fact, the area above the water level is only 1% of the volcanic landmass.

Ascension lies on the South America plate, while the hotspot is on the other side of the Mid Atlantic Ridge under the African plate, and the magma flows along the ridge to reach Ascension Island.

Larger explosive eruptions produce pumice and ash. The ash and pumice can be laid down in two main ways, as pyroclastic and pyroclastic flow, both of which are found on Ascension. Pumice is very light volcanic rock filled with holes, from the rapidly expanding gas that drove the eruption.

Most of the outcrops are scoria cones. These are built up during relatively small-scale explosive eruptions where red-hot rocks are thrown from the vent into the air, cool and then land. The magma on this island is usually basaltic.

Mafic and silicic pyroclastic deposits are distributed across Ascension Island, much of them are trachyte, rhyolite and obsidian, all igneous rocks. These types of rocks have a medium magnetic susceptibility, which is considerable for correlation to Z component. A geological map of Ascension is in figure 4.

The two South Atlantic islands of this paper are better represented by igneous rocks, and basalt is the most common one in both islands. The iron oxide content of basalt can vary from 3.8 to 8.1% and because of this high iron content magnetite is a common mineral in basalts. The magnetic susceptibility of basalt (as in all igneous rocks) is relevant as well, and this is an important feature that can affect the behavior of Z component in these two islands.

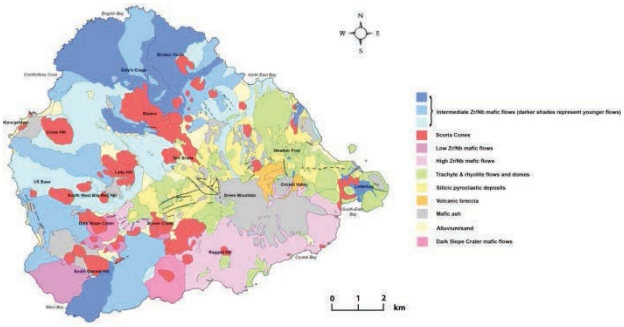

Figure 4. Geological map of Ascension Island

The Tatuoca region has predominantly estuarine sediments, the source of its sediments is both fluvial and marine. They are holocene post-barrier sediments, with variable thicknesses from 2 to 5 meters, compound by fine to very fine sands, well selected with dispersed charcoal fragments and, eventually, ceramic fragments. These sediments cover the older post-barrier lower sediments, which form a package with a thickness of up to 10 meters, consisting predominantly bioturbated sands, from moderate to good selection, fine to medium granulometry, and may be locally coarse to conglomerate.

Kourou has the geology very similar to Tatuoca, having in its majority sedimentary rocks.

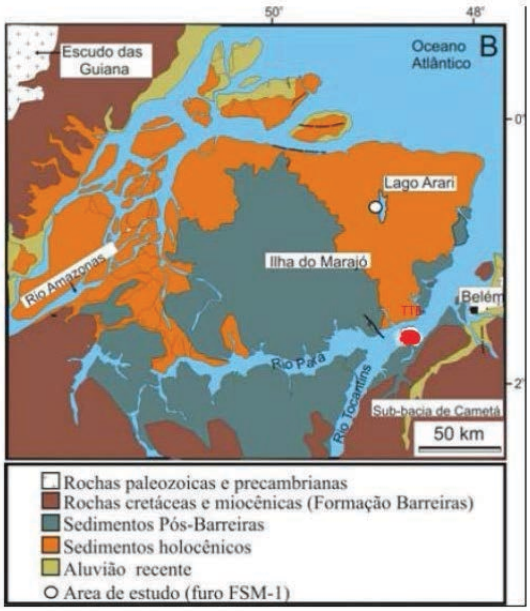

Figure 5. Geological map of the region of Tatuoca

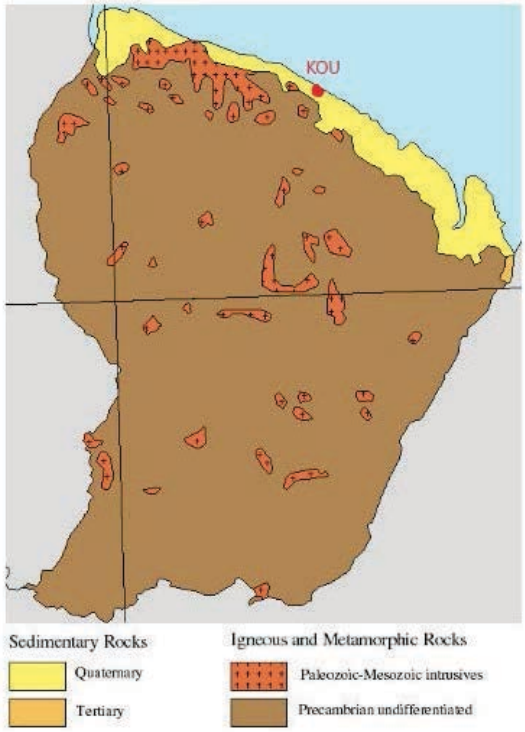

Figure 6. Geological map of the region of Kourou

Conclusions

The present work showed that the morphology of the curves obtained for Z might be interpreted to be due to the Equatorial Electrojet (EEJ) and the SAMA.

It can be seen that the variation in the Z component is a result of the great influence of the Sq current system and in a smaller scale it is due to induction effects in the ocean (Kuvshinov *et al.,* 2007).

The geological influence is imperceptible in the graphs seen, because it is very small when compared with the Sq system.

For a better understanding of the geological influence in the curves, it will be necessary to use a longer period of days, and a statistical analysis should be done using the frequency domain in the same diurnal variation for comparison with the depth of the crust. Finally, a model should be made aggregating all of these influences

The diurnal variation of the Z component displayed an opposite sign from the northern side of the dip equator to the southern side.

The EEJ can enhance the Sq current system in the equatorial region, however, a kind of phase difference was observed between the three stations studied. This phase shift may be attributed to the differences in their latitudinal locations.

The data of Z component from ASC can be a problem in some cases, because of all the variations in the magnetization that a volcanic island can have.

The pattern obtained in the curves revealed that D has deviated from the normal known variation of morning trough and afternoon crest. This could be attributed to change in electric field at the magnetosphere (Okeke et al., 1998).

Acknowledgements

The authors are thankful to the Observatório Nacional, CNPq and CIEE for the financial support. Also, we thank the INTERMAGNET for the KOU, TTB and ASC data and to the II PANGEO's committee for the opportunity.

References

Baker, P. E., Gass, I. G., Harris, P. G., and Le Maitre, R. W., 1964, The volcanological report of the Royal Society expedition to Tristan da Cunha, 1962: Philosophical Philosophical Transactions of the Royal Society of London. Series A, Mathematical and Physical Sciences, v. 256.

Brandl, W., "Erdmagnetische Untersuchungen im Brockenmassif", Abh. der Preuss. Geol. Landes., N. F., 188 (1939) 82 pp.

Freire, L., Laranja, S. R. and Benyosef, L, 2016. Geomagnetic Field Variations in the Equatorial Electrojet Sector, VII Simpósio Brasileiro de Geofísica.

Gelvam A. Hartmann and Igor G. Pacca. Time evolution of the South Atlantic Magnetic Anomaly, Annals of the Brazilian Academy of Sciences (2009) 81(2): 243-255.

International Service of Geomagnetic Indices.

James Cresswell (UK), The geology of Saint Helena, Ascension Island and Tristan da Cunha, Deposits Magazine - Issue 45 (2016), pages 17-23.

Jürgen Matzka, et al.,2009. Geomagnetic observations on Tristan da Cunha, South Atlantic Ocean, ANNALS OF GEOPHYSICS, VOL. 52, N. 1, February 2009.

Kuvshinov, A., C. Manoj, N. Olsen, and T. Sabaka (2007), On induction effects of geomagnetic daily variations from equatorial electrojet and solar quiet sources at low and middle latitudes, J. Geophys. Res., 112, B10102, doi:10.1029/2007JB004955.

Le Sager, P., and T. S. Huang, Longitudinal dependence of the daily geomagnetic variation during quiet time, J. Geophys. Res., 107(A11), 1397, doi:10.1029/2002JA009287, 2002.
Richard A. Geyer, 1951: Geomagnetic Survey of a Portion of Southeastern New York State. Geophysics, vol. 16, issue 2, p. 228.

Susan Macmillan, Chris Turbitt and Alan Thomson, 2009. Ascension and Port Stanley geomagnetic observatories and monitoring the South Atlantic Anomaly, ANNALS OF GEOPHYSICS, VOL. 52, N. 1, February 2009.

Weaver, B. 2002: A Guide to the geology of Ascension Island and Saint Helena, ebook.

Weaver, B. Website:
http://mcee. ou.edu/bweaver/Ascension/sh.htm.

Yamazaki, Y., et al., 2011. An empirical model of the quiet daily geomagnetic field variation, Journal of Geophysical Research, 116, A103112.

Observatorio Geofísico Del Uruguay (Monitoreo Geomagnético Y Sismológico)

Leda Sánchez Bettucci[1,2] , Ramón Caraballo[2]

[1] Área Geofísica-Geotectónica, Instituto de Ciencias Geológicas, Facultad de Ciencias, Universidad de la República (leda@fcien.edu.uy)

[2] Observatorio Geofísico del Uruguay

[3] Facultad de Ingeniería, Universidad de la República

Resumen

Uruguay se encuentra próximo centro de la Anomalía Magnética del Atlántico Sur, comarca del planeta con los menores valores de campo magnético a nivel del globo. Esto puede producir consecuencias como ser una mayor vulnerabilidad a las radiaciones cósmicas nocivas, consecuencias a nivel de las tele y radiocomunicaciones, y generación de corrientes inducidas en líneas de alta tensión y ductos de larga extensión (gaso, minero u oleoductos). Asimismo, la instalación de una red sismológica en el territorio nacional resulta fundamental para conocer la vulnerabilidad del territorio frente a eventos de baja magnitud, como así también colaborar en el monitoreo de explotaciones mineras y la actividad de importantes infraestructuras.

Introducción

En el año 2010 se asumió el compromiso de generar para el país un Observatorio Geofísico dedicado al estudio y monitoreo en dos grandes áreas: una sismología y geomagnetismo con el fin de funcionar como centro de referencia nacional en el estudio y desarrollo de estrategias para la mitigación de riesgos relacionados con fenómenos naturales vinculados a esta temática (Figura1).

El Observatorio Geomagnético, localizado al sur de la localidad de Aiguá (Departamento de Maldonado) cuenta con dos magnetómetros Gem system GSM-90 y dIdD (adquiridos mediante financiación de Pedeciba -Programa de Desarrollo de Ciencias Básicas- y Fondos centrales UDELAR, CSIC), antena VLF (super-SID), para medición de la actividad solar, a través del Dr. Kazuo Makita de la Universidad de Takushoku (Japón), responsable del proyecto SARINET de monitoreo ionosférico para la región de América del Sur, nos fue donado un Riómetro, y en el año 2016 una cámara all sky para detección de transitorios en la alta atmósfera (ondas de gravedad, TIDS, etc), también instalado en Aiguá.

La instalación de una red de instrumentación sísmica en Uruguay, fue iniciada en el año 2013 por el Observatorio Geofísico del Uruguay (OGU) y ha generado un avance significativo en el conocimiento de la sismicidad en nuestro país. Durante los últimos cuatro años, el número de sensores sísmicos en funcionamiento ha aumentado sustancialmente, de uno a once. En Uruguay se han reconocido estructuras con desplazamiento horizontal y fallamiento inverso de escasa extensión. Basado en el conocimiento geológico y en eventos sísmicos históricos y recientes podemos sugerir que algunas reactivaciones de fallas precámbricas y mesozoicas podrían ser los responsables de la generación de eventos sísmicos. Nuestra sismicidad se caracteriza por ser baja a moderada, aunque es capaz de ocasionar daños significativos en los centros urbanos, particularmente en Montevideo donde se encuentra la mayor concentración de población del país. El Observatorio Geofísico del Uruguay (OGU) gestiona la red sísmica nacional, la cual está constituida actualmente por cuatro sismómetros de banda ancha y diez acelerómetros triaxiales de la Dirección Nacional de Minería y Geología (DINAMIGE- MIEM).

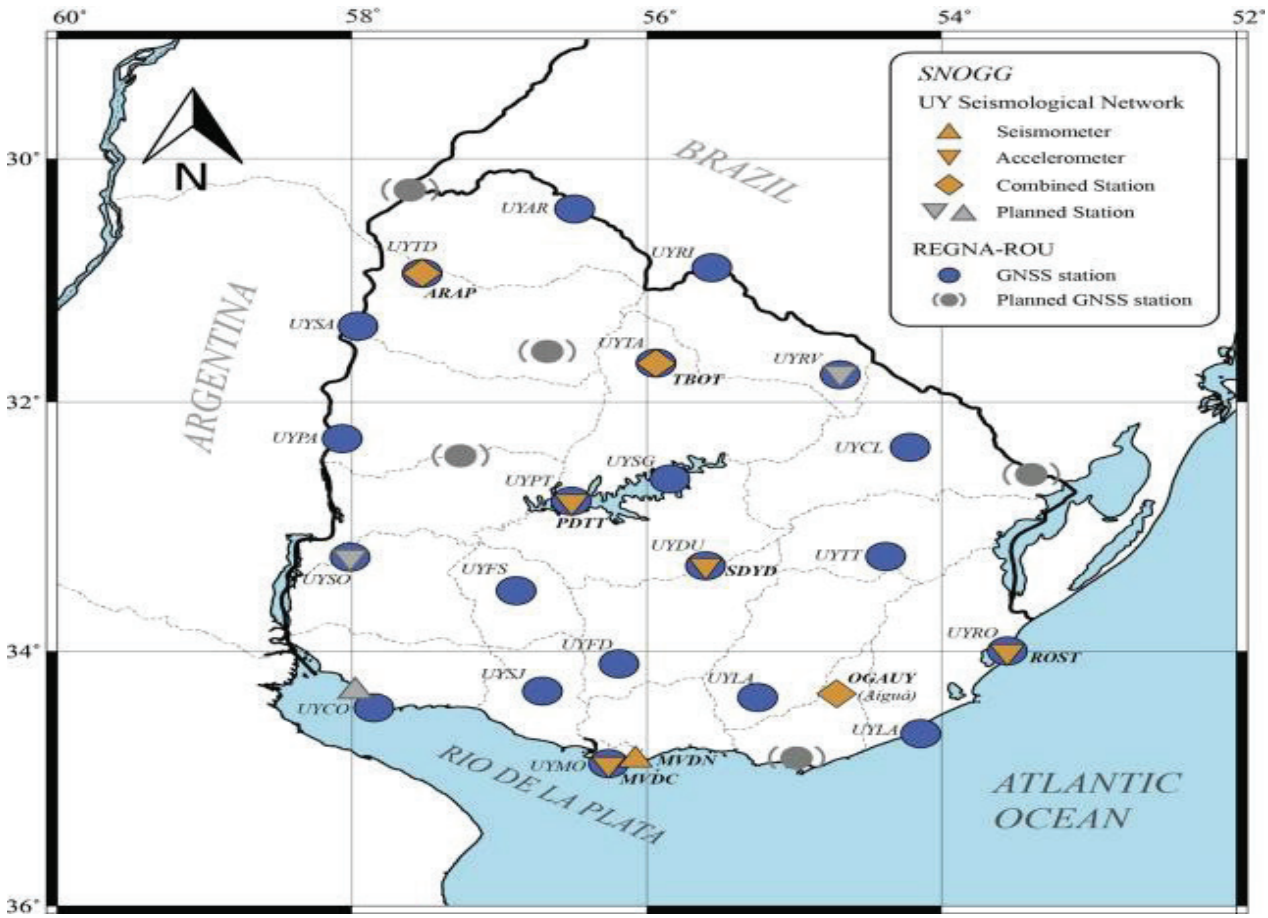

Figura 1. Localización de las estaciones sismológicas, re UY.

Conclusiones

Se pretende poder conocer las variaciones del campo magnético de corto plazo para usos industriales: prospección geofísica, mediciones con equipamiento magnético, en un corto a mediano plazo. Se iniciarán estudios que aporten a la prevención frente a tormentas geomagnéticas y sus efectos asociados: corrientes inducidas en líneas de alta tensión y gaso y oleodcutos, alto flujo de partículas energéticas sobre componentes electrónicos, radiación sobre satélites, efectos sobre la ionosfera y descargas eléctricas, ionización y mutaciones. Así también se pretende determinar los niveles de variación de diurna y anual del campo magnético terrestre y su interacción con el viento solar.

Agradecimientos

El desarrollo y gestión del Observatorio Geofísico del Uruguay no sería posible sin el apoyo que se recibe por parte de Presidencia de la República a través del Sistema Nacional de Emergencias (SINAE), ANTEL, Ministerio de Industria, Energía y Minería MIEM a través de la Dirección Nacional de Minería y Geología y su Director Nacional Lic. Néstor Campal, Ministerio de Defensa- Servicio Geográfico Militar, Universidad de la República – CSIC, PEDECIBA y el dueño de la Estancia de Aiguá Mr. Justin Portma

The Magnetic Observatory of Coimbra (COI): Past, Present operating Status and Future Developments

Paulo Ribeiro [1]; M. Alexandra Pais [1, 2]; Anna L. Morozova [1]
[1] CITEUC, Geophysical and Astronomical Observatory, University of Coimbra, Portugal
[2] Department of Physics, University of Coimbra, Portugal

Abstract

The Magnetic Observatory of Coimbra (COI) is one of the oldest observatories in operation in the world. With a centenary tradition, the geomagnetic measurements started in 1864 in the early site, after missions to the Greenwich and Kew observatories in 1862 and support by the president of the Royal Society of London, Edward Sabine, who offered to supervise the magnetic instruments construction and calibration. The growth of the city during the first quarter of the twentieth century dictated the relocation of the observatory to its current site in 1932 (~ 1.5 km from the city center) in Alto da Baleia. First years in Baleia suffered from very flawed operation and all observations ended up being interrupted around 1941 due to the difficult years of World War. Magnetic observatory routines were resumed in 1951 on a methodical and more accurate basis. By the late 1980s, the COI data began showing some non-negligible perturbations mainly related to the aging and drift of instruments and to the urban magnetic noise. Part of these problems and limitations were overcome in 2007 by replacing the complete old set of instruments with the modern digital variometer (FGE) and the standard absolute instruments (DI-flux and GSM-90F1). This upgrade resulted in a healthier base-line stability and in a clear quality improvement of obtained data series (showing a reduced noise level) as demonstrated by their first time-differences. Nonetheless, the ongoing city growth continued to critically threaten the good functioning and quality of observatory data.

In addition to reporting on the history, instruments and routines of the observatory, this presentation aims to characterize the geomagnetic series currently observed in COI, and to present the plans for future development, which will involve a new relocation of the observatory to a rural area and the application to become an INTERMAGNET network member

A Comparative Study of Pc's 5-6 Geomagnetic Pulsations at Low and Middle Latitudes

Vinicius J. O. Werneck de Carvalho[1] *Luiz Benyosef*[1] *and Angelo De Santis*[2]

[1] *Observatório Nacional - Brazil*

[2] *Istituto Nazionale di Geofísica e Vulcanologia - Italy*

Abstract

In this study Pc5-6 magnetic pulsations were analyzed considering three geomagnetically disturbed days using data from VSS and TTB magnetic observatories (low latitudes) in Brazil and CTS and DUR (middle latitude) in Italy. The Brazilian stations are influenced by Equatorial Electrojet (EEJ) and the South Atlantic Magnetic Anomaly (SAMA), while the Italian stations are free of a strong natural magnetic anomaly. Spectral analyses were performed using the Wavelet techniques.
The results were analyzed and compared showing the effects of different latitudes on the pulsations

Introduction

Magnetic pulsations, or micropulsations, are short-period geomagnetic field fluctuations, with typical amplitudes smaller than one part in 10^4 of the main field, have a transient effect, with periods ranging from 0.2 seconds to 17 minutes [1]. It is known that pulses recorded in both the ground and the magnetosphere originate from the manifestations of plasma waves, known as ultra-low frequency (ULF) hydromagnetic waves, which occur in the magnetosphere, as a result of complex interactions between the solar wind and terrestrial magnetosphere. They can also be originated by sudden Storm Sudden Commencements (SSC) and Sudden Impulses (SI), although it is difficult to confirm.
Micropulsations are classified into two major classes, depending on the wave morphology and duration period: Pulses with quasi-sinusoidal waveforms are called continuous pulsations (Pc), appearing pronouncedly in the day hemisphere, and those with irregular wave patterns are called irregular pulsations (Pi). Pc's 5-6 (1 to 6)*mHz* pulses are more easily found at medium and high latitudes, owing to the nature of their genera equatorial ionosphere and often appear almost simultaneously with those at auroral latitudes, for example [3].ting mechanism [2]. However can also be observed in low latitudes, possibly amplified by the Cowling effect in the equatorial ionosphere and often appear almost simultaneously with those at auroral latitudes, for example [3].

Studies indicate that the generation mechanism is driven by the propagation of resonances in the field line, driven by magnetosphere cavity modes or by waveguides. Ziesolleck and Chamalaun [4], in their work found two peculiar characteristics for Pc's 5-6 pulsations: The first is the increase of their pursuits in the low and middle latitudes during geomagnetically disturbed days and second, there was a sharp fall in the spectral intensity with the increase of latitude. In this study, Pc's 5-6 micropulsation were analyzed considering three geomagnetically disturbed days using data from VSS and TTB magnetic observatories (low latitudes) in Brazil and CTS and DUR (middle latitude) in Italy (Fig.2). The Brazilian stations are influenced by Equatorial Electrojet (EEJ) and the South Atlantic Magnetic Anomaly (SAMA), while the Italian stations are free of a strong natural magnetic anomaly. Spectral analyses were performed using the Wavelet techniques. The results were analyzed and compared showing the effects of different latitudes on the pulsations.

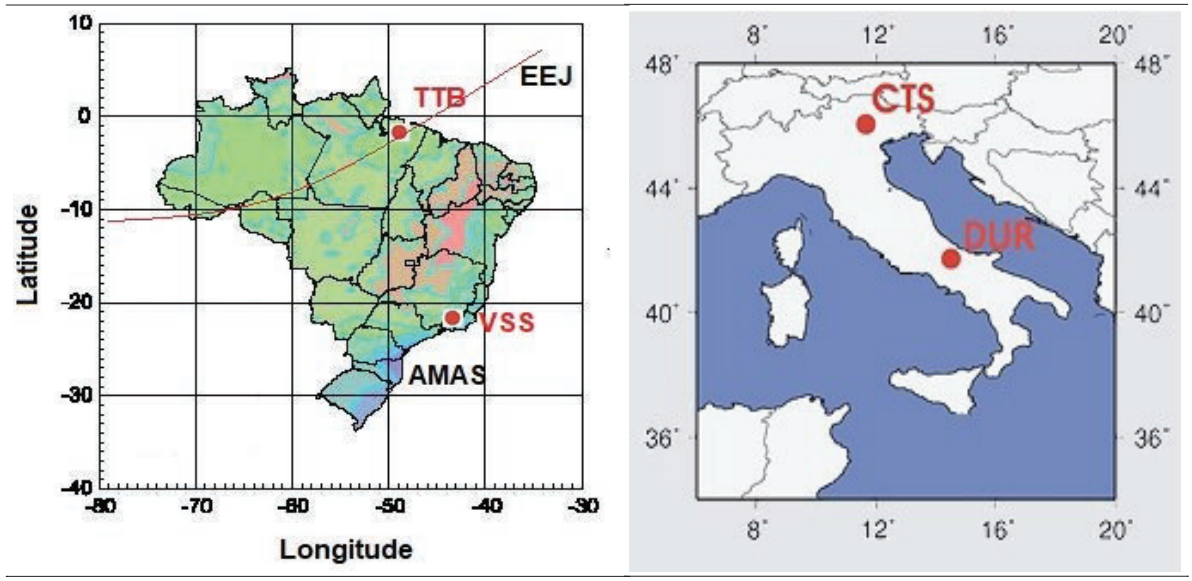

1a *1b*

Figure 1 – Maps showing the locations of the stations, in Brazil (1a) and Italy (1b), for which data were used to this paper.

The geomagnetic and geographic locations of both kinds of stations can seen in table 1:

stations.	Code	G.G Lat	G.G Long.	G.M Lat.	G.M Long.
Cast.Tesino	CTS	46.05 N	11.65 E	37.75 N	85.68 E
Duronia	DUR	41.65 N	14.46 E	35.06 N	88.01 E
Tatuoca	TTB	01.20 S	48.50 W	07.88 N	24.03 E
Vassouras	VSS	22.40 S	43.66 W	13.52 S	27.19 E

Table 1 – List of observatories

Experimental Methodology

Through the indices Kp, two geomagnetically disturbed days were selected: September 17 and 26, 2011. In this work, only the horizontal component H was considered. To high light only the pulses Pc5-6, a digital filtering of the Pass Band type was used. Subsequently, the dominant frequency of events recorded in the observatories was investigated using the Wavelet. The mother wavelet applied in the processing was Morlet, which provides considerable resolution in period and frequency, revealing in which part of the analyzed signal the energy transport and its associated frequencies occur.The Morlet Wavelet consists of a plane wave, modulated by the Gaussian function (1):

$$\psi(t) = \left[\exp(i\beta t)\exp\left(\frac{-\beta^2}{2}\right)\right]\exp\left(\frac{-t^2}{2}\right) \quad (1)$$

Where β is dimension less. This Wavelet function is a complex func tion that allows analyzing the phase and the module of the composite signal. The times are in Universal Time (UT), - 3 hours local time in Brazilian stations and +2 hours local time in Italian stations.

Results

Figure 3 shows the results the Spectra of geomagnetic pulsations at the four stations for day 26, while the Figures 4 and 5 show the filtered signal of component H (Pc5-6) at the four stations for day 17.

Magnetic Observatories - CTS, DUR, VSS and

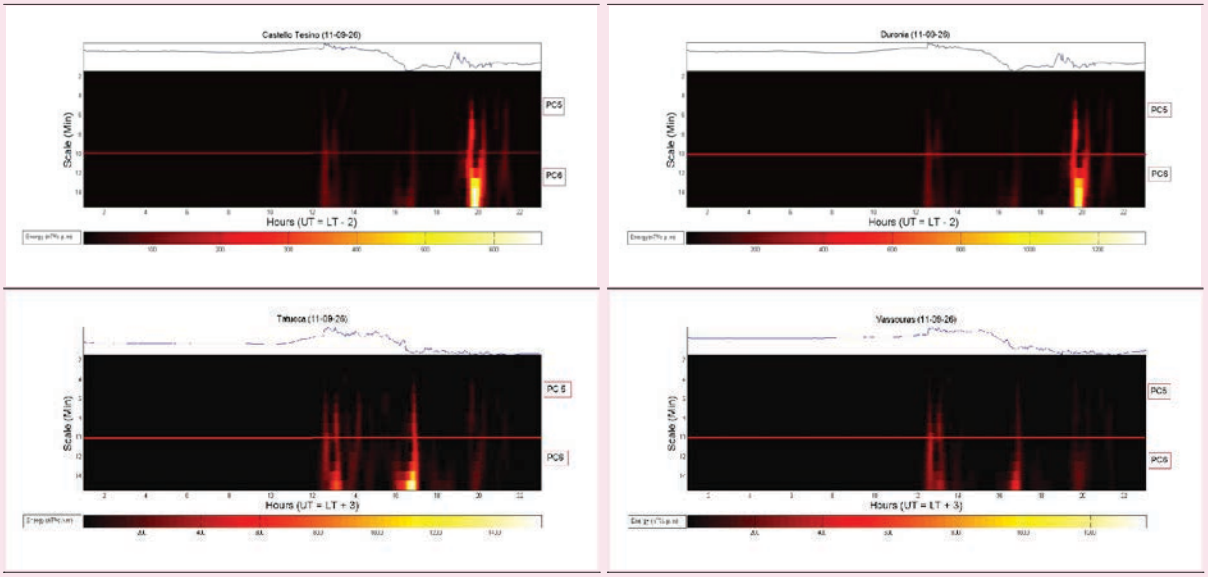

Figure 3:Spectra of geomagnetic pulsations witch Continuous Wavelet Analysis, in component H, on

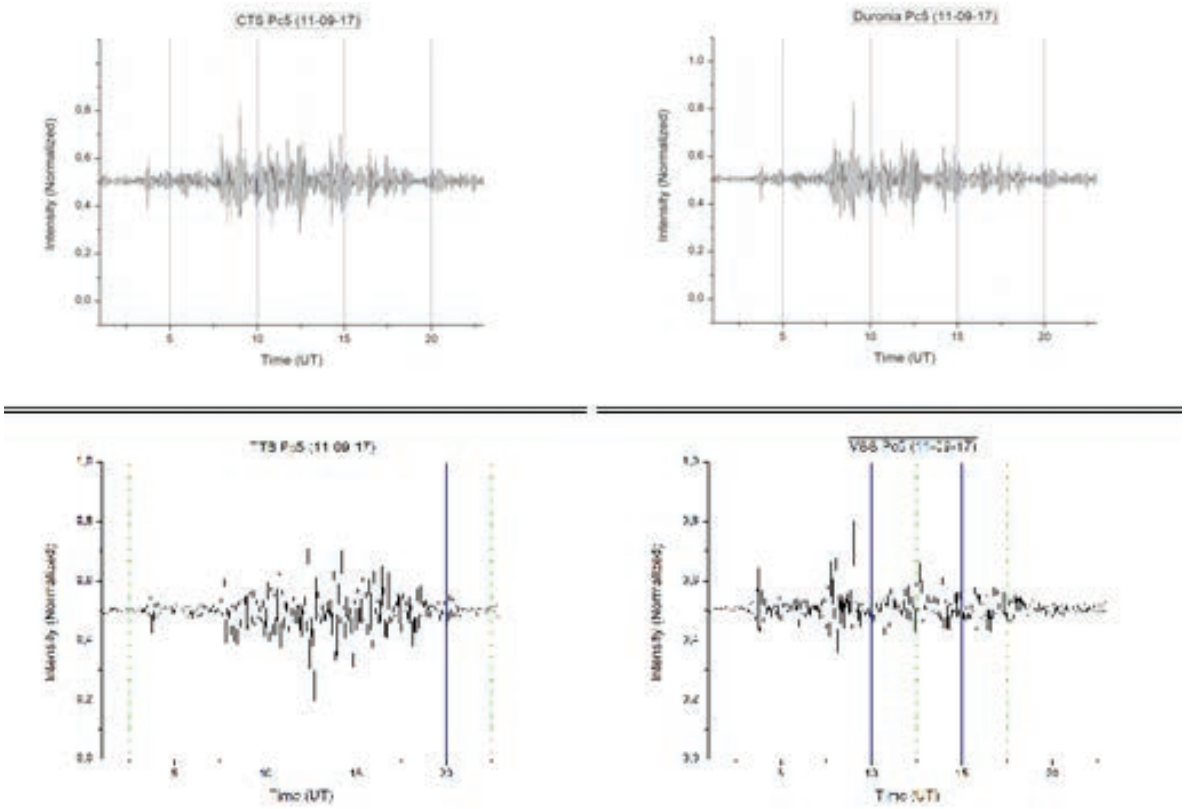

Figures 4 – Filtered pulsations (Pc5) on September 17, 2011.

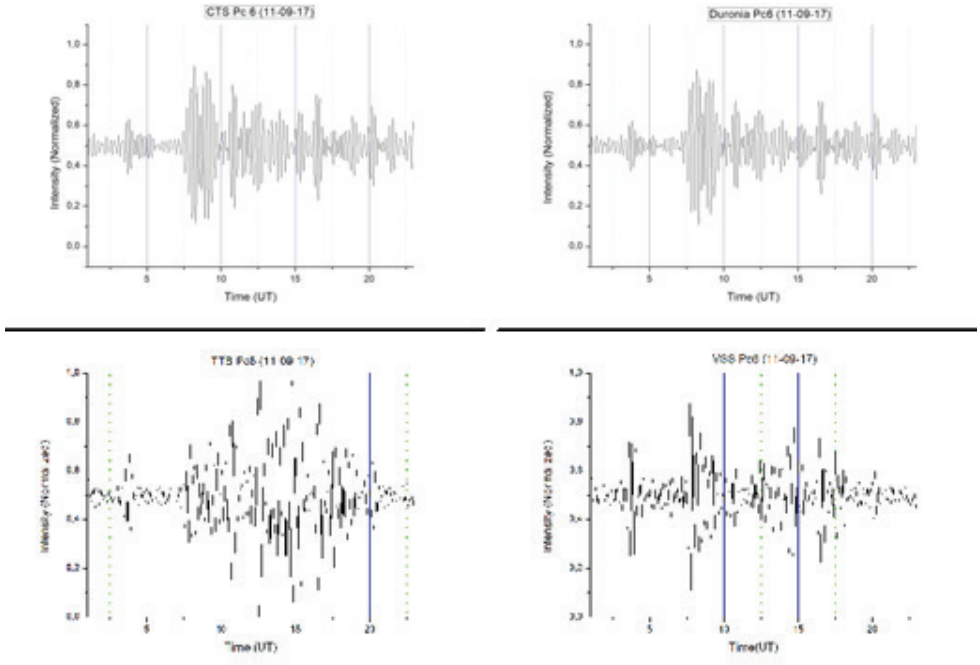

Figure 5 - Filtered pulsations (Pc6) on September 17, 2011.

The analysis of the filtered signals in the Pc5-6 band shows almost simultaneous wave packet registers between 7-15 UT in the CTS, DUR and VSS stations. However, at the TTB station, the mor- phology is very different from the others, concentrating thehighest level of activity between 10-15 UT. It is observed that CTS and DUR record at the same time a strong energy in the frequency Pc6 at 20 UT, while the stations of TTB and VSS they presented very low energy intensity in this period. TTB and VSS show a more pronounced increase in the Pc5 pulse range, while in the CTS and DUR stations, there was little or no occurrence, with the exception of the large event at 20UT.

Discussion

Despite being located at low latitudes, TTB presented high ener- getic levels, registering Pc6 micropulsations of up to approximately $1400nT^2$, highest value among stations. This behavior is pos- sibly related to the performance of the EEJ, which acts in this region as an energy catalyst, thus providing, records of typical micropulsa- tions of medium and high [4], such as Pc5-6. Similar behavior was expected in VSS due to the influence of SAMA, where the innermost part of the Van Allen belt has the closest approach to the Earth's surface. A possible explanation for the low energy level presented, whether its latitude is on the edge of SAMA, where the intensity of radiation is weaker, allowing records of micropulsations, even in a more pleasant way. It was observed a synchrony in the time and morphological in the analyzes Wavelets in pairs of stations CTS- DUR and TTB-VSS. The L-Shell of these regions was calculated through equation (2) in order to find a possible explanation for the behavior.

$$r = Lcos^2(\lambda) \qquad (2)$$

Where *r* is the radial distance (in earth radii) to a point on the line, λ is its geomagnetic latitude, and *L* is the L-shell of interest. The CTS-DUR stations have L-Shell ~1.5**,** while the TTB-VSS station pairs have L-Shel ~1.0. This probably explains the similar behav- ior between these stations, since the origin of the pulse propagation mode is stationary (transverse) along the lines of force. This study shows that the Pc5-6 pulsations have similar forms between the CTS, DUR and VSS stations, having some frequencies and similar ampli- tudes in the Pc5 range mainly. This study makes clear the strong influence of the EEJ on the micropulsations in TTB and a positive correlation between the energetic amplitude of the pulsations with the Kp index.

Acknowledgements

The authors thank the REBOM project (especially Ronaldo M. de Carvalho), CAPES and INGV.

References

Jacobs, J. A., Kato, Y., Matsushita, S. and Troitskaya, A. (1964). Classification of geomagnetic micropulsations. J. geophys. Res. 69, 180

Walker, A. D. M., J. M. Ruohononiemi, K. B. Baker, R. A. Greenwald, and J. C. Samson, Spatial and temporal behavior of ULF pulsations observed by Goose bay HF radar, J. Geophys. Res.

Araki, T., Global structure of geomagnetic sudden commence- ments, Planet. Space Sci., 25,373, (1977).

Ziesolleck, C. W. S. and F. H. A. Chamalaun, A two dimensional array study of low-latitude Pc5 geomagnetic pulsations, J. Geophys. Res., 98, 13705, 1993

Development of an Active Calibration System for Fluxgate Magnetometers

Gustavo G. Cabral, André Wiermann and Luiz Benyosef
Observatorio Nacional - Brazil
gustavocabral@on.br , andrew@on.br , benyosef@on.br

Abstract

The fluxgate magnetometer requires the use of specific calibration and test techniques in order to obtain its calibration coefficients and to assure its technical features. This work aims the development of a set of procedures, electronic systems and computational tools that allow the active testing and calibration of this type of magnetometer. The results obtained can be applied in the development of new magnetometers, functional test of existing instruments and comparison between various instruments.

Introduction

The proposed system is based in a Helmholtz coil controlled by a set of programmable intruments, switches and precision current sources for magnetic excitation. In association to this arrangement a thermal chamber and a magnetic shield are employed to fulfill the characterization requirements.
Calibration coefficients are obtained experimentally by the variation of physical parameters that lead to the change of the values measured by the magnetometer under test. Those coefficients correlate, in the case of triaxial magnetometers, intensity and direction of the magnetic field to which the instrument is subjected, with its response signal. Depending on the type of magnetometer this response signal can be digital or analog.
This project implements the following automated systems:Magnetic characterization system through variation of excitation frequency Offset characterization system Magnetic characterization system Thermo-magnetic characterization system.

Method

The method consists in executing a particular test sequence, starting with the characterization of the sensor core material, continuing with the tests of the electronic circuit and concluding with the exercise of the assembled set to obtain the calibration parameters of the instrument. This method can be summarized by the following steps: External magnetic field response curve survey Thermal dependency curve survey Noise evaluation Operating limits evaluation

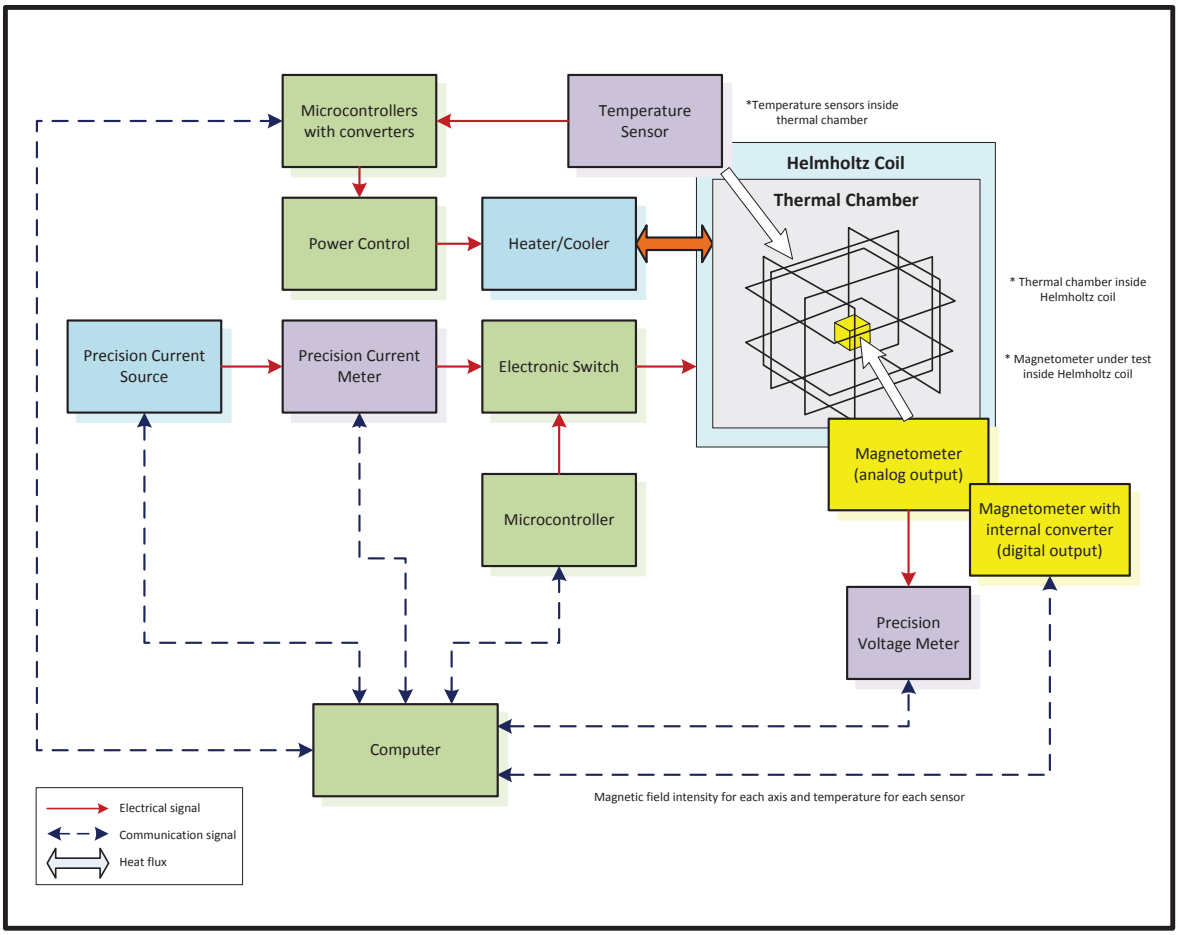

Figure 3 – Thermo-Magnetic Characterization System for Magnetometers with Analog or Digital Outputs

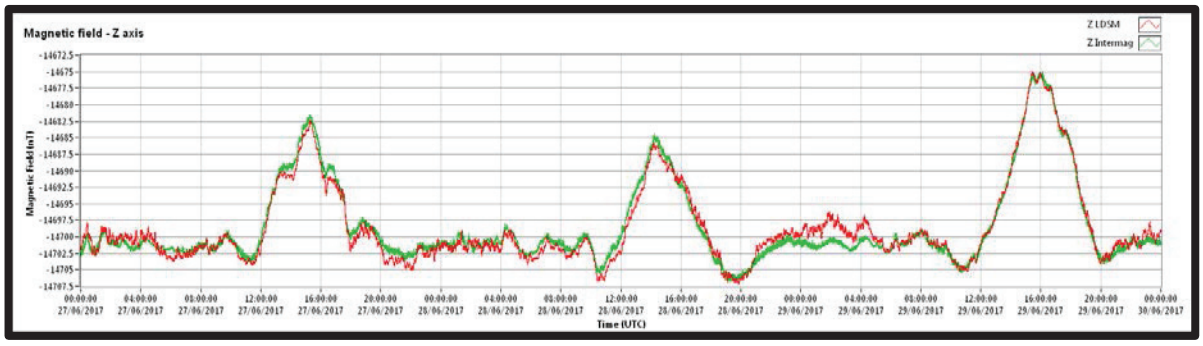

Figure 4 – First results of an instrument calibrated with this system. Measurement performed at the Observatory of Vassouras. Comparison of the LDSM magnetometer measurements with the INTERMAGNET magnetometer.

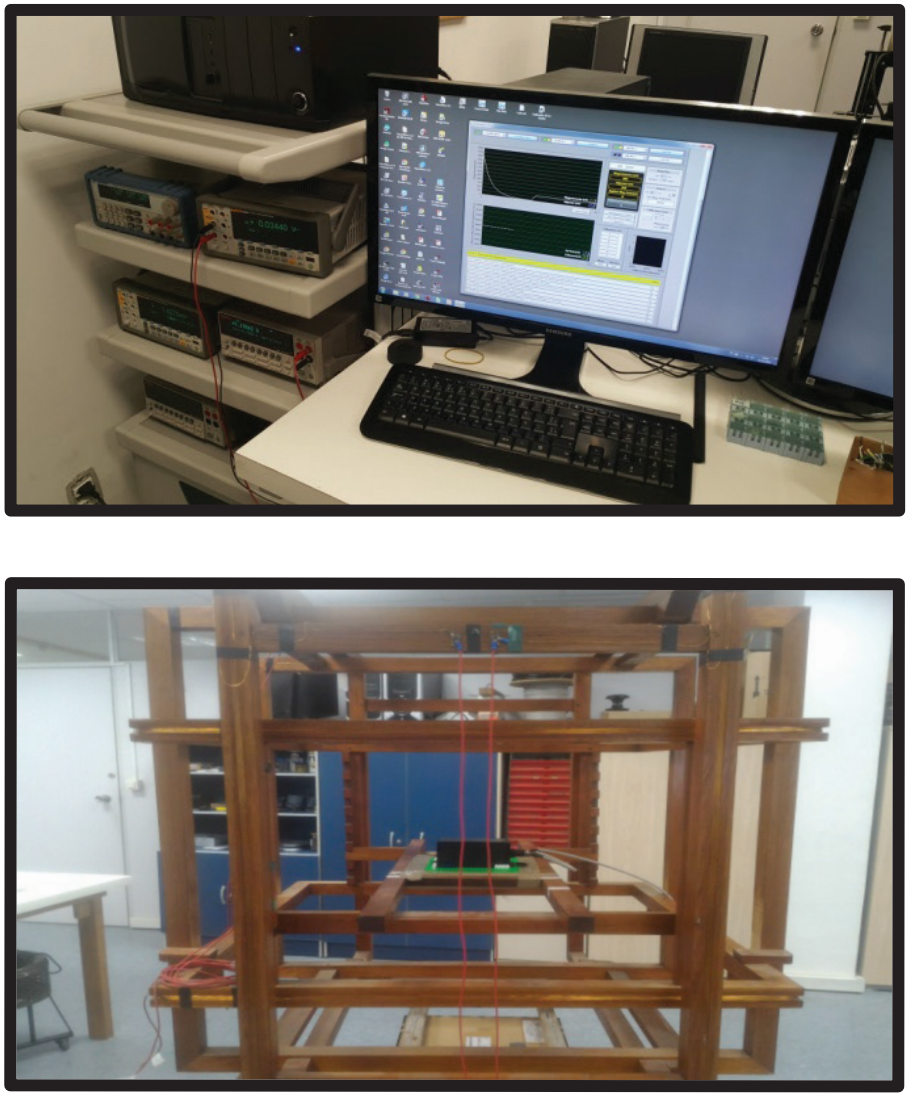

Figure 1 – Computer System with Instruments and Helmholtz Coil

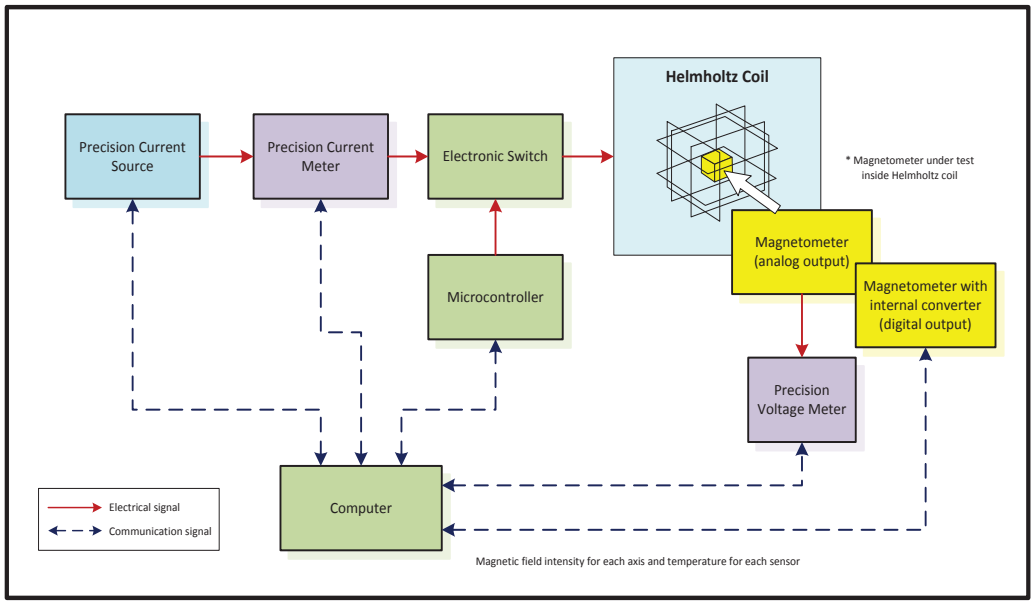

Figure 2 – Magnetic Characterization System for Magnetometers with Analog or Digital Outputs

Development of an Automatic Device for the Determination of the Geographical North from the Measurement of the Solar Ecliptic and Georeferencing

Natacha Oliveira, André Wiermann, Cosme F. Ponte-Neto
Observatório Nacional – Brazil

Abstract

The present work aims at the construction of an electromechanical device based on several sensors and controlled by computational routines, for the automatic determination of the Geographic North direction, from the measurement of the angular position of the sun and the georeferencing information obtained from a GPS module.

Introduction

The geographic (or true) northern direction information is of great importance for several areas of knowledge, such as: geomagnetism, applied geophysics, cartography, topography, civil engineering, georeferencing and navigation. In the context of geophysics, this is particularly important for determining the magnetic declination, which is a parameter directly related to the study of the secular variation of the geomagnetic field. The magnetic declination varies from point to point on the Earth's surface, and varies over time at different rates in different places. All these characteristics contribute to the complexity of determining magnetic declination, which requires that true north be determined with a well-established methodology.

Method

The proposed technique is based on measuring the solar azimuth at any height, other than the zenith, by means of optical sensors and a servocontrolled rotary guide device. The information from this azimuth is then combined with the geodetic position and local time, obtained through the
integrated GPS module. The angle determined from the projection of the ecliptic will guide a sighting strap that will then allow the user to project a line of sight in a north-south direction on local topographic references of his choice.

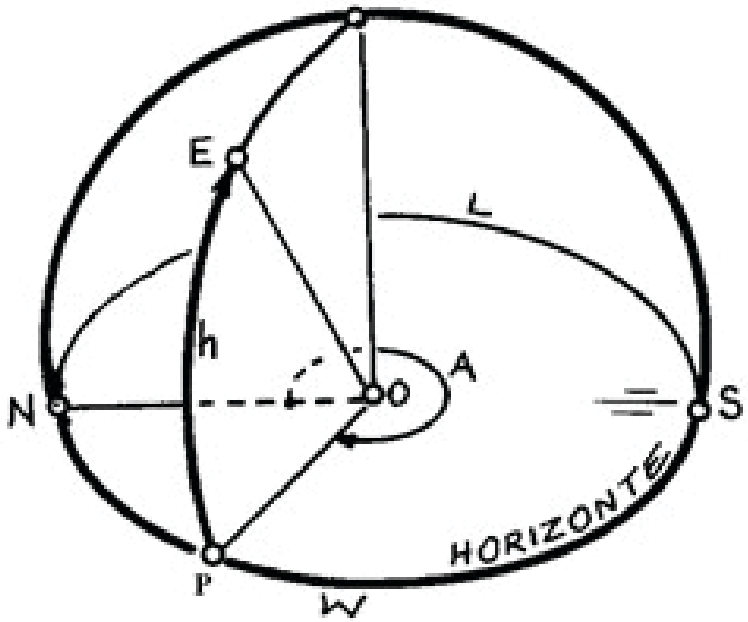

Figure 1 - Coordinate system used: Local Horizontal System

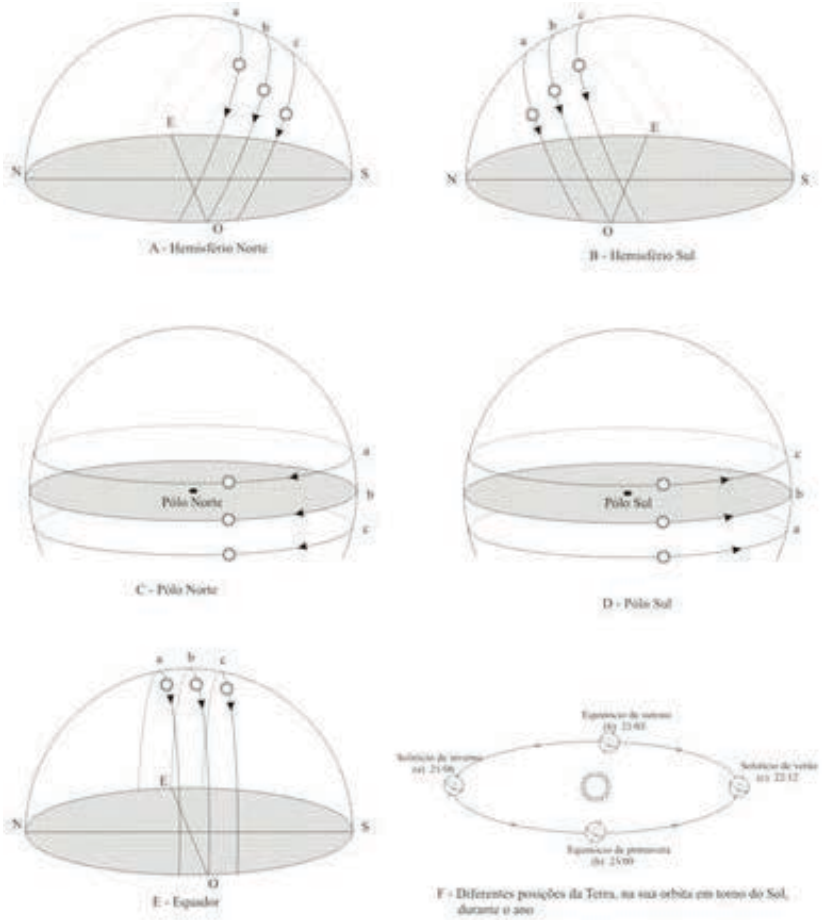

Figure 2 - Position Astronomy

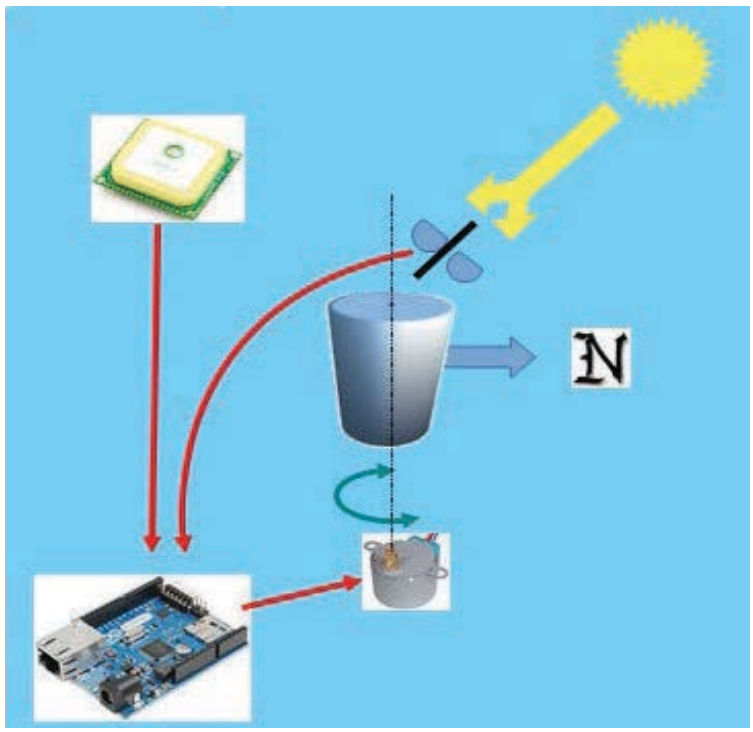

Figure 3 - Diagram illustrating the device

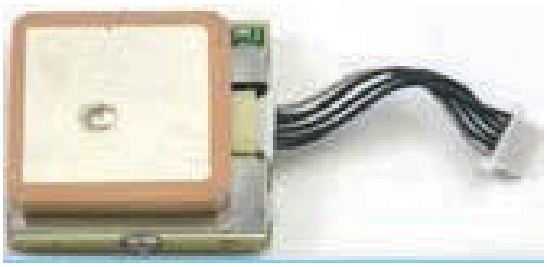

Figure 3.1 - GPS Antenna

Figure 3.2 - Optical sensor

Figure 3.3 - Servo controlled motor

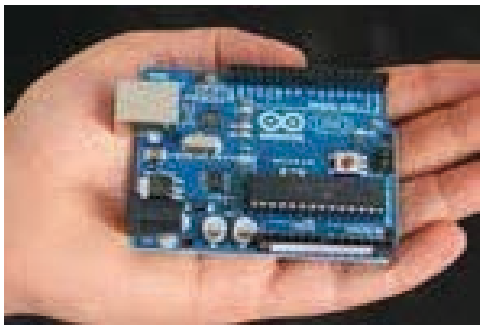

Figure 3.4 - Arduino processor

Análise Comparativa e Interpretação de Dados de Calibração de Um Magnetômetro Fluxgate de Alta Resolução Para Observatórios Geomagnéticos

Thaísa Melo and André Wiermann
Observatório Nacional – Brazil

Introdução

O Laboratório de Desenvolvimento de Sensores Magnéticos (LDSM/ON) vem desenvolvendo sensores do tipo fluxgate desde sua criação, em 1995. O LDSM realiza também serviços de calibração magnética em bússolas aeronáuticas, marítimas e geológicas, além de testes e reparos em instrumentos da rede de monitoramento geomagnético do Observatório Nacional. Recentemente, o LDSM construiu um novo magnetômetro com o propósito de atender aos rigorosos requisitos para uso em observatórios geomagnéticos. Um protótipo funcional foi instalado no Observatório Magnético de Vassouras (VSS), com a finalidade de produzir medidas que possam ser comparadas com os instrumentos da rede INTERMAGNET. Os dados registrados vêm sendo utilizados para auxiliar na determinação de parâmetros tais como, deriva instrumental, variação com a temperatura, sensibilidade e ruído. Os primeiros registros mostram resultados promissores que poderão contribuir para o aperfeiçoamento do equipamento.

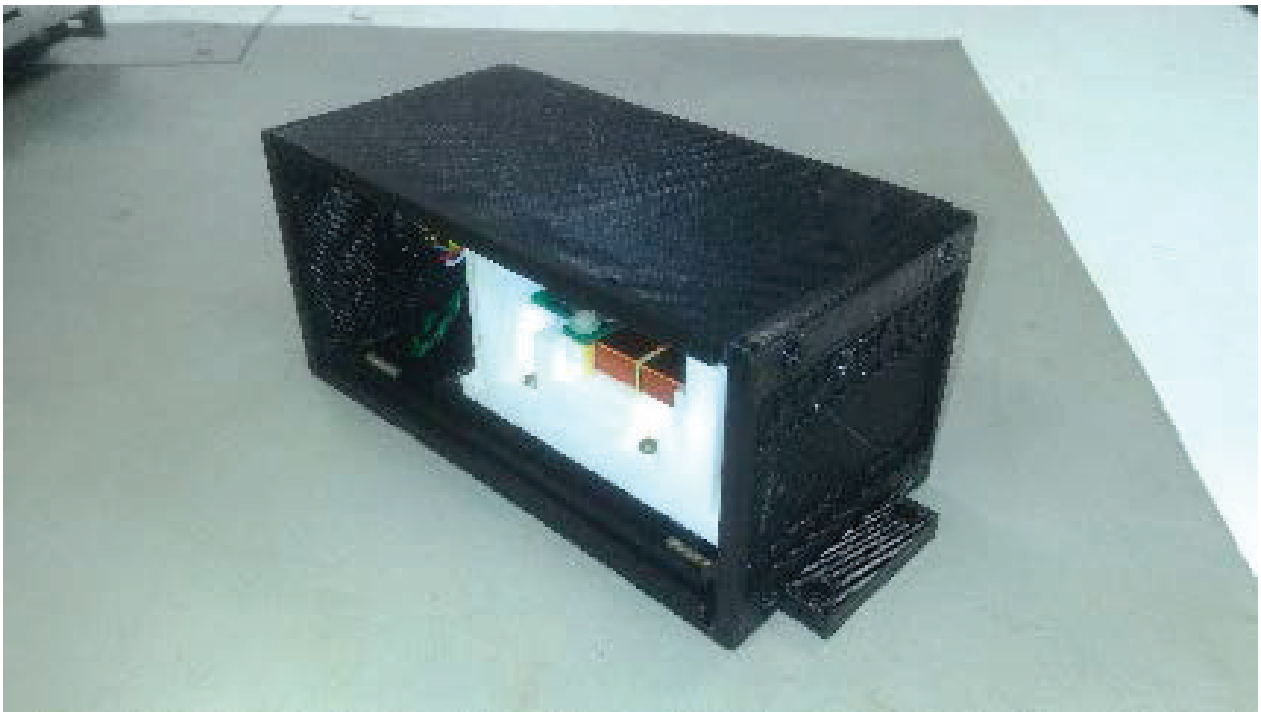

Figura 1 – Protótipo do sensor fluxgate do LDSM para uso em observatórios

Metodologia

Este trabalho tem o propósito de determinar duas principais características do equipamento em teste:
1 – Deriva instrumental em zero e escala
2 – Dependência com a temperatura
A determinação dos parâmetros de operação de um magnetômetro de alta resolução consiste em tarefa complexa e elaborada. Sendo o campo magnéticointensamente pervasivo, seu isolamento é custoso e limitado, dificultando a produção de campos de referência estáveis e precisos, isentos da interferência de ruídos externos, sejam de origem natural ou antropogênica. Para realizar os testes pretendidos, optou-se pela comparação do protótipo com um instrumento de referência (VSS – INTERMAGNET), em regime de operação contínua, onde diferentes valores do campo magnético e de temperatura ocorrem de forma natural. Após as calibrações habituais em laboratório, o instrumento foi então instalado próximo ao variômetro de VSS, onde têm sido coletados os valores de campo e temperatura ao longo de alguns meses. Utilizando ajuste por mínimos quadrados, foram obtidos coeficientes para correção de zero, escala e variação térmica:
$F = a \cdot V + b \cdot (t - t0) + c \cdot Z + d \cdot (t - t0)$
Onde:
F é o campo de referência em NT, V é o valor bruto lido no sensor, t é a temperatura corrente, tO a temperatura de calibração e [a,b,c,d] os parâmetros de ajustes.

Primeiros Resultados

Após dois meses de dados coletados, foram obtidos os parâmetros de calibração [a,b, c, d], posteriormente aplicados aos dados brutos do sensor em teste.

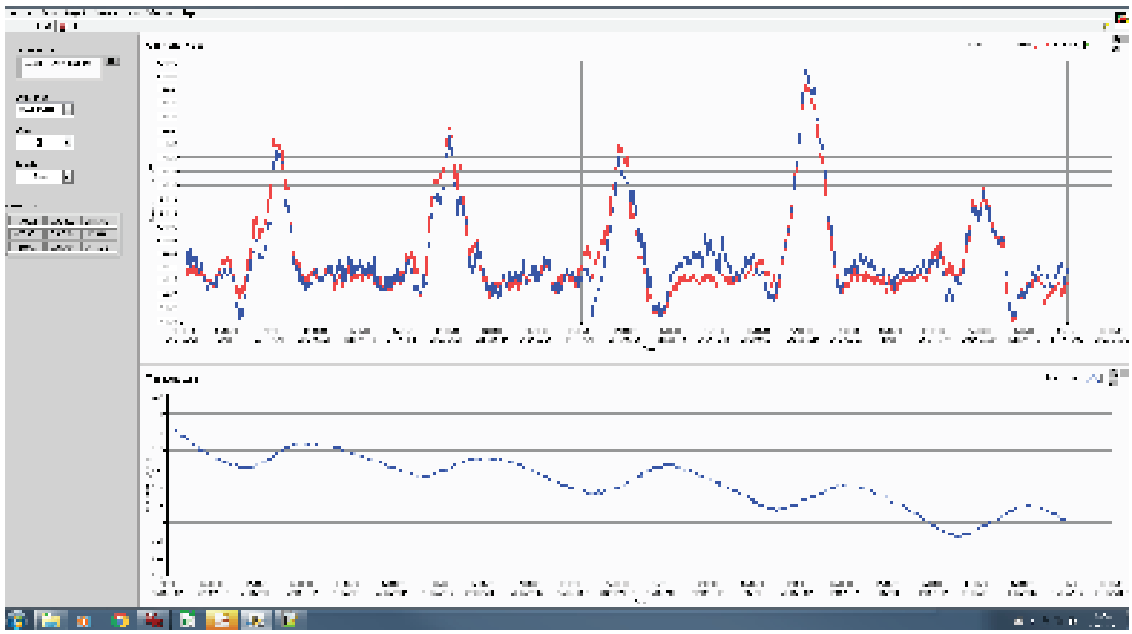

Figura 2 – Leituras brutas acompanhadas do registro das variações de temperatura

Um exemplo dos primeiros resultados, após a aplicação dos coeficientes obtidos, pode ser visto no gráfico a seguir:

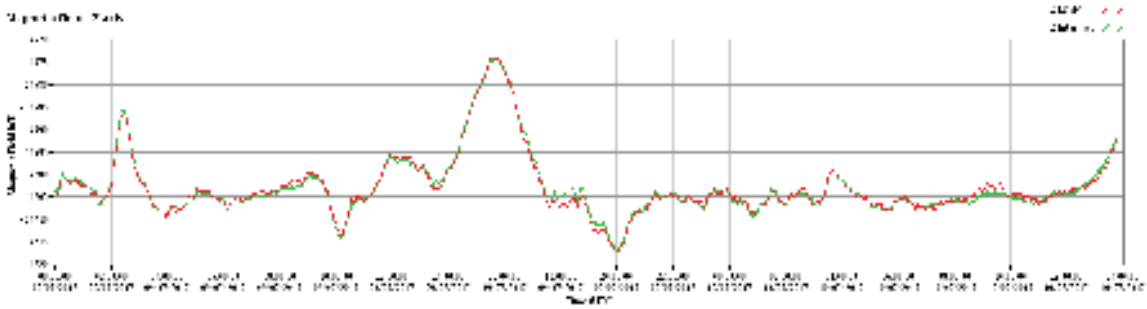

Figura 3 – Leituras comparativas após ajustes nos dados do sensor em teste

Conclusões

Embora ainda em fase inicial, os resultados obtidos pelos ajustes efetuados neste trabalho mostram resultados promissores. Após a obtenção de coeficientes a partir da variação de apenas alguns graus de temperatura e com uma excursão inferior a 100 nT, diferenças médias da ordem de 1nT foram conseguidos, confirmando os testes previamente realizados em bancada no LDSM. Na próxima etapa do projeto, um conjunto maior de dados será utilizado, de forma a melhorar os ajustes. A coleta de dados por um longo período (vários meses), permitirá uma estimativa da deriva do instrumento. Adicionalmente, dois magnetômetros comerciais, de diferentes fabricantes, também estão sendo comparados, permitindo uma melhor avaliação das medidas e dos ajustes efetuados.

Research To Operation (and Operation to Research) In Space Weather

Clezio Marcos De Nardin
Embrace, National Institute for Space Research, 12227-010, S. J. dos Campos - SP, Brazil

Abstract

The present work intends to compile the experience attained with developing the Brazilian Studies and Monitoring of Space Weather (Embrace, from the Portuguese acronym Estudo e Monitoramento Brasileiro de Clima Espacial) Program, which was stablished in August 2007 by a task force composed by public servants of the National Institute for Space Research (INPE) to develop and operate a program of space weather. A revision of the principles of transiting from research to operations in space weather achieved during the evolution of the Embrace Program is presented and discussed based using the case described by the Applied Meteorology Unit (AMU) of bridging the gap between research and operations by provides technology development and transition services to improve operational weather support to the Unites States of America's space program. Also, some highlighted is set under the new Embrace Magnetometer Network and its capability of space weather monitoring and forecast.

Evidence of an Abrupt Secular Variation Change During 2015 in Southern Africa and the Adjacent Atlantic Ocean Region

P.B. Kotzé[1, 2] and J. Matzka[3]

[1] *South African National Space Agency (SANSA), Space Science, Hermanus, South Africa*
[2] *North-West University, Centre for Space Research, Potchefstroom, South Africa*
[3] *GFZ German Research Centre for Geosciences, Potsdam, Germany*

Abstract:
Geomagnetic field data from 5 magnetic observatories located in Southern Africa at Hermanus (HER), Hartebeesthoek (HBK), and Tsumeb (TSU) as well as the adjacent Atlantic Ocean region at St Helena (SHE) and Tristan Da Cunha (TDC) have been analysed to identify abrupt secular variation changes on time scales of less than 1 year. Removal of an annual variation resulting from large-scale magnetospheric and ionospheric currents by means of 12-month differences of the respective observatory monthly mean of northward component X, eastward component Y and vertical component Z, revealed clear evidence of a new geomagnetic jerk that occurred in early 2015 in this area. The results obtained revealed that this 2015 jerk, like the 2014 event, took place with varying amplitudes in the different components at a particular magnetic observatory. In addition, the respective observatories in the region also exhibited strong individual characteristics. To our knowledge, this is the first detailed description of the jerk in early 2015 in this area.
.

Introduction:

The southern African region and the adjacent Atlantic Ocean area have been characterised for several years by strong and abrupt changes in the secular variation pattern of the geomagnetic field (Mandea et al., 2007). In Southern Africa, the three geomagnetic observatories Hermanus, Hartebeesthoek and Tsumeb have been delivering continuous data series for several decades and have previously been used widely to study rapid geomagnetic field changes in this region (Kotzé et al., 2007; Korte et al., 2007; Kotzé and Korte, 2016). The Tristan da Cunha and St. Helena observatories in the South Atlantic are described in several publications (Korte et al., 2009; Matzka et al., 2009; Matzka et al., 2010; Matzka et al., 2011).
Abrupt changes of secular variation trends are also known as geomagnetic jerks (see Mandea et al. 2010 for a review), which make their appearances as distinctive changes of slope in secular variation patterns and generally occur on timescales of a few months to a few years. Since the first identification of a geomagnetic jerk in 1969 by Courtillot et al. (1978) and Malin et al. (1983) several rapid changes in the geomagnetic secular variation (SV) pattern have been identified (Mandea et al., 2010; Pinheiro et al., 2011; Brown et al., 2013). During the recent past several abrupt secular variation change events appeared in quick succession of each other. In Southern Africa the 2007 abrupt SV change as observed at the Hermanus magnetic observatory (Kotzé, 2010, 2011) has been documented, while the 2012 jerk (Chulliat et al., 2015) shows a completely different morphology across the southern African region (Kotzé and Korte, 2016). A characteristic of these most recent events is that they seem to originate from a quick succession of core field acceleration pulses occurring predominantly in West Africa and the South Atlantic region. The 2014 jerk, first reported by Torta et al. (2015) show evidence of intense secular acceleration in the Africa-South Atlantic region extending into Europe. Of particular interest was the variation in strength of the 2014 geomagnetic jerk across Southern Africa (Kotzé, 2017) as revealed by the different field components at each observatory. In this publication we will present evidence of a new abrupt secular variation change event across both Southern Africa and the adjacent Atlantic Ocean area in the beginning of 2015. We will also show how the amplitude of this event varied in the different X, Y and Z components at all five magnetic observatories. There exist conference reports for jerk-like feature in late 2014/early 2015 for Alaskan observatories (Brown et al., 2016), and for a Pacific Ocean (Guam) and a Caribbean (San Juan, Puerto Rico) observatory (Brown et al., 2017), but none describe the 2015 jerk in this area in detail.

DATA, RESULTS AND DISCUSSION:

For the purpose of this study we selected quiet time data of geomagnetic field variations recorded at the INTERMAGNET (www.intermagnet.org) magnetic observatories located at Hermanus (HER), Hartebeesthoek (HBK), Tsumeb (TSU) in southern Africa (Kotzé et al. 2015). At St Helena (SHE) and Tristan de Cunha (TDC) in the South Atlantic region we used monthly means derived from all data available. Hourly mean values at HER, HBK and TSU were required to comply with the Dst ring current index not to change by more than 3nT/h and K-indices less than or equal to 2 in order to eliminate disturbed and active geomagnetic conditions as far as possible. This particular restriction provided the best possible compromise between truly quiet times and the amount of data left to derive monthly means based on hourly mean values. These hourly X, Y and Z observations values were additionally corrected for ionospheric (plus

induced) fields as well as large-scale magnetospheric (plus induced) fields using the CM4 comprehensive field model (Sabaka et al. 2004), updated with the latest indices (ftp://ftp.ngdc.noaa.gov). The latest definitive baseline corrections were also applied, ensuring that the most accurate data were used in this study. Differences between arithmetic mean and median monthly values turned out to be negligibly small. It is, however, suspected that a small amount of external field leakage will still be present in the data in spite of this stringent selection process. In order to eliminate annual and seasonal variations resulting from magnetospheric and ionospheric currents, including the resulting induction effects, secular variation (SV) values were calculated as first differences of the X, Y and Z monthly means at time *t* as the difference between those at time *t* + 6 months and *t* – 6 months. This procedure which is common practice when studying abrupt secular variation changes (Mandea et al 2000, Olsen and Mandea (2007)), however implies that SV information is limited to 6 months after the beginning of the time series and 6 months before the last available main field observations. The time interval in this investigation stretches from 2013.0 to 2016.5 and incorporates data from 2012.5 to 2017.0 (and only to October 2016 in the case of TDC, as it is affected by construction work since November 2016).

The respective rates of SV change were further estimated directly from the time series by piecewise (segmented) linear fits. The piecewise linear fit segments cover the full time range from 2013.0 to 2016.5 for almost all investigated time series. Exceptions are the Y component at TSU (2013.3 to 2016.5) as well as the X component at SHE and the X and Z component at TDC (2013.0 to 2016.0). In order to determine the break points between two consecutive linear segments, a software computer algorithm, called SegReg (http://www.waterlog.info/pdf) searched for an identifiable and distinctive change in the slope of the respective segments. The breakpoint is found numerically by adopting several potential tentative breakpoints and performing a linear regression at both sides of them. The tentative breakpoint that provides the largest coefficient of determination (as a parameter for the fit of the regression lines to the observed data values) is then selected as the true breakpoint. All breakpoints were determined at a 95% statistical confidence level. This procedure also included an iterative method to obtain the best linear fit and the subsequent slope of a particular time interval by optimising the regression coefficient. The scatter in the secular variation data made it almost impossible to obtain a 100% fit of the different linear fits on both sides of some breakpoints. In the present investigation we limited the code to only secular variation data between 2013 and 2016.5 in contrast to a previous investigation where the data ranged between 2006 and 2015 (Kotzé, 2017). As the code is quite sensitive to the range of data provided the present results are to be regarded as more accurate and representative of the trends observed between 2013 and 2016.5 as we also used the latest updated baselines for HER, HBK and TSU.

Results for X, Y and Z components at HER, HBK, TSU, SHE and TDC are shown in figures 1, 2, 3, 4, and 5 respectively as a function of time after applying the procedures described above. In addition, we followed the approach of Torta et al. (2015) and compiled maps of secular acceleration at the Earth's surface in the South Atlantic and African region using the CHAOS-6 geomagnetic field model (Finlay et al., 2016). This geomagnetic field model utilises both ground and satellite data and is able to calculate field information for the period 1999 till 2016.5. Figures 6, 7 and 8 show respectively the X, Y and Z secular acceleration at 2015.0 with the positions of the observatories as indicated.

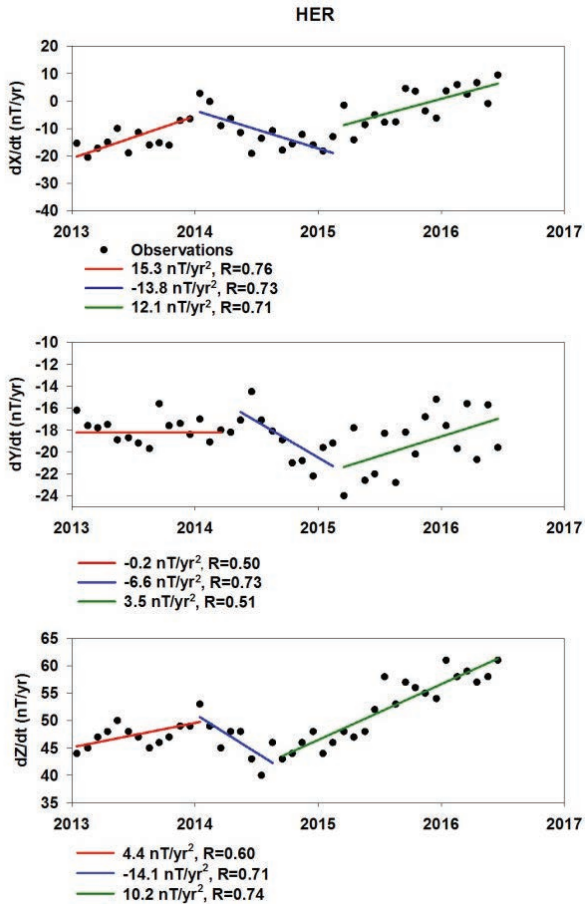

Figure 1. Secular variation of the X, Y and Z components at HER as derived from monthly-means between 2012.5 and 2017.0. The black dots show monthly mean secular variation estimates derived from 12-month differences, while automatically fitted piecewise linear fits to the data provide estimates of secular acceleration as given in the respective legends. Regression coefficients R provide an estimate of the quality for every fit.

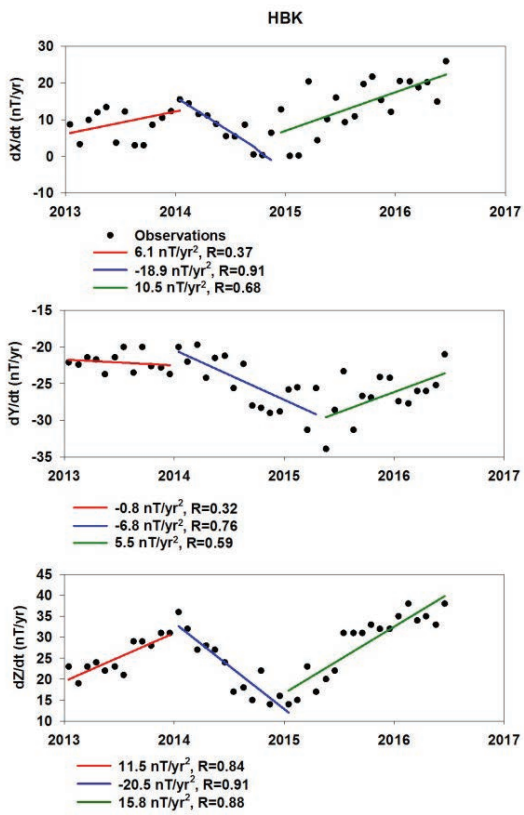

Figure 2. Secular variation of the X, Y and Z components at HBK as derived from monthly-means between 2012.5 and 2017.0. The black dots show monthly mean secular variation estimates derived from 12-month differences, while automatically fitted piecewise linear fits to the data provide estimates of secular acceleration as given in the respective legends. The quality of each fit can be estimated by the respective regression coefficients R.

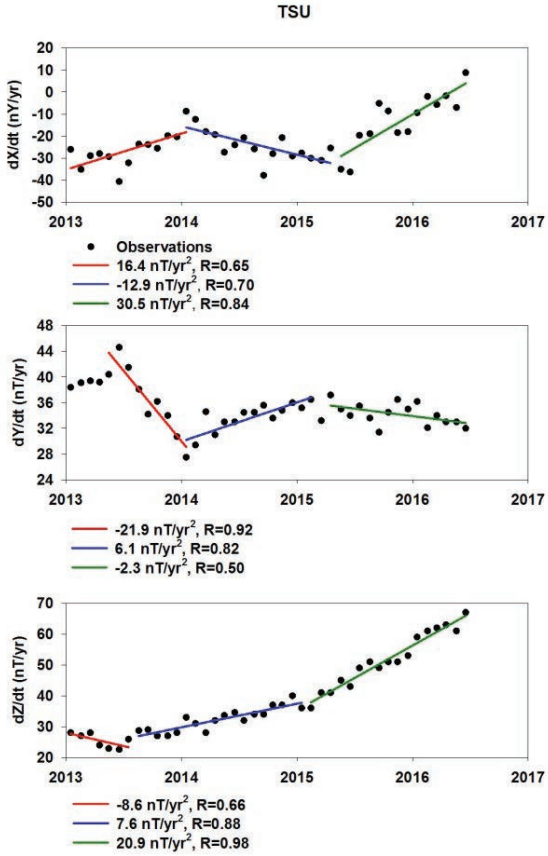

Figure 3. Secular variation of the X, Y and Z components at TSU as derived from monthly-means between 2012.5 and 2017.0. The black dots show monthly mean secular variation estimates from 12-month differences, while automatically fitted piecewise linear fits to the data provide estimates of secular acceleration as given in the respective legends. Regression coefficients R provide an estimate of the quality for every fit.

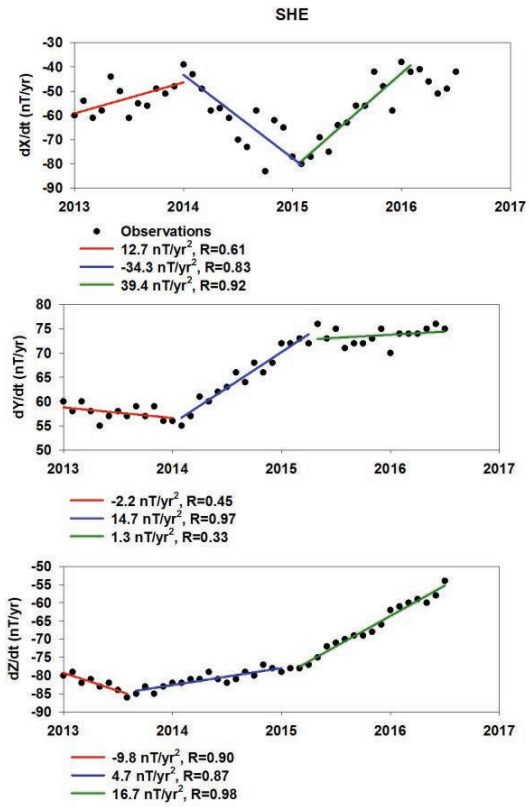

Figure 4. Secular variation of the X, Y and Z components at SHE as derived from monthly-means between 2012.5 and 2017.0. The black dots show monthly mean secular variation estimates from 12-month differences, while automatically fitted piecewise linear fits to the data provide estimates of secular acceleration as given in the respective legends. The quality of each fit can be estimated by the respective regression coefficients R.

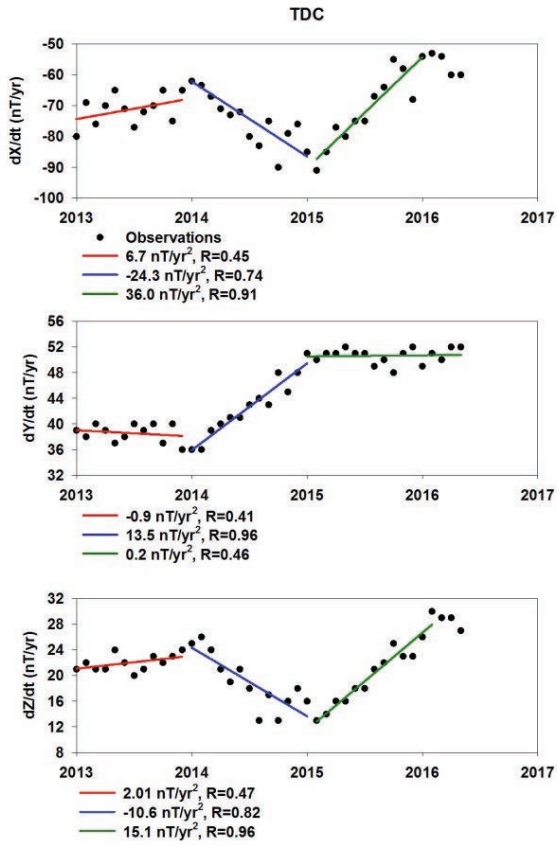

Figure 5. Secular variation of the X, Y and Z components at TDC as derived from monthly-mean measurements between 2012.5 and 2016.83. The black dots show monthly mean secular variation estimates from 12-month differences, while automatically fitted piecewise linear fits to the data provide estimates of secular acceleration as given in the respective legends. The quality of each fit can be estimated by the respective regression coefficients R.

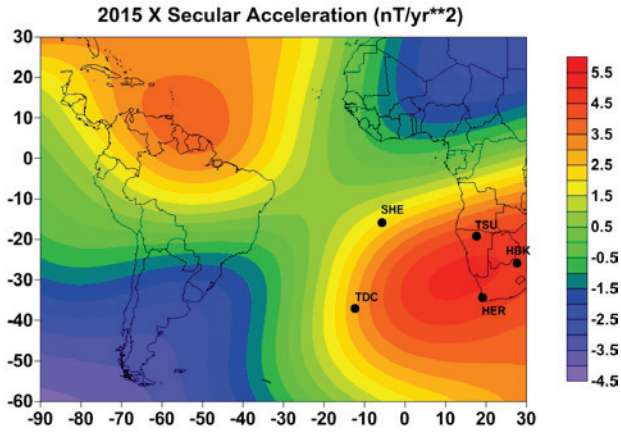

Figure 6. A map showing X-component secular acceleration at the Earth's surface for 2015.0 in the South Atlantic and southern African region as determined using the CHAOS-6 model. The positions of the different observatories used in the investigation are indicated by their respective IAGA codes and black dots.

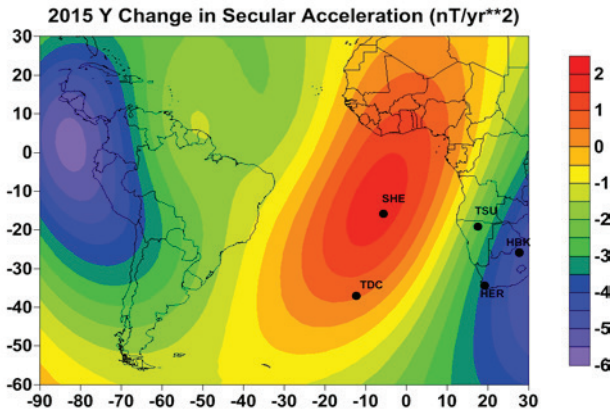

Figure 7. A map showing Y-component changes of secular acceleration at the Earth's surface for 2015.0 across southern Africa and the adjacent South Atlantic according to the CHAOS-6 geomagnetic field model. The positions of the 5 magnetic observatories are as indicated (IAGA codes and black dots).

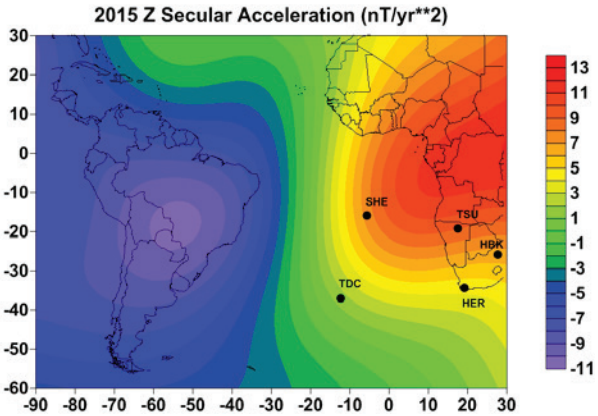

Figure 8. A map showing Z-component secular acceleration at the Earth's surface across the South Atlantic and southern Africa as determined at 2015.0 by the CHAOS-6 field model. The positions of the different magnetic observatories used in the investigation are indicated by black dots and their respective IAGA codes.

From figures 1 to 5 it is evident that the X-component secular variation follows the same pattern at all observatories. However, at TSU, SHE and TDC we notice that between 2015 and 2016.5 the secular acceleration differs quite strongly in magnitude from HER and HBK, where it is observed to be much lower. This is not surprising as according to CHAOS-6 the X-component secular acceleration (Figure 6) in the South Atlantic and southern African region is generally characterised by strong gradients around 2015, with the secular variation change across this region characterised by an increasing tendency. The strength of the 2015 geomagnetic jerk in the X component (i.e. the difference in slope of dX/dt before and after the event) is found to be the weakest at HER. At TDC the absolute magnitude/strength of the 2015 jerk (60.3 nT/yr^2 = 36.0 nT/yr^2-(-24.3) nT/yr^2)) is almost twice the absolute strength of the 2014 event (|-31.0| nT/yr^2).

On the other hand the Y-component secular variation changes at both HER and HBK are in complete contrast to the behaviour at TSU, SHE and TDC. This is not surprising since the Y secular variation at HER and HBK even is of opposite direction to that at TSU, SHE and TDC. It is also evident that the absolute strength of the 2015 jerk (12.3 nT/yr^2) at HBK is almost double the absolute strength of the 2014 event (6.0 nT/yr^2), while at TSU the 2015 event (absolute strength = 8.4 nT/yr^2) is much weaker than the 2014 geomagnetic jerk (absolute strength = 28.0 nT/yr^2). In contrast to TSU, the absolute magnitudes of both the 2014 and 2015 geomagnetic jerks at SHE and TDC are comparable to each other. Figure 7 shows a contour map of the Y secular acceleration change at 2015 as determined by the CHAOS-6 model. It reveals strong gradients over the South Atlantic region as well as southern Africa where the observatories used in this investigation are located. In particular the prominent feature of strong increasing secular variation (d^2Y/dt^2 >0) located along the South Atlantic and western African meridian where both SHE and TDC are located is consistent with observations at these observatories, while decreasing secular variation (d^2Y/dt^2 <0) occurs in the southern African continental and surrounding ocean areas. Similarly HER and HBK are located in a region where the strength of the 2015 is opposite to that of SHE and TDC.

The Z-component SV change at all observatories in this investigation showed a positive tendency (Figures 1-5) between 2015 and 2016.5. This is in strong contrast to the 2003 geomagnetic jerk in 2003 when Olsen and Mandea (2007) found a strong decreasing secular variation (d^2Z/dt^2 <0) in the southern African continental and surrounding ocean area using satellite data. In both the case of TSU and SHE, the two most northerly located observatories in this study, the secular variation at 2015 changes from an increasing tendency to a steeper positive gradient, in contrast to HER, HBK, and TDC. The positive tendency of the SA observed at all observatories is consistent with the Z secular acceleration contour map in figure 8 using the CHAOS-6 model. The behaviour of the Z-component secular variation at TSU and SHE around 2015 does not show a change in sign of the secular acceleration. Therefore, strictly according to the definition of a geomagnetic jerk, one can regard the 2015 Z-component events at TSU and SHE as secular variation changes, rather than a jerk-type feature.

Conclusions:

We used monthly mean X, Y and Z geomagnetic field observations from 5 magnetic observatories across Southern Africa and the adjacent South Atlantic region to identify a new occurrence of rapid secular variation change during 2015. To our knowledge, we are the first to report the 2015 geomagnetic jerk in detail in this area. The data covered the period between 2012.5 and 2017.0, allowing us to determine secular variation values between 2013.0 and 2016.5 based on a 12-month difference technique. The 2014 event (Kotzé, 2017) could also be clearly identified. We were able to clearly identify the 2015 secular variation change event in all components at all 5 observatories. A comparison with the changes in secular variation observed in a previous analysis of the 2014 geomagnetic jerk over southern

Africa (Kotzé, 2017) reveals that in the majority of cases the changes are of the same magnitude as in this investigation. Due to a reduction in noise levels, which was achieved through a stringent data selection process, the upgrading of the CM4 comprehensive magnetic field model with the latest available indices and the application of the most recent baselines, e.g. the Z-component at TSU, we are now able to clearly identify changes around 2014, which was not possible during the previous analysis. This investigation provides an opportunity to make a comparative analysis of the changing secular variation pattern at 5 different magnetic observatories located in a region characterized by rapid and strong field changes (Mandea et al 2007), separated in time by only 1 year. Such a short time in between two jerks is in contrast to the generally accepted assumption and findings proposed by Chulliat et al. (2010) and Chulliat and Maus (2014) that geomagnetic jerks are the resulting consequences of acceleration pulses at the core surface with a 3-4 year separation as observed during the last 10-15 years (see also Torta et al., 2015). The 2014 jerk is generally accepted as the result of the descending phase of an intense acceleration pulse during 2012-2013 (Torta et al., 2015). In order to determine whether the 2015 jerk was the result of the 2012.5 pulse or the manifestation of a new pulse would require a geomagnetic field model based on data extending beyond 2016.5.

According to the findings by Brown et al. (2013) as well as Chulliat and Maus (2014), successive jerks have opposite signs, i.e. if the slope of secular acceleration increases (decreases) with one jerk it decreases (increases) with the next jerk. This behaviour is confirmed for all observatories and all components except for the Z-component for SHE and TSU, which show consecutive increases in secular variation.

Finding the cause of the 2015 geomagnetic jerk and to determine the source mechanism in the core is beyond the scope of this paper. Our main purpose was to report some of its features as observed in southern Africa and the bordering South Atlantic region. A direct consequence of this 2015 jerk following 1 year after the 2014 jerk is that predicting secular variation changes in future are more challenging than previously thought (Torta et al., 2015).

Acknowledgements:

PK was supported by an NRF grant (no. 103610) for rated researchers. The support provided by the GFZ German Research Centre for Geosciences in Potsdam to run and maintain the SHE and TDC magnetic observatories is appreciated. SANSA staff responsible for the data processing from HER, HBK, and TSU observatories are acknowledged.

References:

Brown, W.J., J. E. Mound and P.W. Livermore (2013) Jerks abound: An analysis of geomagnetic observatory data between 1957 and 2008. Phys Earth Planet Interiors, 223, 62-76, doi: 10.1016/j.pepi.2013.06.001.

Brown, W., C. Beggan and S. Macmillan (2016) Geomagnetic jerks in the Swarm era. In: ESA Living Planet Symposium, Prague, Czech Republic, 9-13 May 2016. Spacebooks Online.

Brown, W., C. Beggan and S. Macmillan (2017) Rapid geomagnetic secular variation during the Swarm era and its impact on global field models. [Poster] In: *TSG-VMSG-BGA Joint Assembly 2017, Liverpool, UK, 4-6 Jan 2017*. British Geological Survey. (Unpublished)

Chulliat, A., E. Thébault, and G. Hulot (2010) Core field acceleration pulse as a common cause of the 2003 and 2007 geomagnetic jerks. Geophys. Res. Lett. **37**, L07301, doi:10.1029/2009GL042019.

Chulliat, A. and S. Maus (2014) Geomagnetic secular acceleration, jerks, and a localized standing wave at the core surface from 2000 to 2010. J Geophys Res, **119**, doi:10.1002/2013JB010604.

Chulliat, A., P. Alken, and S. Maus (2015) Fast equatorial waves propagating at the top of the Earth's core. Geophys Res Lett, doi:10.1002/2015GL064067.

Courtillot, V., Ducruix, J., Le Mouel, J.L.(1978) Sur une accélération récente de la
variation séculaire du champ magnétique terrestre. C. R. Acad. Sci. Paris D 287, 1095–1098.

Finlay, C.C., N. Olsen and L. Tøffner-Clausen (2015) DTU candidate field models for IGRF-12 and the CHAOS-5 geomagnetic field model. Earth Planets and Space, **67:114**, doi:10.1186/s40623-015-0274-3.

Korte, M., M. Mandea, P.B. Kotzé, E. Nahayo, and B. Pretorius (2007) Improved observations at the southern African geomagnetic repeat station network. South African Journal of Geology, **110**, p. 175-186, doi:10.2113/gssajg.110.2-3.175.

Korte, M., M. Mandea, H.-J. Linthe, A. Hemshorn, P. Kotzé and E. Ricaldi (2009) New geomagnetic field observations in the South Atlantic Anomaly region. Annals of Geophysics, 52, 65-81.

Kotzé, P.B., M. Mandea, and M. Korte (2007), Modelling the southern African geomagnetic field secular variation using ground survey data for 2005, South African Journal of Geology, **110**, 187-193, doi:10.2113/gssajg.110.3.187.

Kotzé, P.B. (2010) The 2007 geomagnetic jerk as observed at the Hermanus Magnetic Observatory. Phys Comment, **2**, 5-6.

Kotzé, P.B. (2011) Signature of the 2007 geomagnetic jerk at the Hermanus Magnetic Observatory, South Africa. S A Jnl Geol, 114.2, 207-210, doi:10.2113/gssajg.114.2.207.

Kotzé, P. B. and M. Korte (2016) Morphology of the southern African geomagnetic field derived from
observatory and repeat station survey observations: 2005-2014. Earth Planets and Space 68:23, DOI 10.1186/s40623-016-0403-7

Kotzé, P.B., P. J. Cilliers and P. R. Sutcliffe (2015) The role of SANSA's geomagnetic observation network in

space weather: A review. Space Weather, **13**, doi:10.1002/2015SW001279.
Kotzé, P.B. (2017) The 2014 geomagnetic jerk as observed by southern African magnetic observatories. Earth, Planets and Space, 69:17, DOI 10.1186/s40623-017-0605-7
Malin, S.R.C., Hodder, B.M., Barraclough, D.R. (1983) Geomagnetic Secular Variation: A jerk in 1970, in: Publicaciones del Observatorio del Ebro. Memoria, 14. pp.239–256.
Mandea, M., Bellanger,E., and Le Mouël, J.-L. (2000) A geomagnetic jerk for the end of the 20th century? Earth Planet. Sci. Lett., 183, 369-373.
Mandea, M., M. Korte, D. Mozzoni, D., and P. Kotze (2007) The magnetic field changing over the southern African continent – a unique behaviour. South African Journal of Geology, 110, 193-202.
Mandea, M., R. Holme, A. Pais, K. Pinheiro, A. Jackson and G. Verbanac (2010) Geomagnetic jerks: Rapid core field variations and core dynamics. Space Sci Rev, 155, 147–175, doi:10.1007/s11214-010-9663-x.Matzka, J., Olsen, N., Fox Maule, C., Pedersen, L. W., Berarducci, A., Macmillan, S.(2009) Geomagnetic observations on Tristan da Cunha. Annals of Geophysics, 52(1), 97 – 105Matzka, J., Chulliat, A., Mandea, M., Finlay, C.C., Qamili, E.(2010) Geomagnetic observations for main field studies: From ground to space. Space Science Reviews, 155, pp. 29-64, doi:10.1007/s11214-010-9693-4Matzka, J., Husøy, B.-O., Berarducci, A., Wright, D., Pedersen, L.W., Stolle, C., Repetto, R., Genin, L., Merenyi, L. and Green, J.(2011) The geomagnetic observatory on Tristan da Cunha: Setup, operation and experiences. Data Sci. J., 10, pp. IAGA151-IAGA158, DOI:10.2481/dsj.IAGA-22Olsen, N., and M. Mandea (2007) Investigation of a secular variation impulse using satellite data: The 2003 geomagnetic jerk. Earth and Planetary Science Letters, 225, 94-105Pinheiro, K. J., A. Jackson and C. C. Finlay (2011) Measurements and uncertainties of the occurrence time of the 1969, 1978, 1991, and 1999 geomagnetic jerks. Geochem Geophys Geosyst, 12, Q10015, doi:10.1029/2011GC003706.
Sabaka, T.J., Olsen, N., Purucker, M.E. (2004) Extending comprehensive models of the Earth's magnetic field with Ørsted and CHAMP data. Geophys J Int 159:521-547
Torta, J.M., F.J. Pavón-Carrasco, S. Marsal and C. Finlay (2015) Evidence for a new geomagnetic jerk in 2014. Geophys Res Lett, doi: 10.1002/2015GL065501.

A Study for Overhauser Magnetometer Development

André Wiermann and Luiz Benyosef
Observatório Nacional - Brazil

Abstract

Initially a proton precession magnetometer (ppm) was built at the Magnetic Sensor Development Laboratory of the National Observatory (LDSM/ON). Using this ppm platform a new project started seeking to develop an Overhauser magnetometer. In this study electrical and constructive aspects of circuits and materials necessary to develop an Overhauser effect resonance magnetometer were studied.

Introduction

An electric circuit was developed to generate the polarization field and to measure the post polarizing pulse, proton precession frequency with a very high resolution. The figure 1 shows the block diagram of the main portion of the prototype circuit.

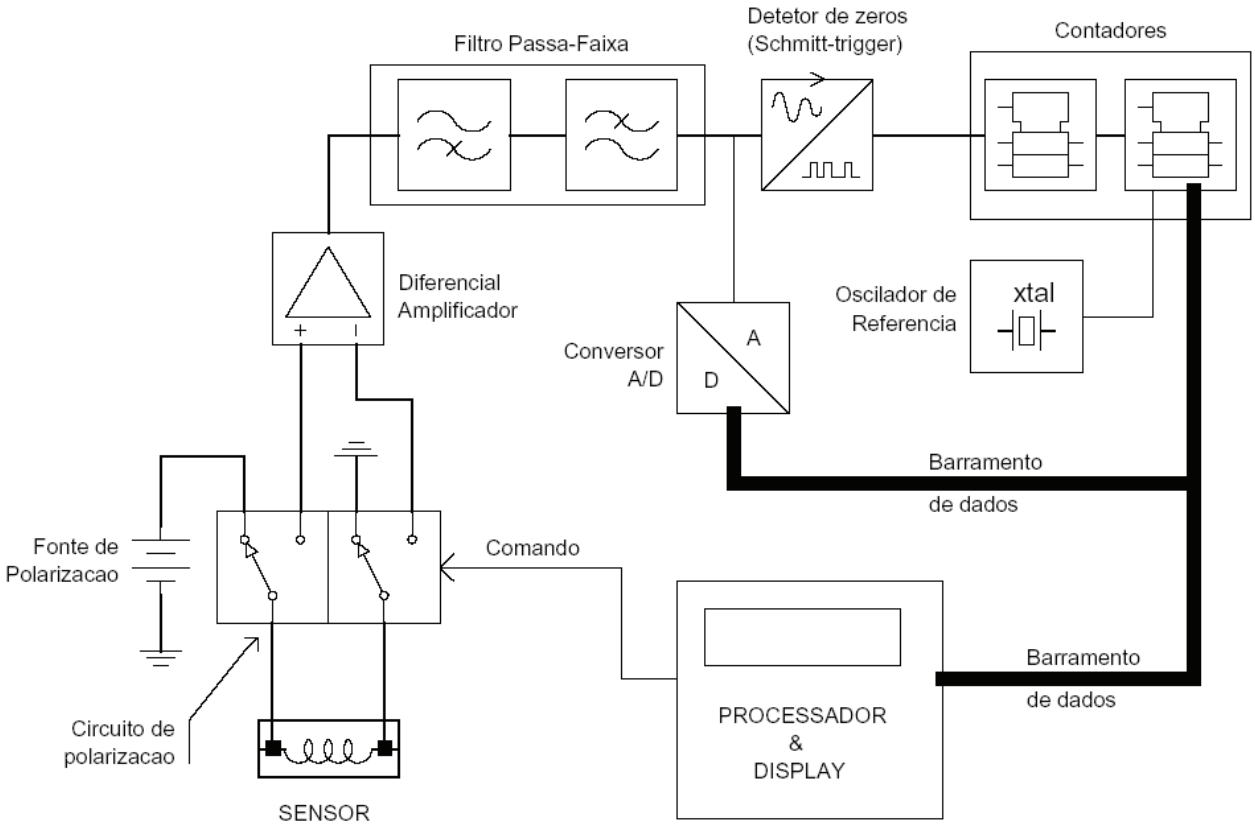

Figure 1 - Block diagram of the prototype.

In the Overhauser magnetometer a large polarization of the electron magnetic moments is transferred to the protons by several couplings between electrons and protons and this effect can offer an alternative for proton spin alignment. The upper energy level of the free electrons in an external dc magnetic field can be continuously saturated using an RF signal in resonance with the corresponding electron spin resonance (ESR) which is determined by the environmental magnetic field. Is possible to maintain the electron spin resonance in a narrow peak meaning that the RF power needed to the polarization saturation of the electron can be small, even if continuous RF pumping of the electrons is maintained. This is the dynamic nuclear polarization (DNP) and the theoretical enhancement of the proton polarization by DNP is multiple of the natural polarization in the same magnetic field. To have a proton-rich liquid sample and at the same time have some free electrons available for RF-ESR, special free radicals compounds must be used. Such chemical compounds feature single unpaired electrons that can be excited to produce the DNP Overhauser effect. Unfortunately as free radicals these compound usually have a tendency to be chemically unstable.

In some nitroxide free radicals, as Tempone (Tetra-Methyl-Piperidine-Oxyde), one unpaired electron near the nitrogen atom is available for ESR polarization. In this project we're using Tempone and two others similar chemical compositions to analysis this Overhauser effects to be applied in the geomagnetic measurements. Some of these nitroxides free radical are basically a carbon ring including one oxidized nitrogen atom, and are used almost universally in Overhauser effect magnetometers. Tempone and its equivalents are long-term chemically stable in a range of solvents and not excessively aggressive to living organisms making handling safe and easy. Over the ppm original platform a RF circuit was assembled to obtain the RF excitation for a new sensor filled with a Tempone doped water.

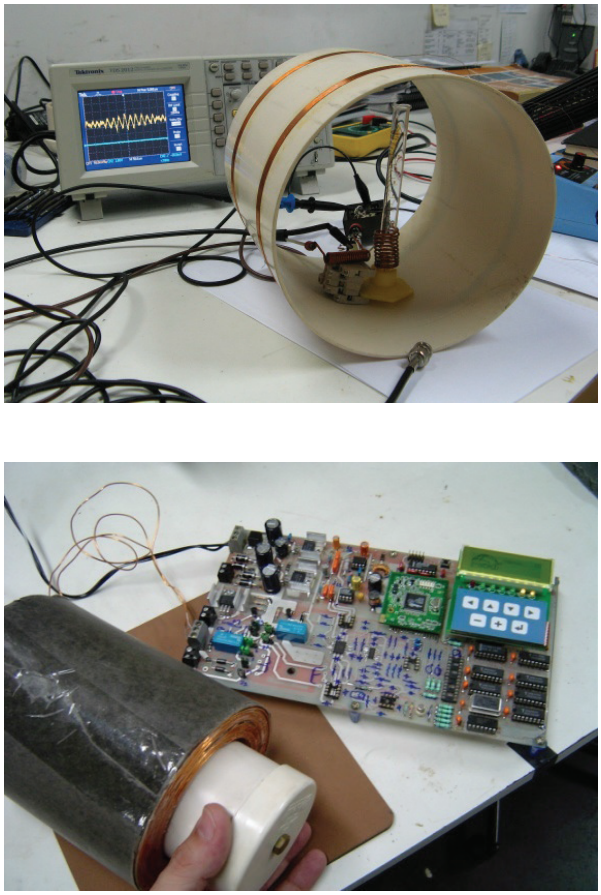

Figure 2 – Test platform used in this study.

In this study electrical and constructive aspects of circuits and materials necessary to develop an Overhauser effect resonance magnetometer were studied. So, an open test platform based on a proton precession magnetometer, built at the Development of Magnetic Sensors at National Observatory (LDSM/ON) was used and an instrumental apparatus was assembled in order to prepare the LDSM/ON for possible future work with resonance magnetometry.

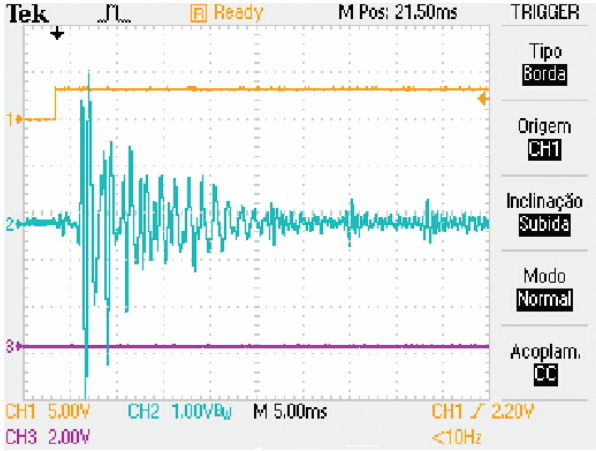

Figure 3 – A precession magnetic signal captured using Overhauser mode with 3W (RF) at 59,875 MHZ applied to the sensor containingTempone in a droped water soluction.

Geomagnetic measurements with resonance instruments in Brazil have severe limitations due to the low magnetic intensities as consequence of South Atlantic Magnetic Anomaly (SAMA) and the Magnetic Equator. Therefore the existence of a apropriated laboratory for testing and develop resonance magnetometers is so important.

Bibliograpy

ABRAGAM A., GOLDMAN M., “Principles of Dynamic Nuclear Polarization”, Rep Prog Phys, **41**, pp 395-467, 1978.

BLOCH F. “Nuclear Induction”, Physical Review v. **70**, 7 & 8, pp 460-474, Oct 1946.

BLOCH F., HANSEN W.W., PACKARD M. “The Nuclear Induction Experiment”, Physical Review v. **70**, 7 & 8, pp 474-489, Oct 1946.

CARVER, Thomas R. and SLICHTER, Charles P. “Experimental Verification of the Overhauser Nuclear Polarization Effect”, Phys. Rev. 102, pp 975-980, 1956.

CORY D., *A Hands on Introduction to NMR - Lecture Notes*, Cambridge, MIT Nuclear Engineering Dept, MIT, 2001.

FAINI G., SVELTO O. “Signal to Noise Considerations in a Nuclear Magnetometer”, Suppl. al Vol. 23, Serie 10 del Nuovo Cimento, pp 55-65, 1962.

FARRAR T.C., BECKER E, D. *Pulse and Fourier Transform NMR - Introduction to Theory and Methods*, New York, Academic Press, 1971.

FUKUSHIMA E., ROEDER S. B.W. *Experimental Pulse Nmr: a Nuts and Bolts Approach*, New York, Westview Press, 1986.

OVERHAUSER A.W. “*Polarization of Nuclei in Metals*”, Phys. Rev. 92, pp 411-412, 1953.

The Fluxgate Magnetometer Past, Present and Future

Luiz Benyosef
Observatório Nacional

Keywords: fluxgate, amorphous ribbons, nanocrystalline ribbons.

The fluxgate magnetometer is a saturated core instrument used with success since its appearence in the 1930's to measure low intensity magnetic fields or its variations. Since its appearance different materials was used as sensor cores, like NiFe crystalline alloys, CoFeBSi amorphous base and nanocrystalline as FeSiBCuNb base. Different geometries, linear or not, and sizes was used also. Its output signal is usually done by second harmonic detection using different ways like phase or amplitude detector. This instrument is largely used for ground, submarine and space applications.

The Magnetic Sensor Development Laboratory of the Observatório Nacional in Rio de Janeiro, Brazil (LDSM/ON) develops and builds high resolution fluxgate sensor cores and their associated analogical and digital circuits. These sensor cores using different geometries are made in our lab using amorphous base FeSiBCo and nanocrystalline FeSiCuNbB ribbons produced by melt-spinning technique. All the annealing steps proceedings are made locally also.

This talk shows magnetometers built by LDSM/ON for scientific, metrological, commercial and military purposes.

Considering the advances in magnetic materials development and new miniaturized electronics, this technology, by its characteristics of three orthogonal vector measurement, high resolution, low power consumption, small weight and size; it had and it has a promising of broad use for large applications in the immediate future.

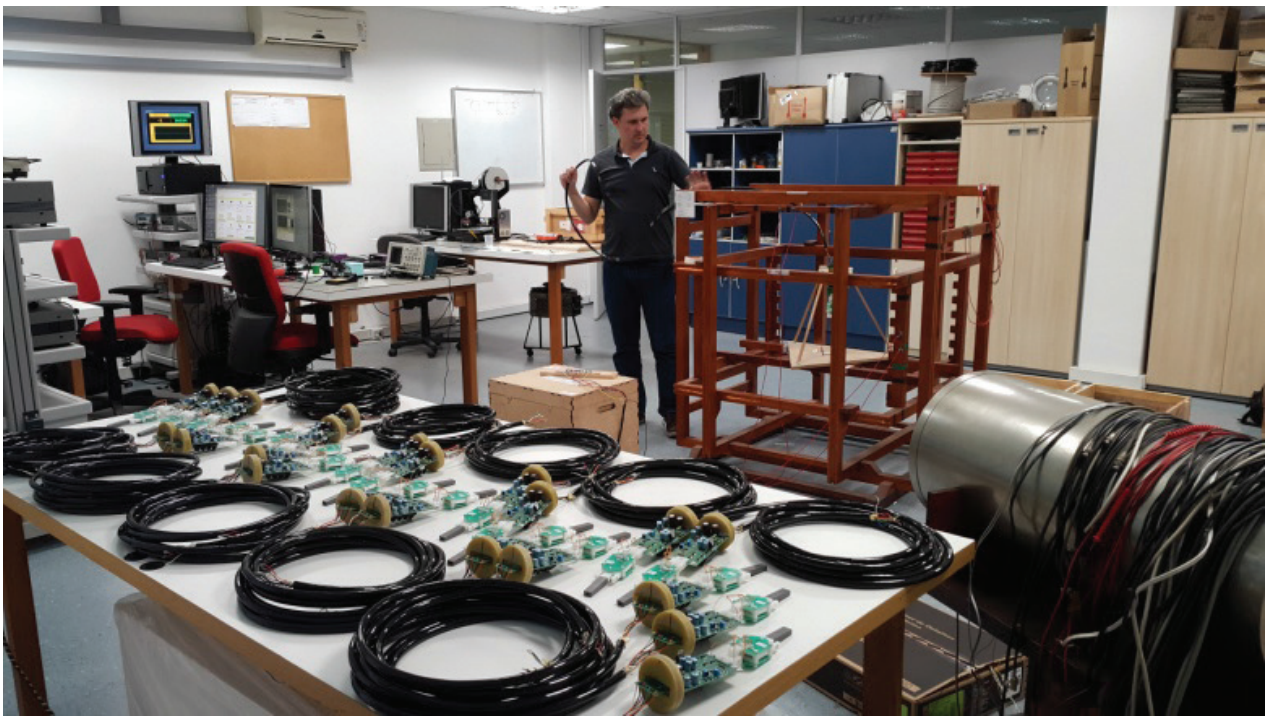

Figure 1 – High resolution fluxgate magnetometers developed and built by LDSM/ON.

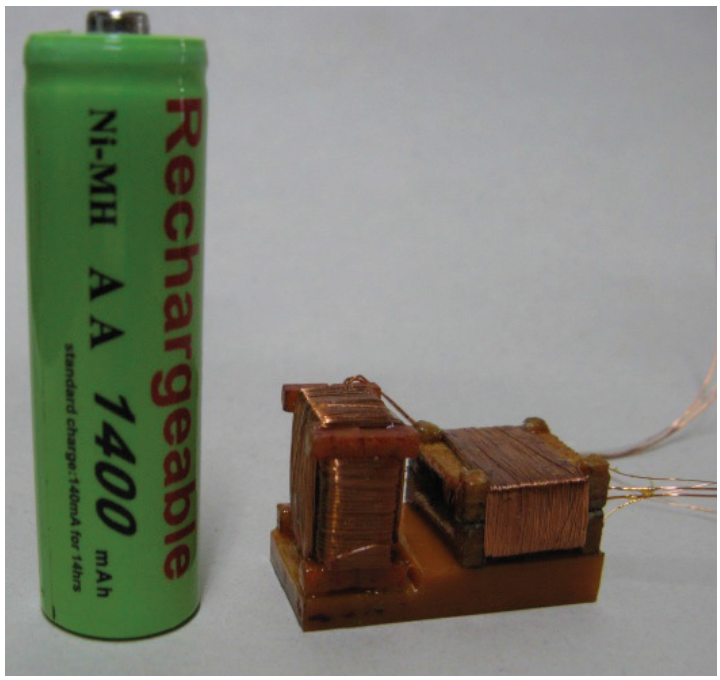

Figure 2 – Miniaturized fluxgate sensor developed and built by LDSM/ON.

Magnetic Indices and their application to Space Weather

Clezio Marcos De Nardin
Embrace, National Institute for Space Research, 12227-010, S. J. dos Campos - SP, Brazil

A brief description

In this curse we are going to provide the students with the necessary background to understand the solar-terrestrial interaction into its extent to the space weather applications, and we will specially focused in the magnetic indices used to monitor the geomagnetic activity in South America.

Main goals

At the end of the curse the students shall be able to:

(a) Identify the different environments components of solar-terrestrial system;

(b) Identify most of the phenomena associated with the solar-terrestrial relationship;

(c) Understand the cause effect relationship in the solar-terrestrial relationship;

(d) Identify the main components of the Earth magnetic field and its variations (internal and external sources);

(e) Identify a magnetic sensor; and

(f) build a magnetic index.

Content of the course:

a. Overview of the Space Weather

b. The Embrace Magnetic Network (equipment, calibration, installation)

c. Different magnetic indices, their deviations and magnetic networks.

Production of a New Calibrated Dataset from the Tatuoca Geomagnetic Observatory in the Brazilian Equatorial Region

Gabriel Soares[1], Jürgen Matzka[2], Katia Pinheiro[1]

[1]Geophysics Department, Observatório Nacional, Rio de Janeiro, 20921-400, Brazil
[2]GFZ German Research Centre for Geosciences, Telegrafenberg, 14473 Potsdam, Germany

Correspondence to: Gabriel Soares (gabrielsoares@on.br)

Abstract

Here we describe the production of a new geomagnetic dataset of the equatorial magnetic observatory Tatuoca (TTB), in Brazil (1.20°S, 48.51°W). We have recovered, processed and calibrated (with regular absolute measurements) 3-component fluxgate raw data from mid 2008 to early 2016. This work has resulted in definitive minute means and hourly mean values of the geomagnetic field components X, Y and Z.
Concerning the removal of artificial disturbances, two versions of the dataset were produced: one in which events of spikes and periods of noise of more than 3 nT (peak to peak) were systematically removed from the records; and a second subset where noise that exceeded 1 nT (peak to peak, by visually checking raw variation 1Hz data magnetograms) was removed from the records, if the noise was not attenuated during the filtering of the 1 Hz data to minute means. We report all steps adopted during the data processing and calibration (baseline construction and application). Our future aim is to include data from 2016 and 2017 in the dataset and to provide it to the scientific community by publishing it through a data repository.

1. Introduction

In this work, we produce a new dataset from the equatorial geomagnetic observatory Tatuoca (TTB, 1.20°S, 48.51°W). The observatory TTB is operated since 1957 by Observatório Nacional (ON) on the Tatuoca Island, in the Amazon River. Although TTB is in operation for more than 60 years, there are only 13 years of hourly means data published in the Word Data Centre for Geomagnetism of Edinburgh so far. Since the year 2015, TTB has been modernized by ON and the German Research Centre for Geosciences GFZ. For the present study, we have recovered, checked and calibrated (with regular absolute measurements) the X, Y and Z geomagnetic field components of fluxgate raw data from mid-2008 to early 2016. This new definitive geomagnetic observatory dataset is denoted here as TTB0816 (TTB dataset from 2008 to 2016). Geomagnetic observatories operations and the applications of their data are described in the literature (e.g., Matzka et al., 2010; Chulliat et al., 2016). Fig. 1 shows the poorly distributed INTERMAGNET observatories in South America, in addition to the TTB location.

We note that TTB is in the Earth's region with the strongest secular variation of the geomagnetic field vertical component (Z): around -200 nT yr^{-1}, corresponding to an inclination rate of change of -0.43° yr^{-1}. This causes a fast movement of the magnetic equator (the line around the globe with I = 0, Z = 0 or F = H) by about 24 km yr^{-1} northwards. TTB0816 documents the magnetic equator crossing at the TTB location in March 2013. For TTB0816, the distance between the magnetic equator and TTB was never more than 120 km (in 2008). Thus, TTB's proximity to the magnetic equator is a transient phenomenon, and in fact, Onwumechilli and Akasofu (1972) and Rastogi et al. (2013) used TTB as a non-equatorial station in their studies. The relative position of the observatories and the magnetic equator line for the years 2008, 2012 and 2016 are also shown in Fig.1.

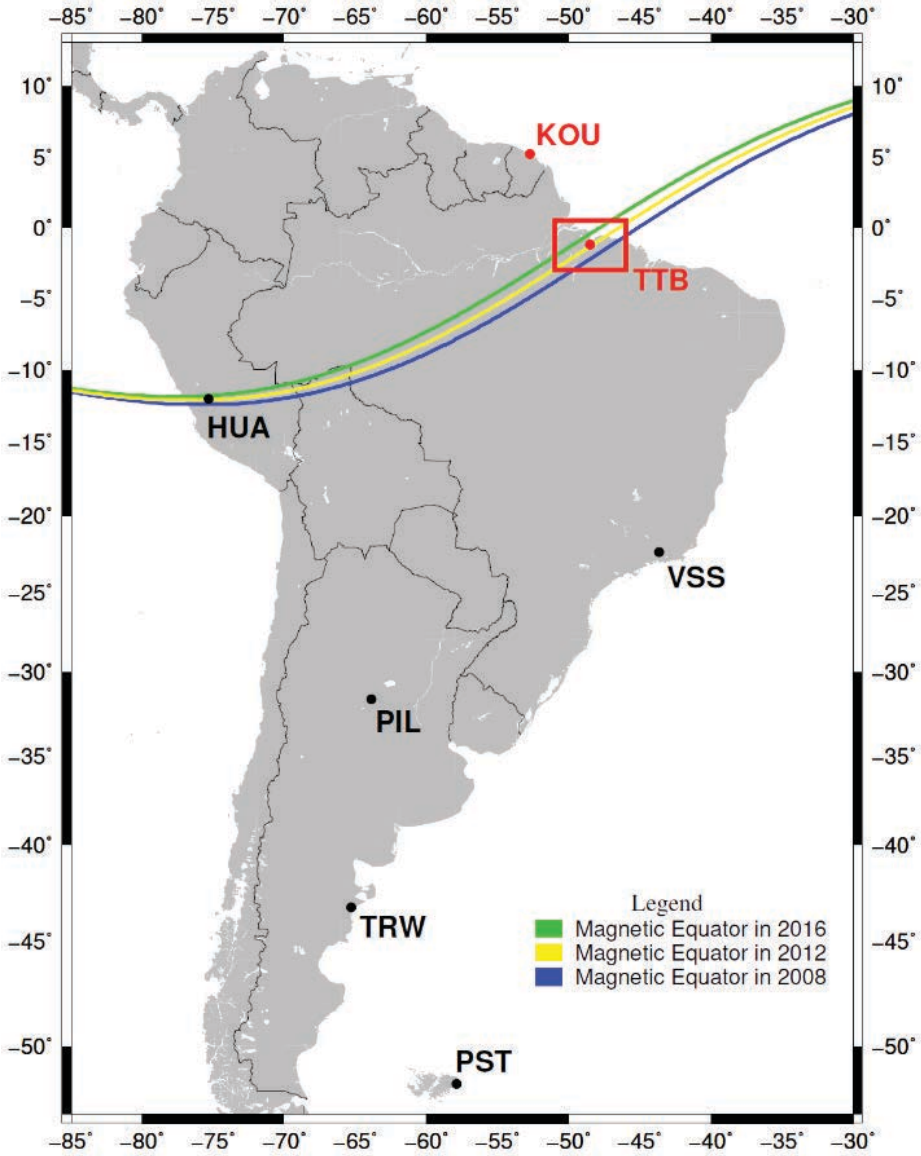

Figure 1. Geographical distribution of the South American INTERMAGNET observatories (KOU, HUA, VSS, PIL, TRW and PST), Tatuoca Observatory (TTB) and the magnetic equator lines for the years 2008, 2012 and 2016. TTB and KOU are highlighted in red as the sources of data from the Brazilian sector.

2. Dataset Preparation

For TTB0816, we quality controlled and calibrated data from the period June 1st, 2008, to January 22nd, 2016. We produced definitive minute means and hourly mean values of the geomagnetic field components X, Y and Z. Variations until November 19th, 2015 were recorded by a LEMI-417M fluxgate magnetometer (sampling rate mostly 1 second, but occasionally 0.25 s to 6 s, see Table 1). From November 20th, 2015 onwards, the variations were recorded by a DTU FGE fluxgate magnetometer (1 second sampling rate), which was installed during the modernization of TTB in November 2015 (see Morschhauser et al, 2017). Table 1 also indicates the H component data availability for each year. We focus in the H component availability due to TTB proximity to the magnetic equator, where H is a good approximation of the total field. Additionally, the H component is important for studies concerning the diurnal variation in the region.

Table 1: Instruments (variometers), sampling rates and H component data availability from TTB, during the period from 2008 to 2016.

Period	Variometer	Sampling Rates (seconds)	Available H data
2008 (since June 1st)	LEMI-417M	0.25	88.4 %
2009	LEMI-417M	0.25 and 1	89.3 %
2010	LEMI-417M	1	85.0 %
2011	LEMI-417M	1	99.3 %
2012	LEMI-417M	1	85.2 %
2013	LEMI-417M	0.25, 1 and 6	97.8 %
2014	LEMI-417M	1 and 6	77.5 %
2015	LEMI-417M + DTU FGE	6 (LEMI) and 1 (FGE)	95.5 %
2016 (until January 22nd)	DTU FGE	1	100 %
2008 to 2016	98 % LEMI-417M and 2 % DTU FGE	0.25 to 6	89.9 %

Each daily magnetogram was visually examined to detect, document and remove spikes, noise and data shifts in the variation records. Artificial disturbances, periods of noise of more than 3 nT (peak to peak), and isolated spikes were systematically deleted from the records. Some recurrent artificial noise during daytime (possibly caused by the photovoltaic power supply or battery charger for the LEMI magnetometer) was found for most of the years, with peak-to-peak amplitude up to 3 nT. Then, the raw data was calibrated by means of absolute measurements of the geomagnetic field and minute means and hourly mean values were calculated. This dataset we now denote as 'TTB0816O' for 'original'.We would like to add one comment regarding the calibration of the raw data by absolute measurements. For the period October 13th, 2014 to May 23rd, 2015, there was no absolutely measured scalar data available at TTB, but there were frequent absolute measurements of the declination D and the inclination I. During this period, we were not able to independently determine the calibration constants. Instead, we calibrated the data with interpolated calibration constants based on absolute measurements before and after this period (this was justified as the difference between the calibration constants before and after this interval is not more than 1.6 nT). Then, we calculated declination and inclination values from our calibrated data and compared it to the absolute measurements of D and I and found good agreement (not shown here). This indicates that the interpolated calibration constants were realistic. Further comments on absolute measurements at the equator can be found in Morschhauser et al. (2017).Because the recurrent artificial noise of relatively low amplitude mentioned above is observed quite often in TTB0816O, we produced a second dataset, here designated as 'TTB0816C' for 'cleaned'. Here, our general rule was to remove data when the noise exceeded 1 nT (peak to peak, by visually checking raw variation data of typically 1 Hz magnetograms). However, we also kept data with noise exceeding the 1 nT level for cases where we expected that the noise in the high time resolution raw data would not affect the minute means. Such cases occurred when the noise is symmetric around the undisturbed data (and minute mean filtering would cancel the noise effectively), or if the apparent noise is only affecting very few samples per minute (such that filtering would lead to a very small error in the minute means). Examples of such occasions are given in Fig. 2, where the period A corresponds to a situation where the minute means curve follows the majority of the 1 Hz data samples with a tiny offset, at the bottom of the blue signal, which represent the undisturbed fraction of data. In this case, data was not excluded from TTB0816C, as the minute means values are following, almost exactly, the 1 Hz undisturbed data and consequently attenuating the noise. The period highlighted by B indicates noise in the 1 Hz raw data that would significantly affect the minute means. Periods similar to the B time interval were removed from the TTB0816C. In total, the cleaned

datasets of the H and Z components contain 0.7 % and 3.3 % less data than the original datasets, respectively.Both the minute means and the hourly mean values of TTB0816O and TTB0816C are included in the TTB0816 dataset.

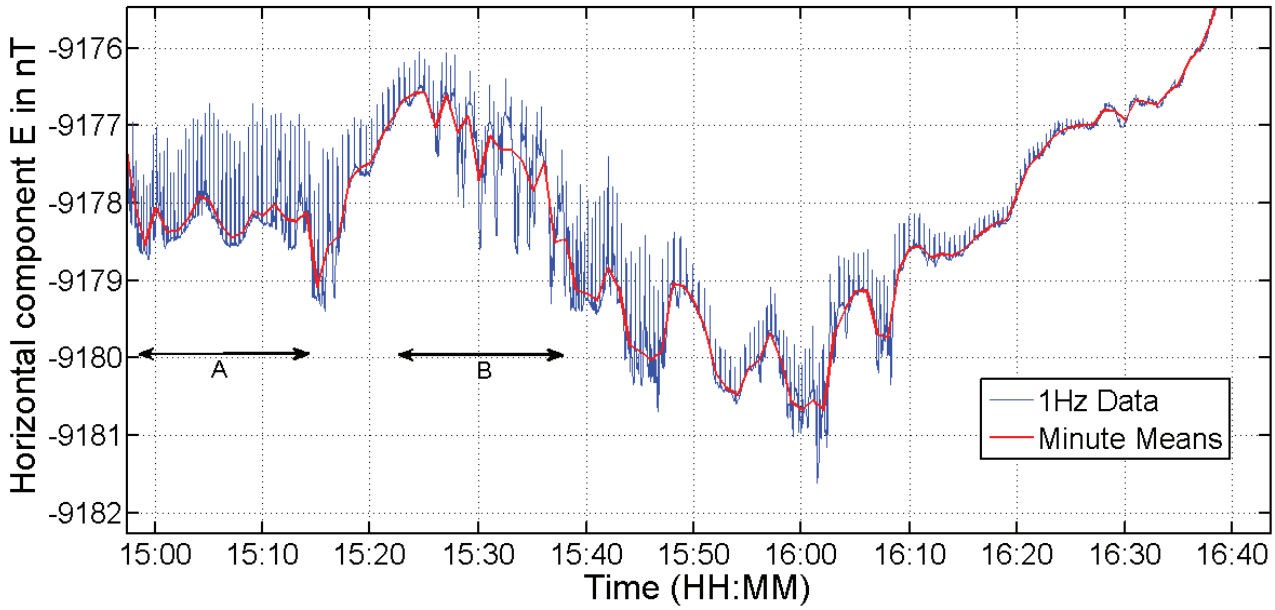

Figure 2: Example of noise interference in TTB 1 Hz data (blue) and minute means (red) for April, 10th 2010. Intervals A and B correspond to different noise types. See text for further details.

3. Applications

The TTB0816O dataset is more suitable for studies based on hourly mean values (e.g. studies concerning the equatorial electrojet or the ring current), while for studies that require 1-minute temporal resolution the cleaned TTB0816C is here suggested.

It is important to emphasize that TTB is one of the few geomagnetic observatories measuring the field at the equatorial region and this will possibly lead to the use of the TTB0816 for new investigations of the equatorial electrojet current (for a review, see Yamazaki and Maute, 2017) in the Brazilian sector, by calculating the difference of the H component measured at TTB and at KOU (indicated by red in Fig. 1), as done in Stolle et al. (2008). The possible forthcoming combination of 2016, 2017 and 2018 TTB data to the TTB0816 would lead to an amount of 11 years, what corresponds to a solar cycle period. This would allow investigations concerning the solar cycle modulation of the equatorial electrojet in the Brazilian sector for the first time.

4. Discussion and Conclusions

The calibration and processing of such a long dataset (seven years and a half) of TTB modern variometers constitutes an expressive result in the Brazilian and international perspectives. The dataset prepared in this study can be addressed to researches concerning the equatorial electrojet ionospheric current, due to the magnetic equator proximity since the last decade.

Concerning the data processing, it is evident that some recurrent artificial disturbances affected the data, which may be associated to the solar panel system used in TTB before 2015 (see Morschhauser et al., 2017). Fortunately, these noises were extinguished after the installation of new variometers and with the modernization of TTB power supply system. Lastly, a significant amount of the noise observed in TTB0816 is attenuated by the minute means filtering. The TTB0816 will be published in data repositories after being combined with additional noise-free TTB data (from 2016 onwards). Therefore, the TTB0816 hourly mean values and minute means will broaden the resources to characterize the geomagnetic field in the Brazilian sector.

5. References

Chulliat, A., Matzka, J., Masson, A., & Milan, S. (2016). Key Ground-Based and Space-Based Assets to Disentangle Magnetic Field Sources in the Earth's Environment. *Space Science Reviews*, 206, 123–156. https://doi.org/10.1007/s11214-016-0291-y

Matzka, J., Chulliat, A., Mandea, M., Finlay, C.C., & Qamili, E., (2010). Geomagnetic observations for main field studies: From ground to space. *Space Science Reviews*, 155, 29-64. https://doi.org/10.1007/s11214-010-9693-4

Morschhauser, A., Soares, G. B., Haseloff, J., Bronkalla, O., Protásio, J., Pinheiro, K., & Matzka, J. (2017). The Geomagnetic Observatory on Tatuoca Island, Brazil: History and Recent Developments. *Geoscientific Instrumentation, Methods and Data Systems*, 6, 367-376. https://doi.org/10.5194/gi-6-367-2017

Onwumechili, A., & Akasofu, S. I. (1972). On the Abnormal Depression of Sq(H) under the Equatorial Electrojet in the Afternoon. *Journal of Geomagnetism and Geoelectricity*, 24 (2), 161-173. http://dx.doi.org/10.5636/jgg.24.161

Rastogi, R. G., Chandra, H., Rahul, S., Trivedi, N. B., & Fontes, S. L. (2013). A comparison of equatorial electrojet in Peru and east Brazil, *The Open Atmospheric Science Journal*, 7, 29–36, https://doi.org/10.2174/1874282320130417003

Stolle, C., Manoj, C., Lühr, H., Maus, S., & Alken, P. (2008). Estimating the daytime equatorial ionization anomaly strength from electric field proxies. *Journal of Geophysical Research*, 113, A09310. https://doi.org/10.1029/2007JA012781

Yamazaki, Y., & Maute, A. (2017). Sq and EEJ - A review on the daily variation of the geomagnetic field caused by ionospheric dynamo currents. *Space Science Reviews*, 206, 299-405. https://doi.org/10.1007/s11214-016-0282-z

Conservation, Scanning and Digitalization of Historical Geomagnetic Data Archives from Brazil

Authors: Daniel R. Franco [1]; Gelvam A. Hartmann [1,2]; Marcelo B. Bianchi [3]; Ozana Hannesch [4]; Ana Cristina de Oliveira Garcia [4]; Alberto Faria dos Santos [1]; Marcio Ferreira Rangel [4]; Amal Abdulmalek [1]; Vanessa Alves da Costa [6]; Ian Muzy Camarão Peixoto [1]; Laisa da Fonseca Aguiar [1]; Etieli da Silva Santos [1]; Everaldo Pereira Frade [4]; André Wiermann [1]; Luci Meri Guimarães [4]; Helder Faria Ladeira [1]; Vitor Bernardes [1]; Andrés R.R. Papa [1]; Ricardo I.F. Trindade [3]; Elder Yokoyama [5]; José Roberto Barbosa [3]

[1] Coordenação de Geofísica, Observatório Nacional (COGEO-ON/MCTIC)
[2] Instituto de Geociências, Universidade Estadual de Campinas (IGc-UNICAMP)
[3] Instituto de Astronomia, Geofísica e Ciências Atmosféricas, Universidade de São Paulo (IAG-USP)
[4] Coordenação de Documentação e Arquivo, Museu de Astronomia e Ciências Afins (CDA-MAST/MCTIC)
[5] Instituto de Geociências, Universidade de Brasília (IGc-UnB)
[6] Laboratório de Engenharia e Exploração de Petróleo, Universidade Estadual do Norte Fluminense (LENEP/UENF)

Keywords: Magnetic observatories; magnetograms, conservation of historical archives; geomagnetic measurements.

This interinstitutional effort of Brazilian research centers aims the cataloging, conservation, digitization and online availability of historical collections of geomagnetic measurements (set of magnetograms, associated with its correspondent books of baseline and scale values) acquired throughout the 20th century in Brazil by the Vassouras and Tatuoca Magnetic Observatories (states of Rio de Janeiro and Pará, respectively). In addition to the valuable historical significance represented by the preservation of this scientific heritage, it will be provided access to the digitized data for both the scientific community and general public by means of an online data repository. Developments achieved so far were related to the VSS datafiles, and can be considered as highly satisfactory: (i) a 'backup' geomagnetic imagery, comprising ~ 87% of the magnetograms (approximately 29,200 documents), 36% of the absolute values books (30 volumes) and 57% of baseline and scale values books (4 volumes); (ii) a high-resolution imagery, comprising ~ 13,870 magnetograms (about 40% of the total), and 10% of absolute measurement and scale value books; (iii) the development of the online repository for this project; and (iv) the onset of digitization step by means of the VSS high-resolution imagery.

Space and Earth Weather – a Cloudy Relationship

Edson Alonso Falla Luza[1,2] *Daniel Ribeiro Franco*[2] *Alexandre Humberto Andrei*[2]

[1] *Universidade Federal Fluminense*
[2] *Observatório Nacional*

Space Weather is the electromagnetic variation of the interplanetary environment caused by the solar activity. It is a new area of broad interdisciplinary interest, in which Geomagnetism is of fundamental importance because it is the terrestrial magnetic field that intermediates the interaction of the Space Weather with the planet Earth. On the other hand, the relationship to the Earth Weather, presumed from the start as the denomination of Space Weather was attributed, is at the same time obvious, because the solar energy is the main source of energy on the climatic systems, and of difficult description given the differences of periods and main amplitudes. Our objective is to study if the Space Weather can impact on Earth Weather and Climate. It has already been verified, analytically and experimentally, that energetic ions passing through the atmosphere favor the formation of condensation nucleotides, increasing the cloud coverage. This impacts directly on both albedo and terrestrial temperature. The dissemination of secondary and tertiary particles from cosmic rays (typified as extra-solar energy ions) is modulated by the Space Weather, by the Forbush Decreases.

The novelty in our approach is to follow for nearly one hundred years what happened in the geographical locations underneath and around the South Atlantic Magnetic Anomaly (SAMA). It thus works as an anti Forbush Decrease. From which the increase or decrease in the air shower can be studied in detail and at length. The main input data are the geomagnetic and meteorological measurements from surrounding stations, the Geomagnetic field rigidity, and the sunspot count. Ancillary, whenever available, also major solar events record and neutrino and muon detectors measurements are taken into account. All these data has to be simultaneously compared along time and space, as the SAMA moved on. Or more to the point, all these data must be normalized and transported towards and idealized standing still SAMA.

In so far we hope to have a considerable relationship. Once we understand all of the above, the main question can be addressed: Solar activity; modulating the flow of charged particles from our galaxy, is it a major player for the enormous climatic variation that has occurred and occurs on Earth?

Absolut observations in the Vassouras Magnetic Observatory during II PANGEO

Antonio Mucussette[1] *and Armindo Nhatsave*[2]
[1] *Nampula Magnetic Observatory – Mozambique*
[2] *Maputo Magentic Observatory – Mozambique*

I Observatory: Nampula

Logger: Vassouras
Observer: MUCUSSETE
Date: 23 Nov 2017
Site Difference: 0.0
Theodolite serial number: 1112
Theodolite vertical scale offset: 90
Fluxgate serial number: 3481
Fixed Mark Reading
CR 1: 000° 04' 15"
CL 1: 180° 00' 45"
CR 2: 000° 06' 00"
CL 2: 180° 02' 30"
Mean: 090° 03' 22"
FM True: 336° 14' 08"
TN Circle: 023° 49' 14"
Declination Observation
VarD(nT)
WU: 12:23 271° 13' 45" 271.2292°
ED: 12:21 270° 48' 45" 270.8125°
WD: 12:20 090° 52' 00" 90.8667°
EU: 12:18 091° 07' 45" 91.1292°
Mean: 12:20 181° 00' 34"
Declination: 12:20 -022° 48' 41" -22.8113°
Inclination Observation
PPMF(nT) VarH(nT) VarZ(nT)
NU: 12:33 230° 44' 30" -39.2583°
SD: 12:35 050° 46' 15" -39.2292°
ND: 12:39 309° 15' 00" -39.2500°
SU: 12:41 129° 12' 45" -39.2125°
Inclination: 12:37 -039° 14' 15" -39.2375°
Baselines
Absolute GDAS Baseline
F (nT): 0.0
D(deg): -22.8113 ° ' "
H (nT):

Z (nT):
I (deg): -39.2375
Collimation Errors
Declination Delta: 000° -10' 11"
Declination Epsilon: 000° 00' 51"
Declination Zo (nT):
Inclination Epsilon: 000° 00' 23"
Inclination Zo (nT):
Gdasview Settings
GDASView Version: V4.63 October 2015
H Baseline (nT): 18421.9
D Baseline (dg): 22.7756
Z Baseline (nT): -14347.9
Site Difference (nT): 0.0
H Offset: 0.0000 Scale: 105.8000
D Offset: 0.0000 Scale: 106.5000
Z Offset: 0.0000 Scale: -106.7500
Sensor Temperature Offset: 0.0000 Scale: 100.0000
Electronics Temperature Offset: 0.0000 Scale: 100.0000
Digitiser Temperature Offset: 0.0000 Scale: 100.0000
Proton (F) Offset: 0.0000 Scale: 1.0000

II Observatory: Nampula

Logger: vassouras
Observer: ARMINDO
Date: 23 Nov 2017
Site Difference: 0.0
Theodolite serial number: 1112
Theodolite vertical scale offset: 90
Fluxgate serial number: 3481
Fixed Mark Reading
CR 1: 000° 06' 00"
CL 1: 180° 02' 00"
CR 2: 000° 04' 30"
CL 2: 180° 02' 30"
Mean: 090° 03' 45"

FM True: 336° 14' 08"
TN Circle: 023° 49' 37"

Declination Observation
VarD(nT)
WU: 12:52 271° 14' 30" 271.2417°
ED: 12:51 270° 49' 30" 270.8250°
WD: 12:49 090° 58' 00" 90.9667°
EU: 12:46 091° 09' 30" 91.1583°
Mean: 12:49 181° 02' 52"
Declination: 12:49 -022° 46' 45" -22.7790°
Inclination Observation
PPMF(nT) VarH(nT) VarZ(nT)
NU: 13:11 230° 42' 45" -39.2875°
SD: 13:12 050° 47' 00" -39.2167°
ND: 13:14 309° 16' 30" -39.2750°
SU: 13:15 129° 14' 00" -39.2333°
Inclination: 13:13 -039° 15' 11" -39.2531°
Baselines
Absolute GDAS Baseline
F (nT): 0.0
D(deg): -22.7790 ° ' "
H (nT):
Z (nT):
I (deg): -39.2531
Collimation Errors
Declination Delta: 000° -09' 08"

Declination Epsilon: 000° -01' 04"
Declination Zo (nT):
Inclination Epsilon: 000° 00' -04"
Inclination Zo (nT):
Gdasview Settings

GDASView Version: V4.63 October 2015
H Baseline (nT): 18421.9
D Baseline (dg): 22.7756
Z Baseline (nT): -14347.9
Site Difference (nT): 0.0
H Offset: 0.0000 Scale: 105.8000
D Offset: 0.0000 Scale: 106.5000
Z Offset: 0.0000 Scale: -106.7500
Sensor Temperature Offset: 0.0000 Scale: 100.0000
Electronics Temperature Offset: 0.0000 Scale: 100.0000
Digitiser Temperature Offset: 0.0000 Scale: 100.0000
Proton (F) Offset: 0.0000 Scale: 1.0000

III Observatory: Nampula

Logger: vassouras
Observer: MUCUSSETE
Date: 23 Nov 2017
Site Difference: 0.0
Theodolite serial number: 1112
Theodolite vertical scale offset: 90
Fluxgate serial number: 3481
Fixed Mark Reading
CR 1: 000° 06' 00"
CL 1: 180° 02' 15"
CR 2: 000° 06' 45"
CL 2: 180° 02' 45"
Mean: 090° 04' 26"
FM True: 336° 14' 08"
TN Circle: 023° 50' 18"
Declination Observation
VarD(nT)
WU: 13:27 271° 15' 45" 271.2625°
ED: 13:25 270° 54' 15" 270.9042°
WD: 13:24 090° 52' 15" 90.8708°
EU: 13:22 091° 10' 45" 91.1792°
Mean: 13:24 181° 03' 15"
Declination: 13:24 -022° 47' 03" -22.7842°

Inclination Observation
PPMF(nT) VarH(nT) VarZ(nT)
NU: 13:37 230° 43' 45" -39.2708°
SD: 13:38 050° 46' 00" -39.2333°
ND: 13:41 309° 14' 45" -39.2458°
SU: 13:42 129° 13' 00" -39.2167°
Inclination: 13:39 -039° 14' 30" -39.2417°
Baselines
Absolute GDAS Baseline
F (nT): 0.0
D(deg): -22.7842 ° ' "
H (nT):
Z (nT):
I (deg): -39.2417
Collimation Errors
Declination Delta: 000° -10' 00"
Declination Epsilon: 000° 02' 09"
Declination Zo (nT):
Inclination Epsilon: 000° 00' 38"
Inclination Zo (nT):

Gdasview Settings
GDASView Version: V4.63 October 2015
H Baseline (nT): 18421.9
D Baseline (dg): 22.7756
Z Baseline (nT): -14347.9
Site Difference (nT): 0.0
H Offset: 0.0000 Scale: 105.8000
D Offset: 0.0000 Scale: 106.5000
Z Offset: 0.0000 Scale: -106.7500
Sensor Temperature Offset: 0.0000 Scale: 100.0000
Electronics Temperature Offset: 0.0000 Scale: 100.0000
Digitiser Temperature Offset: 0.0000 Scale: 100.0000
Proton (F) Offset: 0.0000 Scale: 1.0000

IV Observatory: Nampula

Logger: vassouras
Observer: ARMINDO
Date: 23 Nov 2017
Site Difference: 0.0
Theodolite serial number: 1112
Theodolite vertical scale offset: 90
Fluxgate serial number: 3481
Fixed Mark Reading
CR 1: 000° 06' 15"
CL 1: 180° 02' 45"
CR 2: 000° 05' 45"
CL 2: 180° 02' 45"
Mean: 090° 04' 22"
FM True: 336° 14' 08"
TN Circle: 023° 50' 14"
Declination Observation
VarD(nT)
WU: 13:54 271° 17' 00" 271.2833°
ED: 13:53 270° 51' 15" 270.8542°
WD: 13:51 090° 55' 45" 90.9292°
EU: 13:50 091° 10' 30" 91.1750°
Mean: 13:52 181° 03' 38"
Declination: 13:52 -022° 46' 37" -22.7769°

Inclination Observation
PPMF(nT) VarH(nT) VarZ(nT)
NU: 14:19 230° 44' 45" -39.2542°
SD: 14:20 050° 46' 30" -39.2250°
ND: 14:23 309° 14' 45" -39.2458°
SU: 14:24 129° 11' 30" -39.1917°
Inclination: 14:21 -039° 13' 45" -39.2292°

Baselines
Absolute GDAS Baseline
F (nT): 0.0
D(deg): -22.7769 ° ' "
H (nT):
Z (nT):
I (deg): -39.2292
Collimation Errors

Declination Delta: 000° -10' 08"
Declination Epsilon: 000° 00' 37"
Declination Zo (nT):
Inclination Epsilon: 000° 00' 38"
Inclination Zo (nT):
Gdasview Settings
GDASView Version: V4.63 October 2015
H Baseline (nT): 18421.9
D Baseline (dg): 22.7756
Z Baseline (nT): -14347.9
Site Difference (nT): 0.0
H Offset: 0.0000 Scale: 105.8000
D Offset: 0.0000 Scale: 106.5000
Z Offset: 0.0000 Scale: -106.7500
Sensor Temperature Offset: 0.0000 Scale: 100.0000
Electronics Temperature Offset: 0.0000 Scale: 100.0000
Digitiser Temperature Offset: 0.0000 Scale: 100.0000
Proton (F) Offset: 0.0000 Scale: 1.0000
V Observatory: Nampula
Logger: vassouras
Observer: MUCUSSETE
Date: 23 Nov 2017
Site Difference: 0.0
Theodolite serial number: 1112
Theodolite vertical scale offset: 90
Fluxgate serial number: 3481

Fixed Mark Reading
CR 1: 000° 05' 30"
CL 1: 180° 02' 15"
CR 2: 000° 05' 45"
CL 2: 180° 02' 00"
Mean: 090° 03' 52"
FM True: 336° 14' 08"
TN Circle: 023° 49' 45"
Declination Observation
VarD(nT)
WU: 14:41 271° 17' 15" 271.2875°

ED: 14:39 270° 51' 45" 270.8625°
WD: 14:38 090° 56' 45" 90.9458°
EU: 14:36 091° 11' 45" 91.1958°
Mean: 14:38 181° 04' 23"
Declination: 14:38 -022° 45' 22" -22.7561°

Inclination Observation
PPMF(nT) VarH(nT) VarZ(nT)
NU: 14:55 230° 45' 15" -39.2458°
SD: 14:57 050° 48' 00" -39.2000°
ND: 14:58 309° 13' 00" -39.2167°
SU: 15:00 129° 11' 00" -39.1833°
Inclination: 14:57 -039° 12' 41" -39.2115°
Baselines
Absolute GDAS Baseline
F (nT): 0.0
D(deg): -22.7561 ° ' "
H (nT):
Z (nT):
I (deg): -39.2115
Collimation Errors

Declination Delta: 000° -10' 08"
Declination Epsilon: 000° 00' 09"
Declination Zo (nT):
Inclination Epsilon: 000° 00' 41"
Inclination Zo (nT):
Gdasview Settings
GDASView Version: V4.63 October 2015
H Baseline (nT): 18421.9
D Baseline (dg): 22.7756
Z Baseline (nT): -14347.9
Site Difference (nT): 0.0
H Offset: 0.0000 Scale: 105.8000
D Offset: 0.0000 Scale: 106.5000
Z Offset: 0.0000 Scale: -106.7500

Sensor Temperature Offset: 0.0000 Scale: 100.0000
Electronics Temperature Offset: 0.0000 Scale: 100.0000
Digitiser Temperature Offset: 0.0000 Scale: 100.0000
Proton (F) Offset: 0.0000 Scale: 1.0000

VI Observatory: Nampula

Logger: vassouras
Observer: ARMINDO
Date: 23 Nov 2017
Site Difference: 0.0
Theodolite serial number: 1112
Theodolite vertical scale offset: 90
Fluxgate serial number: 3481

Fixed Mark Reading
CR 1: 000° 04' 00"
CL 1: 180° 01' 30"
CR 2: 000° 03' 30"
CL 2: 180° 01' 15"
Mean: 090° 02' 34"
FM True: 336° 14' 08"
TN Circle: 023° 48' 26"
Declination Observation
VarD(nT)
WU: 15:10 271° 16' 30" 271.2750°
ED: 15:09 270° 51' 30" 270.8583°
WD: 15:08 090° 55' 30" 90.9250°
EU: 15:06 091° 10' 45" 91.1792°
Mean: 15:08 181° 03' 34"
Declination: 15:08 -022° 44' 52" -22.7478°
Inclination Observation
PPMF(nT) VarH(nT) VarZ(nT)
NU: 15:29 230° 45' 15" -39.2458°
SD: 15:31 050° 47' 00" -39.2167°
ND: 15:33 309° 15' 00" -39.2500°
SU: 15:34 129° 11' 45" -39.1958°
Inclination: 15:31 -039° 13' 38" -39.2271°

Baselines
Absolute GDAS Baseline
F (nT): 0.0
D(deg): -22.7478 ° ' "
H (nT):
Z (nT):
I (deg): -39.2271

Collimation Errors
Declination Delta: 000° -10' 04"
Declination Epsilon: 000° 00' 32"
Declination Zo (nT):
Inclination Epsilon: 000° 00' 15"
Inclination Zo (nT):
Gdasview Settings
DASView Version: V4.63 October 2015
H Baseline (nT): 18421.9
D Baseline (dg): 22.7756
Z Baseline (nT): -14347.9
Site Difference (nT): 0.0
H Offset: 0.0000 Scale: 105.8000
D Offset: 0.0000 Scale: 106.5000
Z Offset: 0.0000 Scale: -106.7500
Sensor Temperature Offset: 0.0000 Scale: 100.0000
Electronics Temperature Offset: 0.0000 Scale: 100.0000
Digitiser Temperature Offset: 0.0000 Scale: 100.0000
Proton (F) Offset: 0.0000 Scale: 1.0000

Participants:

Camila Farias - cfarias@smn.gov.ar - Argentina

Soledad Heredia - msoledadheredia@gmail.com - Argentina

Facundo Poblet - fpoblet@fcaglp.unlp.edu.ar - Argentina

Alex Gonsette - alexandre.gonsette@meteo.be - Belgium

Jean Rasson - jr@meteo.be - Belgium

Alberto G.F. Santos - alberto@on.br - Brazil

Alex Benigno Nunes - benigno.alex@gmail.com - Brazil

Alexandre Andrei - oat1@ov.ufrj.br - Brazil

Amanda Piassi - amanda.piassi@inpe.br – Brazil

Andrés Papa - papa@on.br - Brazil

Andreos Vestena Bilibio - andreos.bilibio@inpe.br - Brazil

Caio C. Gonçalves - caiocunha184@gmail.com - Brazil

Cézar F. Bellinghini - cezarbellinghini@gmail.com - Brazil

Clézio De Nardin - clezio.denardin@inpe.br – Brazil

Cosme Ponte Neto - cosme@on.br – Brazil

Cristiano Mendel Martins - mendelmartins@gmail.com - Brazil

Daniel Franco - drfranco@on.br - Brazil

Denise Moura - denise.moura@usp.br - Brazil

Edson A. F. Luza - edsonalonsofl@gmail.com - Brazil

Katia Pinheiro - Kátia J. Pinheiro kpinheirogeomag@gmail.com - Brazil

Karen Sarmiento - karen.sarmiento@inpe.br - Brazil

Laryssa C. F. Silva - laryfreire10@gmail.com – Brazil

Lívia Alves - livia.alves@inpe.br - Brazil

Luiz Benyosef - benyosef@on.br - Brazil

Gabriel Brando Soares - soaresbrando@gmail.com - Brazil

Gustavo Cabral - gustavo.cabral@yahoo.com.br - Brazil

Graziela B.D. Silva - graziela.silva@inpe.br - Brazil

Paulo R. B. Pinto - prbp2005@gmail.com - Brazil

Sophia R. Laranja - sophialaranja@id.uff.br - Brazil

Sony Su Chen - sony.chen@inpe.br - Brazil

Thais Candido Silva - candidothais93@gmail.com - Brazil

Vinicius Werneck - viniciusonrj@gmail.com - Brazil

Vitor Silvério Bernardes - vitorbernardes@on.br - Brazil

Gelvan A. Hartmann - gelvam@ige.unicamp.br - Brazil

Edgar Ricaldi Yarvii - ericaldi@fiumsa.edu.bo - Bolivia

Javier Quispe Mamani - javierlinux21@gmail.com - Bolivia

Wilson Quintero - wquintero65@gmail.com - Colombia

Jorge Brenes Rodriguez - JBrenesR@ice.go.cr - Costa Rica

Armando Ayala Fernandez - AAyala@ice.go.cr - Costa Rica

Maria Elena Muniz - mariaelenam55@gmail.com - Cuba

Jürgen Matzka - jmat@gfz-potsdam.de - Germany

Angelo De Santis - angelo.desantis@ingv.it - Italy

Yvelice Castillo - yvelicesoraya@gmail.com - Honduras

Esteban Hernández - estebanh@geofisica.unam.mx - México

Gerardo Cifuentes Nava - gercifue@geofisica.unam.mx - México

Maria Sergeeva - maria.a.sergeeva@gmail.com - México

Pedro Corona Romero - piter.cr@gmail.com - México

Antonio Eburamo Mucussete - mucussete@gmail.com - Mozambique

Armindo Alberto Nhatsave - armindo.nhatsave@gmail.com - Mozambique

Domingos Rosales - domingo_igp@hotmail.com - Peru

Paulo Ribeiro - pribeiro@ci.uc.pt - Portugal

Ciaran Beggan - ciar@bgs.ac.uk – UK

Carol Finn - cafinn@usgs.gov - USA

Dmitry Koryakin - Dmitry.Koryakin@cgg.com - USA

Leda S. Bettucci - leda@fcien.edu.uy - Uruguay

Ramon Caraballo - jolinar35@gmail.com - Uruguay

Bruno Canosa - brucano1@hotmail.com - Uruguay

Edwin Camacho - edwincmch@gmail.com - Venezuela

Pictures


Observatory coverage


Problems with corrections:
• Remote observatories (thousands kms from survey)
• Data gaps
• Short-period variations (minutes – few hours) usually correlate well, even with remote observatories
• Long-period variations (daily variations) – shifted in phase with longitude and amplitude varies with latitude
• Lead to quasi-systematic residual pseudo-anomalies


D-Z Geomagnetic field variations and geological features measured in low magnetic latitudes
Introduction
Method
Results
Conclusion
Estado actual de los Observatorios Magnéticos perma
Servicio Meteorológico Nacional, Argentina
INTRODUCIÓN
UBICACIÓN